

TECHNISCHE UNIVERSITÄT MÜNCHEN

Professur für Obstbau

Development of a loop-mediated isothermal amplification assay
for the detection of the pear decline agent
Candidatus Phytoplasma pyri

Angela Siemonsmeier

Vollständiger Abdruck der von der Fakultät Wissenschaftszentrum Weihenstephan für Ernährung, Landnutzung und Umwelt der Technischen Universität München zur Erlangung des akademischen Grades eines

Doktors der Naturwissenschaften

genehmigten Dissertation.

Vorsitzende: Prof. Dr. Brigitte Poppenberger-Sieberer

Prüfer der Dissertation: 1. Prof. Dr. Wilfried Schwab
2. apl. Prof. Dr. Ludwig Niessen

Die Dissertation wurde am 18.09.2018 bei der Technischen Universität München eingereicht und durch die Fakultät Wissenschaftszentrum Weihenstephan für Ernährung, Landnutzung und Umwelt am 08.01.2019 angenommen.

Summary

Phytoplasmas pose a severe threat to agriculture and horticulture, causing yellows-type diseases in approximately 1,000 plant species worldwide. *Candidatus* Phytoplasma pyri (*Ca. P. pyri*), the causal agent of pear decline (PD), induces various symptoms on its hosts as stunting and reduced fruit size, leading not only to weakening and dieback of the plants but also to considerable financial losses in pear growing areas. Fighting the disease requires a reliable and inexpensive method for the detection of the pathogen, which can be performed on the spot, also by unexperienced users. The objective of this work was the development of a laboratory-independent, easy-to-use detection procedure for the pear decline phytoplasma. This was achieved with a simplified sample preparation method, an isothermal DNA amplification assay and colorimetric detection of the products.

The loop-mediated isothermal amplification (LAMP) method was chosen for specific amplification of phytoplasma deoxyribonucleic acid (DNA). Four to six LAMP primers were designed based on the 16S rRNA gene, the *pnp* gene and the *rpl22* gene of *Candidatus* Phytoplasma pyri, respectively, and a suitable primer set targeting the 16S rRNA gene was selected. LAMP reaction conditions were optimized for colorimetric detection of the amplification by-product magnesium pyrophosphate. The initially used metal indicator dye hydroxy naphthol blue (HNB) was replaced with the metal indicator Eriochromeblack-T (ErioT). ErioT proved to be a highly suitable alternative to the widely used HNB, showing no fluctuations in colour intensity throughout the experiments as well as a high-contrast colour change from purple to blue in amplified LAMP reactions. No negative impact of ErioT on LAMP performance was observed. The readjustment of the LAMP reaction mix with ErioT resulted in a lowered magnesium chloride concentration as well as the replacement of betaine with polyethylene glycol 8k (PEG 8k). Spectrophotometer analyses of ErioT in LAMP buffer showed distinct absorption peaks at 548 nm in the presence and at 656 nm in the absence of magnesium ions. Absorbance and ability of the dye to form complexes with magnesium ions were found to be pH-dependent. The influence of individual buffer components and the additive PEG 8k on ErioT absorption spectra was investigated. While Tris-HCl (pH 8.8) ensured a suitable solution pH for magnesium complexation, the inorganic salts potassium chloride and ammonium sulfate lowered ErioT absorption maxima of both the free dye and the magnesium complex, probably due to the salt-induced formation of dye aggregates. This effect was compensated when PEG 8k was added, leading to enhanced absorption maxima of similar height irrespective the tested buffer ingredient. However, absorption peaks of both the free dye and the magnesium complex were shifted towards longer wavelengths when the solutions contained PEG 8k compared to solutions without PEG 8k. This bathochromic shift might be caused by PEG 8k-induced formation of J-aggregates or by the azo-hydrazone-tautomerism of ErioT.

The suitability of ErioT for colorimetric detection in LAMP was confirmed in a titration experiment with sodium pyrophosphate. The generation of the amplification by-product

magnesium pyrophosphate was traced with rising amounts of sodium pyrophosphate to determine the amount of by-product required to induce a colour change of EriOT. The colour transition point was determined at 1 mM sodium pyrophosphate. The equivalent DNA yield was calculated to be 0.31 $\mu\text{g}/\mu\text{l}$, which is below the DNA yield of 0.5 $\mu\text{g}/\mu\text{l}$ reported from LAMP reactions with loop primers.

The developed PD LAMP assay detected the pear decline agent with a similar detection limit as conventional PCR (polymerase chain reaction). The sensitivity of realtime PCR was about 100-fold higher than that of LAMP and conventional PCR. The PD LAMP proved to be applicable without limitations to the closely related *Ca. P. mali* and *Ca. P. prunorum*, which are the causal agents of apple proliferation (AP) and European stone fruit yellows (ESFY), respectively. The detection of phytoplasma strains belonging to phylogenetic groups other than 16SrX by the PD LAMP assay was found to be dependent on the applied additive. With the use of 1 M betaine per LAMP reaction, phytoplasma detection was restricted to members of the 16SrX group. In contrast, usage of the molecular crowding agent PEG 8k in the PD LAMP reaction mix enabled the detection of all phytoplasma strains tested in this study. The two additives also had diverging effects on the detection limit of the PD LAMP assay. The use of PEG 8k in PD LAMP reactions led to a detection limit similar to conventional PCR. Replacing PEG 8k with betaine resulted in 10-fold to 100-fold reduced sensitivity of the PD LAMP assay. The finally chosen LAMP reaction mix composition included PEG 8k as additive in order to obtain a LAMP assay with adequate sensitivity. Since mixed infections of diseased plants with a range of phytoplasmas have been reported, the feature of universal phytoplasma detection instead of specific detection of the PD phytoplasma was accepted because all phytoplasmas of a mixed infection are assumed to contribute to the disease.

A simplified sample preparation method based on homogenization of plant tissues in sodium hydroxide (NaOH) solution was developed for the implementation of an entirely laboratory-independent PD detection procedure. The NaOH-based sample preparation method in combination with the PD LAMP assay was successfully applied to field samples of PD-, AP- and ESFY-diseased fruit trees, confirming the applicability of the developed procedure to all fruit tree phytoplasmas of the 16SrX group. A LAMP assay targeting the plant cytochrome oxidase gene was established as internal control to verify the presence of DNA in the diluted NaOH-homogenates. The application of a commercially available direct PCR kit finally enabled the straight comparison of the performances of PD LAMP and PCR when NaOH-treated samples were tested. In an experiment with 40 *in vitro* plants processed with the NaOH sample preparation method, PD LAMP and direct PCR yielded identical results.

The development of a LAMP assay for the detection of *Ca. P. pyri* was successfully accomplished. However, the frequent occurrence of false positives substantially hampered the development process and repeatedly led to the replacement of the malfunctioning primer set with a new one. An intensive search for the putative contamination source remained without result. Finally, it was discovered that the purchased ThermoPol buffer induced the generation

of false positives in the PD LAMP, as demonstrated with a freshly prepared LAMP buffer of equal composition, which yielded clean controls in a comparative experiment. The massive generation of products with distinct sizes, appearing as ladder-like banding pattern on agarose gels, in the absence of any template DNA was unexpected. Furthermore, it was demonstrated that efficient amplification resulting in ladder-like patterns on agarose gels was possible with only two primers present in the reaction solution. The ability of DNA polymerases to perform *ab initio* DNA synthesis, unprimed DNA amplification as well as primer multimerization was demonstrated by various authors. In the light of these reports, the generation of high amounts of amplification products in the absence of template DNA by *Bst* DNA Polymerase is not surprising, given the presence of six different oligonucleotides at an overall concentration of 5.2 μM per reaction. While the exact mechanism of false positive generation in the PD LAMP could not be elucidated within this study, the identification of the LAMP buffer as causal agent of this incidence enabled an efficient strategy to reliably eliminate the distracting malfunction of the PD LAMP.

In conclusion, it can be stated that the loop-mediated isothermal amplification assay developed in this study for the detection of the causal agent of pear decline meets the requirements of a field-suitable pathogen detection procedure by the combination of a simple and rapid sample preparation procedure with a colorimetric isothermal DNA amplification method. Furthermore, the entire procedure was demonstrated to be applicable without limitations to the other fruit tree phytoplasmas of the 16SrX group. The PD LAMP assay is therefore highly suitable for on-site monitoring of the PD, AP and ESFY phytoplasmas on a regular basis.

Zusammenfassung

Phytoplasmen verursachen Welke- und Vergilbungskrankheiten in etwa 1000 Pflanzenarten weltweit und stellen eine ernste Bedrohung für die Landwirtschaft und den Gartenbau dar. *Candidatus Phytoplasma pyri* (*Ca. P. pyri*), der Erreger des Birnenverfalls (pear decline, PD), ruft zahlreiche Symptome bei seinen Wirten hervor, wie beispielsweise Kümmerwuchs und Kleinfrüchtigkeit. Die Erkrankung führt nicht nur zu Schwächung und Absterben der Pflanzen, sondern verursacht auch beträchtliche finanzielle Verluste in Birnenanbaugebieten. Die Bekämpfung dieser Krankheit erfordert eine verlässliche und kostengünstige Methode zur Detektion des Erregers, die vor Ort auch von unerfahrenen Anwendern durchgeführt werden kann. Die Zielsetzung der vorliegenden Arbeit war die Entwicklung einer Labor-unabhängigen, leicht anzuwendenden Nachweismethode für das Birnenverfall-Phytoplasma. Dies wurde erreicht durch eine vereinfachte Methode der Probenaufbereitung, ein isothermales DNA (Desoxyribonukleinsäure)-Amplifikationsassay und eine colorimetrische Detektion der Produkte.

Für die spezifische Amplifizierung von Phytoplasma-DNA wurde die Loop-mediated isothermal amplification (LAMP)-Methode ausgewählt. Jeweils vier bis sechs LAMP-Primer wurden für das 16S rRNA-Gen, das *pnp*-Gen und das *rpl22*-Gen von *Candidatus Phytoplasma pyri* entworfen und ein geeignetes Primer Set zur Amplifizierung des 16S rRNA-Gens wurde ausgewählt. Die LAMP-Reaktionsbedingungen wurden für die colorimetrische Detektion des Nebenproduktes Magnesiumpyrophosphat optimiert. Der anfänglich verwendete Metallindikator Hydroxynaphtholblau (HNB) wurde durch Eriochromschwarz-T (ErioT) ersetzt. ErioT erwies sich als sehr gut geeignete Alternative zu dem häufig in LAMP-Assays verwendeten HNB. Die Farbintensität von ErioT zeigte keine Schwankungen während der Experimente, sowie einen sehr kontrastreichen Farbumschlag von violett zu blau in positiven LAMP-Reaktionen. Negative Auswirkungen von ErioT auf die Leistungsfähigkeit des LAMP-Assays wurden nicht beobachtet. Die erforderliche Nachjustierung des LAMP-Reaktionsgemisches resultierte in einer verringerten Magnesiumchloridkonzentration, sowie der Verwendung von Polyethylenglycol 8k (PEG 8k) anstelle von Betain. Spektrophotometer-Analysen von ErioT in LAMP-Puffer zeigten ausgeprägte Absorptionsmaxima bei 548 nm mit und bei 656 nm ohne Magnesiumionen. Sowohl die Absorption des Farbstoffs als auch seine Fähigkeit zur Komplexbildung mit Magnesiumionen waren abhängig vom pH-Wert des Lösungsmittels. Der Einfluss einzelner Komponenten des LAMP-Puffers sowie des Additivs PEG 8k auf die Absorptionsspektren von ErioT wurden untersucht. Während Tris-HCl (pH 8,8) einen geeigneten pH-Wert der Lösung für die Magnesiumkomplexierung sicherstellte, verringerten die anorganischen Salze Kaliumchlorid und Ammoniumsulfat die Absorptionsmaxima sowohl des unkomplexierten Farbstoffs als auch des ErioT-Magnesium-Komplexes, mutmaßlich aufgrund der Salz-induzierten Bildung von Farbstoff-Aggregaten. Dieser Effekt wurde durch die Zugabe von PEG 8k kompensiert, was unabhängig von der getesteten Pufferkomponente zu erhöhten Absorptionsmaxima mit ähnlichen Höchstwerten

fürte. Im Vergleich zu Lösungen ohne PEG 8k wurden die Absorptionsmaxima des unkomplexierten Farbstoffs sowie des Magnesiumkomplexes jedoch in Richtung längerer Wellenlängen verschoben, wenn die Lösungen PEG 8k enthielten. Dieser bathochrome Effekt könnte durch PEG 8k-induzierte Bildung von J-Aggregaten oder durch die Azo-Hydrason-Tautomerie von ErioT verursacht werden.

Die Eignung von ErioT für die colorimetrische Detektion in LAMP-Assays wurde in einem Titrationsexperiment mit Natriumpyrophosphat bestätigt. Die Bildung des Nebenproduktes Magnesiumpyrophosphat während der DNA-Amplifizierung wurde durch die Titration steigender Mengen von Natriumpyrophosphat simuliert, um die Menge an Nebenprodukt zu bestimmen, die für einen Farbumschlag von ErioT notwendig ist. Der Umschlagspunkt wurde bei 1 mM Natriumpyrophosphat bestimmt. Die äquivalente DNA-Menge wurde mit 0,31 µg/µl errechnet. Dieser Wert liegt unter dem DNA-Ertrag von 0,5 µg/µl, der für LAMP-Reaktionen mit Loop-Primern angegeben wird.

Das entwickelte LAMP-Assay zeigte bei der Detektion des Erregers des Birnenverfalls eine ähnliche Nachweisgrenze wie die konventionelle Polymerasekettenreaktion (PCR). Die Sensitivität des getesteten Realtime-PCR-Assays war etwa 100-fach höher als die Sensitivität des LAMP-Assays und der konventionellen PCR. Die PD LAMP zeigte sich uneingeschränkt einsetzbar für die Detektion der nah verwandten Erreger der Apfeltriebsucht (apple proliferation, AP) und der Europäischen Steinobstvergilbung (European stone fruit yellows, ESFY), *Ca. P. mali* und *Ca. P. prunorum*. Der Nachweis von Phytoplasmen, die nicht der taxonomischen Gruppe 16SrX angehörten, durch die PD LAMP war abhängig vom verwendeten Additiv. Bei der Verwendung von 1 M Betain pro LAMP-Reaktion war die Phytoplasma-Detektion auf die Gruppe 16SrX beschränkt. Der Einsatz von PEG 8k im LAMP-Reaktionsgemisch hingegen ermöglichte den Nachweis aller in dieser Studie getesteten Phytoplasma-Stämme. Darüber hinaus hatten die beiden Additive unterschiedliche Effekte auf die Nachweisgrenze des PD LAMP-Assays. Die Verwendung von PEG 8k in PD LAMP-Reaktionen führte zu einer vergleichbaren Nachweisgrenze wie die konventionelle PCR. Der Einsatz von Betain anstelle von PEG 8k resultierte in einer 10-fach bis 100-fach verringerten Sensitivität des PD LAMP-Assays. Die finale Zusammensetzung des PD LAMP-Reaktionsgemisches beinhaltete PEG 8k als Additiv, um ein LAMP-Assay mit adäquater Sensitivität zu erhalten. Berichte von Mischinfektionen erkrankter Pflanzen mit einer Reihe verschiedener Phytoplasmen finden sich gelegentlich in der Literatur. Die Möglichkeit der universellen Phytoplasma-Detektion mit dem PD LAMP-Assay anstelle einer spezifischen Detektion des PD Phytoplasmas wurde letztlich akzeptiert, da anzunehmen ist, dass alle Phytoplasmen einer Mischinfektion zum Krankheitsgeschehen beitragen.

Zur Implementierung einer vollständig Labor-unabhängigen Nachweisprozedur für das PD Phytoplasma wurde eine vereinfachte Probenaufbereitungsmethode entwickelt, die auf der Homogenisierung von Pflanzengewebe in einer Natriumhydroxid-Lösung (NaOH-Lösung) basiert. Diese Probenaufbereitungsmethode wurde in Kombination mit dem PD LAMP-Assay

erfolgreich zur Testung von Feldproben von Obstbäumen angewendet, die an Birnenverfall, Apfeltriebsucht und Europäischer Steinobstvergilbung erkrankt waren. Die Anwendbarkeit der entwickelten Testprozedur auf alle Obstbaum-Phytoplasmen der Gruppe 16SrX wurde hierdurch bestätigt. Ein LAMP-Assay zum Nachweis des pflanzlichen Cytochrom-Oxidase-Gens wurde als interne Kontrolle etabliert, um das Vorhandensein von DNA in den verdünnten NaOH-Homogenaten zu verifizieren. Die Anwendung eines kommerziell erhältlichen Direct PCR Kits ermöglichte schließlich den direkten Vergleich der Effizienz von PD LAMP-Assay und PCR mit NaOH-behandelten Proben. Ein Experiment mit 40 *in vitro*-Pflanzen, die mit der NaOH-Methode aufbereitet wurden, ergab identische Resultate in der PD LAMP und der Direct PCR.

Die Entwicklung eines LAMP-Assays für den Nachweis von *Ca. P. pyri* wurde letztlich erfolgreich abgeschlossen. Das häufige Auftreten von falsch-positiven Ergebnissen beeinträchtigte den Entwicklungsprozess jedoch erheblich und führte wiederholt dazu, dass das fehlerhafte Primer Set durch ein neues ersetzt wurde. Eine intensive Suche nach der mutmaßlichen Kontaminationsquelle blieb ohne Ergebnis. Schließlich wurde entdeckt, dass der käuflich erworbene ThermoPol-Puffer die Bildung von Falsch-Positiven verursachte, da in einem vergleichenden Experiment gezeigt werden konnte, dass ein frisch angesetzter LAMP-Puffer derselben Zusammensetzung saubere Kontrollen lieferte. Die massive Erzeugung von Produkten mit klar definierten Fragmentgrößen in Abwesenheit jeglicher DNA-Vorlage, die als Leiter-artige Bandenmuster auf Agarose-Gelen erschienen, war zunächst unerwartet. Darüber hinaus konnte gezeigt werden, dass eine effiziente Amplifizierung mit resultierendem Leiter-artigen Bandenmuster auf dem Agarose-Gel mit nur zwei Primern in der Reaktionslösung möglich war. Die Fähigkeit von DNA-Polymerasen zur *ab initio*-DNA-Synthese, DNA-Amplifizierung ohne Beteiligung von Primern sowie zur Multimerisierung von Primern wurde von verschiedenen Autoren demonstriert. Angesichts dieser Berichte ist die Generierung hoher Mengen an Amplifizierungsprodukten in Abwesenheit von Template-DNA durch die *Bst* DNA-Polymerase nicht überraschend, insbesondere da die LAMP-Reaktionslösung sechs verschiedene Oligonukleotide mit einer Gesamtkonzentration von 5,2 μM pro Reaktion enthält. Während der exakte Mechanismus der Entstehung von Falsch-Positiven in der PD LAMP im Rahmen dieser Arbeit nicht ermittelt werden konnte, so ermöglichte doch die Identifizierung des LAMP-Puffers als Verursacher dieser Problematik eine effiziente Strategie zur verlässlichen Eliminierung der störenden Fehlfunktion der PD LAMP.

Abschließend kann festgestellt werden, dass das entwickelte Loop-mediated isothermal amplification-Assay zum Nachweis des Erregers des Birnenverfalls die Anforderungen an eine feldtaugliche Nachweisprozedur durch die Kombination einer einfachen und schnellen Probenaufbereitungsmethode mit einer colorimetrischen, isothermalen DNA-Amplifikationsmethode erfüllt. Darüber hinaus konnte gezeigt werden, dass die gesamte Prozedur uneingeschränkt auf die anderen Obstbaumphytoplasmen der Gruppe 16SrX anwendbar ist. Die PD LAMP ist daher in hohem Maße für ein regelmäßiges Feld-Monitoring der PD-, AP- und ESFY-Phytoplasmen geeignet.

Acknowledgement

The way to this doctoral thesis was a long and challenging journey, and I surely would not have been able to finally arrive here without the help and contribution of all those people I want to thank with the following lines.

First and foremost, I am very grateful to Prof. Dr. Dieter Treutter for giving me the opportunity to work at his institute, for his trust and advice, and I deeply regret that we could not finish what we began together.

Prof. Dr. Wilfried Schwab, who kindly took on the task to be my doctoral thesis supervisor, deserves my special thanks for his time and effort. It was a huge relief to know that he was there to adopt us, a group of “fatherless” and somewhat lost Ph.D. students.

Furthermore, I would like to express my gratitude to Prof. Dr. Ludwig Niessen for taking over as second reviewer and Prof. Dr. Brigitte Poppenberger-Sieberer for chairing the examination board.

I greatly thank Dr. Johannes Hadersdorfer for his support and advice, for seriously considering even my craziest ideas and for always being there when I needed help, whichever day and time it was.

A special thanks goes to Prof. Dr. Gabriele Weber-Blaschke for her continuous support and encouragement during the last months of writing.

I sincerely thank Dr. Bernd Schneider for his help and cooperation throughout the project runtime, and for kindly providing plants, plasmids and pathogen strains. Furthermore, I would like to express my sincere thanks to Prof. Dr. Assunta Bertaccini for providing DNA samples of a broad range of phytoplasmas. To Dietlinde Rißler, Michael Petruschke and all involved employees of the LTZ Augustenberg, I owe special thanks for participating in the inter-laboratory test for the applicability of the PD LAMP to AP samples.

I thank Dr. Michael Neumüller for the good cooperation in this research project and for valuable insights into the world of horticulture, Johanna Stammer for many inspiring and highly creative conversations, Anja Forstner, Ina Tittel, Petra Freynhagen, Gabriele Traute, Rita Wimmer, all involved trainees and the employees of the GHl for their support and a pleasant working atmosphere.

A huge thanks goes to Susanne Hebling for her help and care throughout my time as Ph.D. student, and to Ute Peterskovsky for her encouragement and her imperturbable faith in me even in times when I was near despair. Furthermore, I owe many thanks to Viktoria Stamm and Ute Peterskovsky for linguistic revision of the introduction.

Finally, I want to thank my family for their support and their patience during this long time of waiting for the completion of this thesis.

Table of contents

Summary	III
Zusammenfassung	VI
Acknowledgement.....	IX
List of figures	IX
List of tables	XII
Abbreviations	XIII
1 Introduction	14
1.1 The European pear (<i>Pyrus communis</i> Linn.): Relatives, history and economic importance	14
1.2 Pear Decline – A quarantine disease	17
1.3 Detection of <i>Candidatus</i> Phytoplasma pyri.....	21
1.4 Loop-mediated isothermal amplification.....	22
1.5 Objective of this study	27
2 Materials and Methods	28
2.1 Workflow of the PD LAMP development process.....	28
2.2 Sources of phytoplasmas and DNA samples	28
2.3 DNA extraction.....	29
2.4 Simplified sample preparation.....	30
2.4.1 NaOH-based sample preparation	30
2.4.2 Water-based sample preparation	30
2.5 Conventional nucleic acid based detection methods	31
2.5.1 Nested PCR	31
2.5.2 Conventional PCR.....	31
2.5.3 Direct PCR	32
2.5.4 Realtime PCR.....	33
2.5.5 Agarose gel electrophoresis	34
2.6 Loop-mediated isothermal amplification (LAMP).....	34
2.6.1 LAMP primers.....	34
2.6.2 Reaction conditions	36
2.6.3 Experiments with LAMP buffer ingredients	38

Table of contents

2.6.4	Visualization and documentation of LAMP results	38
2.7	Experiments on the properties of Eriochromeblack-T	39
2.7.1	Measurement of UV/Vis spectra	39
2.7.2	Titration experiments with sodium pyrophosphate	39
3	Results	40
3.1	Development of a colorimetric loop-mediated isothermal amplification assay for the detection of <i>Candidatus</i> <i>Phytoplasma pyri</i> targeting the 16S rRNA gene	40
3.1.1	Experiments with a primer set published by Obura et al. (2011).....	40
3.1.2	Design of LAMP primer sets targeting the 16S rRNA gene of <i>Candidatus</i> <i>Phytoplasma pyri</i>	45
3.1.3	Optimization of the PD LAMP assay with hydroxy naphthol blue for indirect detection of amplification products.....	47
3.2	Detection limit	51
3.3	Evaluation of LAMP primer sets targeting non-ribosomal genes	55
3.4	Development of a simplified sample preparation procedure.....	59
3.5	Detection range: Applicability of the PD LAMP to other members of the 16SrX group.....	69
3.6	Colorimetric detection of LAMP products with Eriochromeblack-T	72
3.6.1	Evaluation of metal indicator dyes for colorimetric product detection in LAMP.....	72
3.6.2	Spectrophotometric investigations of Eriochromeblack-T	77
3.6.3	Titration experiments with sodium pyrophosphate	80
3.6.4	Detection limit and detection range of the PD LAMP with Eriochromeblack-T.....	83
3.7	Occurrence of false positives in LAMP and troubleshooting.....	87
3.7.1	Investigations on the causes of the occurrence of false positives in the PD LAMP.....	87
3.7.2	Experiments with LAMP buffer composition	93
4	Discussion	98
4.1	Targets for LAMP primers	98
4.2	Evaluation of LAMP primer sets for the detection of <i>Candidatus</i> <i>Phytoplasma pyri</i>	99
4.2.1	LAMP primer set PD1 published by Obura et al. (2011).....	99

Table of contents

4.2.2	LAMP primer sets PD2, PD3 and PD4 designed on the 16S rRNA gene of <i>Ca. P. pyri</i>	100
4.2.3	LAMP primer sets targeting the <i>pnp</i> gene and the <i>rpl22</i> gene of <i>Ca. P. pyri</i>	103
4.3	Colorimetric detection with Eriochromeblack-T.....	103
4.3.1	Optimization of the PD LAMP assay with Eriochromeblack-T	105
4.3.2	Investigation of spectrophotometric properties of Eriochromeblack-T	107
4.3.3	Titration experiments with sodium pyrophosphate	111
4.4	Detection limit and detection range of the PD LAMP assay.....	113
4.5	Simplified sample preparation.....	116
4.6	Occurrence of false positives in LAMP	121
4.7	Potential of the PD LAMP assay for on-site applications	130
5	Conclusions	134
5.1	Development of a field-suitable, easy-to-use detection procedure for <i>Candidatus Phytoplasma pyri</i> , the causal agent of pear decline	134
5.2	Brief description of the PD LAMP detection procedure	134
5.3	Recommendations for further development and transfer of the PD detection procedure into practice	136
6	References	137

List of figures

Figure 1: Pear production area in Europe (Eurostat, 2015).....	16
Figure 2: Pear decline symptoms	20
Figure 3: Schematic illustration of the LAMP reaction (Tomita et al, 2008).....	23
Figure 4: Workflow of the development process of the PD LAMP assay	28
Figure 5: First test of LAMP primers published by Obura et al. (2011) with and without initial denaturation step.	41
Figure 6: LAMP reactions with primer set PD1 prepared according to Obura et al. (2011) (LAMP 1) and according to Hadersdorfer et al. (2011) (LAMP 2), with and without initial denaturation step.....	42
Figure 7: LAMP reactions with primer set PD1, magnesium sulfate concentration series	43
Figure 8: LAMP with primer set PD1, application to PD field samples and apple proliferation samples.	43
Figure 9: Occurrence of false positives during the development process of a simplified sample preparation procedure in LAMP reactions with primer set PD1	44
Figure 10: Sequence alignment of the LAMP primer set PD1 obtained from Obura et al. (2011) with the 16S rDNA target sequences of (a) NSP phytoplasma (GenBank access. no. AY736374) and (b) PD phytoplasma (GenBank access. no. AJ542543.1).....	45
Figure 11: Sequence alignment of LAMP primer sets PD2, PD3 and PD4 with the target region of the 16S rDNA sequence of the PD phytoplasma (GenBank access. no. AJ542543.1) ...	46
Figure 12: LAMP reactions with primer sets PD2 and PD3, dNTP concentration series	47
Figure 13: LAMP reactions with primer sets PD2 and PD3, magnesium sulfate concentration series.	49
Figure 14: LAMP reactions with primer set PD4, magnesium sulfate concentration series	49
Figure 15: Colour development of LAMP reactions with primer set PD4 over time, magnesium sulfate concentration series.	50
Figure 16: Detection limit of LAMP with primer set PD3 (A) in comparison to conventional PCR (B) and realtime PCR (C).....	52
Figure 17: Detection limit in the presence of increasing amounts of background DNA: LAMP with primer set PD3 (A) in comparison to conventional PCR (B) and Realtime PCR (C)	53
Figure 18: Detection limit of LAMP with primer set PD4 in comparison to LAMP with primer set PD3 and conventional PCR.....	54
Figure 19: LAMP with primer set pnp after 60, 90 and 120 min of incubation at 63 °C.....	55
Figure 20: LAMP with primer set pnp after 60, 90 and 120 min of incubation at 64 °C.....	56
Figure 21: LAMP with primer set pnp after 90 and 120 min of incubation at 65 °C.....	57
Figure 22: Evaluation of the detection limit of LAMP with primer set pnp (left) in comparison to primer set PD3 (right).....	57
Figure 23: LAMP with primer set rpl22 after 120 min of incubation at 63 °C	58
Figure 24: LAMP with primer set rpl22 after 90 and 120 min of incubation at 65 °C	58
Figure 25: LAMP with primer set rpl22 with enhanced magnesium sulfate and dNTP concentrations and reduced betaine concentration after 90 min of incubation at 65 °C.....	59
Figure 26: LAMP reactions with primer set PD1 and samples prepared by water-based homogenization according to Hadersdorfer et al. (2011) as well as with DNA extracted by DNeasy Plant Mini Kit.	60

List of figures

Figure 27: LAMP inhibition by crude sample preparations from pear, but not from plum	61
Figure 28: Influence of CTAB and NaOH on the colour of LAMP reaction solutions with HNB	61
Figure 29: Influence of the diluent and the dilution step on the formation of amplification products from NaOH-treated samples in LAMP reactions with primer set PD1	62
Figure 30: Influence of NaOH concentration on the formation of amplification products from NaOH-treated bark and leaf samples in LAMP reactions with primer set PD1	63
Figure 31: Influence of NaOH concentration on the formation of amplification products from NaOH-treated bark and leaf samples in LAMP reactions with primer set PD3	64
Figure 32: Application of the NaOH-based sample preparation method to field samples with suspected PD infestation.....	65
Figure 33: COX LAMP as internal control assay for the NaOH-based sample preparation method....	66
Figure 34: Evaluation of the applicability of the NaOH-based sample preparation method and subsequent PD LAMP for the detection of the AP and ESFY phytoplasmas	67
Figure 35: Evaluation of commercially available Direct PCR kits for the detection of 16SrX phytoplasmas in NaOH-based sample preparations.....	68
Figure 36: PD LAMP and Direct PCR results for NaOH-treated pear samples.....	68
Figure 38: PD LAMP reactions with the metal indicator dyes Murexide, Thiazole yellow and Phthalein purple	73
Figure 39: LAMP reactions with the metal indicator dyes hydroxy naphthol blue (HNB) and Eriochromeblack-T (ErioT).....	74
Figure 41: PD LAMP with ErioT, PEG 8k concentration series.....	75
Figure 42: Influence of the additives polyethylene glycol 8k and betaine on LAMP assay sensitivity with either HNB or ErioT.....	76
Figure 43: PD LAMP with either ErioT or the mixed indicator dye ErioT/MO.....	77
Figure 44: Absorption spectra of ErioT and HNB in distilled water and Tris-HCl (pH 8.8), respectively, and in the presence or absence of magnesium ions.....	77
Figure 45: Absorption spectra of ErioT in LAMP buffer, PEG 8k or LAMP buffer and PEG 8k, in the presence or absence of magnesium ions.....	78
Figure 46: Absorption spectra of ErioT in the presence of individual LAMP buffer components	79
Figure 47: Simulation of the ErioT colour change in a LAMP reaction by titration of sodium pyrophosphate.....	80
Figure 48: Development of ErioT absorption values at 648 nm with rising sodium pyrophosphate (NaPP) concentrations	81
Figure 49: Determination of the colour transition points of ErioT and HNB in LAMP reaction solutions in the presence and absence of dNTPs by titration of sodium pyrophosphate.....	82
Figure 50: Determination of the colour transition point of ErioT in LAMP reaction solutions with decreasing dNTP concentrations and increasing sodium pyrophosphate concentrations....	82
Figure 51: Detection limit of the PD LAMP with ErioT and either PEG 8k (A) or betaine (B) in comparison to conventional PCR (C) and realtime PCR with SybrGreen I (D)	84
Figure 52: Detection range of the PD LAMP in dependence of the applied additive	85
Figure 53: Multiple sequence alignment of the PD3 target regions on the 16S rDNA reference sequences of the tested phytoplasma strains as well as of the members of the 16SrX group, and location of the primer binding sites of LAMP primer set PD3	86
Figure 54: Occurrence of false positives in LAMP reactions with primer sets PD2, PD3 and PD4.....	87

Figure 55: Test of LAMP reagents and false positive PD4 LAMP reactions for the presence of target DNA with PCR using primers PD4 F3 and PD4 B3	88
Figure 56: LAMP reactions with primer set PD4, with and without loop primers	89
Figure 57: Comparative test of the primer sets PD3 and PD4 in LAMP reactions with identical composition	89
Figure 58: LAMP reactions with PD4 primers purchased from Eurofins MWG Operon and TIB Molbiol.....	90
Figure 59: LAMP reactions with primer set PD3, with and without loop primers	91
Figure 60: Amplification products formed under LAMP reaction conditions with pairwise combination of PD3 primers	91
Figure 61: Influence of the ThermoPol buffer on the occurrence of false positives in the PD LAMP..	92
Figure 62: Influence of ammonium sulfate on PD LAMP performance	94
Figure 63: Influence of Tris-HCl, ammonium sulfate and potassium chloride concentrations on PD LAMP performance.....	95
Figure 64: Evaluation of glycine as buffering agent in LAMP	96
Figure 65: Schematic illustration of the competition of LAMP reagents for magnesium ions	106
Figure 66: Structural formula and molecular model of the metal indicator Eriochromeblack-T (Skoog et al., 2014)	107

List of tables

Table 1: Pear production and harvested area of the top ten pear producing countries in the world in 2014 (FAO, 2014).	16
Table 2: Published LAMP assays for the detection of phytoplasmas	26
Table 3: Phytoplasma strains used in this study.	29
Table 4: PCR primers used for the detection of fruit tree phytoplasmas.....	33
Table 5: Loop-mediated isothermal amplification (LAMP) primer sets used in this study	35
Table 6: Results of the interlaboratory test series for the comparison of assay performances of LAMP, PCR and nested PCR in combination with different DNA extraction methods for the detection of the AP phytoplasma.	70
Table 7: Diagnostic sensitivity and specificity of the PD LAMP for the detection of the AP phytoplasma in DNA extracts, calculated according to Altman and Bland (1994).....	71
Table 8: Diagnostic sensitivity and specificity of the PD LAMP for the detection of the AP phytoplasma in NaOH-based sample preparations, calculated according to Altman and Bland (1994).	71
Table 9: Diagnostic sensitivity and specificity of the PD LAMP for the detection of the ESFY phytoplasma in NaOH-based sample preparations, calculated according to Altman and Bland (1994).	72
Table 10: Composition of the ThermoPol buffer (New England Biolabs).....	93
Table 11: PD3 Primer sequences.....	135
Table 12: PD3 Primer mix (10x) and LAMP buffer (10x).....	135
Table 13: PD LAMP reaction mix.....	136

Abbreviations

AP	Apple proliferation	PCR	Polymerase chain reaction
AS	Ammonium sulfate	PD	Pear decline
AY	Aster Yellows	PEG 8k	Polyethylene glycol 8k
BIP	Backward inner primer	pnp	Polynucleotide phosphorylase
bp	Base pairs	PPV	<i>Plum pox virus</i>
<i>Bst</i>	<i>Bacillus stearothermophilus</i>	RFLP	Restriction Fragment Length Polymorphism
B3	Backward outer primer	rpl22	Ribosomal protein 22
<i>Ca. P.</i>	<i>Candidatus</i> Phytoplasma	rpm	Rounds per minute
COX	Cytochrome oxidase	sec	Second
CRCA	Cascade rolling circle amplification	SWB	Spartium witches'-broom
Ct	Threshold cycle	<i>Taq</i>	<i>Thermus aquaticus</i>
DAPI	4'-6-diamidino-2-phenylindole	TBE	Tris-borate-EDTA
dNTP	Deoxyribonucleotide triphosphate	T _m	Melting temperature
ErioT	Eriochromeblack-T		
ESFY	European stone fruit yellows		
F3	Forward outer primer		
FIP	Forward inner primer		
HPLC	High pressure liquid chromatography		
HPSF	High Purity Salt Free		
HNB	Hydroxy naphthol blue		
IRPCM	International Research Programme on Comparative Mycoplasmaology		
kb	Kilo bases		
KCl	Potassium chloride		
LAMP	Loop-mediated isothermal amplification		
LB	Backward loop primer		
LF	Forward loop primer		
Mg	Magnesium		
MgCl ₂	Magnesium chloride		
min	Minute		
MO	Methyl orange		
NaOH	Sodium hydroxide		
NaPP	Sodium pyrophosphate		
NASBA	Nucleic acid sequence based amplification		
NSP	Napier stunt phytoplasma		
nt	Nucleotides		

1 Introduction

“... il faut convenir que parmi les Fruits à pevin la nature ne nous donne rien de si beau,
& de si noble à voir que cette Poire ...”

“... it must be confessed that among all those fruits nature does not show us anything
so beautiful nor so noble as this pear ...”

Jean-Baptiste de La Quintinie, 1626-1688.

Director of the royal fruit and vegetable gardens under Louis XIV.

Fruit trees are threatened by a range of infectious diseases and insect pests. Diseases caused by phytoplasma infections are of particular severity since until now, there are no resistant cultivars or rootstocks available. Disease management is therefore restricted to phytosanitary measures and vector control. Consequently, a frequent monitoring is indispensable, which requires suitable and sensitive phytoplasma detection procedures. In the following, the pear as the host for *Candidatus* *Phytoplasma pyri* is portrayed, the disease pear decline is described, the state of the art of phytoplasma detection is summarized and the basic principle of the DNA amplification method used in this study is explained.

1.1 The European pear (*Pyrus communis* Linn.): Relatives, history and economic importance

Pyrus communis, the European pear, is a relative of the apple (*Malus domestica*), both belonging to the family of *Rosaceae*. The number of species within the genus *Pyrus* strongly varies in literature because pears readily cross beyond species' borders, producing a great number of hybrids whose taxonomic classification is difficult (Volk et al., 2006; Wolko et al., 2010; Katayama et al., 2012; Silva et al., 2014). Bell et al. (1996) counted 22 primary *Pyrus* species, Rubstov (1944) numbered 35 pear species, Kutzelnigg and Silbereisen (1995) mentioned more than 70 species to be comprised in the genus *Pyrus*. Furthermore, several interspecific hybrids, of natural occurrence as well as artificial, are known (Bell et al., 1996). Intergeneric hybrids are reported with *Sorbus*, *Cydonia* (Hummer & Janick, 2009) and *Malus* (Fischer et al., 2014). Within this richness of species, forms and varieties, three species are of horticultural importance: *Pyrus communis* Linn., *Pyrus pyrifolia* (Burm. f.) Nakai (Syn. *P. serotina* Rehd.) and *Pyrus nivalis* Jacq. (Hedrick, 1921). *Pyrus pyrifolia*, a species native to Asia called Nashi, is dominating pear cultivation in China and Japan (Bell et al., 1996). The snow pear (*Pyrus nivalis*) is grown mainly in France for the production of perry (Hedrick, 1921). The most widespread pear under cultivation in Europe, America, Africa and Australia is *Pyrus communis* (Bell et al., 1996). Wild ancestors of the domesticated European pear are

presumably the European wild pear, *Pyrus pyraster* (L.) Burgsd., and the Caucasian pear, *Pyrus caucasica* Fed., as well as the snow pear, *Pyrus nivalis* Jacq. (Volk 2006; Yamamoto & Chevreau, 2009; Asanidze et al., 2011; Katayama et al., 2012). However, taxonomic classification of European wild pear and Caucasian pear varies in literature, with several authors considering them as separate species while others state one or both as subspecies of *Pyrus communis*. Dolatowski et al. (2004) reported that semi-wild pears in Poland could not be identified as *Pyrus pyraster* but as *Pyrus* x *amphigenea*, representing various stages of hybridization between *Pyrus pyraster* and *Pyrus communis*. The authors remarked that while *Pyrus pyraster* may have grown in Poland in the past, continuous hybridization with cultivated *Pyrus communis* led to genetic erosion in the taxon *Pyrus pyraster*, which may result in the complete extinction of this species. This demonstrates the difficulties of taxonomic classification within the genus *Pyrus*, which is in part due to natural hybridization and phenotypic plasticity, leading to blurred morphological traits.

The cultivation of *Pyrus communis* has a long tradition in Europe. Originally native to the Caucasus and Eastern Europe, the ancient Greek and Romans verifiably cultivated pears as early as 1000 BC (Volk et al., 2006; Silva et al., 2014). The first written record of cultivated pears in Europe can be found in the epic “The Odyssey”, where Homer named the pear as one of the “gifts of the gods” in the garden of Alcinous (Hedrick, 1921; Janick, 2000). Almost 600 years later Theophrastus, the “Father of Botany”, wrote that propagation of pears from seed resulted in the loss of variety characteristics, proving that different cultivars of the pear were already known at this time. Pliny the Elder described 41 pear varieties in his “Natural History” (77-79 AD; Hedrick, 1921). During the golden era of pomology from the 17th to 19th century in France and Belgium, a vast range of cultivars emerged from extensive breeding efforts. Hedrick (1921) estimated the number of varieties to be around 2,000 to 3,000 in the species *Pyrus communis*. In 2001, the number of *Pyrus communis* cultivars amounted to more than 5,000 (Monte-Corvo et al., 2001).

Nowadays, European pears are cultivated for commercial purposes in more than 50 countries of the temperate regions (Bell et al., 1996). China is the leading pear producing country with more than 18 million tons in 2014, followed by Argentina with 771,271 tons (Table 1). Worldwide pear production covers an area of more than 2.6 million ha (FAO, 2014). In the European Union, the pear production area was about 117,070 ha in 2015, with the top producers being Italy (30,860 ha) and Spain (22,880 ha), followed by Portugal (12,120 ha). Figure 1 shows the pear production in Europe by area (Eurostat, 2015).

Table 1: Pear production and harvested area of the top ten pear producing countries in the world in 2014 (FAO, 2014).

Country	Production (to)	Area harvested (ha)
China	18,098,949	1,118,862
Argentina	771,271	26,995
United States of America	754,415	19,951
Italy	701,558	32,690
Turkey	462,336	24,474
Spain	429,548	23,640
South Africa	404,260	12,024
Belgium	374,300	9,100
Netherlands	349,000	8,603
India	316,700	42,280

In Germany in 2016, the area planted with pear trees intended to produce for the market amounted to 1,925 ha, yielding 34,625 tons of fruit (Federal Statistical Office Germany, 2016). The most important cultivars grown in Germany are ‘Alexander Lucas’, ‘Conference’ and ‘Williams Christ’ (Federal Statistical Office Germany, 2012).

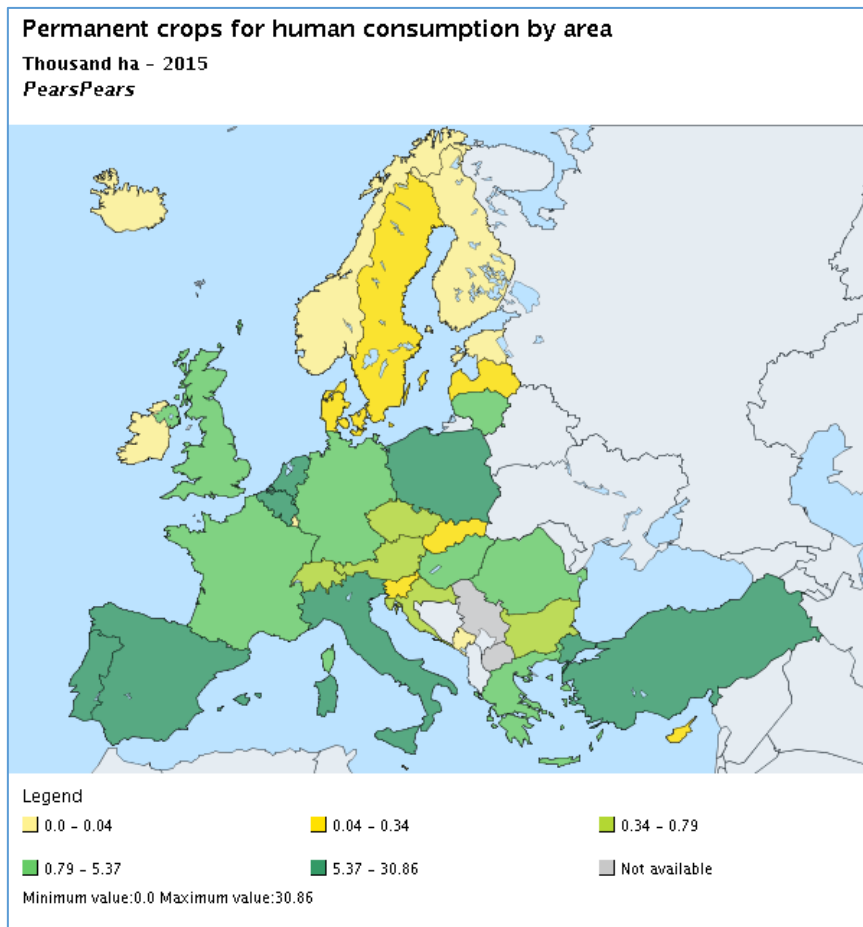


Figure 1: Pear production area in Europe (Eurostat, 2015).

Pears are usually cultivated as composite genetic systems, consisting of a rootstock and a scion, the latter of which is the fruiting pear variety. Rootstocks provide important traits as tolerance towards certain site characteristics, control of size and yield of the scion, precocity as well as, in some cases, resistance to pests or diseases (Maas, 2007; Mudge et al., 2009). European pear varieties are commonly grafted on rootstocks of the same species or on quince (*Cydonia oblonga*) (Webster, 1997). Occasionally, *Pyrus communis* interstocks are used to compensate for the weak frost hardiness of quince rootstocks, to overcome incompatibilities of certain rootstock/scion combinations or to further reduce tree size (Wertheim and Vercammen, 2000). While quince rootstocks show graft incompatibilities with many pear cultivars, they are reported to be less susceptible to the quarantine disease pear decline than *Pyrus communis* rootstocks (Wertheim, 2000; Maas, 2007). However, the contrary was reported by Quartieri et al. (2010), who observed susceptibility to pear decline, when pears were grafted on quince rootstocks, but not on *Pyrus communis* rootstocks.

1.2 Pear Decline – A quarantine disease

Pear decline (PD) is a severe disease affecting pears in Europe, Asia and America (Blomquist & Kirkpatrick, 2002) as well as Australia (Schneider and Gibb, 1997). Carraro et al. (2001) termed it “one of the most dangerous diseases of pear trees” (Carraro et al., 2001, p. 87). The causal agent *Candidatus Phytoplasma pyri* (*Ca. P. pyri*) is listed as a quarantine pest by EPPO (OEPP/EPPO, 2006). PD was first reported in North America, where the pear decline epiphytotic, starting in 1959 in California, affected more than a million pear trees (Schneider, 1970; Carraro et al., 2001; Seemüller & Schneider, 2004). The disease was probably introduced to the U.S. from Europe along with its insect vector (Seemüller & Schneider, 2004; Seemüller et al., 2011). In Italy, PD was known long before as Pear Moria (“moria del pero”), which killed more than 50,000 trees in an outbreak lasting from 1945 to 1947 (Giunchedi et al., 1982).

The causal agent of pear decline is a phytoplasma, which is transmitted by pear psylla. Phytoplasmas are cell wall-less bacteria belonging to the class of mollicutes. They inhabit the phloem of their host plants and cause diseases in approximately 1,000 plant species (Seemüller et al., 2002; Seemüller & Schneider, 2004). Before their discovery in 1967, numerous diseases known as yellows or witches’ broom diseases were attributed to viruses because the respective symptoms were similar to those of virus infections, the causal agents were not culturable in artificial media and were transmitted by insects (Doi, et al., 1967; Hogenhout et al., 2008). Doi et al. (1967) observed small particles in cells of diseased plants showing symptoms of a yellows-type disease, which morphologically resembled mycoplasmas and described them as mycoplasma-like organisms. Since then, numerous diseases of the yellows-type were associated with mycoplasma-like organisms, which later turned out to be phytoplasmas or spiroplasmas (Hogenhout et al., 2008). With the rise of molecular techniques such as polymerase chain reaction (PCR), cloning and sequencing of phytoplasmal DNA, the identity and taxonomic position of these organisms among the prokaryotes was finally elucidated

(Bertaccini & Duduk, 2009). Analysis of the 16S rRNA gene revealed a close relationship to culturable mollicutes rather than to other bacteria (Seemüller et al., 1998). Phytoplasmas form a monophyletic clade within the class of mollicutes. Their closest relatives are species of the genus *Acholeplasma* (Gundersen et al., 1994). Phytoplasmas most likely descended from walled, low G+C Gram-positive ancestors of the *Bacillus-Clostridium* group (Gundersen et al., 1994; Wei et al., 2007; Zhao et al., 2010).

Phytoplasmas belong to the smallest self-replicating organisms with genome sizes ranging from 680 to 1,600 kb (Christensen et al., 2005; Hogenhout et al., 2008; Bertaccini & Duduk, 2009). As a consequence, they lack several metabolic pathways, as for example the ATP synthase pathway (Oshima et al., 2004; Bai et al., 2006). Those metabolic compounds that they cannot produce themselves have to be obtained from the host plant or the insect vector. Phytoplasmas inhabit the sieve tubes of their host plants, which are, despite lacking a nucleus, living cells, but they can also be found occasionally in adjacent phloem parenchyma cells (Doi et al., 1967). This dependence on living cells, delivering essential metabolites to their inhabitants, makes it difficult to maintain these obligate biotrophic organisms in axenic culture. Until 2012, when Contaldo et al. reported the successful axenic culture of phytoplasmas on a patented culture medium, it was not possible to study these pathogens outside their plant hosts or insect vectors. In consequence, it was impossible to determine morphological characteristics of phytoplasmas in pure culture, which is an essential requirement for taxonomic classification of bacteria. In 2004, the IRPCM (International Research Programme on Comparative Mycoplasmaology) Phytoplasma/Spiroplasma Working Team - Phytoplasma taxonomy group decided to erect the provisional taxon '*Candidatus* Phytoplasma' and launched guidelines for the description of new *Candidatus* Phytoplasma species mainly based on the sequence of the 16S rRNA gene (IRPCM, 2004). Since this sequence is highly conserved, this classification system includes threshold values for maximum 16S rDNA sequence similarity of two different phytoplasma species. In detail, a phytoplasma strain is considered a discrete species, if it shares less than 97.5 % sequence similarity of the 16S rRNA gene with any other phytoplasma species previously described (IRPCM, 2004). A second classification system, which arranges phytoplasma strains into groups and subgroups, is commonly used in parallel. This system is based on Restriction Fragment Length Polymorphism (RFLP) profiles of the phytoplasma 16S rRNA gene sequence. Groups are designated by Roman numerals, subgroups carry an additional capital letter (Lee et al., 1993; Lee et al., 1998).

Until now, 33 16Sr groups and 42 *Candidatus* Phytoplasma species are described (Zhao et al., 2015; Zhao & Davis, 2016; Liu et al., 2017). The group 16SrX comprises phytoplasma species infecting temperate fruit trees: apple proliferation phytoplasma (AP, *Candidatus* Phytoplasma mali), pear decline phytoplasma (PD, *Ca. P. pyri*) and European stone fruit yellows phytoplasma (ESFY, *Ca. P. prunorum*). However, with 98.6 – 99.1% sequence similarity, the 16S rDNA sequences are highly conserved among members of this group (Seemüller and Schneider, 2004). While being very closely related, Seemüller and Schneider (2004) proved

these phytoplasmas to be in fact different species. The authors found significant differences in the sequences of the 16S-23S rDNA spacer region and non-ribosomal DNA. Furthermore, the 16SrX phytoplasmas clearly differed in serological comparisons and showed distinct insect vector and host plant specificities. Until now, the complete genomes of four phytoplasma strains have been sequenced, one of which is the apple proliferation phytoplasma, *Ca. P. mali* (Oshima et al., 2004; Bai et al., 2006; Kube et al., 2008; Tran-Nguyen et al., 2008). With a size of 602 kb, its chromosome is among the smallest of bacteria (Kube et al., 2008). In contrast to other phytoplasmas, which have circular chromosomes, *Ca. P. mali* as well as the other fruit tree phytoplasmas of the group 16SrX have a linear chromosome (Kube et al., 2008, 2012). While extrachromosomal elements (plasmids) were reported for several phytoplasma species (Kube et al., 2012), Kube et al. (2008) did not find extrachromosomal DNA in *Ca. P. mali*.

Phytoplasmas are unique bacteria, which live a transkingdom parasitic life (Bai et al., 2006). They reside endocellularly within their plant hosts and insect vectors, exhibiting obligate parasitism during their entire lifecycle without a free-living stage (Zhao et al., 2015). Insect vectors of phytoplasmas belong to phloem suckers of the order *Hemiptera*, mainly planthoppers (*Fulgoridae*) and leafhoppers (*Cicadellidae*) (Bertaccini & Duduk, 2009; Zhao et al., 2015). However, fruit tree phytoplasmas of the 16SrX group are vectored by Psyllids (*Psyllidae*) (Seemüller & Schneider, 2004). The pear decline phytoplasma is spread and transmitted by *Cacopsylla pyricola* and *C. pyri*, as well as by grafting infested propagation material on healthy hosts (OEPP/EPPO, 2006; Seemüller et al., 2011). *C. pyrisuga* also feeds on pears but it is unknown if this species is a vector of *Ca. P. pyri* (Seemüller et al., 2011). Insect vectors acquire the pathogen during feeding on diseased trees. Through the stylet, the phytoplasmas move into the gut and traverse the intestinal walls to invade the haemolymph. They colonize and multiply in the salivary glands, which can take a few days to several weeks to reach an infectious titer (Hogenhout et al., 2008). After this latent period, the pathogens are transmitted to new host plants (Bertaccini & Duduk, 2009). *C. pyri* as well as *C. pyricola* retain the pear decline phytoplasma over winter and were shown to successfully transmit the pathogen in spring (Carraro et al., 2001; Blomquist & Kirkpatrick, 2002). Both psyllids produce up to five generations per year (Seemüller et al., 2011). Phytoplasma infections usually do not negatively impact the insect vectors. In contrast, it was occasionally shown that the colonization with phytoplasmas had beneficial effects on the vectors as for example increased fecundity and elongated lifespan (Beanland et al., 2000; Christensen et al., 2005; Hogenhout et al., 2008). Control of pear decline is carried out by control of its psyllid vectors with an integrated pest management including insecticide spraying and release of predators or application of repellents (Solomon et al. 1989; Jarausch & Jarausch, 2010). Furthermore, phytosanitary measures as clearing of infested trees and use of certified, disease-free propagation material are recommended (OEPP/EPPO, 2006; Seemüller et al., 2011).

The pear decline phytoplasma can induce various symptoms in its host plants, as for example wilt, premature reddening and drop of leaves, stunting and reduced size of fruits (Seemüller et

al., 2011; Bertaccini et al., 2014) (Figure 2). Three courses of the disease are described: Quick decline, slow decline and foliar reddening with leaf curl, as a mild form of slow decline (Seemüller et al., 2011). Quick decline is characterized by sudden wilt, followed by the death of the tree within days or a few weeks. This course of disease is mainly observed, when oriental pear species (*Pyrus pyrifolia* or *P. ussuriensis*) are used as rootstocks for *P. communis* cultivars. Slow decline is expressed by a progressive weakening of pears on less susceptible *P. communis* rootstocks. Depending on the cultivar, symptoms may appear as reduced terminal growth, reduced fruit size, pale leaves or red-coloured leaves in fall instead of the normal yellow autumn colour.

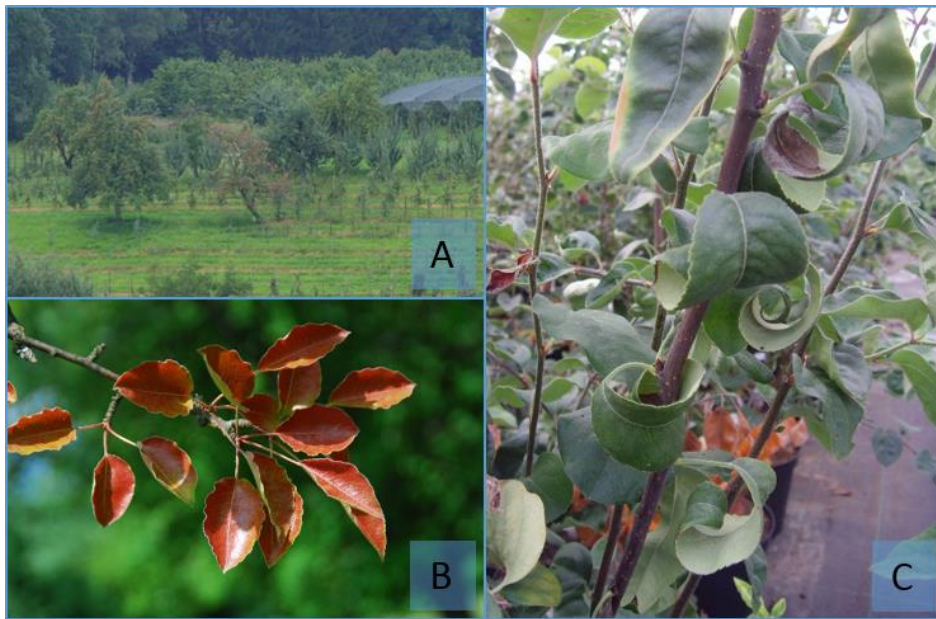


Figure 2: Pear decline symptoms. A: Diseased tree exhibiting red foliage in late summer. B: Red leaves of a diseased pear at the end of May. C: Leaf curling.

Trees exhibiting symptoms of slow decline can survive for years. Drought or other abiotic stress factors may cause a switch to quick decline, finally resulting in the dieback of the tree. The reddening syndrome occurs on more tolerant rootstocks of *P. communis*, *P. betulifoliae* or *P. calleryana* and is often associated with curling of leaves as well as earlier leaf fall. Fluctuating severity of symptoms and temporary symptom remission may be observed (Seemüller et al., 2011). This might in parts be due to the slow recolonization of aerial plant parts in spring from overwintering phytoplasma reservoirs in the roots. The climatic conditions in central Europe account for the functioning of phloem cells in the aerial parts of pear trees to be restricted to one vegetation period, which results in the elimination of the phytoplasmas from stems and branches during late autumn and winter, when the sieve tubes degenerate. In the roots, however, functional phloem cells are present throughout the year and pose a reservoir for overwintering phytoplasmas, which may recolonize the aerial plant parts in spring when new sieve tubes are formed (Seemüller et al., 2011). In contrast, Errea et al. (2002) and Garcia-Chapa et al. (2003) reported the detection of the PD phytoplasma in aerial parts of pear trees during winter in Spain,

indicating that in Mediterranean climates, a proportion of the phloem cells remains active and enables overwintering of phytoplasmas in aerial parts of the trees.

In general, symptom expression and disease development are dependent on the variety and rootstock/scion combination (Garcia-Chapa et al., 2003). However, symptoms of a pear decline infection are not specific and may also be caused by rootstock-scion incompatibility, root rot or abiotic damage, as for example drought or winter injuries (Seemüller et al., 2011). Consequently, a reliable diagnosis by visual inspection is difficult and confirmation of a suspected PD incidence by microscopy, transmission tests or molecular techniques is recommended (OEPP/EPPO, 2006; Seemüller et al., 2011).

1.3 Detection of *Candidatus Phytoplasma pyri*

Several methods for the detection of phytoplasmas have been used in phytoplasma research, such as electron microscopy, fluorescence microscopy of tissues stained with 4',6-diamidino-2-phenylindole (DAPI), indexing or serological procedures. However, routine phytoplasma diagnostics commonly employ PCR techniques for the detection of pathogen DNA in infected host tissues (Seemüller et al., 2011). Phytoplasma-specific universal PCR primers as well as group-specific primers are used with basic PCR, nested PCR and realtime PCR protocols. Primers used for routine phytoplasma detection commonly target the phytoplasmal 16S rRNA gene or the 16S-23S rRNA spacer region (Hodgetts & Dickinson, 2010). Many DNA extraction procedures include a phytoplasma enrichment step. However, the amount of phytoplasma DNA in relation to total DNA extracted from host tissues is reported to be below 1 % (Bertaccini & Duduk, 2009). Various primers, which are applicable for PD phytoplasma detection, are published in pertinent scientific literature of the 1990s (Lorenz et al., 1995 (U3/U5, universal phytoplasma primers, fO1/rO1, 16SrX group-specific primers), Deng & Hiruki, 1991 (P1, universal phytoplasma primer), Schneider et al., 1995 (P7, universal phytoplasma primer)). However, specific detection of *Ca. P. pyri* is difficult due to its close relationship with the other members of the 16SrX group, and cross reactivity of specific primers occurs with DNA of AP and ESFY phytoplasmas. The primer pair fPD/rPDS is reported to be able to discriminate the PD phytoplasma from the other members of the 16SrX group but it cannot detect all strains of *Ca. P. pyri* (Lorenz et al., 1995; Seemüller et al., 2011).

Since the detection of phytoplasmas is often compromised by low phytoplasma titers and heterogeneous distribution in the host, nested PCR is in many cases superior to conventional PCR because it overcomes the restrictions of optical detection of low product amounts via gel electrophoresis. Many protocols use a primer pair for universal phytoplasma detection in first round PCR and a group-specific primer pair for second round PCR (Galetto & Marzachi, 2010). Before the advent of realtime PCR and the availability of affordable realtime PCR cyclers, nested PCR was the most sensitive and therefore the most widespread method for the detection of phytoplasmas. However, conventional PCR as well as nested PCR are susceptible to false positive results due to carry-over contaminations because of the necessity to open reaction tubes

post amplification for the set-up of second round amplification in nested PCR as well as for the execution of gel electrophoresis. Realtime PCR, in addition to speed and sensitivity, offers the advantage of a closed system without the need of post-amplification analysis via gel electrophoresis (Bertaccini & Duduk, 2009). While this method is a lot more expensive than conventional PCR and nested PCR it provides some comfort for the experimenter since optical detection of the products is performed by the thermocycler itself. The application of probes labelled with fluorescent dyes not only makes the product detection inherent, but also enhances sensitivity as well as specificity of the assay since a third oligo nucleotide, apart from the two primers, needs to anneal to the template for generating a signal during amplification. The alternative to labelled probes are DNA intercalating dyes as for example the widely used fluorescent dye SybrGreen I. While product detection with DNA intercalating dyes is rather unspecific, generating a signal also in case of non-specific amplification, this drawback is compensated by performance of a melting curve analysis (Galetto & Marzachi, 2010). However, multiplexing is not possible when using DNA intercalating dyes. TaqMan probes not only enable the simultaneous detection of multiple phytoplasma strains but also the integration of an internal control on plant DNA as for example with primers and probe for the plant cytochrome oxidase gene (Hren et al., 2007) or the plantal 18S rRNA gene (Oberhänsli et al., 2011). The application of an internal control may be particularly useful, when samples derive from woody hosts, which may contain high amounts of PCR inhibitors, such as polyphenols or polysaccharides, in order to confirm that negative results are not due to PCR inhibition (Galetto & Marzachi, 2010). The application of PCR-based detection procedures for phytoplasmas is, however, limited to well-equipped laboratories. In consequence, pear growers and breeders have to send their samples to research institutes for analysis, which provide detection services for plant pathogens. Besides expenditure of time and cost for sample shipping and analysis, DNA extraction may become a bottleneck especially in large-scale screenings since it is recommended to take more than one sample per tree due to the uneven distribution of phytoplasmas in their hosts.

1.4 Loop-mediated isothermal amplification

Since 1983, when Kary Mullis invented the polymerase chain reaction (Mullis, 1990), research on genes and genetics, as well as development of new technologies to study nucleic acids of all types have evolved into an own great world in science, still rapidly expanding, yielding new insights every day, thereby boosting our knowledge on the fundamental code of life. To date, PCR-based technologies are predominating the research landscape, fueling an industry, which provides highly sophisticated and correspondingly expensive equipment. Despite the multitude of discoveries, which have been made possible by the PCR technology, the dependence on a well-equipped laboratory imposes strong limitations on its applicability especially in resource-poor settings. This drawback has pushed efforts to technically simplify the process of DNA amplification as well as the detection of amplification products. Primarily, the temperature-dependent cycling is a key feature developers needed to overcome. Since the early nineties,

various approaches for the isothermal amplification of DNA have been developed, as for example NASBA (nucleic acid sequence-based amplification, Compton, 1991), SDA (strand displacement amplification, Walker et al., 1992), RCA (rolling circle amplification, Fire and Xu, 1995), LAMP (loop-mediated isothermal amplification, Notomi et al., 2000) and HDA (helicase-dependent amplification, Vincent et al., 2004). One of the most promising and currently most widely used isothermal DNA amplification techniques is LAMP, for which the Japanese company Eiken Chemical Co. Ltd. holds a patent. The initial steps of a LAMP reaction are shown in figure 3. LAMP amplifies a target sequence of 130 - 300 nucleotides at a constant temperature of 60 – 65 °C, yielding products of various lengths. A set of four specially designed primers in combination with a DNA polymerase displaying strand-displacement activity but lacking exonuclease activity allows for a temperature-independent autocycling during the DNA amplification process (Notomi et al., 2000).

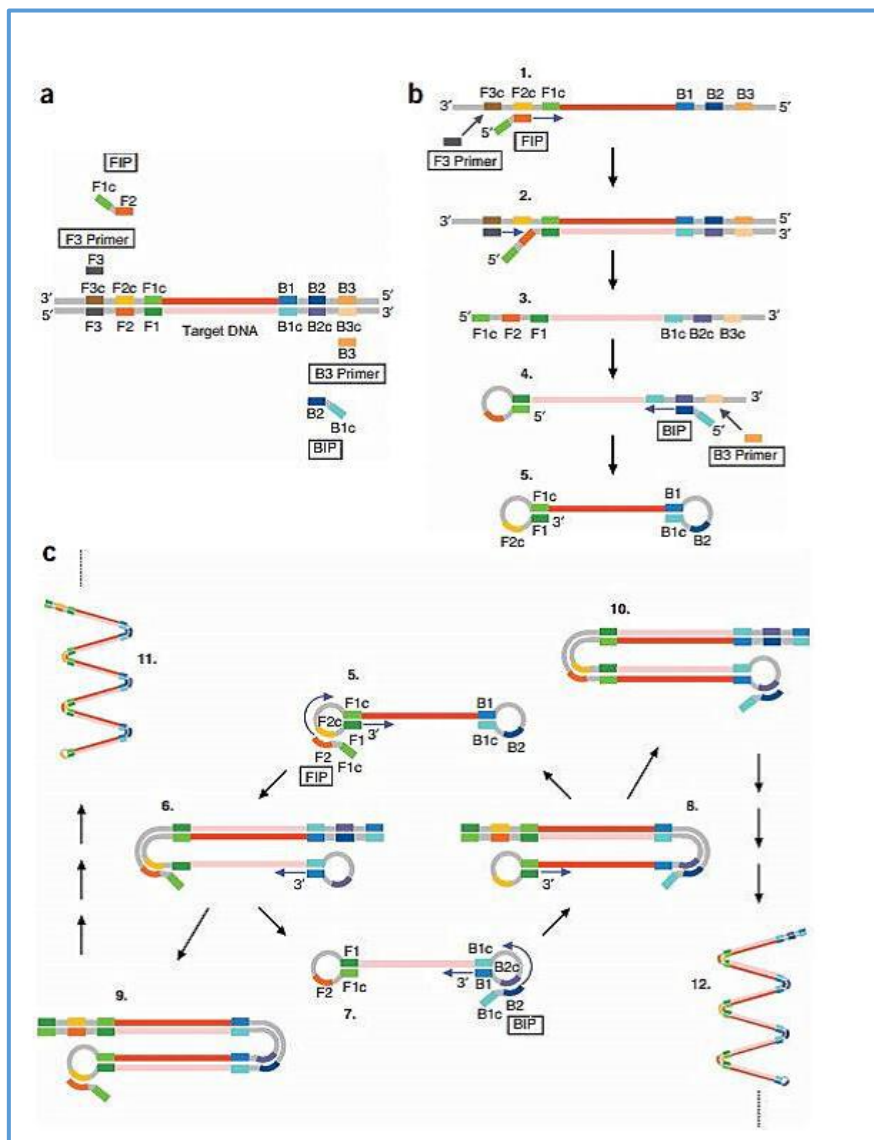


Figure 3: Schematic illustration of the LAMP reaction (Tomita et al, 2008).

The forward and backward inner primers (FIP and BIP, respectively) are composed of a sense (F2 and B2, respectively) and a downstream antisense sequence (F1c and B1c, respectively) of the target DNA (Figure 3a). The outer primers (F3 and B3) hybridize beyond the outer margins of the target sequence, which is framed by F2 and B2. In the initial phase of LAMP, all four primers are used. The F2 sequence of the FIP primer hybridizes to its complementary sequence on the target DNA and initiates amplification of the complementary strand (Figure 3b, step 1). Outer primer F3 hybridizes to F3c on the target DNA and primes strand displacement DNA synthesis, which results in the displacement of the aforementioned amplicon (Figure 3b, step 2). This amplicon now possesses the F1c sequence of the FIP primer and the complementary F1 sequence generated from the target DNA in the same strand (Figure 3, step 3), which leads to the formation of the first loop by hybridization of F1 to F1c at the 5' end of the structure (Figure 3b, step 4). Subsequent amplification and strand displacement DNA synthesis primed by BIP and B3, respectively (Figure 3b, step 4), yield a single stranded DNA containing the sequences B1c, B2 and B1 at the 5' end and F1, F2c and F1c at the 3' end, which results in the formation of loops at both ends ("dumbbell form DNA"; Figure 3b, step 5). Self-primed DNA synthesis by the F1 sequence at the 3' end produces a stem-loop DNA (Figure 3c, steps 5 and 6), which is the starting structure of LAMP autocycling. Subsequent amplification cycles involve hybridization of FIP and BIP to the loops of stem-loop DNAs and intermediates containing several loops and inverted repeats of the target DNA sequence as well as self-priming events of released single stranded DNAs during strand displacement DNA synthesis (Figure 3c, step 7 ff.). LAMP products are stem-loop DNAs and cauliflower-like structures containing several loops and inverted repeats of the target DNA (Notomi et al., 2000). The design of two further primers called loop primers, a forward loop primer (LF) and backward loop primer (LB), is possible to accelerate the reaction (Nagamine et al., 2002). These primers hybridize to the loops of LAMP amplicons not targeted by FIP and BIP, and prime further DNA synthesis. The detection of RNA targets is possible and requires the incorporation of a reverse transcriptase into the LAMP reaction (Reverse transcription (RT) LAMP) (Hadersdorfer, 2013).

For the visualization of LAMP results, several methods have been proposed. Agarose gel electrophoresis of ethidium bromide-stained LAMP products yields characteristic ladder-like banding patterns representing products of a range of different sizes (Notomi et al., 2000, Tomlinson, 2013). Due to the high amplification rate of LAMP reactions, high amounts of the by-product magnesium pyrophosphate are generated, which can be observed by the naked eye as a white precipitate (Mori et al., 2001). Magnesium ions form insoluble complexes with pyrophosphate during the proceeding amplification reaction. Centrifugation of the reaction tubes leads to an accumulation of the precipitate at the bottom of the tubes, forming a white pellet (Mori et al., 2001, Hadersdorfer et al., 2011). The time to reach a distinct level of turbidity was found to correlate linearly with the log of the initial amount of template DNA, and a real-time turbidimeter was introduced for quantitative DNA detection in LAMP (Mori et al., 2004). The first colorimetric detection method for LAMP assays based on pyrophosphate

generation was proposed by Tomita et al. (2008). In this approach, the metal indicator calcein and manganese are added to LAMP reaction solutions. Manganese displaces magnesium in the pyrophosphate complex and the decreasing manganese concentration in the reaction solution is indicated by calcein through a colour change from yellow to green under ambient light. Additionally, free calcein shows green fluorescence when exposed to UV light. However, partial as well as complete inhibition of LAMP assays using calcein and manganese ions has been reported (Goto et al., 2009; Wastling et al., 2010). Goto et al. (2009) introduced the metal indicator hydroxy naphthol blue (HNB) for the indirect detection of DNA amplification in LAMP. This dye indicates decreasing amounts of free magnesium ions in the solution by changing its colour from purple to blue.

HNB is currently widely used for colorimetric detection in LAMP assays (Tomlinson et al., 2010b; Gosch et al., 2012; Ahmadi et al., 2013; Hadersdorfer et al., 2013; Moradi et al., 2014; Vu et al., 2016). Zhang et al. (2014) used ammonium molybdate together with antimonyl potassium tartrate, sulfuric acid and ascorbic acid for the colorimetric detection of phosphate ions derived from pyrophosphatase-catalyzed hydrolysis of pyrophosphate generated in LAMP, as well as in cross-priming isothermal amplification (CPA). However, these reagents have to be added after the amplification reaction, which requires opening the reaction tubes after amplification or a special device that allows merging the reagents without opening the tubes. The necessity to open the reaction tubes post amplification considerably raises the risk of carry-over contaminations, particularly for the highly efficient LAMP reactions. Tanner et al. (2015) demonstrated the applicability of pH indicator dyes for result visualization in weakly buffered LAMP reactions. This method is based on proton release during polymerase-catalyzed DNA amplification, which causes a drop of pH if the solution is not or only weakly buffered. The use of SybrGreen I for LAMP product detection is also reported. However, its addition to LAMP reaction solutions is only possible after incubation because this DNA intercalating dye considerably impairs the LAMP reaction (Goto et al., 2009, Tao et al., 2011; Denschlag et al., 2013, Karthik et al., 2014, Abbasi et al., 2016; Oscorbin et al., 2016).

The potential of LAMP is high especially for medical applications in developing countries. In contrast to other isothermal methods, LAMP does not require other enzymes beyond the polymerase or dye-labelled probes and is therefore comparatively cheap. Additionally, *Bst* DNA Polymerase (large fragment, portion of the *Bacillus stearothermophilus* DNA Polymerase protein that contains the 5' → 3' polymerase activity, but lacks 5' → 3' exonuclease activity) is highly tolerant towards common inhibitors, which allows for the use of “quick-and-dirty”-methods for sample preparation (Kaneko et al., 2007). By now, several diagnostic kits are already commercially available, as for example the Loopamp MTBC detection kit for the detection of *Mycobacterium tuberculosis* or the malaria LAMP kit (Loopamp MALARIA Pan/Pf detection kit; both kits developed by Eiken Chemical Co. Ltd., Tokyo, Japan) (Mori et al., 2013). But also in phytopathology, research and development on LAMP assays is advancing and has already yielded detection protocols for a broad range of pathogens, e.g. for

Phytophthora ramorum and *P. kernoviae* (Tomlinson et al., 2010), *Potato virus Y* (Almasi & Dehabadi, 2013), *Fusarium oxysporum* (Almasi et al., 2013b), *Erwinia amylovora* (Gosch et al., 2012), *Verticillium dahliae* (Moradi et al., 2013) and *Xanthomonas fragariae* (Gétaz et al., 2017), since time expenditure and costs of PCR tests in specialized laboratories are still limiting systematic screenings of cultivated and natural plant populations, for example in case of quarantine diseases. The opportunity to perform high-throughput DNA tests directly in the field is a huge step forward in the challenge of plant health threatened by climate change and globalization of diseases.

Although the LAMP method has been developed 18 years ago, only a limited number of LAMP protocols for the detection of phytoplasmas have been published so far (Table 2).

Table 2: Published LAMP assays for the detection of phytoplasmas

16Sr group	Disease	Target gene	Reference
I	Aster Yellows	16S-23S IGS	Tomlinson et al. (2010b)
	Aster Yellows	16S	Sugawara et al. (2012)
	Aster Yellows	<i>groEL</i>	Sugawara et al. (2012)
II	Witches'-broom disease of lime	IGS/23S	Bekele et al. (2011)
III	X-Disease	16S-23S IGS	Hodgetts et al. (2011)
V	Flavescence dorée	16S	Kogovsek et al. (2015)
X	AP, ESFY, PD	16S	De Jonghe et al. (2017)
XI	Napier stunt disease	16S	Obura et al. (2011)
	Waligama Coconut leaf wilt disease	16S	Siriwardhana et al. (2016)
	Root wilt disease of coconut Arecanut yellow leaf disease	16S	Nair et al. (2016)
XII	Stolbur	IGS/23S	Bekele et al. (2011)
	Bois noir	16S	Gentili et al. (2016)
XIII	Strawberry green petal Mexican periwinkle virescence	<i>groEL</i>	Pérez-López et al. (2017)
XXII	Cape St. Paul wilt	16S-23S IGS	Tomlinson et al. (2010b)
Unspecified (I or II)	Cassava witches'-broom	16S	Vu et al. (2016)

Except Sugawara et al. (2012) and Pérez-López et al. (2017), who designed primers on the *groEL* gene (cpn60), the 16S and 23S ribosomal RNA genes as well as the intergenic spacer region (IGS) are the targets of choice for LAMP assays detecting phytoplasmas. This may be due to the broad availability of ribosomal DNA sequences for all phytoplasma species described since taxonomic classification of an unknown isolate requires sequencing of the 16S rRNA gene (IRPCM 2004).

1.5 Objective of this study

The objective of this work was the development of a nucleic acid based procedure for the detection of *Candidatus* Phytoplasma pyri, the causal agent of pear decline, with the following specified requirements:

1. The detection method should be suitable for on-site application.
2. The entire detection procedure should be laboratory-independent.
3. The detection procedure should be easy to perform, also by unexperienced users.

Loop-mediated isothermal amplification (LAMP) was chosen for reliable detection of the pear decline phytoplasma since it offers a wealth of possibilities for simplifying detection procedures, including sample processing and result visualization. The development of the PD LAMP assay required the following steps:

1. Selection of a suitable LAMP primer set
2. Optimization of LAMP reaction conditions
3. Development of a simplified sample preparation technique
4. Implementation of a suitable LAMP result visualization technique

2 Materials and Methods

2.1 Workflow of the PD LAMP development process

The development process of the PD LAMP assay included the design of suitable LAMP primers, the optimization of reaction conditions as well as the evaluation of assay performance. Readjustments were necessary, whenever a new element was incorporated into the procedure. Figure 4 shows an idealized workflow scheme for the development process of the PD LAMP assay.

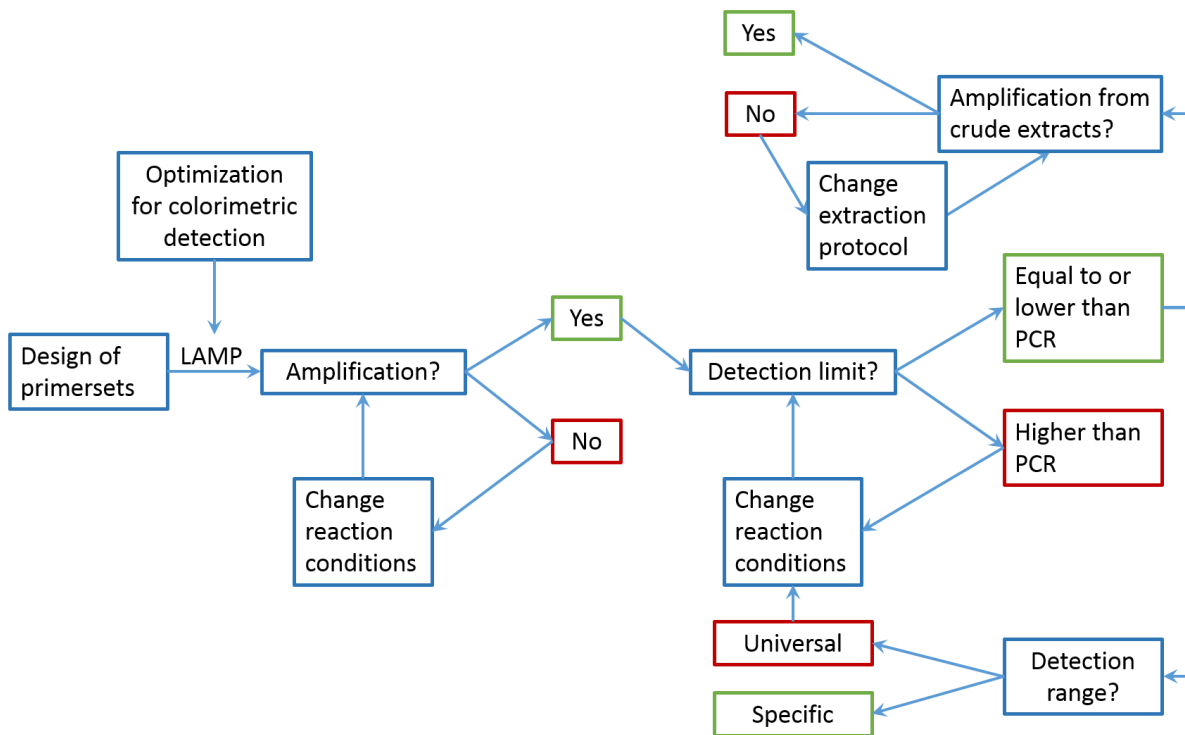


Figure 4: Workflow of the development process of the PD LAMP assay. Green frames = Successful test, continue with next step. Red frames = Unsuccessful test, change a parameter and try again.

2.2 Sources of phytoplasmas and DNA samples

DNA of phytoplasmas belonging to the apple proliferation group was extracted from phytoplasma-infected plants. DNA of all other phytoplasmas was kindly provided by Prof. Assunta Bertaccini (University of Bologna, Italy). A summary of the phytoplasma strains used in this study is given in table 3. The pGemT plasmid containing the P1/P7 fragment of the 16S rDNA sequence of the pear decline phytoplasma was kindly provided by Dr. Bernd Schneider (Julius Kühn-Institut (JKI), Dossenheim, Germany). The P1/P7 insert originated from a PCR with the phytoplasma-specific primer pair P1/P7, which amplifies a fragment of the 16S rRNA gene, the 16S/23S spacer region, tRNA-Ile and a part of the 23S rRNA gene.

PD positive controls in LAMP and PCR reactions derived from pear plants of an *in vitro* culture used to maintain the pear decline phytoplasma. These phytoplasma-infected pears were kindly provided by Dr. Bernd Schneider (JKI, Dossenheim, Germany). PD negative controls derived from healthy Williams pears of an *in vitro* culture. AP positive and negative controls were kindly provided by Dietlinde Rissler (Landwirtschaftliches Technologiezentrum (LTZ) Augustenberg, Baden-Württemberg, Germany). Field samples investigated for the presence of PD, AP and ESFY, respectively, were obtained from orchards located in Baden-Württemberg, Germany, as well as Tyrol, Austria. Samples from pear plants belonging to a PD inoculation trial were obtained from the Bavarian Centre of Pomology and Fruit Breeding, Hallbergmoos, Germany. In this trial, pear cultivars and breeding clones were artificially inoculated with the PD phytoplasma by chip budding. Samples tested with LAMP in this study were collected from shoots of test cultivars as well as sprouted inoculation scions. No template controls of LAMP and PCR reactions contained an equivalent volume of ultrapure water instead of template DNA.

Table 3: Phytoplasma strains used in this study.

Phytoplasma	Disease	Classification	16Sr group ^a
AP	Apple proliferation	<i>Ca. P. mali</i>	X-A
ASHY	Ash Yellows	<i>Ca. P. fraxini</i>	VII-A
AY	Aster Yellows	<i>Ca. P. asteris</i>	I-A
AY-A	Apricot Chlorotic Leafroll	<i>Ca. P. asteris</i>	I-F
BVK	Flower Stunting	<i>Ca. P. oryzae</i>	XI-C
CH-1	Grapevine Yellows	<i>Ca. P. solani</i>	XII-A
CX	Peach X disease	<i>Ca. P. pruni</i>	III-A
ELM WB	Elm Witches`broom	<i>Ca. P. ulmi</i>	V-A
ESFY	European Stone Fruit Yellows	<i>Ca. P. prunorum</i>	X-B
PD	Pear decline	<i>Ca. P. pyri</i>	X-C
PWB	Potato Witches`broom	<i>Ca. P. trifolii</i>	VI-A
TBB	Tomato Big Bud	<i>Ca. P. aurantifolia</i>	II-A

^a based on Lee et al. (1998)

2.3 DNA extraction

Field samples from pear trees were kept in plastic bags in a cooling chamber at +4 °C until DNA extraction. For conventional DNA extraction, shoots and roots were decorticated with a scalpel to obtain bark and phloem tissue. From leaves, midribs were cut out and processed together with the petioles. Fine roots were used directly for DNA extraction. From *in vitro* plants, the callus was removed and DNA was extracted from the whole plants. Sample material was put into falcon tubes, frozen in liquid nitrogen and processed immediately or stored at -80 °C if immediate extraction was not possible. The frozen samples were ground by hand in their falcon tubes with screwdrivers precooled in liquid nitrogen. An amount of 100 mg of each sample was weighed in an analytical balance into 2 ml reaction tubes, which were precooled in liquid nitrogen in order to prevent thawing of the samples before DNA extraction. The weighed

samples in their reaction tubes were cooled again with liquid nitrogen until further processing. Groups of 10 or 20 samples were extracted together. DNA extraction was conducted with the DNeasy Plant Mini kit (Qiagen, Hilden, Germany) following the manufacturer's instructions. DNA extracts were stored at -20 °C until use.

2.4 Simplified sample preparation

2.4.1 NaOH-based sample preparation

Samples intended for NaOH extraction were stored in a fridge or cooling chamber at +4 °C until further processing. From leaves, midveins and petioles were cut out with a sterilized razor blade and used for NaOH extraction. Shoots and roots were decorticated and the bark was used for extraction. Fine roots were used as they were. Samples from different plant organs were treated separately. *In vitro* plants were used on the whole, without the callus. A maximum of 1 g of fresh plant material was weighed into a filter extraction bag (Bioreba, Reinach, Switzerland). Into each filter extraction bag, 1 ml of NaOH solution was added to each 100 mg of plant tissue (FW), up to a maximum of 10 ml of NaOH solution. Leaves were treated with 0.1 M NaOH solution, bark of shoots and roots with 0.5 M NaOH solution. NaOH stock solutions were prepared from NaOH pellets (Merck, Darmstadt, Germany) and kept in 400 ml glass bottles at room temperature. The filled extraction bags were placed into a Homex-6 machine (Bioreba, Reinach, Switzerland) and samples were homogenized. The resulting homogenate was pressed through the filter layer inside the extraction bag and filled into a 2 ml reaction tube. After centrifugation at 13,000 rpm for 5 min, 10 µl of the supernatant was pipetted into a 1.5 ml reaction tube containing 990 µl distilled water to obtain a dilution of 1:100. Two µl of these dilutions were subjected immediately to LAMP or Direct PCR. Storage of the dilutions was at -20 °C for a maximum of one week in case that further tests were required. Older dilutions were discarded.

Unless otherwise stated, NaOH extracts were prepared according to the developed standard protocol described above. Modifications of this protocol were evaluated during the development process of the NaOH sample preparation procedure, as dilution of the homogenates without prior centrifugation, dilution with Tris-HCl (pH 8.8) instead of water and 1:10 or 1:50 dilutions of the homogenates. Applied modifications are given in the results section in the description of the respective experiments.

2.4.2 Water-based sample preparation

The fast plant extraction procedure according to Hadersdorfer et al. (2011) was evaluated for its suitability as simplified sample preparation method for the detection of the pear decline phytoplasma with the PD LAMP. Up to 1 g of fresh plant tissue, which was prepared as described above, was placed into a filter extraction bag (Bioreba, Reinach, Switzerland). Nine ml distilled water or less, respective the amount of tissue, were added and the sample was homogenized with a Homex-6 machine (Bioreba, Reinach, Switzerland). About 1.5 ml of the

homogenate was transferred to a 2 ml reaction tube and centrifuged for 2 min at 13,000 rpm. An aliquot of 100 µl of the supernatant was transferred to a new reaction tube and diluted with 900 µl of distilled water to obtain a dilution of 1:10. Two µl of this dilution were subjected to LAMP.

2.5 Conventional nucleic acid based detection methods

2.5.1 Nested PCR

In the initial experiments of this research project, a nested PCR was used to verify the presence or absence of phytoplasmas in controls and samples before subjecting them to the not yet established PD LAMP. Universal phytoplasma primers P1 (Deng & Hiruki, 1991) and P7 (Schneider et al., 1995) were used to amplify the entire 16S rRNA gene and the 16S/23S spacer region of the phytoplasmal genome, yielding a product of approximately 1800 bp in length (Table 4). According to Green et al. (1999), with minor modifications, the PCR reaction mix contained 1x *Taq* buffer (10 mM Tris-HCl, pH 8.8, 50 mM KCl, 0.08 % (v/v) Nonidet P40), 2 mM magnesium chloride (Fermentas, St. Leon-Rot, Germany), 0.2 mM dNTPs (New England Biolabs, Frankfurt, Germany), 0.5 µM primer P1, 0.5 µM primer P7, 0.05 U/µl *Taq* DNA polymerase (Fermentas, St. Leon-Rot, Germany) and 2.5 µl DNA extract in a total volume of 25 µl. Cycling conditions were as follows: After an initial denaturation step of 3 min at 94 °C, thermal cycling started with denaturation for 45 sec at 94 °C, followed by annealing for 1 min at 55 °C and extension for 2 min at 72 °C. This schedule was repeated 34 times. A final extension step of 5 min at 72 °C completed the amplification reaction.

In the subsequent nested PCR reaction, universal primers fU5 and rU3 (Lorenz et al., 1995) amplified a fragment of the phytoplasmal 16S rRNA gene of about 900 bp in length (Table 4). The PCR reaction mix was prepared according to Lorenz et al. (1995), with minor modifications. In a total volume of 40 µl, the reaction mix contained 1x *Taq* buffer (10 mM Tris-HCl, pH 8.8, 50 mM KCl, 0.08 % (v/v) Nonidet P40), 2 mM magnesium chloride (Fermentas, St. Leon-Rot, Germany), 0.1 mM dNTPs (New England Biolabs, Frankfurt, Germany), 0.5 µM primer fU5, 0.5 µM primer rU3, 0.2 U *Taq* DNA polymerase (Fermentas, St. Leon-Rot, Germany) and 5 µl of the 1:10 diluted product of the preceding PCR with the primer pair P1/P7. Thermal cycling was conducted according to Lorenz et al. (1995), with denaturation for 30 sec at 95 °C, annealing for 75 sec at 55 °C and extension for 90 sec at 72 °C, repeated 34 times.

Desalted PCR primers were purchased from Eurofins MWG Operon (Ebersberg, Germany). PCR was carried out in a C1000 Thermal Cycler (Bio-Rad, Munich, Germany).

2.5.2 Conventional PCR

Since the nested PCR procedure was laborious and time-consuming, it was replaced by a conventional PCR with sufficient sensitivity. The primer pair fO1/rO1 (Lorenz et al. (1995) is specific for fruit tree phytoplasmas of the 16SrX group, yielding a fragment of the 16S rRNA

gene of approximately 1,000 bp in length (Table 4). The PCR reaction mixture was composed of 1x *Taq* buffer (10 mM Tris-HCl, pH 8.8, 50 mM KCl, 0.08 % (v/v) Nonidet P40), 1.5 mM magnesium chloride (Fermentas, St. Leon-Rot, Germany), 0.1 mM dNTPs (New England Biolabs, Frankfurt, Germany), 0.5 μ M primer fO1, 0.5 μ M primer rO1, 1 U *Taq* DNA polymerase (Fermentas, St. Leon-Rot, Germany) and 2 μ l DNA extract in a total volume of 25 μ l. PCR reactions were incubated for 5 min at 95 °C prior to 35 cycles consisting of denaturation for 1 min at 95 °C, annealing for 1 min at 52 °C and extension for 1 min at 70 °C. Complete amplification of the product was assured by a final incubation at 70 °C for 5 min. Conventional PCR with the primer pair fO1/rO1 was used as reference method during the development of the PD LAMP assay, as well as in the final evaluation of the PD LAMP detection limit.

A PCR with the outer primers F3 and B3 of the LAMP primer set PD4 (Table 5) was performed with reaction conditions equal to the PCR with the primer pair fO1/rO1. The size of the amplification product was expected to be 197 bp based on the PD 16S rDNA reference sequence (GenBank accession no. AJ542543.1).

PCR primers were ordered desalted from Eurofins MWG Operon (Ebersberg, Germany). PCR reactions were carried out in a C1000 Thermal Cycler (Bio-Rad, Munich, Germany).

2.5.3 Direct PCR

Due to inconsistent results of DNA extracts and NaOH-based homogenates derived from the same sample, a PCR-based test procedure was established to verify LAMP results for NaOH-treated sample preparations. Two commercially available kits suitable for direct PCR from untreated plant tissues and crude sample preparations were evaluated for their performance with NaOH-based homogenates. Direct PCR from samples prepared with the simplified plant tissue preparation procedure was performed using the primer pair fO1/rO1 (Lorenz et al., 1995) (Table 4) with either the Kapa3G Plant PCR Kit (Peqlab Biotechnologie GmbH, Erlangen, Germany) or the Phire Plant Direct PCR Kit (Thermo Scientific, Dreieich, Germany) according to the manufacturer's instructions. PCR reactions with the Kapa3G Plant PCR Kit comprised 1x Plant PCR buffer, 0.3 μ M primer fO1, 0.3 μ M primer rO1, 0.5 U Kapa3G Plant DNA Polymerase and 2 μ l sample in a total volume of 25 μ l. Recommended cycling conditions were as follows: Initial denaturation for 3 min at 95 °C, 40 cycles with 20 sec at 95 °C, 15 sec at 52 °C and 30 sec at 72 °C, followed by a final extension step for 30 sec at 72 °C. Using the Phire Plant Direct PCR Kit, the reaction mix contained the primers fO1 and rO1 at 0.5 μ M each, 10 μ l 2x Phire Plant PCR buffer, 0.4 μ l Phire Hot Start II DNA polymerase and 1 μ l sample in a total volume of 20 μ l per reaction. Thermal cycling conditions were 5 sec at 98 °C, 5 sec at 52 °C and 20 sec at 72 °C, repeated 39 times, with an initial denaturation step of 5 min at 98 °C and a final elongation step of 1 min at 72 °C.

PCR primers were ordered desalted from Eurofins MWG Operon (Ebersberg, Germany). PCR reactions were carried out in a C1000 Thermal Cycler (Bio-Rad, Munich, Germany).

2.5.4 Realtime PCR

Realtime PCR with the DNA intercalating fluorescence dye SYBR Green I was performed according to Torres et al. (2005). The applied primer pair P1 (Deng & Hiruki, 1991)/R16(x)F1r (Torres et al., 2005) (Table 4) specifically detects phytoplasmas belonging to the taxonomic group 16SrX. Twenty-five μ l of realtime PCR reaction mix contained 1x iQ SYBR Green supermix (Bio-Rad, Munich, Germany), 0.2 μ M primer P1, 0.2 μ M primer R16(x)F1r and 3 μ l sample. Controls and samples were run in triplicates. Reactions were incubated for 10 min at 95 °C and then subjected to 40 cycles composed of denaturation at 95 °C for 15 sec, annealing at 60 °C for 30 sec and extension at 72 °C for 30 sec. Finally, the PCR reactions were heated from 60 to 95 °C in 0.5 °C steps to perform a melting curve analysis.

The detection limit of the realtime PCR assay according to Torres et al. (2005) in comparison to the detection limit of the PD LAMP assay as well as conventional PCR with the primer pair fO1/rO1 was estimated with a 10-fold dilution series of a pGemT plasmid with P1/P7 insert, which was kindly provided by Dr. Bernd Schneider (JKI, Dossenheim, Germany). The tested copy numbers ranged from 10^0 to 10^8 copies per reaction. Each run included no template controls (NTC), which contained ultrapure water instead of DNA, as well as negative controls containing DNA extracts from healthy pears of an *in vitro* culture. Realtime PCR reactions were performed with the MiniOpticon Real-Time PCR System (Bio-Rad, Munich, Germany). Analysis of realtime PCR experiments was carried out with the software CFX Manager 3.1 (Bio-Rad, Munich, Germany). Measurements with deviations of the Ct values of more than 0.3 cycles among the triplicates were excluded from analysis. Samples with Ct values above 32 were appraised as negative. Minimum requirements for standard curves were $R^2 > 0.98$, slope -3.3 to -3.0 and PCR efficiency 90 to 115%. Runs beyond these values were repeated.

Table 4: PCR primers used for the detection of fruit tree phytoplasmas.

Primer	Sequence (5'-3')	Target	Amplicon size	Reference
P1	AAGAGTTTGATCCTGGCTCAGGATT	16S rDNA	1784 bp	Deng & Hiruki (1991)
P7	CGTCCTTCATCGGCTCTT	23S rDNA		Schneider et al. (1995)
fU5	CGGCAATGGAGGAAACT	16S rDNA	876 bp	Lorenz et al. (1995)
rU3	TTCAGCTACTCTTTGTAACA	16S rDNA		Lorenz et al. (1995)
fO1	CGGAAACTTTTAGTTTCAGT	16S rDNA	1071 bp	Lorenz et al. (1995)
rO1	AAGTGCCCAACTAAATGAT	16S rDNA		Lorenz et al. (1995)
P1	AAGAGTTTGATCCTGGCTCAGGATT	16S rDNA	217 bp	Deng & Hiruki (1991)
R16(x)F1r	CATCTCTCAGCATACTTGCGGGTC	16S rDNA		Torres et al. (2005)

2.5.5 Agarose gel electrophoresis

Products of nested PCR and conventional PCR with the primer pair fO1/rO1 were visualized with Tris-borate-EDTA (TBE) gels containing 1 % agarose (Biozym Scientific, Hess. Oldendorf, Germany) and stained with ethidium bromide. Gels for the visualization of products derived from the PCR with the outer primers of LAMP primer set PD4 contained 2 % agarose. Gel electrophoresis was performed at 90 V for 45 min. For the estimation of PCR fragment sizes, the size markers Lambda DNA/Eco 471 (AvaII) Marker, 13 or GeneRuler 1kb plus DNA Ladder (Fermentas, St. Leon-Rot, Germany) were used. The size of the PD4 F3/B3 PCR products was estimated with the GeneRuler 50bp DNA Ladder (Fermentas, St. Leon-Rot, Germany).

2.6 Loop-mediated isothermal amplification (LAMP)

2.6.1 LAMP primers

The design of LAMP primers was conducted using either the LAMP primer design software PrimerExplorer V4 (Eiken Chemical Co., Ltd., Tokyo, Japan; <http://primer-explorer.jp/e/>) or the software LAMP Designer (Premier Biosoft International, Palo Alto, CA, USA). Primer sets PD2, PD3 and PD4 were designed based on the 16S rRNA gene sequence of *Candidatus Phytoplasma pyri* (Genbank Accession No. AJ542543.1). Primer sets pnp and rpl22 were designed from the *pnp* (FN598192.1) and *rpl22* (JQ900579.1) gene sequences of *Ca. P. pyri*, respectively. BLAST analysis (<http://blast.ncbi.nlm.nih.gov/Blast.cgi>) of the designed LAMP primers revealed partial homologies with a range of organisms. However, full homology of complete primer sets was confirmed only for the PD phytoplasma or, in case of primer sets targeting the 16S rRNA gene, for fruit tree phytoplasmas of the 16SrX group. The primer set PD1 was published by Obura et al. (2011), the primer set COX, which targets the plant cytochrome oxidase gene, was borrowed from Tomlinson et al. (2010a). It should be noted that the primer sequences given in the original publication of Obura et al. (2011) exhibited several errors and the PD1 primer sequences used in this study were obtained from the authors by personal communication. Table 5 shows the sequences of all LAMP primer sets used in this study.

Table 5: Loop-mediated isothermal amplification (LAMP) primer sets used in this study

Primer	Sequence (5'-3')	Source
PD1 F3	CGGAATTCCATGTGTAGCG	Obura et al. (2011)
PD1 B3	ACTTCAGTACCGAGTTTCC	
PD1 FIP	TCAGCGTCAGTAAAGACCCAGTAATTTTTATATGGAGGAACAC	
PD1 BIP	CGTGGGGAGCAAACAGGATTTTTAGTACTCATCGTTTACGGC	
PD2 F3	TTAGTGAGACTGCCAATGA	This study (designed with PrimerExplorer V4)
PD2 B3	AGCGATTCCGACTTCATG	
PD2 FIP	ATCACGTTTGTAGCCCAGGTAGGAAGGTGGGGATTACG	
PD2 BIP	ACAATGGCTGTTACAAAGAGTAGCGCAGACTTCAATCCGAACT	
PD2 LB	GAAGCGTGAGTTTTTAGCAAATCTC	
PD3 F3	GTCTTAACTGACGCTGAGG	This study (designed with LAMP Designer)
PD3 B3	CATGCACCACCTGTATCC	
PD3 FIP	ACGTACTACTCAGGCGGAGTACAACGATGAGTACTAAGTGTGG	
PD3 BIP	AATTGACGGGACTCCGCACTGTCAAGACCTGGTAAGGT	
PD3 LF	AATGCGTAACTTCAGCACTG	
PD3 LB	AAGCGGTGGATCATGTTGT	
PD4 F3	ATTCCATGTGTAGCGGTAA	This study (designed with PrimerExplorer V4)
PD4 B3	GCGTAACTTCAGCACTG	
PD4 FIP	GCGTCAGTTAAGACCCAGCAAATGCGTAAAGATATGGAGGAAC	
PD4 BIP	CGTGGGGAGCAAACAGGATTCAACACTTAGTACTCATCGTTA	
PD4 LF	CCGCCTTCGCTACTGGT	
PD4 LB	TACCCTGGTAGTCCACGCC	
COX F3	TATGGGAGCCGTTTTTGC	Tomlinson et al. (2010a)
COX B3	AACTGCTAAGRGCATTCC	
COX FIP	ATGGATTTGRCCTAAAGTTTCAGGGCAGGATTTCACTATTGGGT	
COX BIP	TGCATTTCTTAGGGCTTTCGGATCCRGCGTAAGCATCTG	
COX LF	ATGTCCGACCAAAGATTTTACC	
COX LB	GTATGCCACGTCGCATTCC	
pnp F3	TGGTAGCGGCGGTAA	This study (designed with PrimerExplorer V4)
pnp B3	ACCTTCAACACCAGGAA	
pnp FIP	CAACAATTTCCATATTTTGATGCATATGTTAAAATTGATATTATGCAAGA	
pnp BIP	ACGTTTGTAGAGATAAAATGGATTCTGCTATTGCTCCAAAT	
rpl22 F3	TCTGAAGTTTATGTTAATGAAGGAT	This study (designed with PrimerExplorer V4)
rpl22 B3	CAAACCATTTAGAATCCCAACT	
rpl22 FIP	CCAGAACCTTTAGCTCTCGGTACGTTTAAAACGTTTATTTCCG	
rpl22 BIP	AAGGAGATCAATGTTTCATGGGAACCATTAGGATTAGATTTTTGTCC	

Multiple sequence alignments of LAMP primer sequences with target sequences were conducted with Clustal Omega (<https://www.ebi.ac.uk/Tools/msa/clustalo/>; Larkin et al., 2007). Further editing of the alignments was performed with the software Bioedit, version 7.2.5 (Hall, 1999). Primers F3, B3, LF and LB were ordered with High Purity Salt Free (HPSF) purification, primers FIP and BIP with HPLC purification.

2.6.2 Reaction conditions

Unless otherwise specified, LAMP reaction mixes with the metal indicator hydroxy naphthol blue (HNB) were prepared as follows: LAMP reactions with primer set PD1 (Obura et al., 2011) contained 0.2 μM of each outer primer, 1.6 μM of each inner primer, 120 μM HNB (Sigma-Aldrich, Munich, Germany), 1x ThermoPol buffer (20 mM Tris-HCl (pH 8.8), 10 mM $(\text{NH}_4)_2\text{SO}_4$, 10 mM KCl, 2 mM MgSO_4 , 0.1 % Triton X-100; New England Biolabs, Frankfurt, Germany), 1.6 mM MgSO_4 (New England Biolabs, Frankfurt, Germany), 1 M betaine (Sigma-Aldrich, Munich, Germany), 0.4 mM dNTPs (New England Biolabs, Frankfurt, Germany), 8 U *Bst* DNA Polymerase, large fragment (New England Biolabs, Frankfurt, Germany), and 2 μl sample in a total volume of 25 μl . The original reaction mix as published in Obura et al. (2011) was applied in the initial experiment with primer set PD1 and differed from the reaction mix composition described above in that it did not contain the dye HNB and additional magnesium sulfate. In this same experiment, a reaction mix composition optimized for colorimetric product detection with HNB was adopted from Hadersdorfer et al. (2011) with minor modifications. This reaction mix comprised 6 mM of additional magnesium sulfate and 1 mM dNTPs, with all other components equal to the reaction mix described above. LAMP reactions with primer set PD1 were heated at 95 °C for 5 min prior to incubation at 63 °C for 120 min in a heating block. *Bst* DNA polymerase was added to LAMP reactions after the denaturation step.

LAMP reactions with the primer sets PD2, PD3 and PD4 using HNB for colorimetric product detection were composed of 0.2 μM of each outer primer, 1.6 μM of each inner primer, 0.8 μM of each loop primer, 120 μM HNB (Sigma-Aldrich, Munich, Germany), 1x ThermoPol buffer (20 mM Tris-HCl (pH 8.8), 10 mM $(\text{NH}_4)_2\text{SO}_4$, 10 mM KCl, 2 mM MgSO_4 , 0.1 % Triton X-100; New England Biolabs, Frankfurt, Germany), 4 mM MgSO_4 (New England Biolabs, Frankfurt, Germany), 1 M betaine (Sigma-Aldrich, Munich, Germany), 0.8 mM dNTPs (New England Biolabs, Frankfurt, Germany), 8 U *Bst* DNA Polymerase, large fragment (New England Biolabs, Frankfurt, Germany), and 2 μl sample in a total volume of 25 μl . LAMP reactions with primer set PD2 were incubated at 63 °C for 60 min. Using the primer set PD3, LAMP was performed at 63 °C in initial experiments of the optimization phase. Later, the incubation temperature was raised to 65 °C in order to suppress the generation of false positives. LAMP reactions with primer set PD4 were incubated at 65 °C. Unless otherwise specified, LAMP reactions with the primer sets PD2, PD3 and PD4 were incubated for 60 min.

In experiments with magnesium sulfate concentration series, during the optimization process with the metal indicator dye HNB, specified values of magnesium sulfate concentrations refer to amounts added separately to the magnesium containing ThermoPol buffer.

The optimized reaction mix composition with HNB was also used in tests with the primer sets pnp and rpl22. The applied reaction temperatures are given in the description of the respective experiments in the chapter “Results”.

A LAMP assay targeting the plant cytochrome oxidase (COX) gene was adopted from Tomlinson et al. (2010a) and supplemented with the metal indicator dye HNB. Twenty-five μl of LAMP reaction mix contained 120 μM HNB (Sigma-Aldrich, Munich, Germany), 1x ThermoPol buffer (20 mM Tris-HCl (pH 8.8), 10 mM $(\text{NH}_4)_2\text{SO}_4$, 10 mM KCl, 2 mM MgSO_4 , 0.1 % Triton X-100; New England Biolabs, Frankfurt, Germany), 6 mM MgSO_4 (New England Biolabs, Frankfurt, Germany), 0.8 M betaine (Sigma-Aldrich, Munich, Germany), 1.4 mM dNTPs (New England Biolabs, Frankfurt, Germany), 0.4 μM of each outer primer, 4 μM of each inner primer, 2 μM of each loop primer, 16 U *Bst* DNA Polymerase, large fragment (New England Biolabs, Frankfurt, Germany), and 2 μl sample. LAMP reactions with COX primers were incubated at 65 °C for 60 min. Heat inactivation of the *Bst* DNA polymerase as described in Tomlinson et al. (2010a) was omitted.

Experiments with alternative metal indicator dyes were conducted with primer set PD3 and the following reaction mix composition: 0.2 μM of each outer primer, 1.6 μM of each inner primer, 0.8 μM of each loop primer, 20 mM Tris-HCl (pH 8.8) (AppliChem, Darmstadt, Germany), 10 mM $(\text{NH}_4)_2\text{SO}_4$ (Merck, Darmstadt, Germany), 10 mM KCl (Merck, Darmstadt, Germany), 0.1 % Tween-20 (AppliChem, Darmstadt, Germany), 5.2 mM MgCl_2 (Merck, Darmstadt, Germany), 4.8 % (w/v) polyethylene glycol (PEG) 8k (Sigma-Aldrich, Munich, Germany), 0.8 mM dNTPs (New England Biolabs, Frankfurt, Germany), 8 U *Bst* DNA Polymerase, large fragment (New England Biolabs, Frankfurt, Germany), and 2 μl sample in a total volume of 25 μl . Concentrations of the dyes were 120 μM Eriochromeblack-T (ErioT) (Merck, Darmstadt, Germany), 120 μM or 240 μM Murexide (AppliChem, Darmstadt, Germany), 120 μM Phthalein purple (Merck, Darmstadt, Germany) or 600 μM Thiazole yellow (Merck, Darmstadt, Germany) per reaction, respectively. The mixed indicator consisted of ErioT and the pH indicator dye Methyl orange (MO) (Merck, Darmstadt, Germany) in a ratio of 2.5:1. The dye was prepared as 10 ml stock solution, composed of 0.064 g ErioT powder (corresponding to a concentration of 10 mM) and 0.018 g MO powder dissolved in distilled water. Per LAMP reaction, 0.3 μl of the dye solution was added.

The optimized LAMP reaction mix with the metal indicator dye Eriochromeblack-T and the primer set PD3 was composed of 0.2 μM of each outer primer, 1.6 μM of each inner primer, 0.8 μM of each loop primer, 120 μM ErioT (Merck, Darmstadt, Germany), 20 mM Tris-HCl (pH 8.8) (AppliChem, Darmstadt, Germany), 10 mM $(\text{NH}_4)_2\text{SO}_4$ (Merck, Darmstadt, Germany), 10 mM KCl (Merck, Darmstadt, Germany), 0.1 % Tween-20 (AppliChem, Darmstadt, Germany), 4.8 mM MgCl_2 (Merck, Darmstadt, Germany), 4.8 % (w/v) PEG 8k (Sigma-Aldrich, Munich, Germany), 0.8 mM dNTPs (New England Biolabs, Frankfurt, Germany), 8 U *Bst* DNA Polymerase, large fragment (New England Biolabs, Frankfurt, Germany), and 2 μl sample in a total volume of 25 μl , unless otherwise specified.

LAMP primers were synthesized by Eurofins MWG Operon (Ebersberg, Germany) unless otherwise stated. Primers FIP and BIP were ordered with HPLC purification. Primer sets for the detection of the PD phytoplasma were premixed as 10x concentrated primer mix. Stock

solutions of LAMP reaction mix ingredients were stored at -20 °C except PEG 8k (30 % w/v), which was stored in a fridge at +4 °C. LAMP reactions were incubated in a heating block (Grant QBT, Grant Instruments Ltd., Shepreth, UK).

2.6.3 Experiments with LAMP buffer ingredients

The original composition of the ThermoPol buffer (New England Biolabs, Frankfurt, Germany) was adopted for the self-made LAMP buffer, except that the detergent Triton X-100 was replaced with Tween-20. Furthermore, magnesium sulfate was removed from the buffer and magnesium ions were added separately to LAMP reaction solutions in the form of magnesium chloride. The 10x concentrated LAMP buffer consisted of 200 mM Tris-HCl (pH 8.8, adjusted at room temperature) (AppliChem, Darmstadt, Germany), 100 mM (NH₄)₂SO₄ (Merck, Darmstadt, Germany), 100 mM KCl (Merck, Darmstadt, Germany) and 1 % Tween-20 (AppliChem, Darmstadt, Germany). For experiments with varying concentrations of the buffer ingredients, the respective concentrations are given in the results section. The 10x concentrated LAMP buffer was stored in 1.5 ml aliquots at -20 °C. The buffer was freshly assembled from stock solutions of the individual ingredients every three weeks. Ten ml stock solutions of the buffer ingredients were stored at -20 °C except the detergent Tween-20, which was stored at room temperature.

Experiments with alternative buffering substances to Tris-HCl were conducted with glycine (Sigma-Aldrich, Munich, Germany) and 3-(N-morpholino)propanesulfonic acid (MOPS) (AppliChem, Darmstadt, Germany). The applied concentrations are given in the results section.

2.6.4 Visualization and documentation of LAMP results

End-point detection of LAMP results was performed by colorimetric detection of the amplification by-product magnesium pyrophosphate with a metal indicator dye. The colour change was judged by eye and documented as follows: 0.2 ml reaction tubes were placed into white racks derived from pipette tips boxes. Thusly arranged tubes were positioned on a customary scanner (Epson GT-1500), shaded with a cardboard box and scanned. The presence of precipitated magnesium pyrophosphate was confirmed by centrifugation of the reaction tubes. Positive reactions showed a white pellet at the bottom of the tubes. Agarose gel electrophoresis of LAMP products was performed to verify LAMP results as indicated by the colour change. TBE gels for the visualization of LAMP products contained 2 % agarose (Biozym Scientific, Hess. Oldendorf, Germany) and were stained with ethidium bromide. Gel electrophoresis was performed at 90 V for 45 min. The size of LAMP products was estimated with the GeneRuler 50bp DNA Ladder (Fermentas St. Leon-Rot, Germany).

2.7 Experiments on the properties of Eriochromeblack-T

2.7.1 Measurement of UV/Vis spectra

UV/Vis absorption spectra of ErioT in the presence of different solvents were investigated with a Kontron Uvikon 931 spectrophotometer (Kontron Instruments, Milan, Italy). Test solutions were prepared at room temperature on a 1.2 ml scale and contained 120 μ M ErioT and 20 mM Tris-HCl (pH 8.8) or distilled water, as well as 4.8 mM magnesium chloride when the ErioT-Mg-complex was investigated. The influence of the complete LAMP buffer, the LAMP buffer components potassium chloride and ammonium sulfate as well as the additive PEG 8k on absorption spectra was examined individually as well as in combination. These reagents were added in their respective LAMP concentrations to ErioT/Tris-HCl (pH 8.8) solutions. All preparations were vortexed and then transferred to quartz cuvettes. Distilled water served as blank. Absorption spectra were measured from 350 to 750 nm.

2.7.2 Titration experiments with sodium pyrophosphate

Titration experiments were performed on a 1.2 ml scale in order to investigate ErioT absorbance in a sodium pyrophosphate concentration series with the Kontron spectrophotometer, or on a 100 μ l scale in 0.2 ml reaction tubes to compare the behavior of ErioT and HNB as well as to examine the influence of dNTPs on the colour transition point. Test solutions for measurements with the spectrophotometer contained the following reagents corresponding to their respective LAMP concentrations: 120 μ M ErioT (Merck, Darmstadt, Germany) or HNB (Sigma-Aldrich, Munich, Germany), 1x LAMP buffer (20 mM Tris-HCl (pH 8.8) (AppliChem, Darmstadt, Germany), 10 mM $(\text{NH}_4)_2\text{SO}_4$ (Merck, Darmstadt, Germany), 10 mM KCl (Merck, Darmstadt, Germany), 0.1 % Tween-20 (AppliChem, Darmstadt, Germany)), 4.8 mM MgCl_2 (Merck, Darmstadt, Germany), 4.8 % PEG 8k (Sigma-Aldrich, Munich, Germany), distilled water. Primers, dNTPs as well as *Bst* DNA polymerase were excluded from these experiments for financial considerations. Sodium pyrophosphate ($\text{Na}_4\text{P}_2\text{O}_7$, abbreviated as NaPP) (Merck, Darmstadt, Germany) was added in a concentration series from 1 mM to 2.5 mM in 0.5 mM steps. Two reference solutions without sodium pyrophosphate, and with 0 mM and 4.8 mM magnesium chloride, respectively, were included in the experiment. After incubation at 65 °C for 60 min in a heating block, the reaction tubes were centrifuged for 2 min at 13,000 rpm. One ml of the supernatant was transferred into a 1.5 ml quartz cuvette and absorbance spectra were measured.

Test solutions at a 100 μ l scale were composed as described above. The dNTPs (New England Biolabs, Frankfurt, Germany) were added when their interaction on the colour change was studied. The respective concentrations are given in the results section. Sodium pyrophosphate was added in a concentration series from 0.1 mM to 2.5 mM. The solutions were incubated for 60 min at 65 °C and then centrifuged for 2 min at 13,000 rpm. The colour change of the test solutions was judged by eye and photographed for documentation.

3 Results

3.1 Development of a colorimetric loop-mediated isothermal amplification assay for the detection of *Candidatus Phytoplasma pyri* targeting the 16S rRNA gene

Four primer sets targeting the 16S rRNA gene of *Ca. P. pyri* were evaluated for their performance in a LAMP assay intended for on-site application, which involved a metal indicator dye for indirect product detection and a simplified sample preparation procedure. The primer set with the designation PD1 was developed by Obura et al. (2011) for the detection of the Napier stunt phytoplasma (NSP; group 16SrXI), which causes the Napier stunt disease of Napier grass. The authors reported the successful detection of the PD phytoplasma in specificity tests. Hence, the applicability of this primer set in a LAMP assay for the detection of the PD phytoplasma was evaluated at first in this study. Primer sets PD2, PD3 and PD4 were designed on the 16S rDNA sequence of the *Ca. P. pyri* reference strain (GenBank accession no. AJ542543.1). Optimization was conducted with the metal indicator dye hydroxy naphthol blue (HNB) in the first instance.

3.1.1 Experiments with a primer set published by Obura et al. (2011)

First efforts to develop a LAMP assay suitable to detect PD in the field were conducted with a primer set developed for the detection of the Napier stunt phytoplasma, which was reported to detect *Ca. P. pyri* in specificity tests (Obura et al., 2011). The first experiment was performed with the original reaction conditions described in Obura et al. (2011). Since the authors applied an initial denaturation step in their NSP LAMP, two variants were tested: Reactions of the first variant were heated for 5 min at 95 °C prior to amplification according to Obura et al. (2011); reactions of the second variant were subjected to incubation immediately without prior denaturation. Controls for pear decline were tested in duplicates. A no template control (NTC) was included in the variant without prior denaturation. After incubation at 63 °C for 60 min, LAMP products were subjected to agarose gel electrophoresis. Faint laddering was observed in one of the positive controls of the denatured variant. Weak, unspecific smear was visible in the second positive control as well as the negative controls. In the non-denatured variant, no specific amplification product was detected (Figure 5).

Results

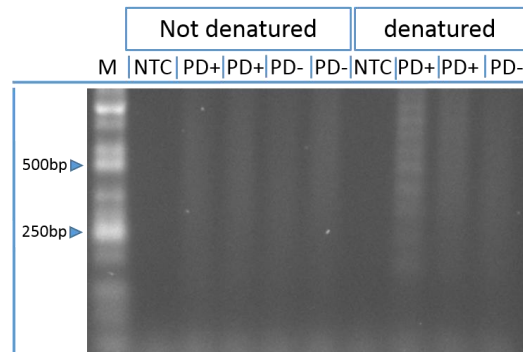


Figure 5: First test of LAMP primers published by Obura et al. (2011) with and without initial denaturation step. M = Size marker; NTC = No template control; PD+ = PD positive control; PD- = PD negative control.

Since one hour of incubation appeared insufficient, reaction time was extended by further 60 min in the following experiments. For the incorporation of the metal indicator dye HNB into the LAMP assay, two different reaction mix compositions were tested:

- (1) A reaction mix prepared according to Obura et al. (2011) supplemented with HNB.
- (2) A reaction mix prepared according to Hadersdorfer et al. (2011) without a reverse transcriptase, which is needed for the transcription of the RNA template in the respective LAMP assay for the detection of the *Plum pox virus* (PPV). This LAMP assay was optimized for colorimetric product detection with HNB and contained additional 6 mM MgSO₄ to the basic amount of 2 mM MgSO₄ included in the ThermoPol buffer (New England Biolabs, Frankfurt, Germany), as well as 1 mM dNTPs instead of 0.4 mM comprised in the preparation of Obura et al. (2011).

Both reaction mix preparations were tested with and without initial denaturation. As expected, no colour change was visible after 1 hour of incubation. However, after 2 hours of incubation, specific amplification of positive controls was obtained only with prior denaturation of the template in the modified Obura preparation. The colour of these positive controls was light blue and clearly distinguishable from the dark blue negative controls and unamplified controls of the non-denatured variant (Fig 6, LAMP 1). Reaction mixes prepared according to Hadersdorfer et al. (2011) yielded amplification products in both variants with and without prior denaturation after 120 min of incubation, but unspecific amplification products occurred throughout the controls. Due to the higher magnesium sulfate concentration, these reaction solutions showed a purple colour with a weak bluish tint in the positive controls (Fig 6, LAMP 2).

Results

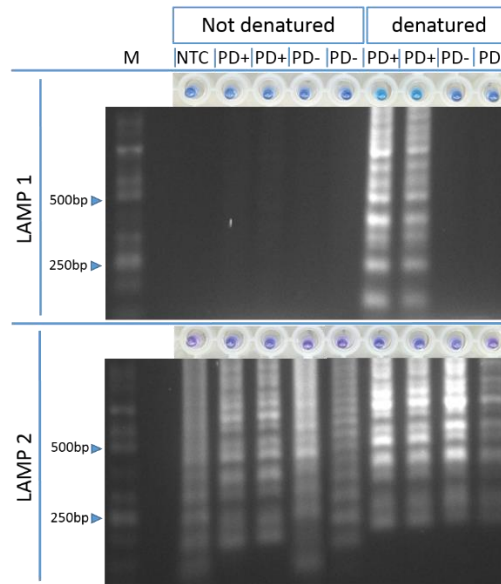


Figure 6: LAMP reactions with primer set PD1 prepared according to Obura et al. (2011) (LAMP 1) and according to Hadersdorfer et al. (2011) (LAMP 2), with and without initial denaturation step. M = Size marker; NTC = No template control; PD+ = PD positive control; PD- = PD negative control. Dye: HNB.

The modified Obura preparation with HNB was the most promising one, with specific amplification products in the positive controls only. However, the dark blue colour of the unamplified controls indicated that a considerable amount of HNB was in its free form because of a too low magnesium sulfate concentration. A concentration series of magnesium sulfate was tested with all other components held equal. In addition to 2 mM MgSO_4 , which are included in the ThermoPol buffer, several magnesium sulfate concentrations from 0 mM up to 3.2 mM were evaluated (Figure 7). Increasing magnesium ion concentrations led to a general change in colour of the reaction solutions before the onset of the LAMP reaction. With 1.2 mM MgSO_4 or more, the reaction solutions were stained purple, indicating a high amount of HNB-magnesium-complexes. At 0.8 mM MgSO_4 , the positive control showed a colour change after incubation and the expected ladder-like banding pattern was visible on the agarose gel. Negative and no template controls remained negative. The variants with 0 mM and 0.4 mM MgSO_4 also yielded specific amplification of the positive control with all other controls remaining negative. However, no colour change of the positive controls was observed in these variants. The ground colour of unamplified controls was still bluish. Reactions containing 1.2 mM or 1.6 mM MgSO_4 showed a definite colour change from purple to blue in positive controls and a bright purple colour in negative and no template controls. The observed colour change matched perfectly the results obtained by agarose gel electrophoresis. Addition of 2.4 mM and 3.2 mM MgSO_4 yielded dark blue colours with a purple tint instead of the expected light blue colour in amplified samples. Compared to the initial colour of the reaction solutions before the onset of the reaction, the colour change was weak, which indicated high amounts of remaining free magnesium ions after the amplification reaction. However, false positive amplification occurred in all negative and no template controls of the two highest magnesium sulfate concentrations tested. 1.6 mM

Results

MgSO₄ was determined as optimal concentration in this LAMP assay, yielding the most pronounced colour change of the amplified positive control.

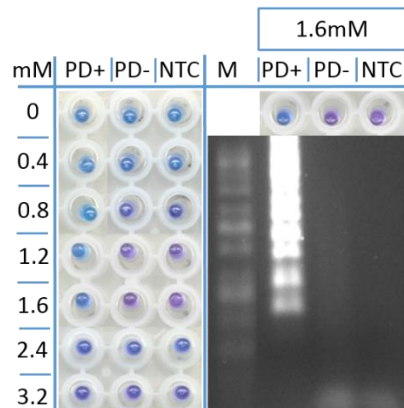


Figure 7: LAMP reactions with primer set PD1, magnesium sulfate concentration series. Left: Colour change in dependence of the applied magnesium sulfate concentration. Right: Colour change and agarose gel at 1.6 mM MgSO₄. mM = Concentration of additional magnesium sulfate per reaction [mM]; M = Size marker; NTC = No template control; PD+ = PD positive control; PD- = PD negative control. Dye: HNB.

After the optimization of the reaction mix, a test for application to apple proliferation samples was performed. Since the apple proliferation phytoplasma (AP) is closely related to the pear decline phytoplasma, the applicability of this primer set for AP detection was most likely. However, while successfully detecting AP in the positive controls, the primer set consistently produced false positives with AP negative controls. Presence of the pathogens in the positive controls for AP and PD as well as their absence in negative controls was confirmed by nested PCR. Additionally, a first test on field samples derived from pear orchards located in Baden-Württemberg, Germany, with suspected PD infestation was performed. Nested PCR gave positive results for three out of four samples. All samples were positive in LAMP (Figure 8).

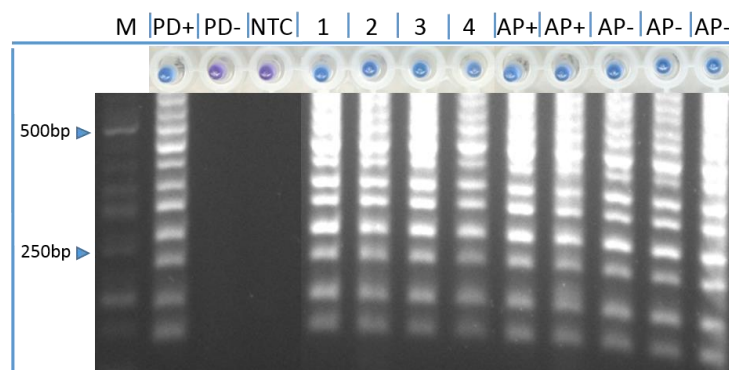


Figure 8: LAMP with primer set PD1, application to PD field samples and apple proliferation samples. M = Size marker; PD+ = PD positive control; PD- = PD negative control NTC = No template control; 1 - 4 = pear field samples with suspected PD infection; AP+ = AP positive control; AP- = AP negative control. Dye: HNB.

In following tests of field samples as well as preliminary experiments to develop a simplified sample preparation procedure, false positives in samples derived from healthy pears, negative

Results

controls as well as no template controls were accumulating. Figure 9 shows the results of an experiment to evaluate the influence of 1 µl of a 0.5 M NaOH solution diluted 1:5 or 1:50 with 100 mM Tris-HCl (pH 8.8) on the LAMP reaction as pretest for a NaOH-based sample preparation procedure (for details on the development of the simplified sample preparation procedure, see chapter 3.4).

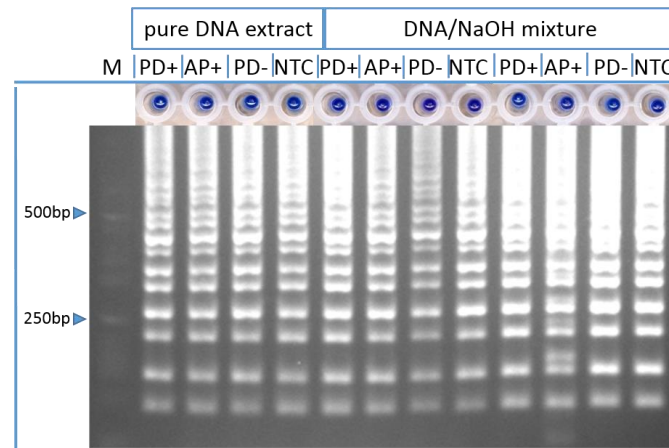


Figure 9: Occurrence of false positives during the development process of a simplified sample preparation procedure in LAMP reactions with primer set PD1. M = Size marker; NTC = No template control; PD+ = PD positive control; PD- = PD negative control; AP+ = AP positive control. Dye: HNB.

False positives were observed throughout all variants and controls. Contaminations originating from opening the reaction tubes after the initial denaturation step were assumed to be the source. Hence, it was attempted to eliminate this contamination source by altering the reaction mix with the objective of redundanzing the initial denaturation step. Enhancing the concentrations of several components of the reaction mix enabled amplification without prior denaturation (data not shown). However, with 2 hours of incubation and a still unsatisfying colour change which varied in intensity from experiment to experiment, the assay did not meet the expectations of a detection system suitable for field use. In a final effort, it was attempted to design loop primers, which ought to speed up the reaction, reducing the incubation time of 2 hours and improving amplification efficiency, thereby leading to a more pronounced colour change. The underlying assumption that inefficient amplification was responsible for the slow and weak colour change proved true when a sequence alignment of the LAMP primers with the 16S rDNA reference sequence of *Candidatus Phytoplasma pyri* (GenBank accession no. AJ543542) was performed, which revealed mismatches of the target sequence with LAMP primers F3, B3 and FIP (Figure 10b). Furthermore, it was discovered that the sequences of the LAMP primers did not fit the original target sequence from the Napier stunt phytoplasma deposited under the denoted GenBank accession number by Obura et al. (2011) (Figure 10a). As a consequence, work with this primer set was abandoned and design of new LAMP primers was undertaken.

Results

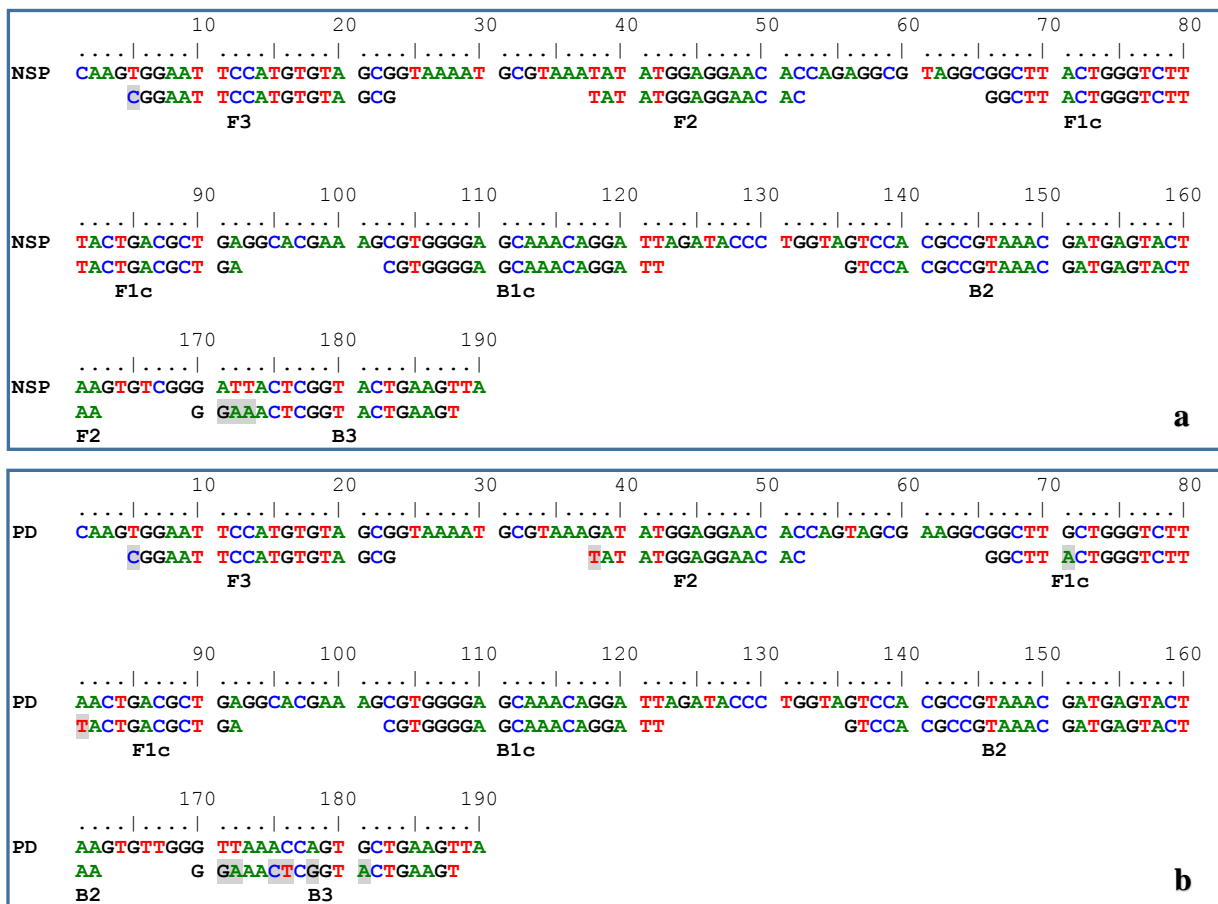


Figure 10: Sequence alignment of the LAMP primer set PD1 obtained from Obura et al. (2011) with the 16S rDNA target sequences of (a) NSP phytoplasma (GenBank access. no. AY736374) and (b) PD phytoplasma (GenBank access. no. AJ542543.1). Mismatches at the primer binding sites are shaded. F3, B3 = outer LAMP primers; F2, F1c = FIP sequence components; B2, B1c = BIP sequence components.

3.1.2 Design of LAMP primer sets targeting the 16S rRNA gene of *Candidatus Phytoplasma pyri*

The 16S rRNA gene was chosen as target for LAMP primers because of the availability of sequence information for all formally described phytoplasma species. The reference sequence of *Candidatus Phytoplasma pyri* (GenBank accession no. AJ542543.1) was used to generate primer sets with the free online tool PrimerExplorer V4 (<http://primerexplorer.jp/e/>) as well as with a test version of the commercially available primer design software LAMP Designer. During the project runtime, three different primer sets targeting the 16S rRNA gene of *Ca. P. pyri* were evaluated. Figure 11 shows the position of the primers on the target sequence. All primers were tested with a BLAST analysis for possible cross-reactivity with other organisms. As expected, most primers showed sequence similarities with other phytoplasmas of the group 16SrX up to 100 %. The applicability of the primer sets to the AP phytoplasma was evaluated during the optimization process. Several primers showed partial sequence similarities with a range of organisms. However, full homology of more than one primer within a primer set was not observed.

Results

```

660      670      680      690      700      710      720      730
.....|.....|.....|.....|.....|.....|.....|.....|
TGGAATTCCA TGTGTAGCGG TAAAATGCGT AAAGATATGG AGGAACACCA GTAGCGAAGG CGGCTTGCTG GGTCTTAACT
ATTCCA TGTGTAGCGG TAA ATGCGT AAAGATATGG AGGAACACCA GTAGCGAAGG CGG TTGCTG GGTCTTAACT
PD4 F3 PD4 F2 PD4 LF PD4 F1c
GTCTTAACT
PD3 F3

740      750      760      770      780      790      800      810
.....|.....|.....|.....|.....|.....|.....|.....|
GACGCTGAGG CACGAAAGCG TGGGGAGCAA ACAGGATTAG ATACCCTGGT AGTCCACGCC GTAACGATG AGTACTAAGT
GACGC CG TGGGGAGCAA ACAGGATT TACCCTGGT AGTCCACGCC TAAACGATG AGTACTAAGT
PD4 F1c PD4 B1c PD4 LB PD4 B2
GACGCTGAGG AACGATG AGTACTAAGT
PD3 F3 PD3 F2

820      830      840      850      860      870      880      890
.....|.....|.....|.....|.....|.....|.....|.....|
GTTGGGTTAA ACCAGTGCTG AAGTTAACGC ATTAAGTACT CCGCCTGAGT AGTACGTACG CAAGTATGAA ACTTAAAGGA
GTTG CAGTGCTG AAGTTAACGC
PD4 B2 PD4 B3
GTTGG CAGTGCTG AAGTTAACGC ATT GTACT CCGCCTGAGT AGTACGT A
PD3 F2 PD3 LF PD3 F1c PD3 B1c

900      910      920      930      940      950      960      970
.....|.....|.....|.....|.....|.....|.....|.....|
ATTGACGGGA CTCCGCACAA GCGGTGGATC ATGTTGTTTA ATTCAAGAT ACACGAAAAA CCTTACCAGG TCTTGACATA
ATTGACGGGA CTCCGCACAA GCGGTGGATC ATGTTGT A CCTTACCAGG TCTTGACA
PD3 B1c PD3 LB PD3 B2

980      990      1,000      1010      1020      1030      1040      1050
.....|.....|.....|.....|.....|.....|.....|.....|
CTCTGCAAAG CTATAGAAAT ATAGTGGAGG TTATCAGGGA TACAGGTGGT GCATGGTTGT CGTCAGCTCG TGTCTGAGGA
GGA TACAGGTGGT GCATG
PD3 B3

1060      1070      1080      1090      1100      1110      1120      1130
.....|.....|.....|.....|.....|.....|.....|.....|
TGTGGGTTA AGTCCCGCAA CGAGCGCAAC CCTTATCGCT AGTTACCATC ATTTAGTTGG GCACCTTAGT GAGACTGCCA
TTAGT GAGACTGCCA
PD2 F3

1140      1150      1160      1170      1180      1190      1200      1210
.....|.....|.....|.....|.....|.....|.....|.....|
ATGATAAATT GGAGGAAGGT GGGGATTACG TCAAATCATC ATGCCCTTA TGACCTGGGC TACAAACGTG ATACAATGGC
ATGA AGGAAGGT GGGGATTACG ACCTGGGC TACAAACGTG ATACAATGGC
PD2 F3 PD2 F2 PD2 F1c PD2 B1c

1220      1230      1240      1250      1260      1270      1280      1290
.....|.....|.....|.....|.....|.....|.....|.....|
TGTACAAAG AGTAGCTGAA GCGTGAGTTT TTAGCAAATC TCAAAAAAAC AGTCTCAGTT CGGATTGAAG TCTGCAACTC
TGTACAAAG AGTAGC GAA GCGTGAGTTT TTAGCAAATC TC AGTT CGGATTGAAG TCTGC
PD2 B1c PD2 LB PD2 B2

1300      1310      1320
.....|.....|.....|
GACTTCATGA AGTCGGAATC GCTAGTAATC
CATGA AGTCGGAATC GCT
PD2 B3

```

Figure 11: Sequence alignment of LAMP primer sets PD2, PD3 and PD4 with the target region of the 16S rDNA sequence of the PD phytoplasma (GenBank access. no. AJ542543.1). F3 (green), B3 (red) = outer LAMP primers; LF, LB (pink) = forward and backward loop primers; F2 (blue), F1c (black) = FIP sequence components; B2 (orange), B1c (violet) = BIP sequence components.

3.1.3 Optimization of the PD LAMP assay with hydroxy naphthol blue for indirect detection of amplification products

In the following, several experiments on magnesium and dNTP concentrations with different primer sets and the metal indicator hydroxy naphthol blue (HNB) are presented. As recommended by Goto et al. (2009), 120 μ M HNB per reaction were applied in the PD LAMP. For the use of Eriochromeblack-T as metal indicator dye and polyethylene glycol 8k as additive, a minor adjustment of magnesium ion concentration was necessary. The respective experiments are presented in chapter 3.6 “Colorimetric detection of LAMP products with Eriochromeblack-T”.

3.1.3.1 Optimization of dNTP concentration

For the primer sets PD2 and PD3, dNTP concentration was varied in a concentration series from 0.4 to 1 mM per reaction. The experiment included positive and negative controls for pear decline and apple proliferation as well as no template controls. The concentration of additional magnesium sulfate was held as low as possible in order to avoid unspecific or false positive reactions. However, the initial magnesium sulfate concentration of 2 mM, which is included in the ThermoPol buffer, was sufficient for a dNTP concentration of 0.4 mM but needed to be enhanced to 4 mM MgSO_4 for 0.8 mM and 1 mM dNTPs because the colour of the reaction solution immediately turned to blue after addition of dNTPs during the preparation of the LAMP reaction mix. Figure 12 shows the results of the dNTP concentration series experiment.

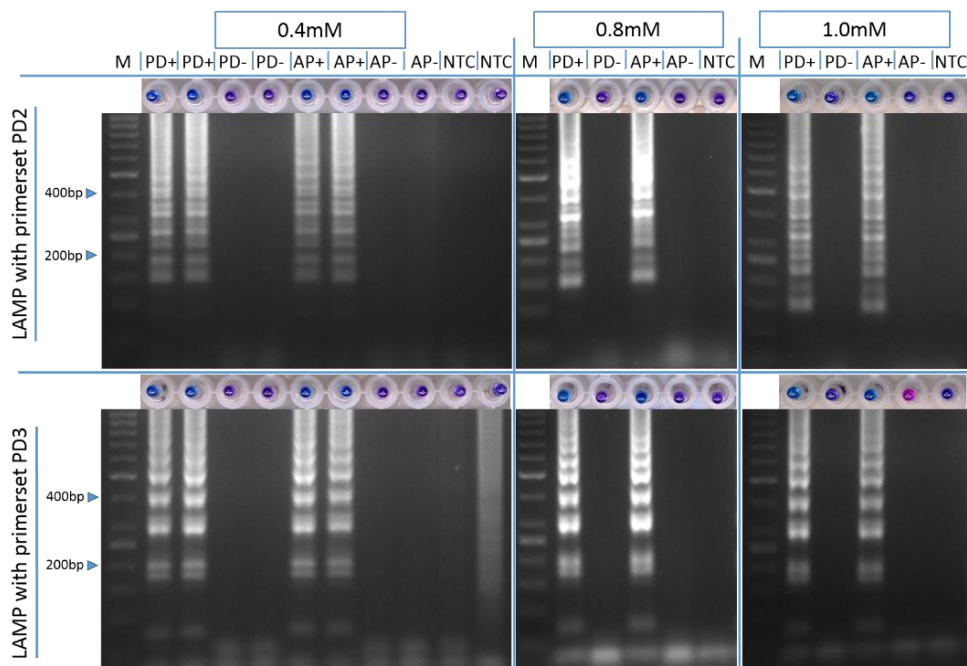


Figure 12: LAMP reactions with primer sets PD2 and PD3, dNTP concentration series. M = Size marker; NTC = No template control; PD+ = PD positive control; PD- = PD negative control; AP+ = AP positive control; AP- = AP negative control. Dye: HNB.

Sixty min of incubation at 63 °C were sufficient to yield a clearly distinguishable colour change in positive reactions. A concentration of 0.8 mM dNTPs was determined as optimal

concentration for both assays because the colour change showed the best contrast between blue positive and purple negative controls. The contrast was less pronounced at 0.4 mM dNTPs due to the low concentration of magnesium sulfate in the reaction solution. At 1 mM dNTPs, the ground colour of reactions, which did not yield amplification products, showed a blue tint as a result of increased magnesium complexation by dNTPs. This impaired visual differentiation of blue-stained positive controls from negative controls. An AP negative control of this variant showed a bright magenta colour after incubation, which might be due to an accidental degradation of the metal indicator dye. However, this unusual staining did not influence the result of the LAMP reaction. False positive amplifications were not observed throughout this experiment. At the lowest dNTP concentration, a no template control showed a smear on the agarose gel. However, this unspecific amplification did not result in a colour change of the metal indicator.

For the primer set PD4, the dNTP concentration was adopted from the reaction mix composition for the primer sets PD2 and PD3 since it worked equally well in the respective LAMP assay.

3.1.3.2 Optimization of magnesium sulfate concentration

Initially, magnesium ions were added as magnesium sulfate in addition to 2 mM MgSO₄, which were included in the ThermoPol buffer (New England Biolabs). Later, magnesium sulfate was replaced by magnesium chloride as source of magnesium ions for reasons of assay stability (see chapter 3.7.2 “Experiments with LAMP buffer composition”). As the complexing behavior of the two metal indicators used in this study is different, magnesium chloride concentration had to be readjusted after changing the metal indicator dye (see chapter 3.6 “Colorimetric detection of LAMP products with Eriochromeblack-T”).

Using HNB in the LAMP assays with primer sets PD2 and PD3, a magnesium sulfate concentration series from 4 mM to 5.6 mM (in addition to 2 mM MgSO₄ provided by the ThermoPol buffer) was tested on controls for pear decline and apple proliferation in order to determine the optimal magnesium ion concentration. Results are shown in figure 13. In the LAMP assay with the primer set PD2, generation of false positives occurred at 4.8 mM and 5.6 mM MgSO₄. With the primer set PD3, no false positive reactions were observed at the applied magnesium sulfate concentrations. At 5.6 mM MgSO₄, weak unspecific amplification in the negative controls was observed as faint bands on the agarose gel, which did not result in a colour change of the respective reaction solutions. Sixty min of incubation were sufficient to develop a clearly distinguishable colour change in the LAMP assay with primer set PD2 irrespective the magnesium sulfate concentration. LAMP reactions with the primer set PD3 and 4 mM MgSO₄ also showed a distinct colour change after 60 min of incubation. In the PD3 variants with higher magnesium sulfate concentrations, it was not possible to clearly distinguish positive from negative controls by the colour change of the metal indicator after 60 min. Elongation of the reaction time to 90 min yielded the expected colour change of the positive controls. For LAMP reactions with primer sets PD2 or PD3, 4 mM MgSO₄ was determined as

Results

optimal concentration, yielding a clearly distinguishable colour change within a reaction time of 60 min.

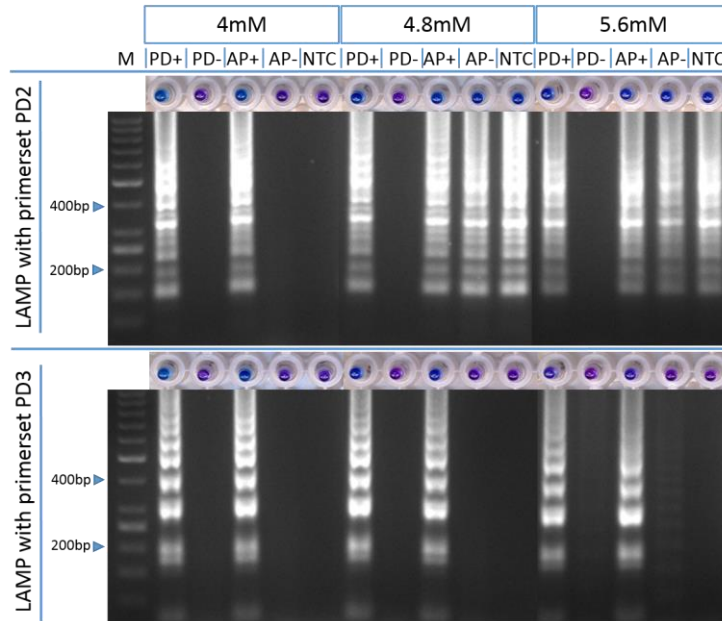


Figure 13: LAMP reactions with primer sets PD2 and PD3, magnesium sulfate concentration series. M = Size marker; NTC = No template control; PD+ = PD positive control; PD- = PD negative control; AP+ = AP positive control; AP- = AP negative control. Supplemental magnesium sulfate concentrations per reaction are given in the headline boxes. Dye: HNB.

With the primer set PD4, a magnesium sulfate concentration series from 2.4 mM to 5.6 mM (supplemental to 2 mM MgSO₄ included in the ThermoPol buffer) was investigated with PD controls in duplicates (Figure 14). Occasional false positives were observed in all variants except for the variant with 3.6 mM MgSO₄ as judged by the colour change and confirmed by agarose gel electrophoresis.

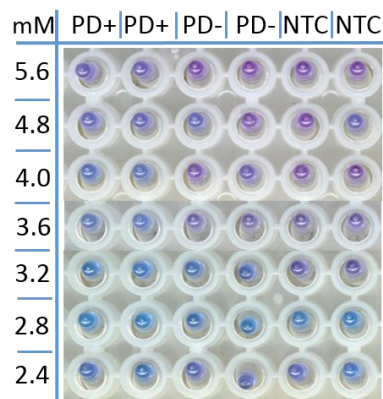


Figure 14: LAMP reactions with primer set PD4, magnesium sulfate concentration series. PD+ = PD positive control; PD- = PD negative control; NTC = No template control. Supplemental magnesium sulfate concentrations per reaction [mM] are given in the left column. Dye: HNB.

LAMP reactions with magnesium sulfate concentrations up to 3.6 mM were terminated after 30 min of incubation since the fully developed colour change indicated amplification products

in positive controls as well as several false positives in negative and no template controls. With higher magnesium sulfate concentrations, it took 60 min of incubation to distinguish positive from negative controls by the colour change. LAMP reactions with the highest concentration of 5.6 mM MgSO₄ showed a very weak colour change of positive controls after 60 min. Incubation for further 30 min did not change this result. Agarose gel electrophoresis of LAMP products revealed unspecific amplification in negative and no template controls of this variant. Figure 15 shows a time course of the colour change development in the variants with 4 mM, 4.8 mM and 5.6 mM MgSO₄. Four mM MgSO₄ was identified as optimal concentration for the PD4 using LAMP assay.

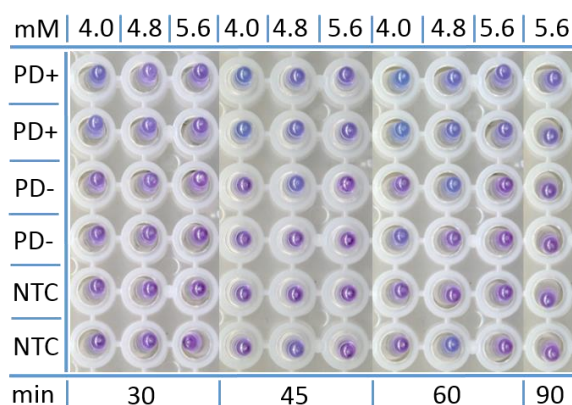


Figure 15: Colour development of LAMP reactions with primer set PD4 over time, magnesium sulfate concentration series. PD+ = PD positive control; PD- = PD negative control; NTC = No template control. Supplemental magnesium sulfate concentrations per reaction [mM] are given in the headline. Dye: HNB.

3.1.3.3 Optimization of incubation temperature

All primer sets were tested in the first instance at a reaction temperature of 63 °C as the medium temperature within the optimum range of *Bst* DNA polymerase activity, which is the recommended LAMP reaction temperature in the PrimerExplorer V4 Manual (Eiken Chemical Co., Ltd., Tokyo, Japan). LAMP reactions with the primer set PD4 were conducted in a temperature gradient from 60 to 65 °C to determine the optimal reaction temperature, at which unspecific and false positive amplification products did not occur. Positive and negative controls for pear decline as well as no template controls were run in duplicates. LAMP performed equally well at all temperatures tested. Unspecific amplification was occasionally observed as smear or faint unspecific laddering on agarose gels. However, these amplifications did not result in a colour change of the metal indicator except in one negative control incubated at 60 °C (data not shown).

Continuous work with the primer sets PD3 and PD4 revealed that unspecific and false positive amplifications occurred more frequently at lower reaction temperatures and consequently, the highest possible reaction temperature of 65 °C as determined by the temperature range of *Bst* DNA polymerase activity was finally chosen for the PD LAMP assay.

3.2 Detection limit

Sensitivity tests were performed for primer sets PD3 and PD4 at various stages of the optimization process and in several variants from experiments with simple dilution series of positive controls to dilution series of a plasmid containing the 16S rDNA target sequence. In the following, experiments to evaluate the detection limit of PD3 and PD4 LAMP assays with HNB for colorimetric product detection are presented. Sensitivity of primer set PD2 was not examined since it continuously produced false positives and unspecific reactions during the optimization process and was therefore excluded from further experiments. The final evaluation of the detection limit of the LAMP assay with the primer set PD3 and the optimized reaction mix using Eriochromeblack-T for colorimetric detection of amplification products is presented in the chapter 3.6.3 “Detection limit and detection range of the PD LAMP with Eriochromeblack-T”.

Primer set PD3

First experiments to estimate the detection limit of LAMP with HNB and the primer set PD3 were performed with a 10-fold dilution series of a DNA extract derived from *in vitro* cultured pears infected with the PD phytoplasma. The pure DNA extract and dilutions up to 1:10,000 were tested with LAMP using the primer set PD3, PCR with primers fO1/rO1 and realtime PCR according to Torres et al. (2005) with the primer pair P1/R16(x)F1r and SybrGreen I (Figure 16). LAMP yielded positive results up to a dilution of 1:1,000. The colour change of amplified dilutions was well distinguished from the unamplified dilution and controls. Subsequent agarose gel electrophoresis confirmed LAMP results as indicated by the colour change. Unlike PCR, banding patterns of LAMP products showed no weakening in intensity with increasing dilution of the DNA extract. PCR reactions were positive up to dilution 1:1,000, showing only a weak band at this last positive dilution. Realtime PCR showed specific amplification for all dilutions including the highest one of 1:10,000. Deviations of the fluorescence signals of more than 0.5 cycles were observed for one out of three repetitions of the 1:1,000 and 1:10,000 dilutions, respectively. The negative control yielded fluorescence signals beyond cycle 33. However, melt curve analysis confirmed specific amplification in the dilutions of the DNA extract from the PD containing *in vitro* plant. The fluorescence signals observed in the triplicates of the negative control proved to be unspecific in the melt curve analysis.

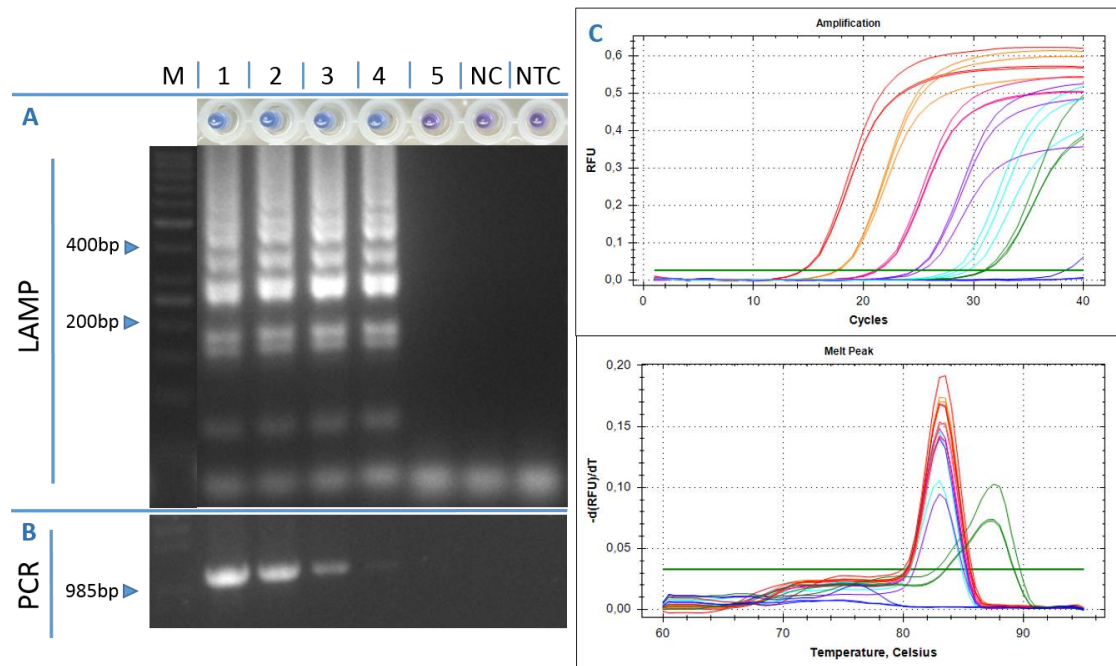


Figure 16: Detection limit of LAMP with primer set PD3 (A) in comparison to conventional PCR (B) and realtime PCR (C). M = size marker; 1-5 = dilution series of a PD-positive DNA extract (1 = undiluted; 2 = diluted 1:10; 3 = diluted 1:100; 4 = diluted 1:1,000; 5 = diluted 1:10,000); NC = negative control; NTC = no template control. Dye: HNB. Realtime PCR amplification curves and melt curve analysis are given on the right. Red lines = undiluted DNA extract; orange = diluted 1:10; magenta = diluted 1:100; violet = diluted 1:1,000; turquoise = diluted 1:10,000; green = negative control; blue = no template control.

In order to examine the detection limit of the LAMP assay with the primer set PD3 in the presence of increasing amounts of background DNA, a dilution series of the same DNA extract used in the experiment described above was prepared with a DNA extract derived from healthy *in vitro* pears as diluent, which also served as negative control. Dilution steps were 1:1, 1:5, 1:10, 1:100, 1:1,000 and 1:10,000. The dilution series was tested with LAMP using primer set PD3, PCR with the primer pair fO1/rO1 and realtime PCR according to Torres et al. (2005). Results are presented in figure 17. PD LAMP showed specific amplification up to a dilution of 1:1,000. The observed colour change was in perfect agreement with the results of subsequent agarose gel electrophoresis. PCR with primers fO1/rO1 yielded positive results for all dilutions tested. However, as already observed in the previous experiment, the intensity of PCR products on the agarose gel weakened with every dilution step, showing only a very faint band at the highest dilution (1:10,000). This was not the case for LAMP products which showed equal intensities on the agarose gel for all amplified dilutions. Realtime PCR yielded fluorescence signals for all dilutions, which proved to be specific in the melt curve analysis. The negative control again produced fluorescence signals beyond cycle 33, which were due to unspecific amplification.

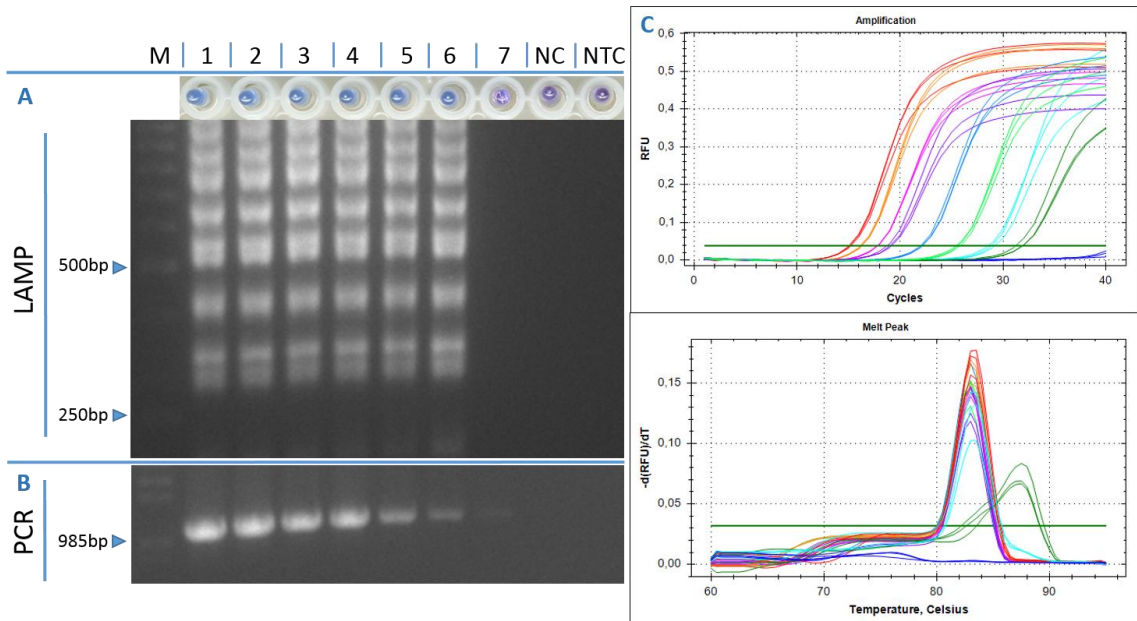


Figure 17: Detection limit in the presence of increasing amounts of background DNA: LAMP with primer set PD3 (A) in comparison to conventional PCR (B) and real-time PCR (C). M = size marker; 1-7 = dilution series of a PD-positive DNA extract with plant DNA (1 = undiluted; 2 = diluted 1:1; 3 = diluted 1:5; 4 = diluted 1:10; 5 = diluted 1:100; 6 = diluted 1:1,000; 7 = diluted 1:10,000); NC = negative control; NTC = no template control. Dye: HNB. Realtime PCR amplification curves and melt curve analysis are given on the right. Red lines = undiluted DNA extract; orange = diluted 1:1; magenta = diluted 1:5; violet = diluted 1:10; light blue = diluted 1:100; light green = diluted 1:1,000; turquoise = diluted 1:10,000; green = negative control; blue = no template control.

Primer set PD4

The detection limit of primer set PD4 was estimated with a 10-fold dilution series of a DNA extract of *in vitro* pear plants infected with the PD phytoplasma and compared with results of conventional PCR with primers fO1/rO1. It should be noted that this dilution series was not prepared with the same DNA extract as in the experiments described above, although both extracts derived from pear plants belonging to the same *in vitro* culture. Therefore, this experiment was also conducted with primer set PD3 in order to compare assay performances depending on the primer set. Furthermore, it was attempted to enhance assay sensitivity by altering the concentrations of magnesium sulfate (+ 2 mM), dNTPs (+ 0.6 mM) and betaine (- 0.2 M). Dilutions were tested in duplicates. Results are shown in figure 18.

Results

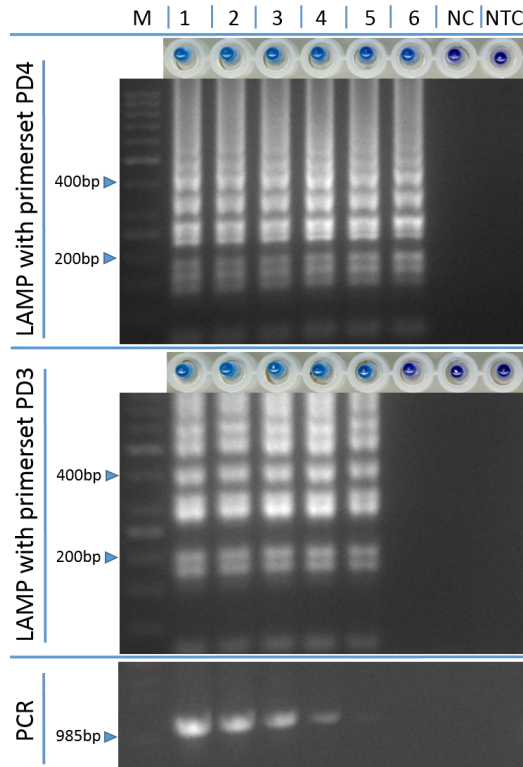


Figure 18: Detection limit of LAMP with primer set PD4 in comparison to LAMP with primer set PD3 and conventional PCR. M = size marker; 1-6 = dilution series of a PD-positive DNA extract (1 = undiluted; 2 = diluted 1:10; 3 = diluted 1:100; 4 = diluted 1:1,000; 5 = diluted 1:10,000; 6 = 1:100,000); NC = negative control; NTC = no template control. Dye: HNB.

The primer set PD4 successfully amplified dilutions up to the factor 1:10,000 in both replicates. The dilution 1:100,000 was amplified in one out of two replicates with this primer set. Primer set PD3 yielded positive results up to dilution 1:10,000 for both replicates but failed to amplify the highest dilution. PCR with primers fO1/rO1 showed positive amplification until dilution 1:10,000. However, bands at this dilution were extremely weak. The colour change observed in LAMP reactions of this experiment was less pronounced than in the experiment described above, which was due to the differences in reaction mix composition. These alterations did not influence the detection limit of the LAMP assay with the primer set PD3, which was similar to the detection limit of PCR as observed earlier.

Finally, primer set PD3 proved to be superior to primer set PD4 although the latter provided a 10-fold higher sensitivity. This was mainly due to the considerable vulnerability of LAMP reactions with primer set PD4 to the occurrence of false positives, which appeared less frequent in LAMP reactions with primer set PD3.

3.3 Evaluation of LAMP primer sets targeting non-ribosomal genes

Two primer sets were designed based on the *pnp* gene and the *rpl22* gene sequences of *Ca. P. pyri*, respectively. LAMP performance with these primer sets was tested with the reaction mix composition optimized for the 16S rRNA primer sets and colorimetric product detection with HNB.

Primer set pnp

A first experiment with the LAMP primer set pnp was conducted at 63 °C (Figure 19). In addition to PD controls, a positive control for AP was included in the experiment. After 60 min, the reaction tubes were scanned and then returned to the heating block for another 30 min of incubation because no colour change was visible. After 90 min, a second scan was taken. All positive controls as well as the no template controls had turned blue. After a total of 120 min of incubation, the remaining negative control had changed its colour to dark blue. Subsequent agarose gel electrophoresis showed ladder-like banding patterns in the PD and AP positive controls, which were almost identical apart from some faint bands representing short fragments of 100-200 bp that appeared in the lanes of the two PD controls but not in the AP control. Laddered banding patterns were also observed in the negative and no template controls, but they differed from those of the positive controls and were therefore considered unspecific.

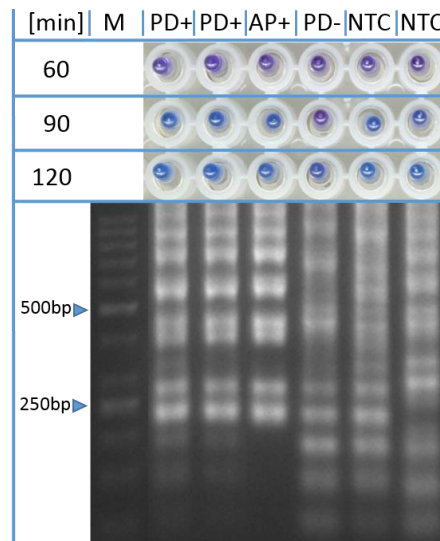


Figure 19: LAMP with primer set pnp after 60, 90 and 120 min of incubation at 63 °C. M = size marker; PD+ = PD positive control; AP+ = AP positive control; PD- = PD negative control; NTC = no template control. Dye: HNB.

In a second experiment, the incubation temperature was raised by 1 °C in order to avoid unspecific amplifications in negative and no template controls. A 10-fold dilution series of a DNA extract derived from a PD infected pear maintained in the greenhouse was tested in addition to the controls (Figure 20). Reaction tubes were scanned at 60, 90 and 120 min of incubation. After 60 min of incubation, only the PD positive control showed a colour change to dark blue. After further 30 min, the PD and AP positive controls had turned to light blue.

Results

However, the dilution series was positive at dilutions 1:10 and 1:1,000, while the dilution 1:100 did not show any colour change. At a final reaction time of 120 min, the dilution 1:100 still remained purple, signaling a failure of amplification, whereas the no template control showed a colour change to blue. Subsequent agarose gel electrophoresis revealed specific banding patterns only in the PD and AP positive controls. Unspecific laddering was observed in all samples of the dilution series including the undiluted DNA extract, as well as in the no template control.

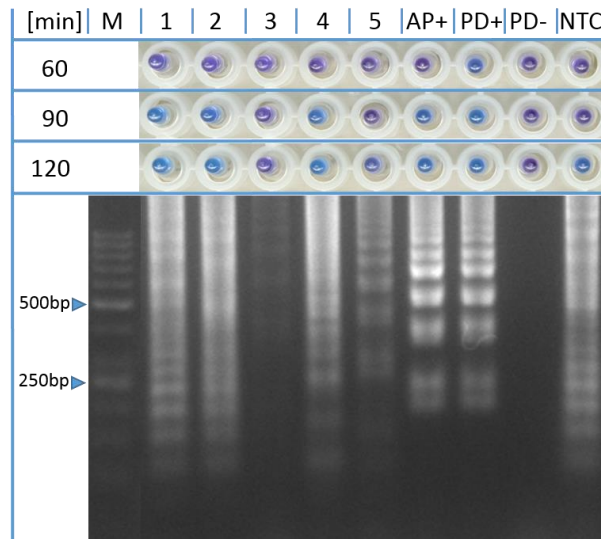


Figure 20: LAMP with primer set pnp after 60, 90 and 120 min of incubation at 64 °C. M = size marker; 1-5 = dilution series of a PD-positive DNA extract (1 = undiluted; 2 = diluted 1:10; 3 = diluted 1:100; 4 = diluted 1:1,000; 5 = diluted 1:10,000); AP+ = AP positive control; PD+ = PD positive control; PD- = negative control; NTC = no template control. Dye: HNB.

The dilution series was tested again with a LAMP reaction temperature of 65 °C. The controls used in the previous experiment were substituted with diluted NaOH homogenates derived from the same healthy and PD infected pear *in vitro* cultures, which provided the DNA extracts used as controls in LAMP and PCR (for details on the NaOH-based sample preparation method, see chapter 3.4 “Development of a simplified sample preparation procedure”). The presence and absence of the pathogen in the positive and negative control, respectively, was confirmed by LAMP with primer set PD3.

After 60 min of incubation, no colour change was visible (data not shown). While after 90 min, only the 1:1,000 dilution as well as the no template control showed a faint colour change, dilutions up to 1:1,000 had turned blue after 120 min of incubation. However, the positive control stayed purple whereas the negative and no template controls showed a definite colour change (Figure 21). Agarose gel electrophoresis of the amplification products revealed unspecific banding patterns in the dilutions indicated as positive by the colour change, except the 1:10 dilution, which showed a banding pattern resembling that of successfully amplified positive controls in the first two experiments. Amplification of the positive control had failed. The negative and no template controls showed unspecific laddering on the agarose gel.

Results

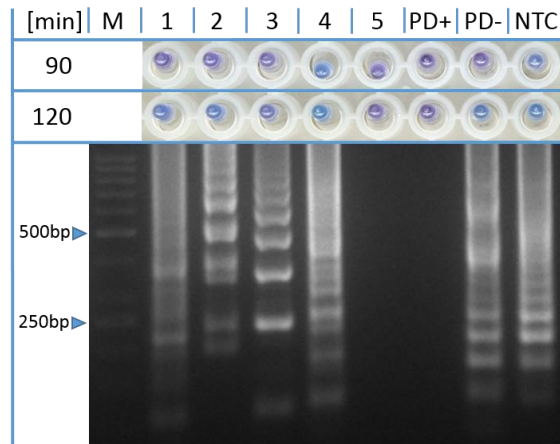


Figure 21: LAMP with primer set pnp after 90 and 120 min of incubation at 65 °C. M = size marker; 1-5 = dilution series of a PD-positive DNA extract (1 = undiluted; 2 = diluted 1:10; 3 = diluted 1:100; 4 = diluted 1:1,000; 5 = diluted 1:10,000); PD+ = PD positive control; PD- = negative control; NTC = no template control. Dye: HNB.

Since the pnp primer set performed poorly with the reaction conditions optimized for the 16S rRNA primer sets, it was attempted to increase amplification efficiency with raised concentrations of magnesium sulfate (+ 2 mM), dNTPs (+ 0.6 mM) and a reduced betaine concentration (- 0.2 M). This reaction mix composition was tested with a 10-fold dilution series of a PD positive control. In order to compare LAMP performances of primer sets pnp and PD3, respectively, the dilution series was also tested with the primer set PD3 in the same reaction mix composition (Figure 22). Dilutions and controls were tested in duplicates.

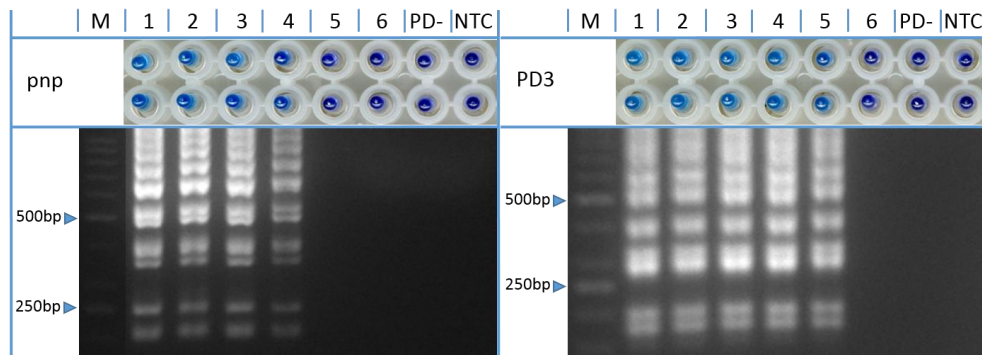


Figure 22: Evaluation of the detection limit of LAMP with primer set pnp (left) in comparison to primer set PD3 (right). M = size marker; 1-6 = dilution series of a PD-positive DNA extract (1 = undiluted; 2 = diluted 1:10; 3 = diluted 1:100; 4 = diluted 1:1,000; 5 = diluted 1:10,000; 6 = diluted 1:100,000); PD- = negative control; NTC = no template control. Dye: HNB.

LAMP with primer set pnp successfully amplified the diluted DNA extract to 1:1,000 after 90 min of incubation. LAMP with primer set PD3 showed a 10-fold higher sensitivity as well as a higher reaction speed, requiring only 60 min to yield a colour change in both replicates of the 1:10,000 dilution. Subsequent agarose gel electrophoresis confirmed the results as indicated by the colour change. No unspecific or false positive amplifications of the two primer sets were

observed in this experiment. However, due to the poor performance of the primer set pnp in comparison to PD3, further experiments with this primer set were not conducted.

Primer set rpl22

Experiments with the primer set rpl22 were performed in parallel to the experiments with the primer set pnp. The first test was carried out at 63 °C, and reaction tubes were scanned after 60, 90 and 120 min of incubation. A positive control for AP was included in the experiment. After 120 min of incubation, no colour change was visible. Failed amplification was confirmed by subsequent agarose gel electrophoresis (Figure 23)

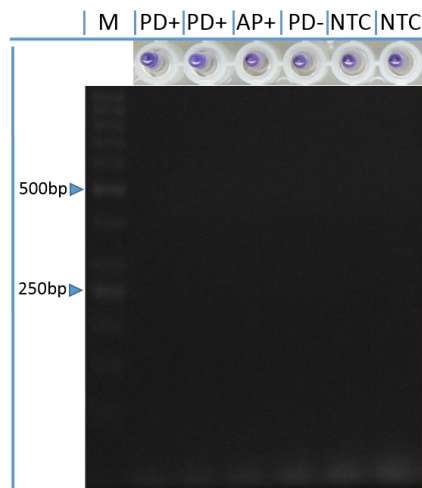


Figure 23: LAMP with primer set rpl22 after 120 min of incubation at 63 °C. M = size marker; PD+ = PD positive control; AP+ = AP positive control; PD- = PD negative control; NTC = no template control. Dye: HNB.

A second experiment was performed at a reaction temperature of 65 °C. A 10-fold dilution series of a DNA extract derived from a PD infected pear maintained in the greenhouse was tested in addition to the controls. The reaction tubes were scanned after 90 and 120 min, respectively (Figure 24). Again, no colour change was visible and no amplification products were observed on the agarose gel (data not shown).

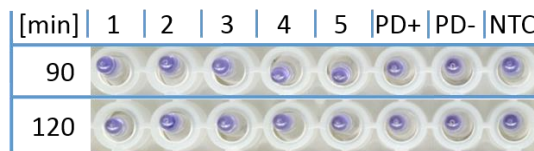


Figure 24: LAMP with primer set rpl22 after 90 and 120 min of incubation at 65 °C. 1-5 = dilution series of a PD-positive DNA extract (1 = undiluted; 2 = diluted 1:10; 3 = diluted 1:100; 4 = diluted 1:1,000; 5 = diluted 1:10,000); PD+ = PD positive control; PD- = negative control; NTC = no template control. Dye: HNB.

Along with the primer sets pnp and PD3, the primer set rpl22 was tested in a modified reaction mix with altered magnesium sulfate, dNTP and betaine concentrations as described above. The experiment included PD controls as well as a 10-fold dilution series of a PD positive control.

Results

LAMP reactions were incubated at 65 °C. The experiment was terminated after 90 min. As figure 25 shows, LAMP with primer set rpl22 did neither amplify the PD positive control nor any of the dilutions, as indicated by the absence of a colour change and confirmed by subsequent agarose gel electrophoresis. Work with this primer set was discontinued after the third unsuccessful experiment.

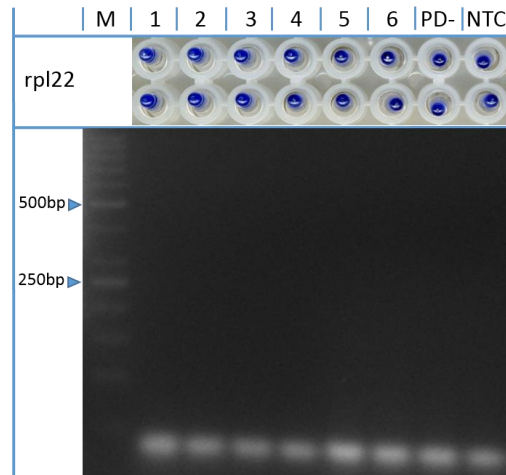


Figure 25: LAMP with primer set rpl22 with enhanced magnesium sulfate and dNTP concentrations and reduced betaine concentration after 90 min of incubation at 65 °C. M = size marker; 1-5 = dilution series of a PD-positive DNA extract (1 = undiluted; 2 = diluted 1:10; 3 = diluted 1:100; 4 = diluted 1:1,000; 5 = diluted 1:10,000; 6 = diluted 1:100,000); PD- = negative control; NTC = no template control. Dye: HNB.

3.4 Development of a simplified sample preparation procedure

First experiments with crude plant extracts were performed with the primer set PD1, published by Obura et al. (2011). Since homogenization of leaf tissues in distilled water and subsequent dilution of these homogenates according to Hadersdorfer et al. (2011) worked well with the PPV LAMP established at our institute, it was attempted to adopt this procedure for the PD LAMP. From shoots used in an inoculation trial for artificial inoculation of pears with the PD phytoplasma, bark including the phloem tissue was decorticated with a razor blade and placed in filter extraction bags (Bioreba, Reinach, Switzerland). After addition of about 1 ml distilled water per 100 mg plant tissue, the samples were homogenized with a Homex-6 machine (Bioreba, Reinach, Switzerland). About 1.5 ml of the resulting homogenate was transferred into a 2 ml reaction tube and centrifuged for 2 min at 13,000 rpm. One hundred μ l of the supernatant was transferred into a new 1.5 ml reaction tube and 900 μ l distilled water was added to obtain a 1:10 dilution. Two μ l of the diluted homogenate was subjected to LAMP. After 2 hours of incubation at 63 °C, all water-based preparations were negative. Conventional DNA extraction (DNeasy Plant Mini Kit, Qiagen) from the same shoots and subsequent testing with the PD LAMP yielded positive results for all samples (Figure 26).

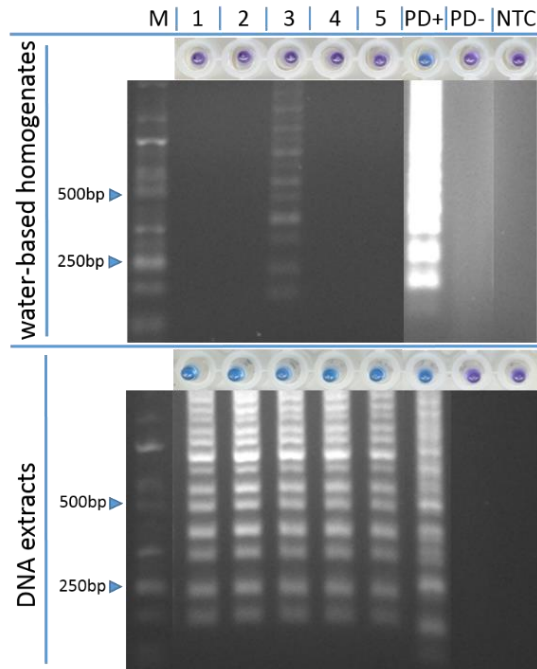


Figure 26: LAMP reactions with primer set PD1 and samples prepared by water-based homogenization according to Hadersdorfer et al. (2011) as well as with DNA extracted by DNeasy Plant Mini Kit. Plant material of samples no. 1-5 was divided between water-based homogenization and conventional DNA extraction. M = Size marker; PD+ = PD positive control; PD- = PD negative control; NTC = No template control. Dye: HNB.

There were two possible reasons for the failure of LAMP to amplify from the water preparations:

- (1) The water extract from pear bark contained substances inhibiting the *Bst* DNA polymerase.
- (2) The amount of phytoplasma DNA was too low to be detected by LAMP.

In order to test hypothesis (1), the 10-fold diluted homogenate of sample no. 2 was supplemented with the respective DNA extract, which had been tested positive in the previous experiment, in a ratio of 10:1. Additionally, a further 10-fold dilution was tested, resulting in a final dilution of 1:100 of the water extract. A plum sample prepared with the water extraction method and mixed with a DNA extract positive for PD was included. Figure 27 shows the results. The amplification was clearly inhibited by the pear homogenate at any dilution, but not by the plum homogenate. The pear water extract mixed with DNA yielded no amplification product. The plum sample enriched with a DNA extract positive for PD showed a positive amplification in LAMP, as indicated by a colour change of the reaction solution to blue. Results were confirmed by subsequent agarose gel electrophoresis.

Results

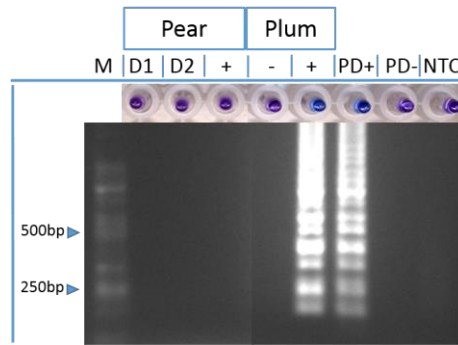


Figure 27: LAMP inhibition by crude sample preparations from pear, but not from plum. A PD positive DNA extract was supplemented with diluted plant sap from pear or plum, respectively. Pear D1 = Crude plant sap diluted 1:10; Pear D2 = Crude plant sap diluted 1:100; Pear + = crude plant sap diluted 1:10, supplemented with the PD positive DNA extract of the same sample; Plum - = crude plant sap from plum diluted 1:10; Plum + = crude plant sap from plum diluted 1:10, supplemented with the PD positive DNA extract derived from the pear sample; M = Size marker; NTC = No template control; PD+ = PD positive control; PD- = PD negative control. Primer set PD1; dye: HNB.

Since water based homogenates of pear leaves impaired the LAMP reaction, homogenization in a suitable buffer was the next attempt to create a simplified extraction procedure. Two solutions were chosen for a first test: (1) Cetyltrimethylammonium bromide (CTAB) buffer, widely used for homogenization of plant tissues. CTAB forms complexes with genomic DNA. Because polysaccharides are insoluble in CTAB-containing lysates at high salt concentrations, they can be removed from the solution by centrifugation. (2) Sodium hydroxide (NaOH) solution, proposed by Wang et al. (1993) for a simplified plant sample preparation intended for subsequent PCR analysis. At first, the solutions to be tested were examined for their influence on the colour of the LAMP reaction mix. To 23 μ l of LAMP reaction mix, 2 μ l of 0.5 M NaOH or CTAB buffer (without mercaptoethanol) at different dilutions were added, respectively. A control containing 2 μ l of water was included in the experiment. The result is shown in figure 28.



Figure 28: Influence of CTAB and NaOH on the colour of LAMP reaction solutions with HNB. Two μ l of the test solution was added to 23 μ l of LAMP reaction solution. Test solution no. 1 = CTAB diluted 1:100 with water; 2 = CTAB diluted 1:10 with water; 3 = CTAB undiluted; 4 = NaOH (0.5 M) diluted 1:10 with water; 5 = NaOH (0.5 M) diluted 1:10 with Tris-HCl (pH 8.8; 100 mM); 6 = NaOH (0.5 M) diluted 1:100 with water; 7 = NaOH (0.5 M) diluted 1:100 with Tris-HCl (pH 8.8; 100 mM).

While CTAB buffer caused an immediate colour change to blue at any dilution, the NaOH variants did not cause a colour change to blue in the reaction solutions, indicating that they did not interact with the metal indicator or the magnesium ions. However, colours of NaOH-containing LAMP reaction solutions appeared brighter than the water-containing control, rather magenta than purple, which might have been due to an altered reaction solution pH.

Results

Further tests confirmed that 0.5 M NaOH solutions diluted with water and supplemented with DNA extracts did not interfere with DNA amplification in LAMP (data not shown). For the treatment of plant tissues with NaOH, the homogenization procedure of Hadersdorfer et al. (2011) was adopted with minor modifications. Instead of water, 0.5 M NaOH solutions were used for homogenization of pear samples in filter extraction bags. The resulting homogenate was transferred to a 1.5 ml reaction tube and diluted without prior centrifugation. Two μ l of the diluted homogenate was subjected to LAMP. The first test with NaOH-treated field samples from material that had been tested positive in earlier experiments showed sporadic amplification products in homogenates, which were diluted 1:100 with either Tris-HCl (pH 8.8) or distilled water, but not with homogenates diluted 1:10. Additionally, positive samples derived from leaves while bark samples were not amplified. The 0.5 M NaOH solution seemed appropriate for treatment of leaves, as reported by Wang et al. (1993), but not for bark, as indicated by the failure of LAMP to generate amplification products from the bark samples treated with 0.5 M NaOH (Figure 29).

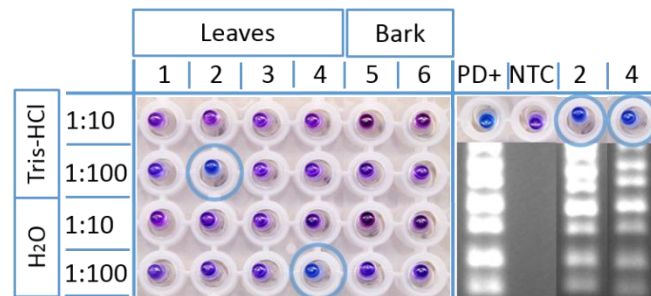


Figure 29: Influence of the diluent and the dilution step on the formation of amplification products from NaOH-treated samples in LAMP reactions with primer set PD1. Crude NaOH homogenates of pear leaves (Samples no. 1-4) or bark (samples no. 5-6) were diluted 1:10 or 1:100 with either Tris-HCl (pH 8.8) or distilled water. All samples were negative except the encircled samples no. 2 and 4. Results of agarose gel electrophoresis of these samples together with the controls are given on the right. PD+ = PD positive control; NTC = No template control. Dye: HNB.

Remaining material of two leaf samples and one bark sample tested in the previous experiment was used to investigate the influence of NaOH concentration applied in the homogenization of leaf and bark tissues on LAMP performance (Figure 30). The sample material was split and treated with 0.1 M, 0.3 M and 0.5 M NaOH, respectively. Since 1:10 dilutions were not amplified in the previous experiment, the dilutions tested in this experiment were 1:50 and 1:100 with either distilled water or Tris-HCl (pH 8.8). The best result for the bark sample was achieved with the lower NaOH concentrations at a dilution of 1:100 with water. LAMP products from leaf samples were generated preferentially when the samples were treated with 0.5 M NaOH.

However, the colour of the reaction mixes containing the samples was slightly impaired in both experiments because the homogenates were not centrifuged prior to dilution, which resulted in brownish or greenish solutions that more or less stained the reaction mixes. The negative control

Results

was false positive in both runs, hence presumably contaminated (data not shown). It was therefore replaced in further experiments.

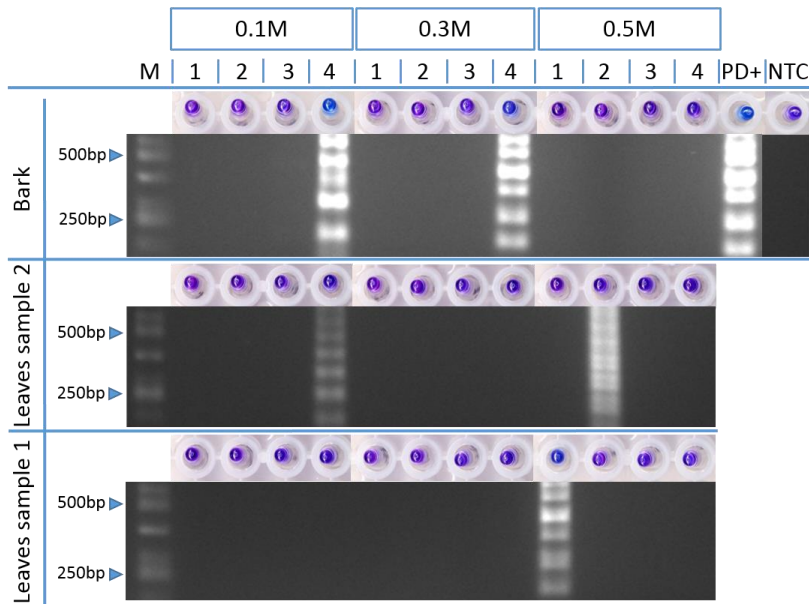


Figure 30: Influence of NaOH concentration on the formation of amplification products from NaOH-treated bark and leaf samples in LAMP reactions with primer set PD1. NaOH concentrations used for tissue homogenization are given in the headline boxes. 1 = crude plant sap diluted 1:50 with Tris-HCl; 2 = diluted 1:100 with Tris-HCl; 3 = diluted 1:50 with distilled water; 4 = diluted 1:100 with distilled water; PD+ = PD positive control; NTC = No template control. Dye: HNB.

After these first, promising experiments, the Obura-primer set was discarded (for details, see chapter 3.1.1 “Experiments with a primer set published by Obura et al. (2011)”) and work was continued with the newly designed primer set PD3. Very early in the optimization process with these primers, the last NaOH experiment, extended by centrifugation of the homogenates for 2 min at 13,000 rpm prior to dilution, was repeated and despite the frequent occurrence of false positives in controls, NaOH-treated samples showed amplification products in distinct variants and dilutions only (Figure 31). The tendency observed earlier that low NaOH concentrations were suitable for bark samples while higher NaOH concentrations served better for leaf samples was supported. Furthermore, dilution of the homogenates with Tris-HCl (pH 8.8) was less appropriate to support amplification in LAMP, whereas dilution with water worked best at factor 1:100. The newly implemented centrifugation step of the crude homogenates led to dilutions which did no longer stain the LAMP reaction mixes.

Results

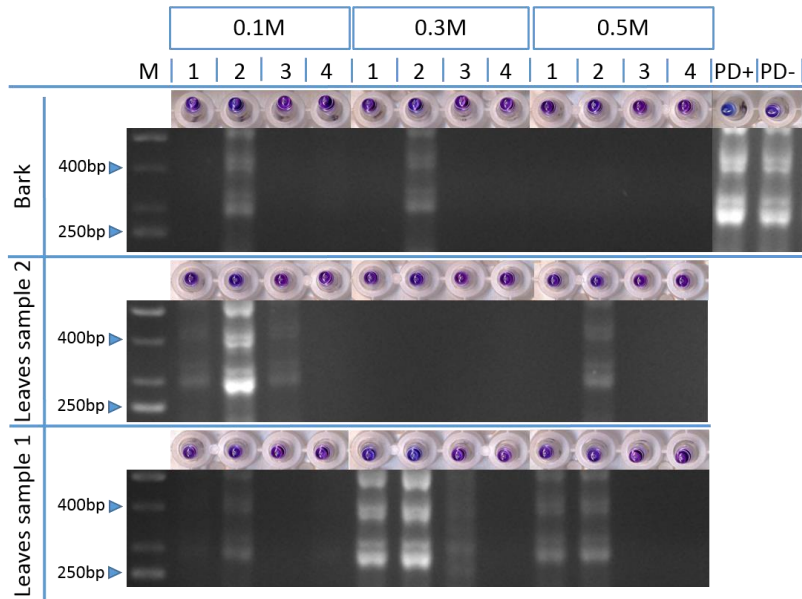


Figure 31: Influence of NaOH concentration on the formation of amplification products from NaOH-treated bark and leaf samples in LAMP reactions with primer set PD3. NaOH concentrations used for tissue homogenization are given in the headline boxes. 1 = crude plant sap diluted 1:50 with distilled water; 2 = diluted 1:100 with distilled water; 3 = diluted 1:50 with Tris-HCl; 4 = diluted 1:100 with Tris-HCl; PD+ = PD positive control; PD- = negative control (false positive). Dye: HNB.

After optimization of the PD3 LAMP, the next step was the tentative application of the NaOH-based sample preparation method to a larger bulk of samples. For this purpose, material of ten field samples from a pear orchard presumably affected by pear decline (located near Lake Constance, Baden-Württemberg, Germany) was processed with the NaOH sample preparation method as well as the DNeasy Plant Mini Kit (Qiagen) as reference method, respectively. Bark and leaves were processed separately. From leaves, midribs and petioles were used for extraction. Leaf material was treated with 0.5 M NaOH solution in the NaOH-based sample preparation variant. Bark was treated with 0.1 M NaOH solution. The resulting homogenates were centrifuged and diluted 1:100 with distilled water. Diluted homogenates were subjected to LAMP with primer set PD3. Reactions of this run were incubated for 90 min because there was no colour change observable in the samples after 60 min. A nested PCR with the primer pair P1/P7 in first round PCR and U3/U5 in second round PCR did not amplify any of the NaOH extracts (data not shown). DNA extracts prepared with the DNeasy Plant Mini kit were tested with LAMP and PCR with the primer pair fo1/rO1. For LAMP reactions with the DNA extracts, 60 min of incubation were sufficient to produce a definite colour change. Figure 32 shows the results of LAMP and PCR for both extraction methods.

Results

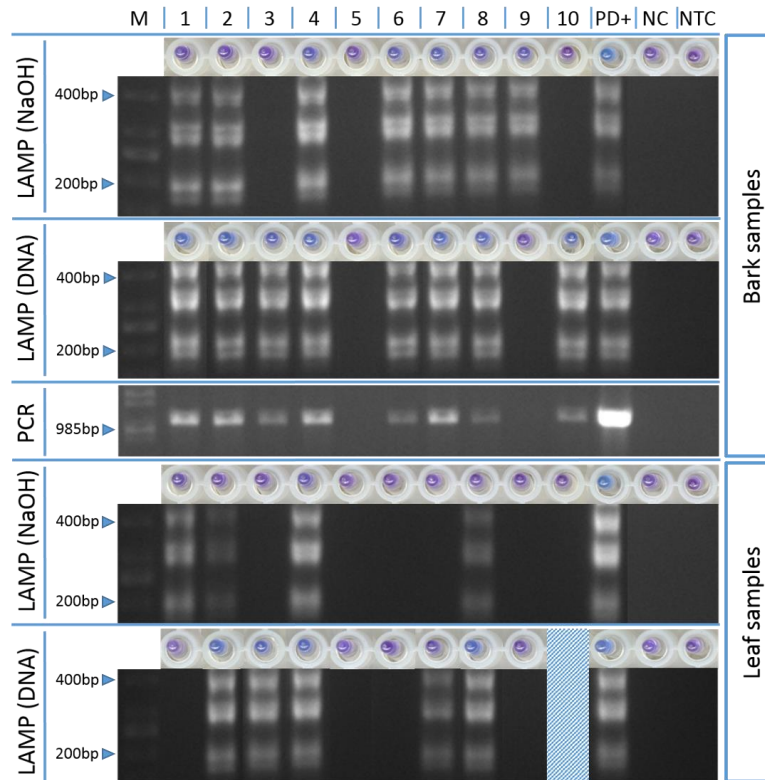


Figure 32: Application of the NaOH-based sample preparation method to field samples with suspected PD infestation. Sample material of leaves or shoots, respectively, was divided between conventional DNA extraction (DNeasy Plant Mini Kit) and the NaOH sample preparation method. DNA extracts and diluted homogenates were subjected to LAMP with primer set PD3. DNA extracts were as well tested with conventional PCR with primers fo1/rO1 (DNA extracts from leaves were negative in PCR, data not shown). 1-10 = field samples; PD+ = PD positive control; NC = negative control; NTC = No template control. Blue-shaded column: Leaf sample no. 10 was not subjected to conventional DNA extraction due to shortage of sample material. Dye: HNB.

The results for bark samples extracted with the DNeasy Plant Mini Kit (Qiagen) agreed to 100 % when tested with either LAMP or PCR. In total, eight out of ten samples yielded positive results. DNA extracts of leaf samples yielded no amplification products in PCR (data not shown). In LAMP, five out of ten leaf samples extracted with the DNeasy Plant Mini Kit were tested positive. They all derived from shoots whose bark samples showed positive results in PCR as well as LAMP. NaOH-treated bark samples yielded seven, leaf samples four positive results in LAMP. A comparison of LAMP results of NaOH preparations and DNA extracts showed concordant results for seven out of ten bark samples and six out of nine leaf samples (one leaf sample was treated with NaOH only because of shortage of sample material). Inconsistent results were obtained from three bark samples and three leaf samples, with both tissue types yielding two false negatives and one false positive in their NaOH preparations, respectively.

In order to exclude in prospective experiments the possibility that false negative results were caused by the absence of DNA in NaOH-based homogenates, a LAMP on the plant cytochrome oxidase gene (COX) according to Tomlinson et al. (2010a) was implemented as internal control

Results

assay. The original reaction mix composition published in Tomlinson et al. (2010a) was extended by the metal indicator HNB to sustain the field applicability of the test procedure. Further optimization of reaction conditions was not required. Samples derived from a PD inoculation trial were prepared with the NaOH extraction method and tested with the PD LAMP assay. The modified COX LAMP served as internal control for the NaOH extraction method. Diluted homogenates were subjected to LAMP immediately or after storage in a freezer for a maximum of seven days. In total, 339 leaf samples from sprouted inoculation scions and shoots of test cultivars were analyzed with the PD LAMP. The presence of DNA in the diluted homogenates was verified with COX LAMP. Twelve out of 339 (3.54 %) samples yielded negative results in the COX LAMP assay and were therefore excluded from further analysis. However, only four samples amplified in the PD LAMP assay. Figure 33 shows an example of the COX LAMP performed in the large scale testing described above. Except the water containing no template control, all samples showed a bright colour change to blue and a specific banding pattern on the agarose gel, corresponding to the pattern of the DNA extract, which served as positive control.

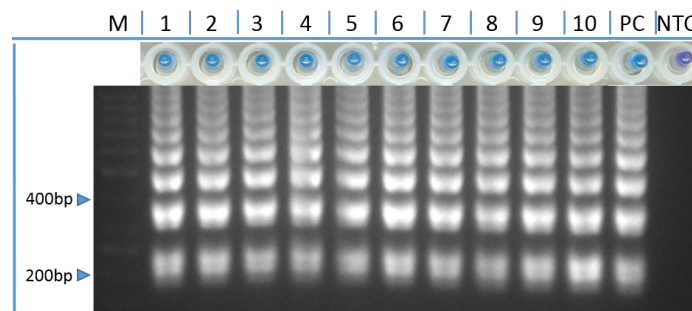


Figure 33: COX LAMP as internal control assay for the NaOH-based sample preparation method. M = size marker; 1-10 = Leaf samples prepared with the NaOH extraction method; PC = positive control; NTC = no template control. Dye: HNB.

In order to examine if the NaOH extraction method together with the PD LAMP assay were applicable to the two closely related phytoplasmas infecting temperate fruit trees, AP phytoplasma and ESFY phytoplasma, an experiment was conducted with samples kindly provided by Dietlinde Reißler and Michael Petruschke (LTZ Augustenberg, Germany). In total, samples from roots, shoots and leaves of seven apple trees with known AP infection and one apricot infected with ESFY were prepared with 0.1 M NaOH for bark of shoots and roots as well as feather roots, and 0.5 M NaOH for midribs and petioles of leaves. Crude homogenates were diluted 1:100 with distilled water and subjected to PD LAMP and COX LAMP (Figure 34). NaOH extraction was successful as proven by COX LAMP with positive results for all samples tested. PD LAMP yielded positive results for all root and leaf samples and five out of seven shoot samples from apple. Shoot and leaf samples from apricot did not yield LAMP products. The root sample from apricot, however, gave a positive result in PD LAMP. Subsequent agarose gel electrophoresis confirmed the results as indicated by the colour change of the LAMP reactions (data not shown).

Results

The applicability of the PD LAMP assay in combination with the NaOH sample preparation method to apple proliferation samples was further evaluated in an interlaboratory experiment in collaboration with the LTZ Augustenberg (Germany). Results of this experiment are given in chapter 3.5 “Detection range: Applicability of the PD LAMP to other members of the 16SrX group”.

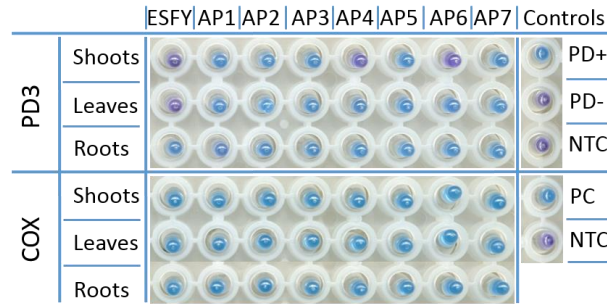


Figure 34: Evaluation of the applicability of the NaOH-based sample preparation method and subsequent PD LAMP for the detection of the AP and ESFY phytoplasmas. COX LAMP served as internal control. Shoots, leaves and roots of each sample were processed separately. ESFY = sample from apricot infected with the ESFY phytoplasma; AP1-7 = samples from apple trees infected with the AP phytoplasma. The processed tissue type is given on the left. Controls for the PD LAMP assay: PD+ = PD positive control; PD- = PD negative control; NTC = no template control. Controls for the COX LAMP assay: PC = positive control; NTC = no template control. Dye: HNB.

Since the tested DNA extracts and NaOH preparations did not originate from exactly the same material, there was a possibility that phytoplasmas at a low titer were detectable in one half of the sample and in the other one not. In order to overcome the problem that LAMP results of NaOH-treated samples were not verifiable with PCR, two commercially available Direct PCR kits, the Kapa3G Plant PCR Kit (Peqlab) and the Phire Plant Direct PCR Kit (Thermo Scientific) were tested for their applicability to NaOH extracts. Both kits utilize artificially modified DNA polymerases, which exhibit a high tolerance towards common PCR inhibitors present in plants. Two NaOH samples from the interlaboratory experiment with apple proliferation samples, described in chapter 3.5 “Detection range: Applicability of the PD LAMP to other members of the 16SrX group”, one positive and one negative, as well as three pear samples from the inoculation trial, one positive, one negative and one with inconsistent results, were chosen for a first test, together with conventionally extracted controls derived from *in vitro* plants. All samples were tested at the standard dilution of 1:100 applied in LAMP tests. The positive pear sample and the positive apple sample were tested additionally as 1:10 dilution of the crude homogenate. PCR was performed with the primer pair fO1/rO1. Reaction mixes were prepared according to the manufacturers instructions. Results are shown in figure 35. While the Kapa3G Plant PCR Kit (Peqlab) only amplified the target in the positive pear sample at a dilution of 1:100, the Phire Plant Direct PCR Kit (Thermo Scientific) yielded positive results for the positive apple proliferation sample and the positive pear sample, for both 1:10 and 1:100 dilutions, respectively. Negative samples as well as the one sample with inconsistent results in previous tests were negative. Controls were clean in both variants.

Results

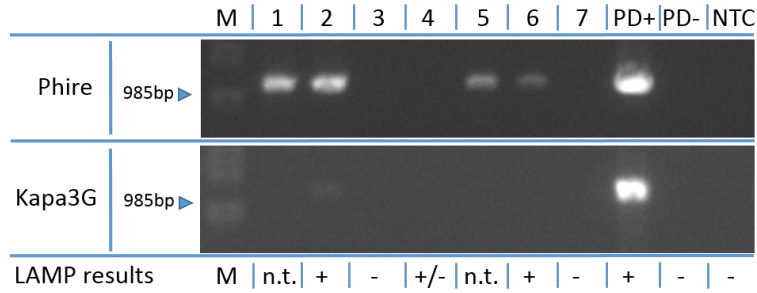


Figure 35: Evaluation of commercially available Direct PCR kits for the detection of 16SrX phytoplasmas in NaOH-based sample preparations. The applied kits are given on the left: Phire = Phire Plant Direct PCR Kit (Thermo Scientific); Kapa3G = Kapa3G Plant PCR Kit (Peqlab). Previous LAMP results of the tested samples are given below the PCR results (n.t. = 1:10 dilutions were not tested with PD LAMP). M = size marker; 1 = PD positive pear sample diluted 1:10; 2 = PD positive pear sample diluted 1:100; 3 = PD negative pear sample; 4 = pear sample with inconsistent results in previous experiments; 5 = AP positive apple sample diluted 1:10; 6 = AP positive apple sample diluted 1:100; 7 = AP negative apple sample; PD+ = PD positive control; PD- = PD negative control; NTC = no template control.

In order to evaluate the consistency of results of PD LAMP and Direct PCR for samples prepared with the NaOH extraction method, 40 individual *in vitro* cultured plants, of which 10 were healthy 'Williams' pears and 30 belonged to a culture used to maintain the PD agent, were treated with the NaOH sample preparation method and subjected to PD LAMP and Direct PCR with the primer pair fO1/rO1 using the Phire Plant Direct PCR Kit (Thermo Scientific). LAMP results were judged by the colour change of the metal indicator dye Eriochromeblack-T (ErioT). Results of PD LAMP and Direct PCR are presented in figure 36.

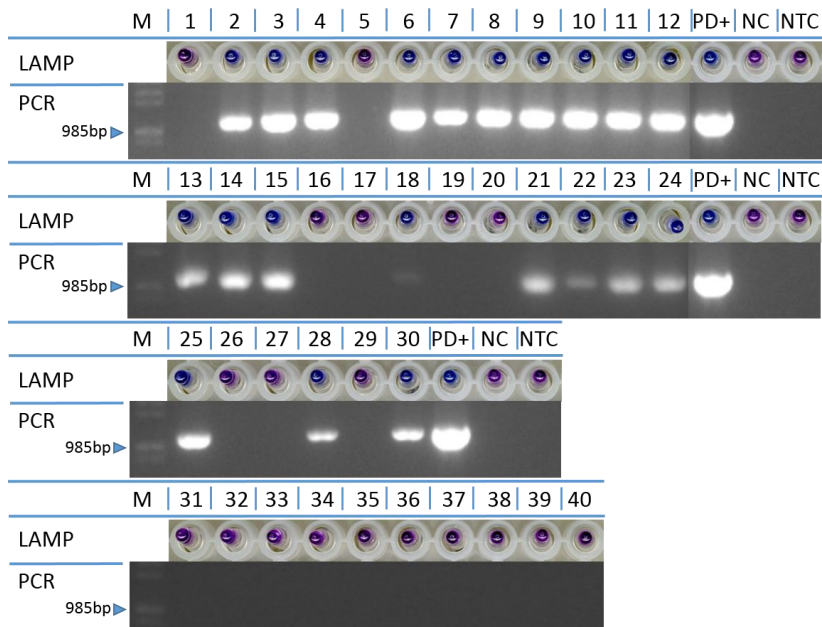


Figure 36: PD LAMP and Direct PCR results for NaOH-treated pear samples. M = size marker; 1-30 = *in vitro* pear plants with expected PD infection; 31-40 = healthy *in vitro* pear plants. PD+ = PD positive control; PD- = PD negative control; NTC = no template control. LAMP dye: ErioT.

Results of PD LAMP and Direct PCR matched 100 %. Out of 30 pears with expected PD infection, 21 proved to be positive in LAMP and PCR. Sample no. 18 yielded only a weak band in PCR, but produced a definite colour change in LAMP, indicating that LAMP was able to efficiently generate high product amounts from low titers of pathogen DNA in the diluted homogenate. All samples from healthy pears were negative.

3.5 Detection range: Applicability of the PD LAMP to other members of the 16SrX group

The highly conserved nature of the 16S rRNA gene among members of the apple proliferation group made a successful detection of these close relatives of the pear decline phytoplasma with LAMP primers targeting the PD 16S rRNA gene most likely. Since the applicability of the PD3 LAMP to apple proliferation samples was confirmed during the optimization process, an inter-laboratory test series was performed in cooperation with the Center for Agricultural Technology Augustenberg (LTZ Augustenberg, Baden-Württemberg, Germany) to compare the assay performances of LAMP, PCR and nested PCR in combination with different DNA extraction methods. Samples were taken by employees of the LTZ Augustenberg from roots, shoots and leaves of apple trees repeatedly tested for the presence or absence of the AP phytoplasma and sent as blind samples to the laboratory of the LTZ plant health department as well as to the laboratory of the Associate Professorship of Fruit Science of the TUM. In the LTZ laboratory, samples were treated with a conventional DNA extraction method including a phytoplasma enrichment step and subsequently tested with nested PCR for the presence of the AP phytoplasma. In the TUM laboratory, the sample material was divided between DNA extraction with the DNeasy Plant Mini Kit (Qiagen) and the simplified sample preparation method with NaOH. DNA extracts were tested with PD LAMP as well as PCR with the primer pair fO1/rO1. NaOH extracts were tested with LAMP only because the Direct PCR protocol was not yet established at the time of this experiment. In total, 32 samples were analyzed. Detailed results from both laboratories and the expected results based on previous tests are presented in table 6. DNA extracts prepared with the DNeasy Plant Mini Kit (Qiagen) and tested with LAMP yielded the same results as those obtained in the laboratory of the LTZ Augustenberg with conventional DNA extraction and nested PCR. LAMP on NaOH-treated samples showed three divergent results from those of nested PCR, one false negative and two false positives. However, one of the two false positive samples did not show a colour change but a weak laddering on the agarose gel. In this case, a contamination derived from the adjacent positive control during application of the samples to the agarose gel is likely. Both false positive samples were tested again and yielded negative results which indicates a pipetting error or another handling mistake rather than an error of the LAMP method itself. PCR with the primer pair fO1/rO1 on the DNA extracts showed six divergent results as compared to nested PCR, out of which five were false negatives and one was false positive. The results obtained by nested PCR differed from the expected outcome in 4 out of 32 samples. However, results of conventional PCR as well as LAMP assays with both extraction methods were in perfect agreement with nested PCR results

Results

in these samples. Consequently, these results were considered as true negatives or true positives, respectively.

Table 6: Results of the interlaboratory test series for the comparison of assay performances of LAMP, PCR and nested PCR in combination with different DNA extraction methods for the detection of the AP phytoplasma.

Sample No.	Type	expected	Nested PCR	LAMP (NaOH)	LAMP (DNA)	PCR
1	Shoot	+	+	-	+	-
2	Shoot	+	+	+	+	+
3	Shoot	+	+	+	+	+
4	Shoot	+	+	+	+	+
5	Shoot	+	-	-	-	-
6	Shoot	+	+	+	+	+
7	Shoot	+	+	+	+	+
8	Shoot	-	-	-	-	-
9	Shoot	-	-	-	-	-
10	Shoot	-	-	-	-	-
11	Shoot	-	-	-	-	-
12	Root	+	+	+	+	-
13	Root	+	+	+	+	-
14	Root	+	+	+	+	+
15	Root	+	+	+	+	-
16	Root	+	+	+	+	+
17	Root	+	+	+	+	+
18	Root	-	+	+	+	+
19	Root	-	-	-	-	-
20	Root	-	-	+	-	-
21	Root	-	-	-	-	-
22	Leaf	+	-	-	-	-
23	Leaf	+	+	+	+	+
24	Leaf	+	+	+	+	+
25	Leaf	+	+	+	+	+
26	Leaf	+	-	-	-	-
27	Leaf	+	+	+	+	-
28	Leaf	+	+	+	+	+
29	Leaf	-	-	-	-	-
30	Leaf	-	-	-	-	-
31	Leaf	-	-	-	-	+
32	Leaf	-	-	+	-	-

Based on the results of this comparative trial, the diagnostic sensitivity and specificity of the LAMP assay for the detection of the apple proliferation phytoplasma were calculated according to Altman and Bland (1994). In this approach, sensitivity is defined as the proportion of true positives, which are detected as positive by the assay in question. Specificity is defined as the proportion of true negatives, which are identified as negative by the assay. Tables 7 and 8 show

Results

the results. True positives and true negatives were determined based on nested PCR results. Diagnostic sensitivity as well as specificity of the LAMP assay in combination with DNA extraction using the DNeasy Plant Mini Kit (Qiagen) were 100 % (Table 7). NaOH-treated samples yielded contradictory results in 3 out of 32 samples. Consequently, the calculated diagnostic sensitivity of the LAMP assay in combination with the NaOH-based sample preparation procedure was 94.4 % and the diagnostic specificity was 85.7 % (Table 8).

Table 7: Diagnostic sensitivity and specificity of the PD LAMP for the detection of the AP phytoplasma in DNA extracts, calculated according to Altman and Bland (1994).

		Nested PCR	
		True positive	True negative
		18	14
LAMP (DNA)	Positive	18	0
	Negative	0	14
Sensitivity [%]	Pos.(LAMP)/True Pos.*100	100	
Specificity [%]	Neg.(LAMP)/True Neg.*100		100

Table 8: Diagnostic sensitivity and specificity of the PD LAMP for the detection of the AP phytoplasma in NaOH-based sample preparations, calculated according to Altman and Bland (1994).

		Nested PCR	
		True Positive	True Negative
		18	14
LAMP (NaOH)	Positive	17	2
	Negative	1	12
Sensitivity [%]	Pos.(LAMP)/True Pos.*100	94.4	
Specificity [%]	Neg.(LAMP)/True Neg.*100		85.7

The applicability of the PD LAMP assay for the detection of the European stone fruit yellows phytoplasma (ESFY) was evaluated with field samples derived from an orchard in Tyrol, Austria. The trees showed various ESFY symptoms including leaf roll and yellowing, except two trees, which were sampled as negative controls. A total of 66 leaf samples from 21 apricot trees, 3 peach trees, 2 nectarine trees and 2 Japanese plums were treated with the simplified sample preparation method and subjected to PD LAMP as well as Direct PCR with the primer pair fO1/rO1. LAMP was repeated two times, yielding identical results for 65 out of 66 samples. Results of LAMP and PCR agreed for 57 out of 66 samples. Nine samples yielded contradictory results, out of which were eight negative in PCR and positive in both LAMP replications. One sample showed a weak colour change in one LAMP replication but no colour change in the second replication. However, the specific laddering on the agarose gel was observed in both cases. The failure of the colour change in this sample may be due to low amounts of pathogen DNA close to the detection limit of the PD LAMP assay. Diagnostic sensitivity and specificity

were calculated according to Altman and Bland (1994) for ESFY detection by the PD LAMP assay (Table 9).

Table 9: Diagnostic sensitivity and specificity of the PD LAMP for the detection of the ESFY phytoplasma in NaOH-based sample preparations, calculated according to Altman and Bland (1994).

		Direct PCR	
		True Positive	True Negative
		29	37
LAMP (NaOH)	Positive	29	9
	Negative	0	28
Sensitivity [%]	Pos.(LAMP)/True Pos.*100	100	
Specificity [%]	Neg.(LAMP)/True Neg.*100		75.7

Diagnostic sensitivity amounted to 100 %, specificity to 75.7 %. However, seven out of eight samples, which yielded positive results in LAMP and negative results in Direct PCR, derived from trees with at least one further sample being consistently positive in all tests. This may indicate low pathogen amounts close to or beyond the detection limit of the applied PCR assay, or PCR inhibition due to secondary substances in the crude plant sap.

3.6 Colorimetric detection of LAMP products with Eriochromeblack-T

3.6.1 Evaluation of metal indicator dyes for colorimetric product detection in LAMP

The metal indicator hydroxy naphthol blue exhibited an unsteady performance in the PD LAMP assay over time, with strong variations in the ground colour of the reaction mix prior to incubation from purple to rather blueish staining. In consequence, the difference in the colour of negative and positive reactions was occasionally not as distinct as expected and in some cases, an agarose gel electrophoresis was necessary to determine the result. Figure 37 shows scans of LAMP reactions displaying a range of colours, which were performed within four weeks.

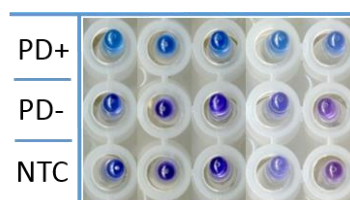


Figure 37: LAMP reactions with the metal indicator dye HNB displaying strong variations of the colour in negative and no template controls. PD+ = PD positive control; PD- = PD negative control; NTC = no template control.

Several alternative metal indicator dyes were examined for their applicability in LAMP: Eriochromeblack-T, Murexide, Thiazole yellow and Phthalein purple. The dyes were tested at a concentration of 120 μ M, except Murexide, which was tested at 120 μ M and 240 μ M. All other LAMP reaction components were held equal. Results of the first tests with Murexide,

Results

Thiazole yellow and Phthalein purple are presented in figure 38. Murexide and Phthalein purple were tested with controls in duplicates. Thiazole yellow was tested with a dilution series of the positive control.

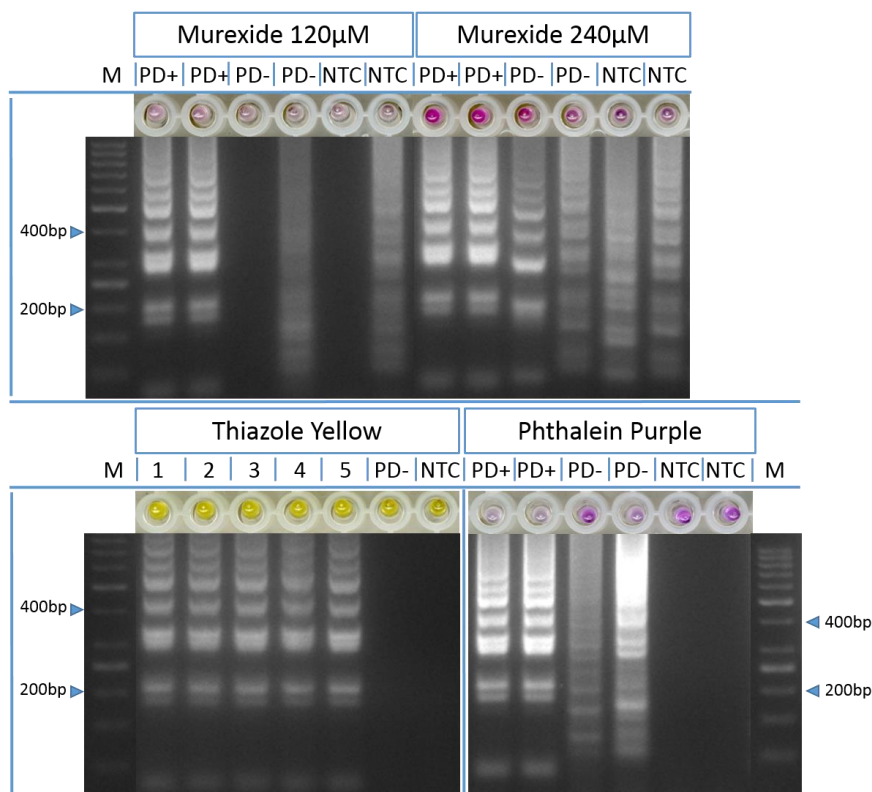


Figure 38: PD LAMP reactions with the metal indicator dyes Murexide, Thiazole yellow and Phthalein purple. M = size marker; PD+ = PD positive control; PD- = PD negative control; NTC = no template control; 1-5 = dilution series of a PD positive control (1 = diluted 1:10; 2 = 1:100; 3 = 1:1,000; 4 = 1:10,000; 5 = 1:100,000).

Murexide at a concentration of 120 µM did not respond to changes in the magnesium ion concentration caused by the LAMP reaction. The ground colour at this concentration was pale. Specific banding patterns were observed in the positive controls, indicating that Murexide did not impair the LAMP reaction. Unspecific laddering occurred in one negative control and one no template control, respectively. With 240 µM Murexide, positive controls and one negative control showed an intensification of the pink base colour as compared to no template controls. However, subsequent agarose gel electrophoresis revealed unspecific amplifications in all negative and no template controls. Specific amplification of the positive controls was confirmed.

Thiazole yellow did not change its colour although the LAMP reactions were not inhibited and turbidity was observed in positive reactions. Successful amplification of all dilutions of the dilution series was confirmed by subsequent agarose gel electrophoresis. The negative and no template controls were not amplified. Reducing the magnesium ion concentration in the reaction mix as well as enhancing the dye concentration did not enable a colour change of Thiazole yellow in positive LAMP reactions (data not shown).

Results

The metal indicator Phthalein purple was discoloured in successfully amplified positive controls. However, the ground colour of the LAMP reaction mix was pale, and unspecific amplification occurred in negative controls, which resulted in a weakening of the colour and in one case almost in a discolouration of the reaction solution.

Most promising results were obtained from a test with Eriochromeblack-T (ErioT), an azo dye commonly used for the determination of water hardness. Figure 39 shows the dyes HNB and ErioT by comparison in a dilution series of a PD-positive sample, with optimized reaction mixes for the respective dyes (in this experiment, the additive PEG 8k was used instead of betaine in both reaction mixes).

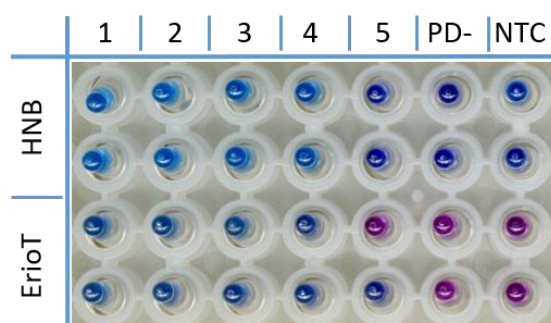


Figure 39: LAMP reactions with the metal indicator dyes hydroxy naphthol blue (HNB) and Eriochromeblack-T (ErioT). 1-5 = dilution series of a PD positive sample (1 = diluted 1:10; 2 = 1:100; 3 = 1:1,000; 4 = 1:10,000; 5 = 1:100,000); PD- = PD negative control; NTC = no template control.

The colours of positive and negative LAMP reactions with ErioT exhibited a higher contrast and were judged easier by the naked eye than the colours of corresponding LAMP reactions with HNB. The results as indicated by the colour change of ErioT were in perfect agreement with results of subsequent agarose gel electrophoresis (see figure 42, LAMP reactions with polyethylene glycol 8k). Sensitivity of the preparations was almost identical, confirming that ErioT did not impair the LAMP reaction. Unspecific laddering was observed in the no template controls of the HNB LAMP but not in the ErioT LAMP.

The concentration of ErioT was chosen equal to that of HNB because complexing behavior of both metal indicators was expected to be similar. Lowering the concentration of the dye resulted in weak colours although the colour change was well-defined (data not shown). Total magnesium ion concentration was readjusted to 4.8 mM per reaction in an experiment testing a 10-fold dilution series of a DNA extract derived from sample material of a pear *in vitro* culture used to maintain the PD phytoplasma (Figure 40). The dilutions were tested in duplicates. LAMP reaction mixes contained magnesium chloride in a concentration series from 4 mM to 6 mM per reaction in 0.4 mM steps. A concentration of 4.8 mM $MgCl_2$ in the reaction mix provided the highest sensitivity as well as a high contrast colour change between positive and negative reactions. At lower or higher magnesium chloride concentrations, assay sensitivity was considerably reduced. High magnesium ion concentrations caused dark blue colours in positive reactions and bright purple colours in negative reactions, whereas low magnesium ion

Results

concentrations resulted in light blue colours in positive reactions and dark, bluish stained purple colours of negative reactions. Based on 4.8 mM MgCl₂ as optimal concentration, the contrast of the colour change declined with increasing as well as decreasing magnesium chloride concentrations.

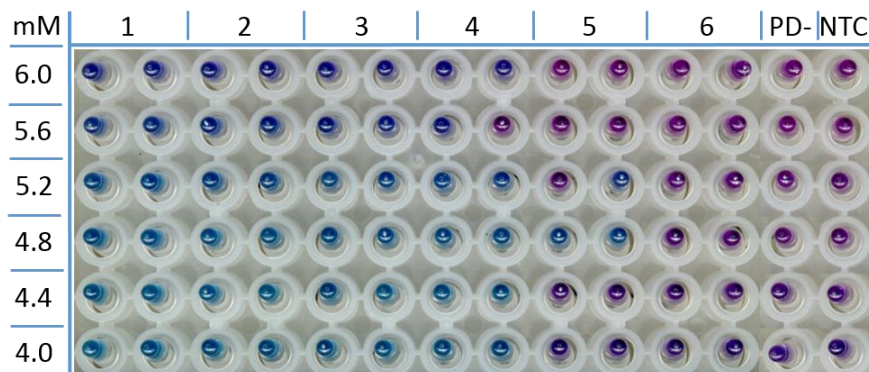


Figure 40: PD LAMP with ErioT, magnesium chloride concentration series. Applied concentrations of magnesium chloride [mM] per reaction are given on the left, sample designations in the headline. 1-6 = dilution series of a PD positive sample (1 = diluted 1:10; 2 = 1:100; 3 = 1:1,000; 4 = 1:10,000; 5 = 1:100,000; 6 = 1:1,000,000); PD- = PD negative control; NTC = no template control.

During the optimization process of the PD LAMP with ErioT, the additive polyethylene glycol 8k (PEG 8k) was tested as alternative to betaine. A concentration series from 2 to 6 μ l of a 30 % (w/v) PEG 8k solution, representing a concentration of 2.4 % to 7.2 % of PEG 8k per LAMP reaction, was tested with a 10-fold dilution series of a PD positive control (Figure 41). The highest sensitivity was obtained from the preparations with 4 μ l PEG 8k (30 %), which corresponded a concentration of 4.8 % per reaction. Agarose gel electrophoresis confirmed the absence of unspecific reactions at any applied PEG 8k concentration (data not shown). However, the blue staining of positive reactions appeared increasingly pale with rising PEG concentrations.

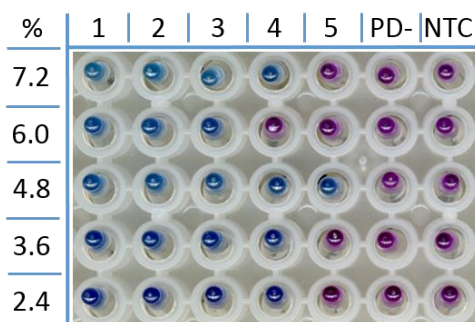


Figure 41: PD LAMP with ErioT, PEG 8k concentration series. The concentration of PEG 8k per reaction [%] is given on the left. 1-5 = dilution series of a PD positive control (1 = diluted 1:10; 2 = 1:100; 3 = 1:1,000; 4 = 1:10,000; 5 = 1:100,000); PD- = PD negative control; NTC = no template control.

The influence of the additives betaine and PEG 8k on LAMP performance with either ErioT or HNB was examined in a comparative experiment with a 10-fold dilution series of a PD positive control (Figure 42). For each metal indicator dye, the respective optimized LAMP reaction mix

Results

was applied. Betaine was applied at 1 M, which corresponded to the concentration in the optimized LAMP reaction mix with HNB. PEG 8k was used in the optimum concentration of 4.8 % per reaction as determined in the concentration series described above.

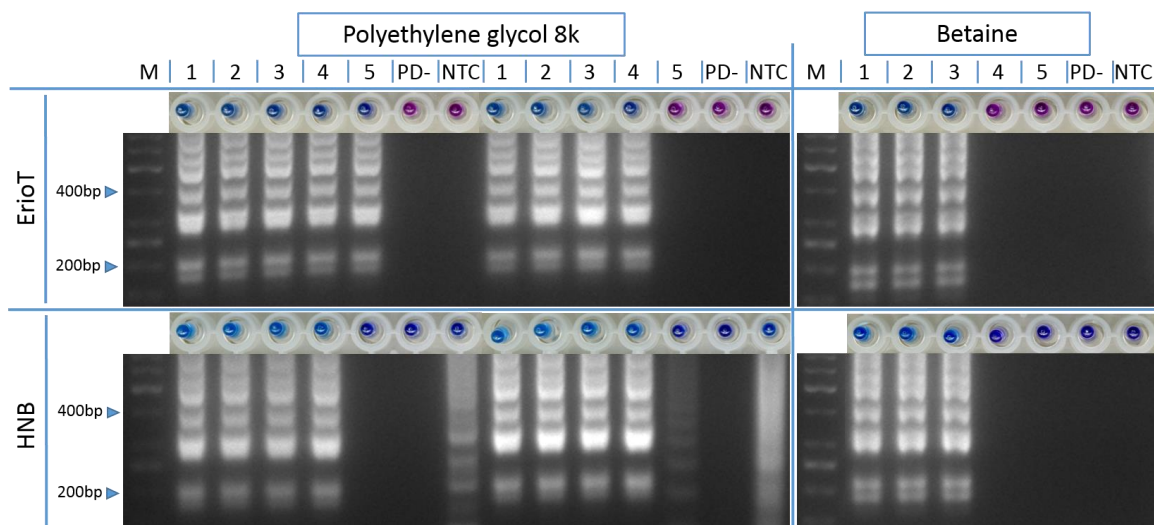


Figure 42: Influence of the additives polyethylene glycol 8k and betaine on LAMP assay sensitivity with either HNB or ErioT. M = size marker; 1-5 = dilution series of a PD positive control (1 = diluted 1:10; 2 = 1:100; 3 = 1:1,000; 4 = 1:10,000; 5 = 1:100,000); PD- = PD negative control; NTC = no template control.

The PEG 8k using variant was run in duplicates and yielded positive results to a dilution of 1:10,000 in both replicates and 1:100,000 in one out of two replicates when ErioT was the dye. While the detection limit of LAMP reactions with HNB was almost equal to LAMP reactions with ErioT, yielding positive results to dilution 1:10,000 in both replicates, unspecific laddering was observed on the agarose gel in the no template controls of the HNB LAMP. Using betaine, controls were clean in both variants, but the detection limit was reduced by one order of magnitude. No differences in the colours of the reaction mixes were observed, whichever additive was used. The colour change of positive reactions was in perfect agreement with the occurrence of specific banding patterns on the agarose gels.

In several publications dealing with the conventional use of ErioT in the titration of metal ions, the addition of the pH indicators Methyl orange (MO) or Methyl red to pure ErioT was proposed to enhance the contrast of the colour change (Münch, 1965; List & Hörhammer, 1967; Latscha et al., 2004). Mixing ErioT with Methyl orange results in a colour change from red to green upon decreasing magnesium ion concentrations, instead of purple to blue as with pure ErioT. In a series of experiments, a suitable mixing ratio of the two dyes was determined. Figure 43 shows LAMP reactions with pure ErioT in comparison to the mixed dye ErioT/MO. Controls were tested in duplicates.

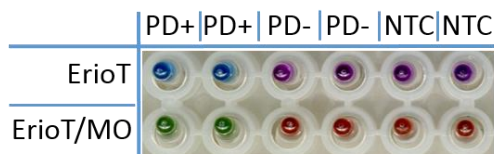


Figure 43: PD LAMP with either ErioT or the mixed indicator dye ErioT/MO. PD+ = PD positive control; PD- = PD negative control; NTC = no template control.

Specific amplification was observed in positive controls only, as indicated by the colour change. LAMP results were confirmed by agarose gel electrophoresis (data not shown). In sensitivity tests, LAMP reactions with the mixed indicator proved to be similarly sensitive as preparations with pure ErioT, confirming that Methyl orange did not impair the LAMP reaction. However, colours of the mixed dye became pale and showed a decreasing contrast with time and repeated use of the same dye aliquot while pure ErioT solutions remained stable over a considerably longer period of time. In consequence, further experiments were conducted with ErioT.

3.6.2 Spectrophotometric investigations of Eriochromeblack-T

Absorption spectra of ErioT in different solvents and in the presence of a range of compounds used in LAMP reactions were investigated with a spectrophotometer and compared to the respective spectra of HNB. Figure 44 shows absorption spectra of ErioT and HNB dissolved in either distilled water or 20 mM Tris-HCl (pH 8.8) and in the presence or absence of magnesium ions. Aqueous solutions of ErioT were only weakly coloured and showed very low absorption peaks with as well as without magnesium. Both dyes did not respond to presence of magnesium ions in the solution. Using Tris-HCl (pH 8.8) as solvent, the absorption peaks of ErioT were raised by approximately 0.5 units but curves were still flat compared to the spectra of HNB. The absorbance maximum for the ErioT-magnesium complex was determined at 538 nm, the maximum of the free dye at 566 nm. The corresponding maxima of HNB were measured at 578 nm and 644 nm, respectively.

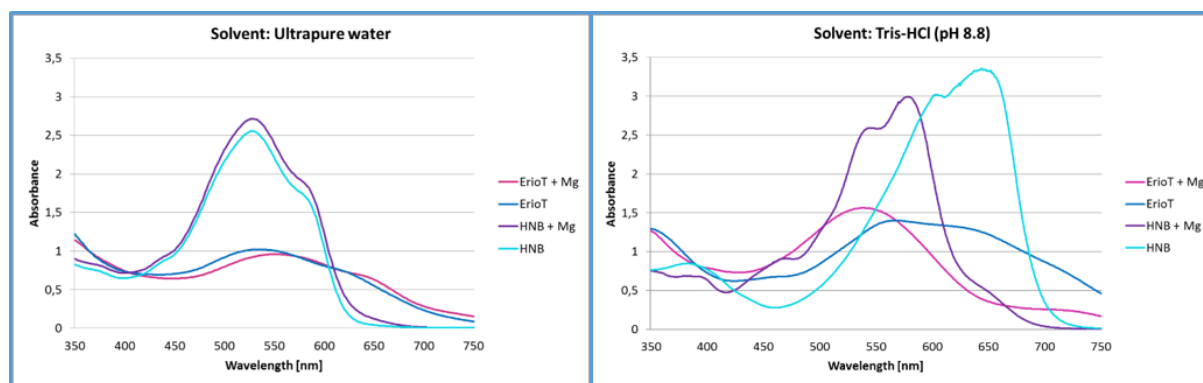


Figure 44: Absorption spectra of ErioT and HNB in distilled water and Tris-HCl (pH 8.8), respectively, and in the presence or absence of magnesium ions.

Measurements of ErioT spectra were repeated with solutions containing LAMP buffer and PEG 8k corresponding to the respective concentrations in the LAMP reaction solution

Results

(Figure 45). Spectra of ErioT in LAMP buffer showed distinct absorption peaks at 548 nm with and at 656 nm without magnesium chloride in the solutions. ErioT in solutions containing LAMP buffer and PEG 8k displayed very similar absorption curves, with a slightly lower absorption peak at 549 nm in the magnesium chloride containing solution than in the respective solution with LAMP buffer alone. The absorption peak of the free dye in LAMP buffer with PEG 8k showed a shift of 5 nm towards shorter wavelengths in comparison to the respective solution without PEG 8k. The appearance of an additional shoulder at longer wavelengths was observed in both variants and in the magnesium-containing as well as the magnesium-deficient solutions, respectively. ErioT solutions containing PEG 8k only exhibited flat absorption curves similar to those of aqueous solutions and did not respond to the presence of magnesium ions.

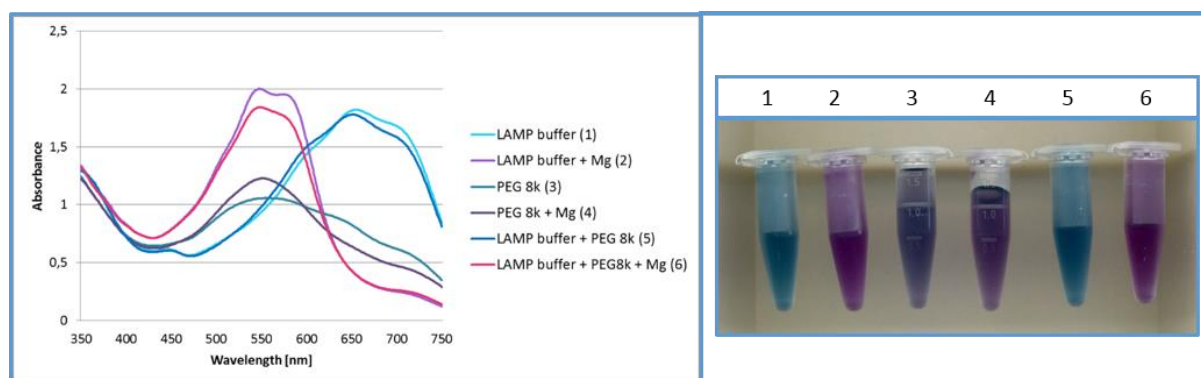


Figure 45: Absorption spectra of ErioT in LAMP buffer, PEG 8k or LAMP buffer and PEG 8k, in the presence or absence of magnesium ions. A photograph of the investigated solutions is given on the right. 1 = LAMP buffer without magnesium chloride; 2 = LAMP buffer with magnesium chloride; 3 = PEG 8k without magnesium chloride; 4 = PEG 8k with magnesium chloride; 5 = LAMP buffer and PEG 8k without magnesium chloride; 6 = LAMP buffer and PEG 8k with magnesium chloride.

Spectrophotometer measurements of HNB in LAMP buffer and PEG 8k yielded absorption peaks at 581 nm for the magnesium-complex and at 656 nm for the free dye (data not shown). In general, absolute absorbance values of ErioT were about 0.5 to nearly 1.5 units lower than absorbance values of HNB measured in previous experiments, irrespective the used solvent. However, the observed stronger contrast of the ErioT colour change in comparison to HNB was confirmed by the spectrophotometer measurements, which yielded a difference in the absorption maxima between the free dye and the magnesium complex of 108 nm for ErioT, but only of 75 nm for HNB, when the dyes were measured in LAMP buffer and PEG 8k corresponding to the optimized PD LAMP reaction conditions.

The influence of individual buffer components on absorption spectra of free ErioT and the metal indicator-magnesium-complex was examined (Figure 46). All solutions were prepared with Tris-HCl (pH 8.8) as solvent in order to provide a suitable surrounding for ErioT to form differently coloured complexes with magnesium. The buffer components ammonium sulfate (AS) and potassium chloride (KCl) both lowered the absorption peaks of the magnesium complex as well as the free dye, but caused only minor shifts of the maxima. For the magnesium complex, AS shifted the absorption peak by 1 nm towards longer wavelengths, KCl by 2 nm as

compared to the dye solution without any buffer component added. Solutions without magnesium chloride showed identical absorption peaks in the reference solution and the KCl containing solution, but a shift of 4 nm towards shorter wavelengths when the solution comprised AS.

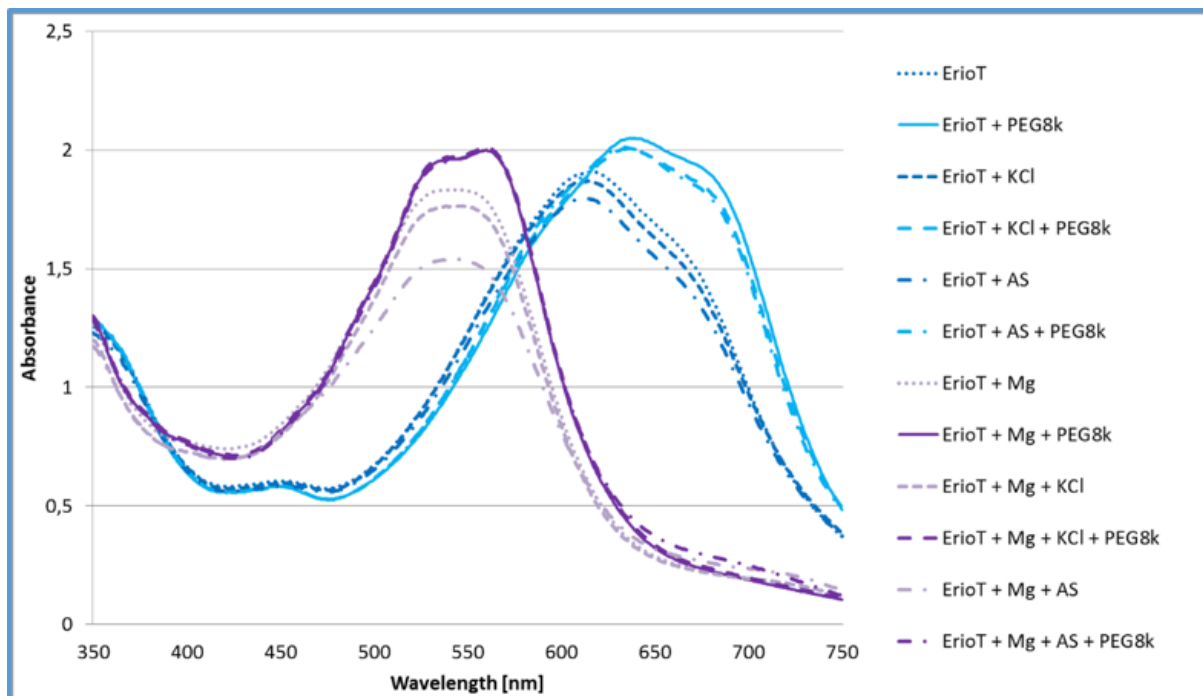


Figure 46: Absorption spectra of EriOT in the presence of individual LAMP buffer components. AS = ammonium sulfate; KCl = potassium chloride; Mg = magnesium (added as magnesium chloride).

AS was the buffer ingredient, which lowered the absorption peaks of both magnesium-containing and magnesium-deficient solutions the most compared to all other variants of this trial as well as to previous measurements of solutions with the complete LAMP buffer. This effect was more pronounced in the solution with magnesium than in the solution without magnesium. KCl also lowered the absorption peaks, but to a lesser extent than AS. The addition of PEG 8k led to enhanced absorption peaks for both magnesium-containing and magnesium-deficient variants, irrespective the tested buffer component. Furthermore, the absorption peaks were shifted to higher wavelengths by approximately 20 nm in solutions containing PEG 8k compared to solutions without PEG 8k. Interestingly, PEG 8k-containing solutions with magnesium showed nearly identical absorption curves, whichever buffer component was tested, whereas the respective solutions without PEG 8k displayed considerably different absorption curves. Furthermore, solutions containing KCl or AS showed distorted isobestic points. This effect was compensated by PEG 8k. The appearance of a shoulder at longer wavelengths than the absorption maximum was again observed in solutions without magnesium chloride, being more pronounced in solutions containing PEG 8k than in solutions without PEG 8k. In contrast to previous measurements, absorption spectra of the magnesium complex displayed a shoulder at shorter wavelengths than the absorption maximum when the solutions contained PEG 8k. This shoulder disappeared in spectra of PEG 8k-deficient solutions.

3.6.3 Titration experiments with sodium pyrophosphate

The colour change of EriOT in positive LAMP reactions is caused by a drop of magnesium ion concentration due to the precipitation of the amplification by-product magnesium pyrophosphate. A simulation of the EriOT colour change through gradual generation of magnesium pyrophosphate during a LAMP reaction was performed by titrating sodium pyrophosphate (NaPP) in a LAMP reaction solution at a 2 ml scale. It was expected that sodium ions were replaced by magnesium ions, forming the magnesium pyrophosphate complex. Due to financial considerations, the tested solutions did not contain primers, dNTPs and *Bst* DNA polymerase. At a constant magnesium chloride concentration corresponding to the concentration in a real LAMP reaction, different amounts of NaPP were added. Preliminary tests had shown that the colour change did not take place within two hours when the solutions were prepared and left at room temperature. In order to simulate the reaction as accurately as possible, the solutions were incubated at 65 °C for 60 min, which corresponds to the reaction conditions of the PD LAMP assay. As expected, the formation of water insoluble magnesium pyrophosphate with increasing NaPP concentration reduced the amount of free magnesium ions in the solution, resulting in a colour change of the metal indicator EriOT from purple to blue. Figure 47 shows the absorption spectra of the NaPP concentration series at constant magnesium chloride concentration and of control solutions with and without magnesium ions, as well as a photograph of the preparations after centrifugation. Magnesium pyrophosphate is visible as whitish pellet at the bottom of the tubes.

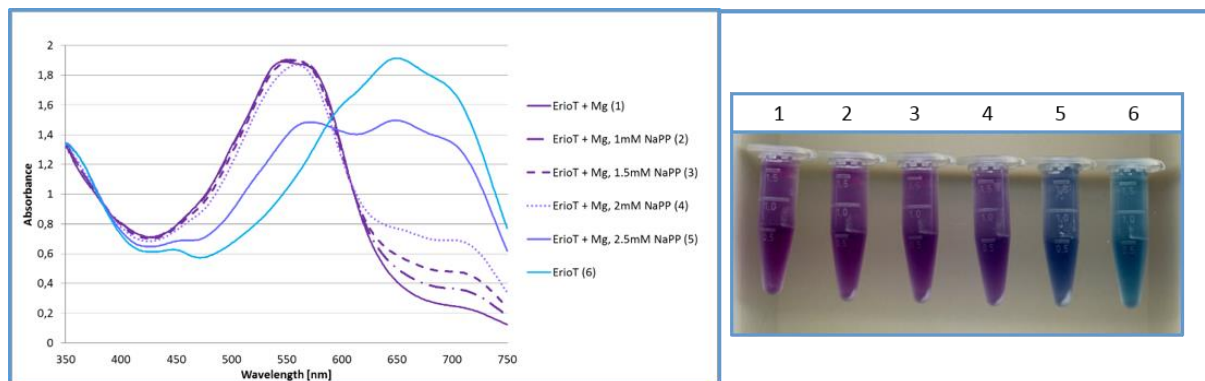


Figure 47: Simulation of the EriOT colour change in a LAMP reaction by titration of sodium pyrophosphate. Mg = magnesium (added as magnesium chloride); NaPP = sodium pyrophosphate, concentration given in [mM]. Absorption spectra are given on the left, a photograph of the centrifuged solutions on the right. 1 = reference solution with magnesium chloride, 0 mM NaPP; 2 = with magnesium chloride, 1 mM NaPP; 3 = with magnesium chloride, 1.5 mM NaPP; 4 = with magnesium chloride, 2 mM NaPP; 5 = with magnesium chloride, 2.5 mM NaPP; 6 = reference solution without magnesium chloride.

The magnesium-containing reference solution without NaPP showed a distinct absorption maximum at 547 nm. Upon addition of 1 mM NaPP, this peak was first shifted by 2 nm towards longer wavelengths. Enhancing the NaPP concentration to 1.5 mM and 2 mM, the absorption maximum was red-shifted by further 10 nm. At 2.5 mM sodium pyrophosphate, a distinct colour change from purple to blue became visible and the absorption curve showed two peaks in the

regions of the maxima of the reference solutions. The absorption band representing the metal chelate occurred at 572 nm, displaying a red-shift of 25 nm as compared to the magnesium-containing reference solution. However, the second peak occurred at 647 nm, which corresponds to the wavelength of the absorbance maximum of the magnesium-free reference solution (648 nm). Figure 48 shows the development of absorbance values at 648 nm, which is the wavelength of the absorption peak of the free dye, with rising sodium pyrophosphate concentrations. The absorbance value of the reference solution without magnesium at 648 nm is shown as light blue baseline in the graph. The massive release of dye molecules from their metal chelates at a sodium pyrophosphate concentration of 2.5 mM results in a sharp increase of absorbance values, marking the colour transition point of ErioT under the given reaction conditions.

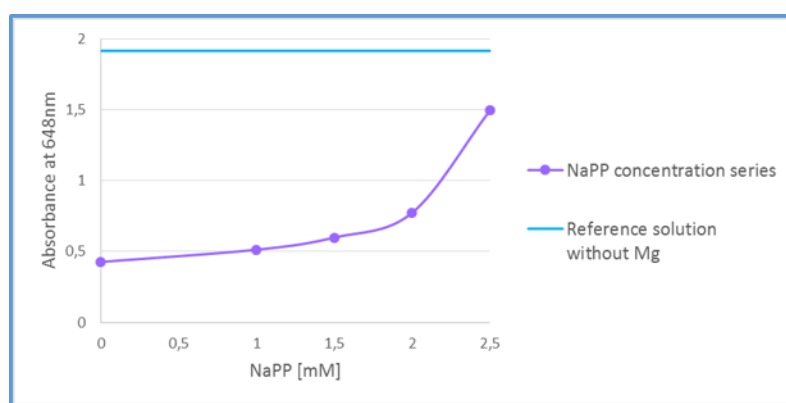


Figure 48: Development of ErioT absorption values at 648 nm with rising sodium pyrophosphate (NaPP) concentrations. The blue baseline represents the value of the absorption peak of the free dye in the reference solution.

The influence of dNTPs on the colour transition point was examined in a separate experiment, because dNTPs also form complexes with magnesium ions. Figure 49 shows a NaPP concentration series with ErioT as well as HNB in the absence of dNTPs, in comparison to the same concentration series with dNTPs added in the concentration used in PD LAMP. Solutions were prepared at a 100 μ l scale and contained all LAMP components except *Bst* DNA polymerase. The colour change was judged by eye. In the presence of dNTPs, the colour change of both metal indicator dyes occurred at a lower NaPP concentration than in the NaPP titration without dNTPs. As observed in the experiment described above, 2.5 mM NaPP were necessary to cause a colour change of ErioT as well as of HNB when the solutions did not contain dNTPs. When dNTPs were added, the colour change occurred considerably earlier. At 1.5 mM NaPP, the solution with ErioT exhibited a definite colour change to blue. At 1 mM NaPP, the solution had an intermediate colour, appearing more bluish than purple. With HNB, the colour change at 1.5 mM NaPP was visible but weak, compared to the clearly distinguishable colours of the ErioT solutions. However, ErioT solutions with dNTPs showed a darker ground colour than without dNTPs at NaPP concentrations below the colour transition point. This demonstrates

that dNTPs, as strong magnesium-complexing agents, are in direct competition to ErioT for magnesium ions.

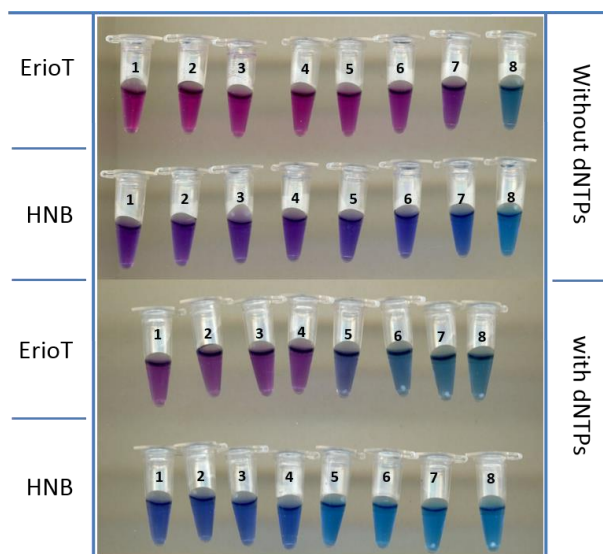


Figure 49: Determination of the colour transition points of ErioT and HNB in LAMP reaction solutions in the presence and absence of dNTPs by titration of sodium pyrophosphate (NaPP). Applied NaPP concentrations: 1 = 0.1 mM; 2 = 0.2 mM; 3 = 0.3 mM; 4 = 0.4 mM; 5 = 1 mM; 6 = 1.5 mM; 7 = 2 mM; 8 = 2.5 mM.

In order to better simulate this competitive situation in LAMP, a concentration series with NaPP and dNTPs in opposite directions was investigated. Starting with the original concentration of dNTPs in the PD LAMP, the dNTP concentration was lowered stepwise by the same amount, by which the NaPP concentration was raised. Figure 50 shows these concentration series in opposite directions in LAMP reaction solutions with ErioT. The colour change occurred at 1 mM NaPP, which was also the colour transition point in the previous experiment with constant dNTP concentration.



Figure 50: Determination of the colour transition point of ErioT in LAMP reaction solutions with decreasing dNTP concentrations and increasing sodium pyrophosphate concentrations. 1 = 0 mM NaPP, 3.2 mM dNTPs; 2 = 0.1 mM NaPP, 3.1 mM dNTPs; 3 = 0.2 mM NaPP, 3.0 mM dNTPs; 4 = 0.3 mM NaPP, 2.9 mM dNTPs; 5 = 0.5 mM NaPP, 2.7 mM dNTPs; 6 = 0.7 mM NaPP, 2.5 mM dNTPs; 7 = 1 mM NaPP, 2.2 mM dNTPs; 8 = 1.5 mM NaPP, 1.7 mM dNTPs; 9 = 2 mM NaPP, 1.2 mM dNTPs; 10 = 2.5 mM NaPP, 0.7 mM dNTPs.

Based on this value, the DNA yield required to produce a colour change of ErioT in LAMP was calculated. When a nucleotide is processed during amplification, a pyrophosphate moiety is dissociated. The ratio of dNTP consumption and pyrophosphate generation therefore is 1:1.

Taking the average molar mass of desoxynucleosid monophosphates of 308.95 g/mol as a basis, a DNA yield of 0.30895 µg/µl is calculated for the production of 1 mM pyrophosphate.

3.6.4 Detection limit and detection range of the PD LAMP with Eriochromeblack-T

The final evaluation of the detection limit of the PD LAMP assay with the primer set PD3 and the optimized reaction mix using ErioT for colorimetric detection of amplification was performed with a 10-fold dilution series of a pGemT plasmid containing the P1/P7-fragment of the 16S rDNA sequence of *Candidatus* Phytoplasma pyri as insert. The dilution series was tested with PD LAMP, PCR with primers fO1/rO1 and realtime PCR according to Torres et al. (2005) (Figure 51). Additionally, two additives were investigated for their influence on LAMP sensitivity, individually and in combination: Betaine, which is a denaturing additive commonly used in LAMP, and polyethylene glycol 8k (PEG 8k), a macromolecular crowding agent. Concentrations of the target ranged from 10^8 to 10^0 copies per reaction in the experiments with PCR, realtime PCR and PD LAMP with PEG 8k, whereas in LAMP assays with betaine and the betaine/PEG 8k combination, the highest copy number was omitted. Experiments with the original PD LAMP assay using PEG 8k were repeated three times, PCR two times, realtime PCR three times. LAMP with PEG 8k detected 10^2 copies per reaction in two out of three experiments. In the third experiment, the assay successfully detected 10^3 copies, but failed to amplify 10^2 copies. The detection limit of LAMP with betaine was 10^4 copies in all replications. The combination of betaine with PEG 8k did not result in an enhanced sensitivity compared to the assay using betaine only. PCR reached a sensitivity of 10^2 copies per reaction. PCR and LAMP assays failed to amplify 10^1 and 10^0 copies per reaction. The colour change of positive LAMP reactions correlated well with banding patterns on agarose gels. Samples beyond the detection limit yielded no colour change, hence no banding patterns were visible on the gel. While PCR products showed a weakening of intensity on the gel with reduced target concentration, LAMP products were at equal intensity at all dilutions as observed in earlier experiments. Realtime PCR according to Torres et al. (2005) using the DNA-intercalating dye SybrGreen I and the primer pair P1/R16(X)F1r for group-specific detection of fruit tree phytoplasmas belonging to the taxonomic group 16SrX was able to detect one copy of the target per reaction. Melt curve analysis confirmed specific amplification in all replicates. However, Ct values for the one and ten copies per reaction, respectively, showed deviations of more than 0.5 cycles among the replicates, indicating stochastic effects of target distribution in the replicates. Negative controls yielded fluorescence signals beyond cycle 32 in all experiments. Melt curve analysis proved these amplifications to be unspecific in all cases.

Results

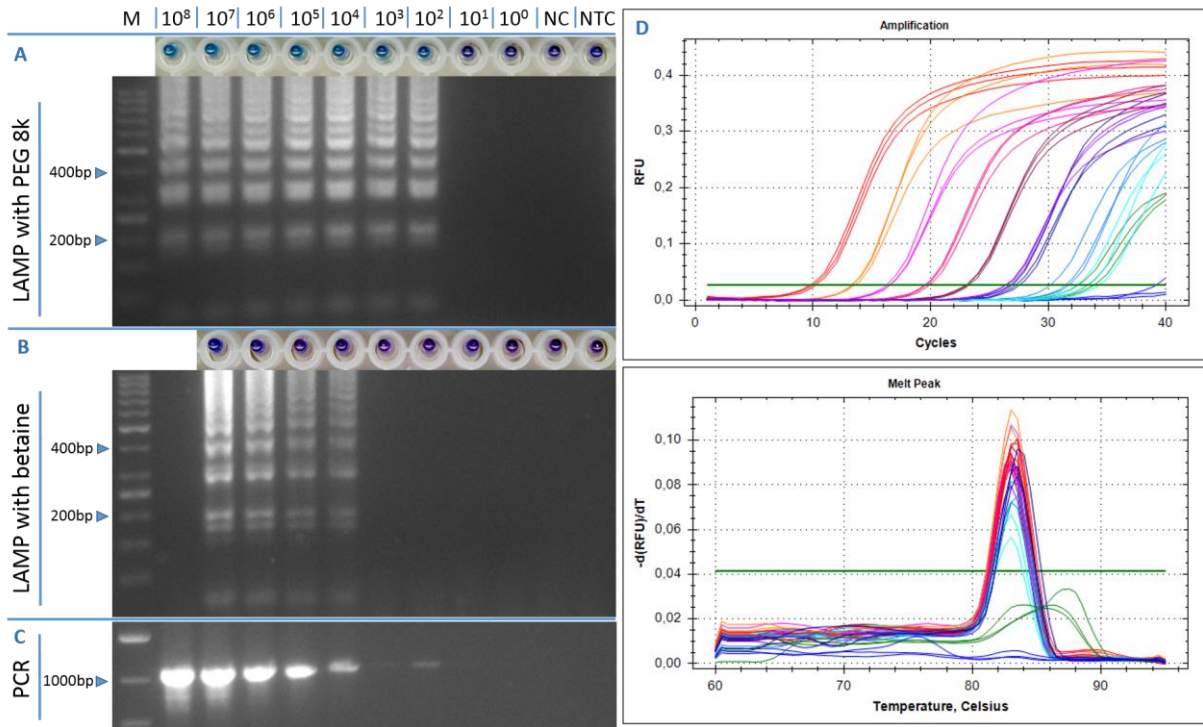


Figure 51: Detection limit of the PD LAMP with ErioT and either PEG 8k (A) or betaine (B) in comparison to conventional PCR (C) and realtime PCR with SybrGreen I (D). Copy numbers of the target per LAMP or PCR reaction are given in the headline on the left. M = size marker; NC = negative control; NTC = no template control. Realtime PCR amplification curves and melt curve analysis are given on the right. Red lines = 10⁸ copies per reaction; orange = 10⁷; pink = 10⁶; magenta = 10⁵; dark red = 10⁴; violet = 10³; dark blue = 10²; light blue = 10¹; turquoise = 10⁰; green = negative control; blue = no template control.

In order to investigate the applicability of the PD LAMP assay with primer set PD3 to other phytoplasma strains, both versions of the LAMP assay, either with PEG 8k or betaine, were tested on DNA samples from a range of phytoplasmas representing different phylogenetic groups (Figure 52). Using betaine as additive in the LAMP reaction, no colour change of the reaction mixture and no or very weak unspecific banding patterns on agarose gels were observed for phytoplasmas other than *Candidatus* Phytoplasma pyri. However, the PEG-containing LAMP assay successfully amplified all phytoplasma strains tested in this study. A definite colour change to blue was visible in these reactions, and ladder-like banding patterns were observed on the agarose gel. These banding patterns showed subtle differences to the PD positive control in some cases, with several bands missing or new bands being generated. A combination of PEG 8k and betaine suppressed the amplification from some, but not all phytoplasma strains. DNA extracts from phytoplasmas of the group 16SrI were not amplified in a LAMP reaction mix with 4.8 % PEG 8k and 0.8 M betaine, whereas raising the betaine concentration to 1 M with PEG 8k concentration held equal led to the failure of amplification of DNA extracts from phytoplasmas of groups I, VII and XII. In the sample of a group 16SrVI member, a very faint banding pattern was observed on the agarose gel. DNA extracts from phytoplasmas of the groups II, III, V and XI were amplified, but the reactions did not yield a

Results

colour change and the respective banding patterns were weak, again showing differences to the banding pattern derived from the pear decline phytoplasma.

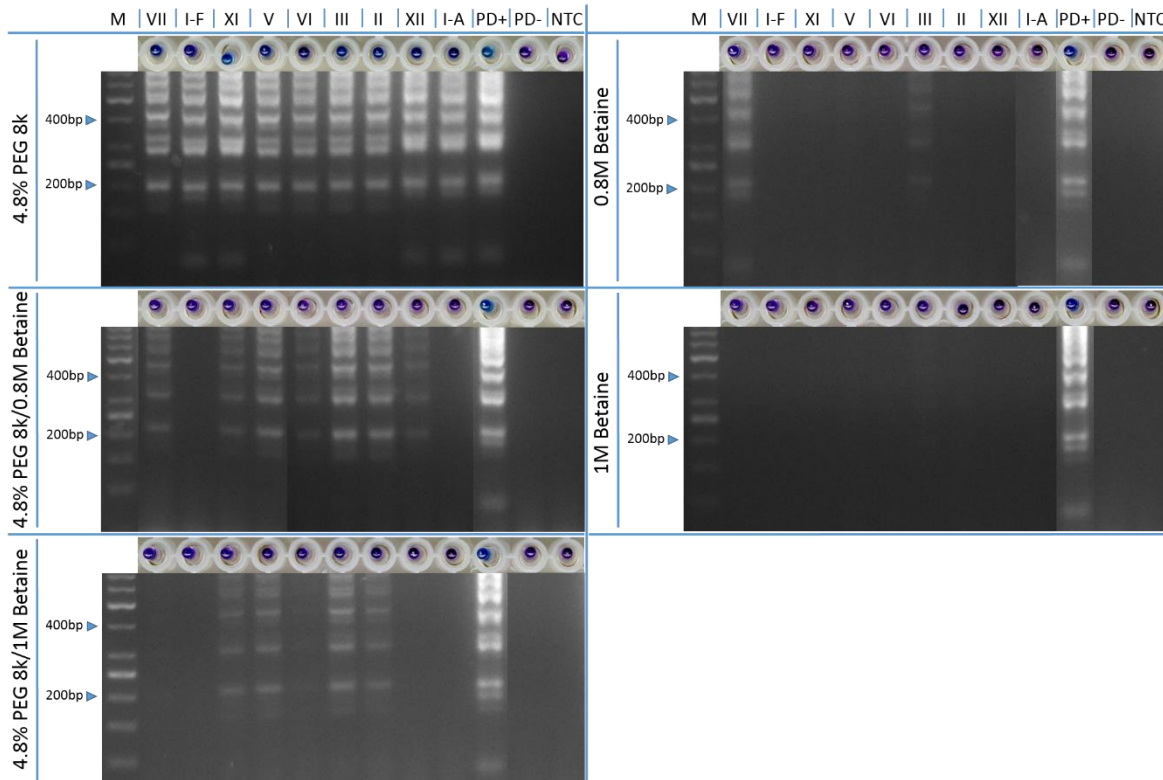


Figure 52: Detection range of the PD LAMP depending on the applied additive. Tested representatives of the 16Sr groups: VII = *Ca. P. fraxini* (Ash yellows); I-F = *Ca. P. asteris* (Apricot chlorotic leafroll); XI = *Ca. P. oryzae* (Flower stunting); V = *Ca. P. ulmi* (Elm Witches' broom); VI = *Ca. P. trifolii* (Potato Witches' broom); III = *Ca. P. pruni* (Peach X disease); II = *Ca. P. aurantifolia* (Tomato big bud); XII = *Ca. P. solani* (Grapevine yellows); I-A = *Ca. P. asteris* (Aster yellows). M = size marker; PD+ = PD positive control; PD- = PD negative control; NTC = no template control. Dye: ErioT.

A sequence alignment of the 16S rDNA sequence of *Candidatus Phytoplasma pyri* with reference sequences of the tested phytoplasma strains revealed three deletions and three insertions in the PD3 target region as well as sporadic mismatches at the primer binding sites (Figure 53). Members of the 16SrX group AP and ESFY, which had already been tested earlier and which were fully amplified throughout all experiments (see chapter 3.5), showed identical sequences with the PD phytoplasma in the target region and at the primer binding sites except for one mismatch at the forward loop primer (LF) binding site. The Spartium witches' broom phytoplasma (SWB), which is also a member of the 16SrX group, showed one mismatch with primer LF and two mismatches with outer primer B3. However, the SWB phytoplasma was not tested with the PD LAMP assay in this study.

Results

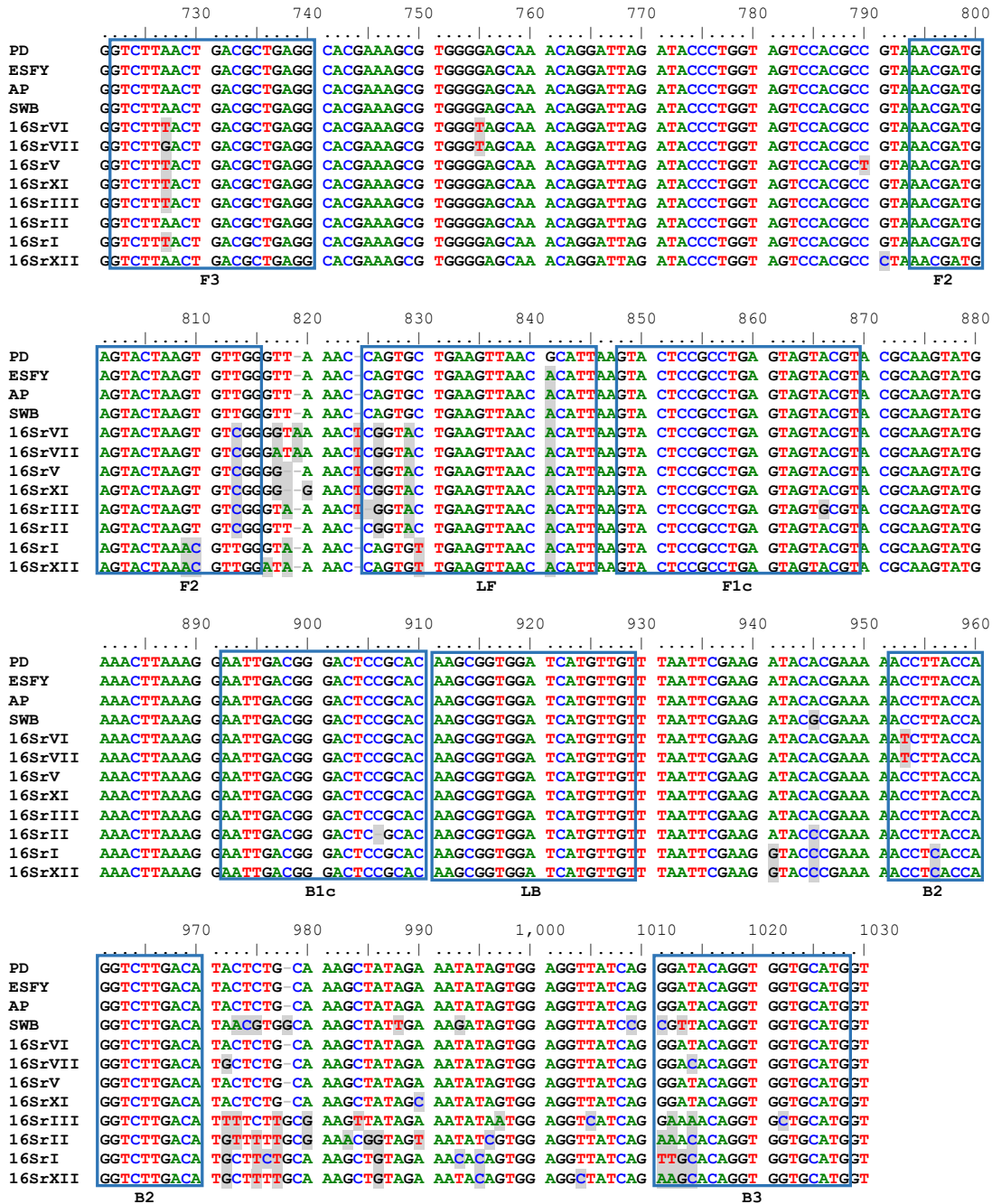


Figure 53: Multiple sequence alignment of the PD3 target regions on the 16S rDNA reference sequences of the tested phytoplasma strains as well as of the members of the 16SrX group, and location of the primer binding sites of LAMP primer set PD3. Mismatches of the 16S rDNA sequences with the PD reference sequence are shaded. LAMP primer locations are framed. Members of group 16SrX: PD = Pear decline; ESFY = European stone fruit yellows; AP = Apple proliferation; SWB = Spartium witches' broom. F3, B3 = outer LAMP primers; LF, LB = forward and backward loop primers; F2, F1c = FIP sequence components; B2, B1c = BIP sequence components.

3.7 Occurrence of false positives in LAMP and troubleshooting

3.7.1 Investigations on the causes of the occurrence of false positives in the PD LAMP

The occurrence of false positives was a recurrent problem with all LAMP primer sets applied for the detection of the PD phytoplasma, which substantially hampered work with the LAMP method. Figure 54 shows false positive LAMP reactions with primer sets PD2, PD3 and PD4. Agarose gel electrophoresis revealed that banding patterns of negative and no template controls were identical with those of positive controls in all cases. Furthermore, false positive amplifications produced as high amounts of DNA as true positives, leading to a definite colour change of the metal indicator dye as well.

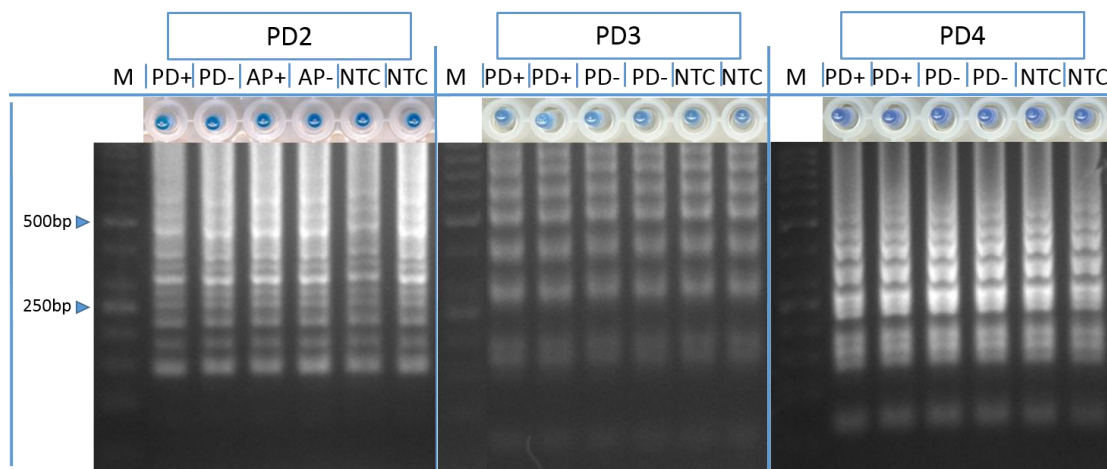


Figure 54: Occurrence of false positives in LAMP reactions with primer sets PD2, PD3 and PD4. M = size marker; PD+ = PD positive control; PD- = PD negative control; AP+ = AP positive control; AP- = AP negative control; NTC = no template control. Dye: HNB.

This phenomenon affected whole runs rather than individual samples and controls in most cases. Standard measures were taken to avoid contaminations. LAMP reaction mixes were prepared in a PCR workstation, which was subjected to UV irradiation for 10 min before use. Pipets, pipet tips, reaction tubes and racks were maintained in the workstation and used exclusively for the preparation of LAMP and PCR reaction mixes. Samples were added to reaction mixes outside the PCR workstation.

The primer set PD2 started to produce false positives already during the optimization phase. The primer set PD3 was tested in parallel and these runs stayed clean in most cases. However, occasional occurrence of false positives was observed also with the primer set PD3 in this period. Replacing LAMP reagents with fresh aliquots as well as ordering new primers did not eliminate the false positive amplifications. Primer set PD2 was abandoned and a newly designed primer set, PD4, was tested with promising results in the first instance. After two months of work with PD4, this primer set also started to produce false positives, which affected entire experiments. Again, substitution of reagents did not solve the problem. Preparing the reaction mix in different rooms and with different equipment yielded the same results. A PCR with the

Results

outer LAMP primers of primer set PD4 was conducted with the LAMP reagents as samples, in order to examine if the LAMP reagents were contaminated with target DNA (Figure 55). Products of a preceding LAMP run were diluted 1:10 and tested as well. Agarose gel electrophoresis of PCR products displayed a distinct band in the PD positive control as well as a weak band of the same size in the diluted positive controls of the LAMP reaction. False positive LAMP products showed weak banding patterns due to insufficient dilution but no band corresponding to the expected PCR product, indicating that the false positive amplifications did not originate from the proper target. PCR negative and no template controls as well as the LAMP reagents showed no products.

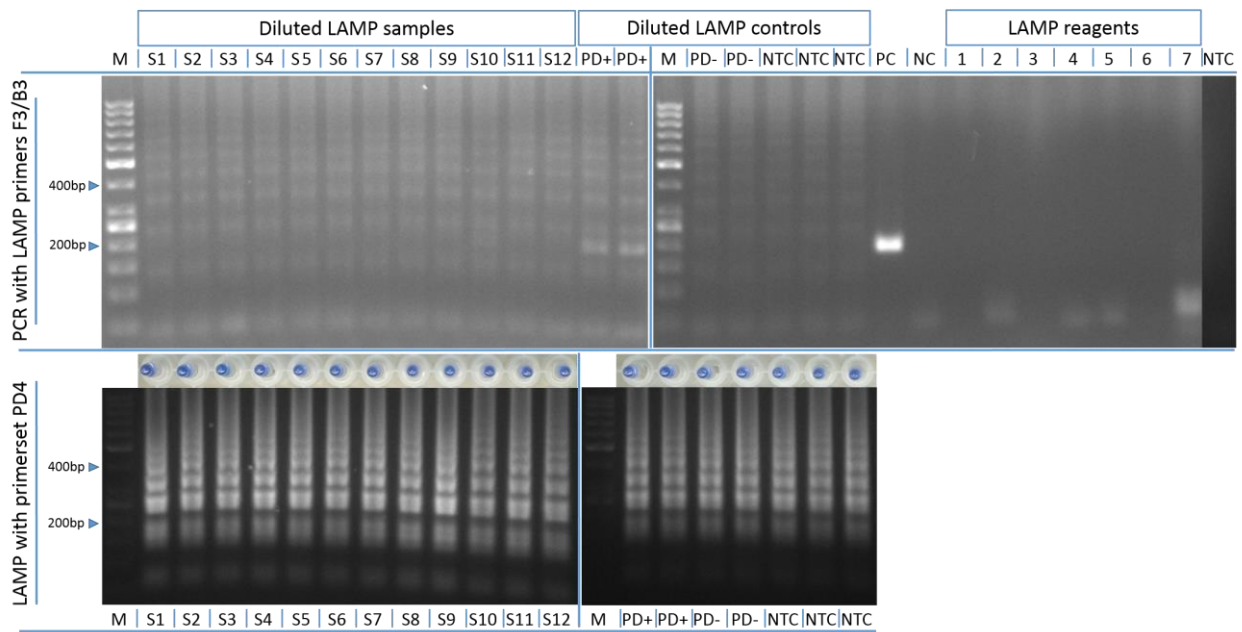


Figure 55: Test of LAMP reagents and false positive PD4 LAMP reactions for the presence of target DNA with PCR using primers PD4 F3 and PD4 B3. The tested false positive LAMP reactions are shown below the respective PCR results. M = size marker; S1-S12 = samples tested with PD4 LAMP. The respective LAMP products of samples and controls were diluted 1:10 and subjected to PD4 F3/B3 PCR. PD+ = PD positive control; PD- = PD negative control; NTC = no template control. LAMP dye: HNB. PCR controls: PC = PD positive control; NC = PD negative control; NTC = no template control. LAMP reagents: 1 = dNTPs; 2 = MgSO₄; 3 = HNB; 4 = betaine; 5 = ThermoPol buffer; 6 = *Bst* DNA polymerase; 7 = PD4 Primer mix.

An experiment was conducted using the complete primer set PD4 in one variant and the primer set without loop primers in another variant in order to examine if a deceleration of the LAMP reaction would give insights in the cause and development of false positives. Controls were tested in duplicates. LAMP reactions without loop primers were not only slower than the reactions with loop primers, requiring additional 30 min of incubation to achieve a colour change, but also showed a markedly different banding pattern on the agarose gel (Figure 56). However, both variants displayed false positives in all controls, indicating that their generation did not depend on the loop primers.

Results

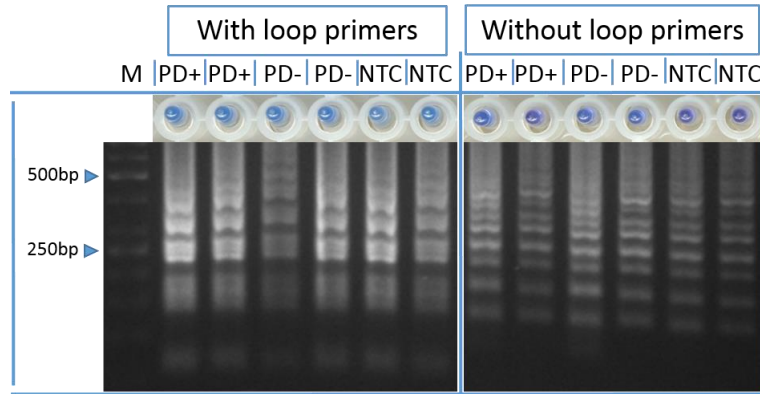


Figure 56: LAMP reactions with primer set PD4, with and without loop primers. M = size marker; PD+ = PD positive control; PD- = PD negative control; NTC = no template control. Dye: HNB.

The primer set PD3 was tested in comparison to primer set PD4 in LAMP reactions containing the same reagents in the same concentrations in both variants (Figure 57). LAMP reactions with PD4 resulted, as expected, in the formation of false positives, whereas reactions with PD3 yielded clean controls. This result finally eliminated the hypothesis that a contamination with genomic target DNA was the source of false positive LAMP reactions. In order to further exclude the possibility of amplicon-contaminated reaction tubes, additional aliquots of both reaction mixes were incubated in their respective 2 ml tubes, in which they had been prepared. Two ml reaction tubes intended for the preparation of LAMP and PCR mastermixes were always kept in the PCR workstation, packed in plastic bags, in which they had been delivered. These tubes were not opened outside the PCR workstation and therefore, contact with LAMP amplicons was excluded.

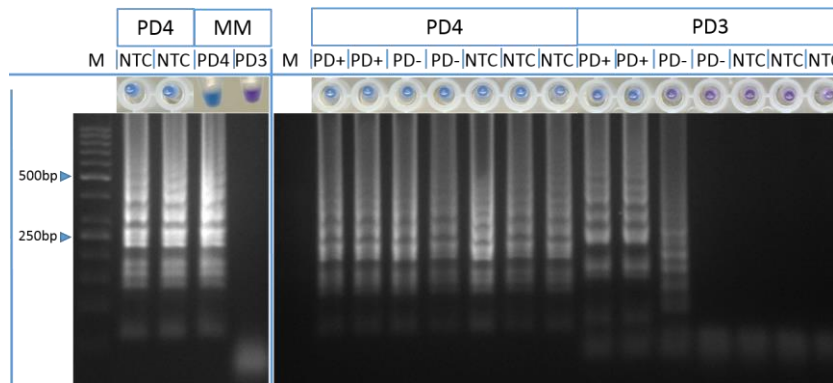


Figure 57: Comparative test of the primer sets PD3 and PD4 in LAMP reactions with identical composition. M = size marker; MM = LAMP Mastermix with PD3 and PD4 primers, respectively, incubated in 2 ml reaction tubes, in which the MMs had been prepared. PD+ = PD positive control; PD- = PD negative control; NTC = no template control. Dye: HNB.

Corresponding to the results of the other LAMP reactions, the reaction mix with PD4 primers in the 2 ml tube turned blue after 60 min of incubation at 65 °C, while the reaction mix with PD3 primers stayed purple. Agarose gel electrophoresis confirmed false positive amplifications in LAMP reactions with the primer set PD4, whereas LAMP reactions with the primer set PD3 showed specific banding patterns in positive controls only.

Results

To investigate the possibility of producer-related quality differences of primers and their influence on the occurrence of false positives, PD4 primers were ordered from two different companies, Eurofins MWG Operon (Ebersberg, Germany) and TIB Molbiol (Berlin, Germany), and applied in LAMP reactions with all other components held equal. Figure 58 shows that LAMP reactions with primers from the two companies produced different banding patterns, but the occurrence of false positives was not influenced. Shorter amplicons predominated in LAMP reactions with primers obtained from TIB Molbiol as compared to LAMP reactions with MWG primers. Consequently, the blue colour of reactions with TibMolbiol primers appeared darker than those with MWG primers, reflecting a reduced generation of the by-product magnesium pyrophosphate. The cause for the false positive amplifications with the primer set PD4, however, remained unclear.

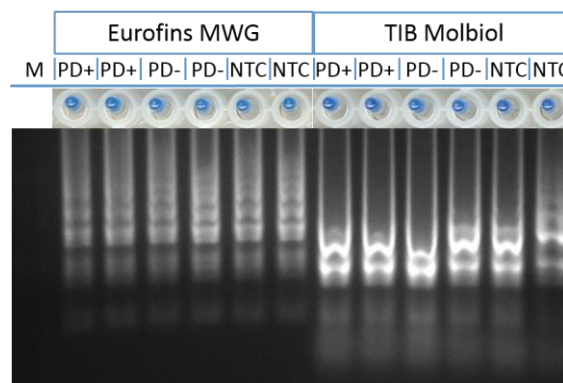


Figure 58: LAMP reactions with PD4 primers purchased from Eurofins MWG Operon and TIB Molbiol. M = size marker; PD+ = PD positive control; PD- = PD negative control; NTC = no template control. Dye: HNB.

Since the primer set PD3 yielded clean LAMP runs, work was continued with these primers. Several hundred samples derived from pears of an inoculation trial were tested successfully. The assay worked reliably for half a year before false positives persistently occurred also with this primer set. As observed before, replacing LAMP reagents was not a successful measure. In an attempt to determine if an individual primer failed to work properly, the PD3 primer set was at first reduced to its basic components, the outer and inner primers. Figure 59 shows LAMP reactions without loop primers in comparison to LAMP with the complete primer set. As before, LAMP reactions with the complete primer set showed a colour change to blue in all controls. False positive amplification in all negative and no template controls was confirmed by subsequent agarose gel electrophoresis. However, a complete failure of amplification was observed in LAMP reactions without loop primers, as indicated by the absence of a colour change even after an elongated incubation time of 120 min, which was confirmed by agarose gel electrophoresis. This was unexpected, because in general, loop primers are not required for amplification in LAMP, leading to the speculation that one of the inner primers failed to work.

Results

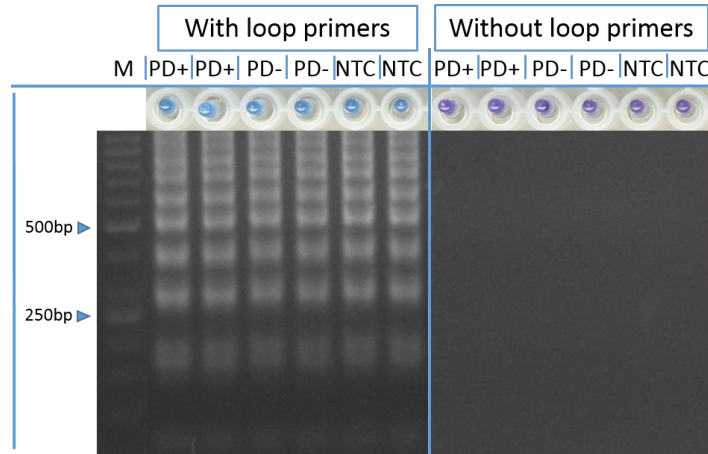


Figure 59: LAMP reactions with primer set PD3, with and without loop primers. M = size marker; PD+ = PD positive control; PD- = PD negative control; NTC = no template control. Dye: HNB.

Several combinations of PD3 primers were tested for their ability to amplify under LAMP reaction conditions in the presence and absence of target DNA. Figure 60 shows LAMP reactions with two primers only. The forward inner primer (FIP) was tested with the backward outer primer (B3), forward outer primer (F3) as well as the backward loop primer (LB) in equal concentrations, respectively. Two types of negative controls were tested, one prepared with the DNeasy Plant Mini kit (Qiagen), one with the NaOH sample preparation method, from healthy pears maintained in an *in vitro* culture.

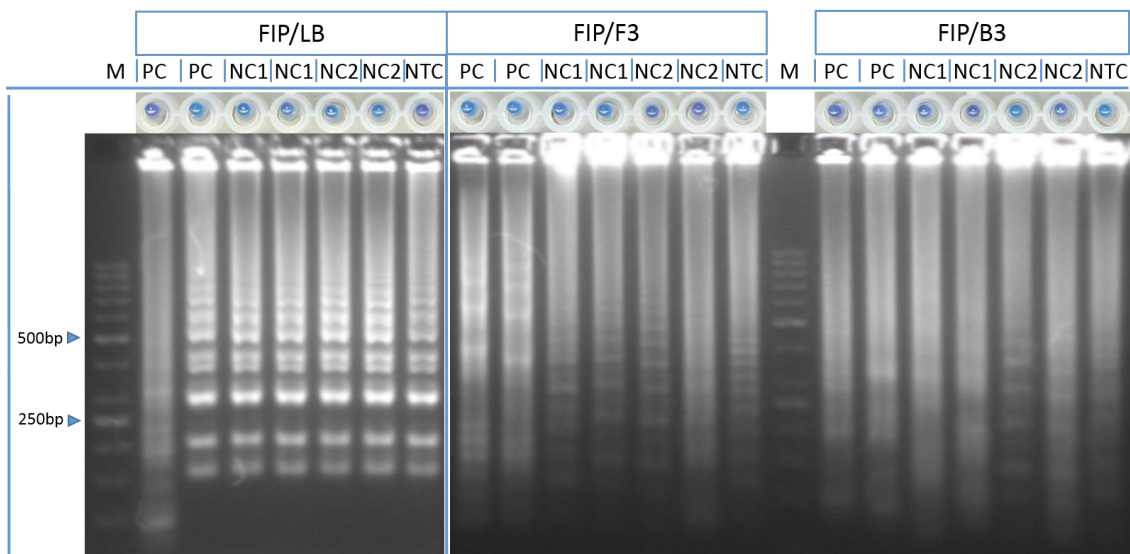


Figure 60: Amplification products formed under LAMP reaction conditions with pairwise combination of PD3 primers. FIP = forward inner primer; LB = backward loop primer; F3 = forward outer primer; B3 = backward outer primer; M = size marker; PC = PD positive control; NC1 = PD negative control (DNA extract); NC2 = PD negative control (NaOH extract); NTC = no template control. Dye: HNB.

All controls were amplified in the three variants, yielding a more or less pronounced colour change to blue. Variants with FIP and B3 or F3 showed diverse banding patterns or smear on the agarose gel that appeared unspecific. The combination of FIP and LB, however, produced a distinct banding pattern, which was identical for positive, negative and no template controls,

Results

except one positive control, which showed unspecific laddering on the gel. The banding pattern produced with FIP and LB was not identical to the pattern observed when the complete primer set was used, which indicates that at least one further primer participates in the generation of false positives. This proved that efficient amplification took place in the absence of target DNA, even in the no template controls with only two types of oligonucleotides present in the reaction solution. However, only the combination of FIP and LB yielded a distinct and recurring product, indicating that a defective action of at least two primers was necessary to cause the generation of false positives rather than unspecific products.

Since ordering fresh primers had repeatedly proven unsuccessful to eliminate false positives, it was supposed that one or more components of the chemical reaction surrounding were responsible for the unusual behavior of the primers. In order to investigate this possibility, the LAMP buffer was considered first to influence primer binding. An experiment was conducted with a buffer prepared freshly in our laboratory, containing the same ingredients as the ThermoPol buffer (New England Biolabs) usually applied in the PD LAMP. The formerly used ThermoPol buffer aliquot purchased from New England Biolabs was used in a separate run as control. All other reagents were held equal. Controls were tested in duplicates. The results are presented in figure 61.

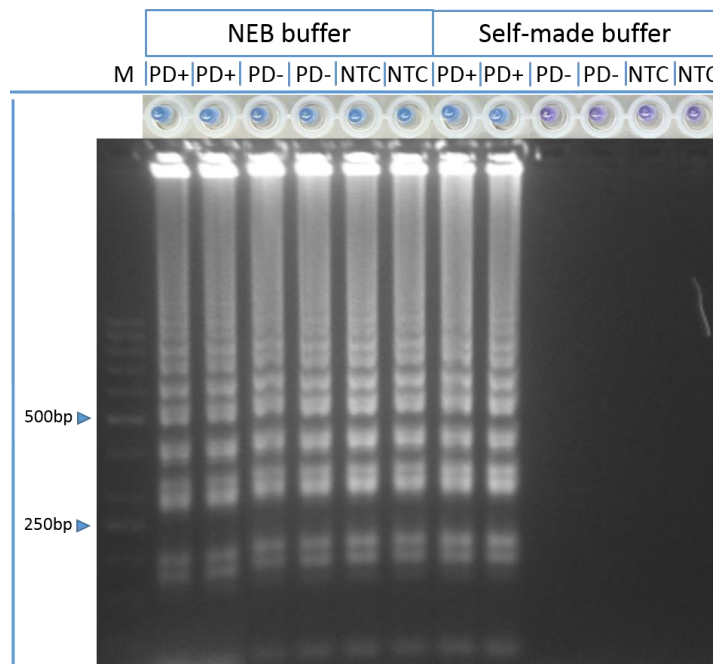


Figure 61: Influence of the ThermoPol buffer on the occurrence of false positives in the PD LAMP. LAMP reactions with the purchased ThermoPol buffer (NEB buffer) are shown on the left, LAMP reactions with freshly prepared LAMP buffer of equal composition on the right. M = size marker; PD+ = PD positive control; PD- = PD negative control; NTC = no template control. Dye: HNB.

LAMP reactions with the purchased ThermoPol buffer yielded the same result as before, displaying blue colours throughout all controls with the corresponding positive-appearing banding patterns on the agarose gel. However, LAMP reactions with the self-made buffer

yielded clean negative and no template controls as confirmed by subsequent agarose gel electrophoresis.

Since the date of preparation was known, continuous work with the self-made buffer revealed that false positives frequently occurred after approximately four weeks when the buffer was kept in aliquots in a freezer at -20 °C, which indicated that the malfunction of the buffer was a matter of storage duration. Consequently, the buffer was freshly assembled every three weeks from frozen stock solutions of the individual components. This procedure proved to be successful, avoiding false positives for the remaining time of the project.

3.7.2 Experiments with LAMP buffer composition

The discovery that the buffer was responsible for the occurrence of false positives in LAMP reactions led to a series of experiments evaluating alternatives for and altered concentrations of individual buffer components in order to avoid the observed instabilities or to elongate usability. ThermoPol buffer (10x) as provided by New England Biolabs consists of the following ingredients (Table 10):

Table 10: Composition of the ThermoPol buffer (New England Biolabs)

Reagent	Concentration (10x)
Tris-HCl (pH 8.8)	200 mM
(NH ₄) ₂ SO ₄	100 mM
KCl	100 mM
MgSO ₄	20 mM
Triton X-100	1 %

The combination of ammonium sulfate with magnesium sulfate in the buffer solution was considered to be problematic, because both salts dissociate sulfate anions, thereby influencing their respective dissociation equilibria. Additionally, sulfate is a large, hydrated anion that increases ionic strength fourfold compared to a monovalent anion. The ionic strength of the reaction solution influences primer T_m . Moreover, occasional problems occurred with purchased magnesium sulfate solutions, indicating fluctuant concentrations, which, in the worst case, led to an immediate colour change from purple to blue during reaction mix preparation after the addition of dNTPs. As a consequence, the first measure was to replace magnesium sulfate with magnesium chloride and then to exclude it from the buffer, since 2 mM MgSO₄, which are integrated into the 1x ThermoPol buffer, are not sufficient for a LAMP assay with colorimetric detection, and supplemental magnesium has to be added when a LAMP reaction mix is prepared. The substitution of magnesium sulfate with magnesium chloride did not influence assay performance (data not shown).

Figure 62 shows the results of LAMP reactions in the presence and absence of ammonium sulfate (AS). The influence on assay sensitivity was evaluated with a 10-fold dilution series of

Results

a PD positive control. Magnesium chloride was used as source for magnesium ions. The variant V1 with AS representing the standard buffer showed negative reactions with a dark purple colour, while in the variant without AS, the colour of negative reactions was bright purple (Figure 62, V1 and V2). However, incubation time of the assay without AS was elongated by further 30 min due to a weak colour change of positive reactions. The experiment was repeated with enhanced dNTP (+ 0.6 mM) and magnesium chloride (+ 2 mM) concentrations and reduced betaine concentration (- 0.2 M) in order to verify the observed tendency of reduced sensitivity of an AS deficient assay (Figure 62, V3 and V4). As before, the variant without AS showed a bright purple colour in negative reactions, whereas addition of AS resulted in bluish staining of negative reactions. Reduced sensitivity by one order of magnitude was confirmed for the AS deficient assay. An elongated incubation time by 30 min intensified the contrast of the colour change, but did not raise assay sensitivity. Enhancing the magnesium chloride concentration by further 1 mM did not alter the bluish colour of negative reactions in the presence of ammonium sulfate (data not shown).

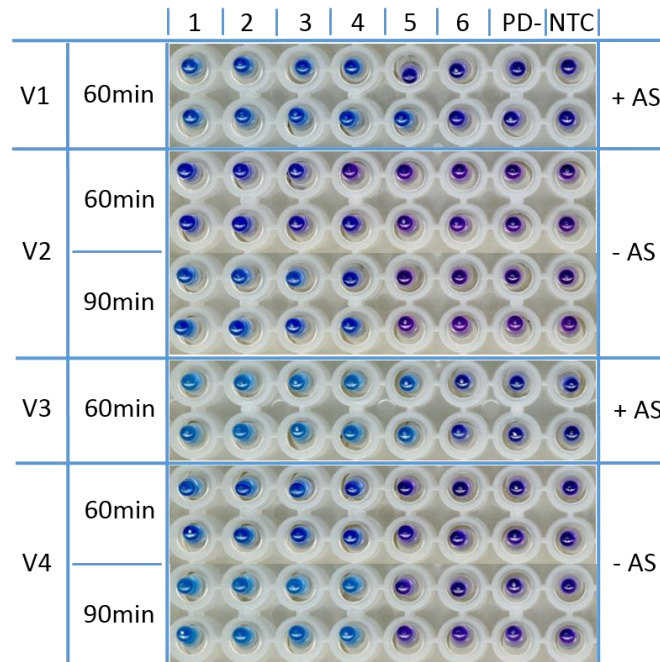


Figure 62: Influence of ammonium sulfate on PD LAMP performance. V1, V2 = optimized PD LAMP reaction mix composition with and without ammonium sulfate (AS), respectively. V3, V4 = PD LAMP reactions with enhanced magnesium chloride, dNTP and reduced betaine concentrations, with and without AS. 1-6 = dilution series of a PD positive control (1 = undiluted; 2 = diluted 1:10; 3 = 1:100; 4 = 1:1,000; 5 = 1:10,000; 6 = 1:100,000); PD- = PD negative control; NTC = no template control; +AS = with ammonium sulfate; -AS = without ammonium sulfate. Dye: HNB.

Figure 63 shows a series of experiments with varying concentrations of Tris-HCl (pH 8.8) (Tris), AS and potassium chloride (KCl). A dilution series of a PD positive control was tested in duplicates, starting with the 1:10 dilution.

Conc. [mM] (10x)			1	2	3	4	5	PD- NTC
Tris	AS	KCl						
200	50	100						
200	50	200						
300	75	200						
400	75	200						
400	75	300						

Figure 63: Influence of Tris-HCl, ammonium sulfate and potassium chloride concentrations on PD LAMP performance. Varied concentrations of individual buffer components [mM] in the 10-fold concentrated buffer preparation are given on the left. Tris = Tris-HCl (pH 8.8); AS = ammonium sulfate; KCl = potassium chloride; 1-5 = dilution series of a PD positive control (1 = diluted 1:10; 2 = 1:100; 3 = 1:1,000; 4 = 1:10,000; 5 = 1:100,000); PD- = PD negative control; NTC = no template control. Dye: HNB.

Sensitivity of the preparations varied from 1:1,000 to 1:10,000, with the higher dilution being positive in one repetition only in many cases. A significant influence of the concentration of an individual buffer component on assay sensitivity was not observed in the range of the evaluated concentrations. However, increasing concentrations of the buffer ingredients resulted in a weak contrast of the colour change because negative reactions displayed a bluish staining similar to positive reactions. No false positives were observed throughout these experiments.

During DNA amplification in LAMP, a constant reaction solution pH is maintained by Tris-HCl. However, Tris buffers are temperature sensitive, showing considerable decrease of pH values with increasing temperature. Therefore, fluctuations of the buffer pH were suspected as possible source of error in LAMP reactions producing false positives. Enhancing the Tris-HCl concentration to increase buffer capacity as conducted in the concentration series experiment described above results in a higher ionic strength, which has a direct impact on primer melting temperatures. Two alternative buffer substances, glycine and 3-(N-morpholino)propanesulfonic acid (MOPS) were evaluated for their suitability in LAMP reactions.

Glycine was tested at two concentrations, 200 mM, corresponding to the concentration of Tris-HCl in the 10x ThermoPol buffer, and 20 mM, respectively. Stock solutions of 1 M and 0.1 M glycine were adjusted with NaOH to a pH of 9. LAMP buffer with glycine was prepared in 10-fold concentration with KCl, AS and MgCl₂ corresponding to the respective concentrations in the ThermoPol buffer. The influence of the non-ionic detergent Tween-20 on

Results

buffer capacity was also evaluated, testing both glycine concentrations with and without 1 % Tween-20. The pH of the complete buffer preparations was measured. The variants with 200 mM glycine both yielded a pH value of 8.34 after LAMP buffer assembly with or without detergent. Preparations with 20 mM glycine showed a larger drop of pH, with 7.54 in the presence and 7.64 in the absence of Tween-20. The control buffer with Tris-HCl yielded a pH of 8.68 after LAMP buffer preparation.

PD LAMP reactions were incubated at 65 °C for 60 min. Controls were tested in duplicates. The variants with 200 mM glycine in the 10-fold buffer concentrate yielded ladder-like banding patterns on the agarose gel in the positive controls, which were identical to those observed in the control reactions with Tris-HCl. However, LAMP reactions containing glycine showed no colour change (Figure 64). In both variants with low glycine concentration, the positive controls were not amplified. The non-ionic detergent Tween-20 had no influence on LAMP performance in this experiment.

Glycine [mM] (10x)	Buffer pH	M	PD+	PD+	PD-	PD-	NTC	NTC		
Tris-HCl	8.68									
200	8.34									- T
20	7.64									- T
200	8.34									+ T
20	7.54									+ T

Figure 64: Evaluation of glycine as buffering agent in LAMP. Tested glycine concentrations [mM] in the 10-fold concentrates of the LAMP buffer as well as pH values of the LAMP buffers are given on the left. M = size marker; PD+ = PD positive control; PD- = PD negative control; NTC = no template control; +T = LAMP buffer with Tween-20; -T = LAMP buffer without Tween-20. Dye: HNB.

According to Denschlag et al. (2013), the applicability of 20 mM MOPS with a preset pH of 8.8 as buffering agent in LAMP with HNB for colorimetric product detection was examined.

Unfortunately, it became obvious already during reaction mix preparation that MOPS leads to an immediate blue staining of the HNB-containing reaction solution in the presence of magnesium ions. The reaction mix was discarded and the experiment was repeated with a MOPS buffer whose pH was adjusted to 7.48 in order to examine if the pH value influenced the effect of MOPS on the colour of reaction solutions. However, this buffer again led to intensely blue staining of reaction mixes (data not shown). Since MOPS was incompatible with colorimetric detection based on the metal indicator dye HNB, the applicability of this buffer in LAMP was not further examined.

Continuous work with the self-made buffer, which was freshly prepared every three weeks, confirmed that this procedure worked well for the PD LAMP. However, a LAMP assay targeting the *Plum pox virus*, which was performed in the same laboratory, showed occasionally false positives although the same buffer was used. An experiment was conducted with the PPV primer set used with the LAMP reaction mix composition, which was optimized for the primer set PD3, extended by a reverse transcriptase, since PPV is an RNA target. Surprisingly, these reactions displayed no false positives in the controls although comprising the same reagents as before, when the assay produced false positives. This indicates that, in addition to the LAMP buffer, there are other reagents in a LAMP reaction, which are able to provoke false positives. Since both assays contained the same reagents but applied different concentrations, the PD LAMP assay is considered more stable than the PPV assay, which uses higher concentrations of magnesium ions (added as magnesium sulfate) and dNTPs.

4 Discussion

4.1 Targets for LAMP primers

In this work, six LAMP primer sets were evaluated for their performance in a LAMP assay intended for on-site detection of the PD phytoplasma. The chosen target genes were the 16S rRNA gene, the *pnp* gene and the *rpl22* gene.

The 16S rRNA gene encodes a ribosomal RNA, which is part of the 30S ribosomal subunit of prokaryotic ribosomes. In fruit tree phytoplasmas of the 16SrX group, the 16S rRNA gene is 1521 nt in length (Seemüller & Schneider, 2004). The 16S rRNA has a distinct secondary structure, acting as scaffold for the proteins of the ribosomal 30S subunit. At the 3' end it binds to the Shine-Dalgarno sequence of the mRNA, ensuring the correct positioning of the mRNA start codon prior to protein synthesis. The phytoplasma genome contains two copies of the 16S rRNA gene (Schneider & Seemüller, 1994).

Since the pioneering work of Woese (1987), the 16S rRNA gene is the marker of choice for phylogenetic studies of prokaryotes. While being universal within the prokaryotes and highly conserved in a functional regard, the 16S rRNA gene possesses variable regions, which contain specific signatures suitable for identification and classification of eubacteria (Seemüller et al., 1994). The availability of universal primers for the bacterial 16S rRNA gene made a phylogenetic classification of the unculturable phytoplasmas via RFLP analysis and sequencing of the PCR-amplified 16S rDNA finally possible (Weisburg et al., 1991; Schneider et al., 1993; Seemüller et al., 1994). In 1995, the International Committee on Systematic Bacteriology accepted the proposal of Murray and Schleifer (1994) to implement a new taxonomic rule for the description of uncultured organisms in a provisional taxon with the designation *Candidatus*, for which sequence information of the 16S rRNA gene is mandatory (Murray & Stackebrandt, 1995). Following this taxonomic rule, the IRPCM Phytoplasma/Spiroplasma Working Team – Phytoplasma taxonomy group formally described the provisional taxon *Candidatus* Phytoplasma (IRPCM, 2004). In consequence, for every phytoplasma strain described as *Candidatus* Phytoplasma species, the sequence of the respective 16S rRNA gene is deposited in the NCBI nucleotide sequence database GenBank, making this sequence a preferred target for PCR and LAMP assays intended for phytoplasma detection. The 16S rRNA gene is the most often sequenced gene in phytoplasmas (Sugawara et al., 2012). The broad availability of sequence information hence was the main factor determining the decision to design LAMP primers on the 16S rRNA gene of *Ca. P. pyri* in this study.

However, the highly conserved nature of the 16S rRNA gene imposes constraints on the classification of certain phytoplasma strains and isolates at subgroup level and below (Hodgetts & Dickinson, 2010). Several attempts to achieve a better resolution between closely related strains led to the design of PCR primers targeting non-ribosomal genes, which are applicable within certain 16Sr groups, as for example primers targeting the *tuf* gene of 16SrI group

phytoplasmas (Schneider et al., 1997; Marcone et al., 2000) or the *secY* gene of 16SrV phytoplasmas (Arnaud et al., 2007). LAMP assays for phytoplasma detection are in most cases designed to target the 16S rRNA gene (e.g. Tomlinson et al., 2010; Bekele et al., 2011; Obura et al., 2011). However, Sugawara et al. (2012) reported the development of a LAMP assay targeting the *groEL* gene, which specifically amplifies the target from phytoplasma strains of the AY group (16SrI).

The *pnp* gene encodes the polynucleotide phosphorylase (syn. polyribonucleotide nucleotidyltransferase), which degrades mRNA by catalyzing phosphorolysis in 3'-5'-direction, using magnesium ions as cofactors. Danet et al. (2011) used the *pnp* gene besides others to investigate the genetic diversity of 16SrX phytoplasmas. The authors reported that among the three fruit tree phytoplasmas, 5-6 % of nucleotide positions of the *pnp* gene sequence were substituted. At the time of writing, *pnp* gene sequences of isolates from *Ca. P. mali*, *Ca. P. pyri*, *Ca. P. prunorum* and *Ca. P. asteris* were available in the GenBank database.

The nucleotide sequence used for the design of a primer set targeting the *rpl22* gene actually comprises partial coding sequences of the ribosomal protein 22 gene (*rpl22*) as well as of the ribosomal protein s3 gene (*rps3*). The ribosomal protein 22 is involved in the assembly process of the large subunit of the phytoplasmal ribosome. It binds to different domains of the 23S rRNA of the assembled 50S subunit. The ribosomal protein s3 is a part of the 30s subunit. It binds to the mRNA, adjusting its position for the translation process. The binding sites of the designed LAMP primers are located in the transition region of the *rpl22* gene to the *rps3* gene, hence the resulting LAMP amplicon covers the terminal region of the *rpl22* sequence and the initial part of the *rps3* sequence. The *rpl22* gene sequence is available from a broad range of phytoplasma strains. A search with the keywords "Phytoplasma" and "rpl22" in the NCBI nucleotide sequence database yielded 569 hits at the time of writing. Martini et al. (2007) used sequences of *rpl22* and *rps3* genes in combination with the 16S rRNA gene to construct a phylogenetic tree of phytoplasmas and related mollicutes and Gram-positive walled bacteria, which provided a finer resolution within 16Sr groups than 16S rRNA gene based phylogeny alone. The authors reported an average sequence similarity among members of the 16SrX group of 93.4-96.5 % based on the studied rp genes. The *rpl22* gene is a single copy gene (Duduk et al., 2013).

4.2 Evaluation of LAMP primer sets for the detection of *Candidatus Phytoplasma pyri*

4.2.1 LAMP primer set PD1 published by Obura et al. (2011)

In this study, first attempts to develop a LAMP assay for the detection of the PD phytoplasma were conducted with a LAMP primer set targeting the phytoplasmal 16S rRNA gene, which was obtained from Obura et al. (2011) for the detection of the Napier stunt phytoplasma (NSP). The authors reported successful detection of *Candidatus Phytoplasma pyri* with this primer set

in specificity tests. Initial tests with this primer set, hereinafter referred to as primer set PD1, conducted in this project yielded promising results, confirming that the PD1 LAMP primers were able to prime amplification of the 16S rDNA of *Ca. P. pyri* (Figures 6 - 8). The incorporation of the metal indicator dye hydroxy naphthol blue (HNB), which was proposed by Goto et al. (2009) for colorimetric detection of LAMP reactions, required a modification of the original reaction mix composition specified in Obura et al. (2011). In detail, the magnesium ion concentration in the LAMP reaction mix had to be carefully enhanced in order to achieve a distinct contrast of the HNB colour change while avoiding unspecific amplification, which may be caused by high magnesium ion concentrations. The optimized LAMP reaction mix with primer set PD1 successfully detected the PD phytoplasma in field samples, as indicated by the HNB colour change and as confirmed by agarose gel electrophoresis. The application to the closely related apple proliferation phytoplasma was confounded by continuous false positive amplification in AP negative controls (Figure 8), which was assumed to be caused by mispriming of apple DNA since the absence of the pathogen was confirmed by nested PCR. However, sensitivity as well as speed of the reaction were not satisfying. Various attempts to create an efficient assay with this primer set failed. This was probably due to several mismatches of the PD1 LAMP primers with their respective binding sites on the 16S rDNA sequence of *Ca. P. pyri*. Furthermore, an alignment of the PD1 primer sequences with the target DNA sequence of NSP denoted in Obura et al. (2011) revealed mismatches also with this DNA sequence (Figure 10). Consequently, work with this primer set was no longer continued.

Nonetheless, it was observed during work with primer set PD1 that template DNA denaturation as described by Obura et al. (2011) in the reaction conditions for the NSP assay is not required in LAMP, which is in accordance with Nagamine et al. (2001). An initial denaturation step is reported to enhance sensitivity of LAMP assays by up to 200-fold (Aryan et al., 2010). However, initial denaturation of the template DNA was not incorporated in the PD LAMP since *Bst* DNA polymerase does not survive the required high temperatures, making a subsequent addition of the enzyme necessary, which was considered a potential contamination risk. Furthermore, short-time heating to high temperatures in combination with an additional pipetting step would run counter to the intended field applicability and simplicity of the assay.

4.2.2 LAMP primer sets PD2, PD3 and PD4 designed on the 16S rRNA gene of *Ca. P. pyri*

Based on the 16S rDNA sequence of the *Candidatus* Phytoplasma pyri reference strain, three primer sets were designed. The concentration of the metal indicator dye HNB was adopted from Goto et al. (2009), which was confirmed as optimum concentration in LAMP by Hadersdorfer et al. (2011). Concentration series of dNTPs and magnesium ions were tested with each primer set individually. However, the ratio of magnesium ions chelated by metal indicator molecules and dNTPs, which also form complexes with magnesium ions, is independent of the primer set. The ideal amount of magnesium ions saturates the dNTPs, leaving enough free magnesium ions to complex with the metal indicator and work as cofactor for the polymerase. The amplification has to be highly efficient, generating enough product, and thereby enough pyrophosphate as

by-product, to produce the insoluble magnesium-pyrophosphate-complex, which detracts magnesium ions from the complexes with the metal indicator dye at such a rate that the colour of the reaction solution changes. In this regard, the required magnesium ion concentration is connected with the performance of a primer set in the LAMP reaction.

The LAMP reaction mix composition using HNB for indirect product detection was continuously optimized during experiments with changing primer sets. This was possible because parameters for the design of LAMP primers are narrow and consequently, the properties of individual primers are similar if the target sequence is the same. However, performance of the primer sets was different under identical reaction conditions, which might be due to secondary structures of the template DNA and the resulting accessibility of the target. This was also reported by Sugawara et al. (2012) who designed and evaluated 16 LAMP primer sets based on the 16S rDNA sequence of the onion yellows phytoplasma (*Ca. Phytoplasma asteris*). Out of these 16 primer sets, only two primer sets were able to amplify the target. The authors hypothesized that the failure of the 14 primer sets was due to secondary structures of the template DNA since the 16S rRNA gene encodes a ribosomal structural RNA. Furthermore, the two primer sets showed markedly different sensitivities, with one primer set being 10-fold less sensitive, and the other 100-fold more sensitive than PCR. In this work, all primer sets designed on the 16S rRNA gene of *Ca. P. pyri* successfully amplified the target, but differences in the performance of the primer sets were observed in terms of assay sensitivity as well as vulnerability to the occurrence of false positives. It was also observed that reaction speed, as judged by the time necessary to obtain a distinguishable colour change of positive reactions, varied between the primer sets. Khorosheva et al. (2016) remarked that reaction speed of isothermal amplification methods might in parts depend on the secondary structures of the template DNA. Since the binding sites of the three primer sets are located in different sections of the 16S rDNA sequence, they might encounter different situations regarding the secondary structure of the template, resulting in the observed discrepancies of LAMP performance.

Although the recommended reaction temperature for LAMP assays is 63 °C (PrimerExplorer V4 Manual, Eiken Chemical Co., Ltd., Tokyo, Japan), the highest possible reaction temperature as determined by the optimum temperature range of *Bst* DNA polymerase was chosen for the PD LAMP assay because unspecific and false positive amplifications occurred more frequently at lower temperatures. Since the occurrence of false positive reactions was a persistent problem throughout the development process, the suppression of these undesired amplifications by high temperatures was of paramount importance in the selection of a suitable reaction temperature. While many authors state the application of the recommended reaction temperature of 63 °C without evaluating LAMP performance over the full temperature range of *Bst* DNA polymerase, Kogovšek et al. (2015) investigated sensitivity and reaction speed of LAMP assays targeting the 16S and 23S rRNA genes of the Flavescence dorée phytoplasma (16SrV group), respectively, at different reaction temperatures. The authors found that the 16S rRNA LAMP assay performed best at 65 °C, whereas the 23S rRNA LAMP assay performed best at 62 °C.

LAMP assays targeting the 16S rRNA gene of phytoplasmas are either published with a reaction temperature of 63 °C (Bekele et al., 2011; Obura et al., 2011; Sugawara et al., 2012) or 65 °C (Tomlinson et al., 2010b; Siriwardhana et al., 2012; Gentili et al., 2016).

The primer set PD2 was eliminated from further examinations very early in the development process due to the frequent occurrence of unspecific and false positive reactions. Primer sets PD3 and PD4 were less susceptible in this regard. However, problems with false positive amplifications occurred more frequently with primer set PD4 than with PD3 and finally, although the primer set PD4 showed a 10-fold higher sensitivity than PD3, the robustness of primer set PD3 made it superior to PD4, making PD3 the primer set of choice for the PD LAMP. Since false positive amplifications in LAMP reactions were the most challenging problem during the development of the PD LAMP assay, establishing a robust and reliable assay was of paramount importance in the choice for a suitable LAMP primer set.

A first estimation of the detection limit of the optimized PD LAMP assay with the primer set PD3 and HNB for indirect product detection in comparison to conventional and realtime PCR showed that the PD LAMP was similarly sensitive as conventional PCR and 10-fold less sensitive than realtime PCR (Figure 16). While bands of PCR products on agarose gels weakened with increasing dilution of the template, LAMP yielded banding patterns of equal intensity in all amplified dilutions, a phenomenon, which was also observed by Tomlinson et al. (2010b). The colour change of the metal indicator dye HNB was in perfect agreement with the results obtained from agarose gel electrophoresis, indicating that the applied concentration of magnesium sulfate was well balanced. A similar observation was reported by Hadersdorfer et al. (2011), who used HNB in a RT LAMP assay detecting the *Plum pox virus*. The final evaluation of the detection limit of the PD LAMP assay with the metal indicator dye Eriochromeblack-T is discussed in chapter 4.4 “Sensitivity and specificity of the PD LAMP assay”.

Since with 98.6-99.1 % sequence similarity, the 16S rRNA gene is highly conserved among members of the 16SrX group, it was expected that the LAMP primer sets designed on this gene would also amplify the AP and ESFY phytoplasmas. Several experiments proved the suitability of the PD LAMP for the detection of the AP and ESFY agents, using DNA extracts as well as crude sample preparations. A multiple sequence alignment of the target region of the primer set PD3 showed that sequences of the three fruit tree phytoplasmas were identical at the primer binding sites except for one mismatch with the forward loop primer (Figure 53). Due to the high sequence similarity, PCR primers targeting the 16S rRNA gene of 16SrX phytoplasmas are in most cases group specific (Lee et al., 1995; Lorenz et al., 1995). Those primers, which were designed to specifically detect the PD phytoplasma are not able to amplify all PD strains (Lorenz et al., 1995). A recently published LAMP assay for group specific detection of the fruit tree phytoplasmas of the 16SrX group also employs primers targeting the highly conserved 16S rRNA gene (De Jonghe et al., 2017).

4.2.3 LAMP primer sets targeting the *pnp* gene and the *rpl22* gene of *Ca. P. pyri*

Due to the high sequence similarity of the 16S rRNA gene among the 16SrX fruit tree phytoplasmas, LAMP with primers designed on this gene was not able to discriminate the AP and ESFY phytoplasmas from the PD phytoplasma. The *pnp* and *rpl22* gene sequences of phytoplasmas were reported to be more variable than the highly conserved 16S rDNA sequence (Martini et al., 2007; Danet et al., 2011). In an attempt to create a LAMP assay specific for *Ca. P. pyri*, LAMP primers were designed targeting the *pnp* gene and the *rpl22* gene of the PD phytoplasma, respectively. A similar approach was made by Sugawara et al. (2012) who presented a LAMP assay targeting the *groEL* gene of the onion yellows phytoplasma (AY group). This gene shows sequence similarities among the AY phytoplasmas ranging from 93.8-100 %. However, the authors reported that LAMP with *groEL* primers successfully amplified the target also in other phytoplasma strains of the AY group.

First tests with the primer sets *pnp* and *rpl22* were largely unsuccessful, yielding mostly unspecific products with primer set *pnp* (Figures 19 – 21), whereas LAMP with primer set *rpl22* repeatedly failed (Figures 23 – 25). Enhancing dNTP and magnesium sulfate concentrations as well as reducing the betaine concentration finally led to specific amplification of the target in LAMP with primer set *pnp*. However, the detection limit of LAMP with this primer set was one order of magnitude lower than with primer set PD3, which targets the 16S rRNA gene (Figure 22). Furthermore, LAMP reactions with *pnp* primers required an additional 30 min of incubation to yield a clearly distinguishable colour change in positive reactions as compared to LAMP with primer set PD3. Amplification with primer set *rpl22* was not achieved throughout the LAMP test series. This might be a result of the higher variability, which was reported for this gene among 16SrX phytoplasmas (Martini et al., 2007). On the other hand, failure of some LAMP primer sets to amplify the target while other primer sets designed on the same gene sequence yielded a high performance in LAMP was reported by Sugawara et al. (2012) for primers targeting the 16S rRNA gene as well as the *groEL* gene of the onion yellows phytoplasma. Hence, the systematic screening of a range of primer candidates with standardized reaction conditions appears to be more suitable than examining and optimizing individual primer sets as it was done in this study. Due to the poor performance of LAMP with the primer sets *pnp* and *rpl22* compared to LAMP with primer sets PD3 or PD4, work with *pnp* and *rpl22* primers was discontinued and primer specificity was not evaluated.

4.3 Colorimetric detection with Eriochromeblack-T

The enzymatic incorporation of a nucleotide during a nucleic acid amplification reaction results in the release of a pyrophosphate anion (Mori et al., 2001; Jansson and Jansson, 2002). Several attempts have been made to detect PCR amplification by the detection of inorganic pyrophosphate or orthophosphate after pyrophosphatase-catalyzed hydrolysis (Jansson and Jansson, 2002; Shiddiky et al., 2006). However, drawbacks of pyrophosphate detection in PCR arise mainly from the small amounts of pyrophosphate generated in PCR reactions, as well as

the heat-induced hydrolysis of pyrophosphate to orthophosphates during the denaturation step. Moreover, promoting the generation of higher amounts of pyrophosphate in PCR by altering reaction conditions or target length may provoke unspecific amplifications (Mori et al., 2001). In cases where the generation of pyrophosphates impairs the amplification reaction due to product inhibition, thermostable pyrophosphatases can be used to push the equilibrium towards DNA synthesis by the removal of the by-product pyrophosphate, thereby enhancing PCR yield (Lee et al., 2009; Park et al., 2010).

In LAMP, DNA yields of 0.4 µg/µl are reported (Mori et al., 2001; Tomita et al., 2008). This high amplification efficiency is accompanied by the generation of large amounts of inorganic pyrophosphate. Mori et al. (2001) demonstrated that the white precipitate responsible for the occurring turbidity in LAMP reactions with ongoing amplification consists of water insoluble magnesium pyrophosphate complexes. The application of the metal indicator hydroxy naphthol blue (HNB) for colorimetric detection based on pyrophosphate generation and magnesium complexing in LAMP was introduced by Goto et al. (2009), and this dye is currently widely used in various LAMP protocols that employ colorimetric product detection (e.g. Tomlinson et al., 2010b; Hadersdorfer et al. 2011; Gosch et al., 2012; Ahmadi et al., 2013; Moradi et al., 2014; Vu et al., 2016). Also in this study, colorimetric detection of LAMP results was intended to be performed with HNB since this dye provides all benefits necessary for in-field-applicability of a LAMP assay: easy judgement of LAMP results, no post-amplification treatment necessary, no negative influence on assay performance and low cost. However, HNB appeared progressively unstable during the development process of the PD LAMP, which was expressed by varying intensities and tints of the colour over time, and occasionally in repetitions of the same experiments (Figure 37). Moreover, the dye yielded only a deficient contrast between positive and negative samples, frequently necessitating an additional analysis of the LAMP products with agarose gel electrophoresis. In consequence, several alternative metal indicator dyes were tested for their applicability in LAMP: Murexide, Phthalein purple, Eriochromeblack-T and Thiazole yellow (Figures 38 – 39). The best results were obtained with Eriochromeblack-T (ErioT), an azo dye mainly used in complexometric titrations as for example the determination of water hardness with EDTA (Biedermann and Schwarzenbach, 1948; Betz and Noll, 1950). Beyond this traditional use, the applications of this dye are manifold. Obuchowski and Wegrzyn (1991) proposed ErioT as Bromphenol blue-alternative for agarose gel electrophoresis of DNA. Morris et al. (1997) demonstrated ErioT to have angiostatic properties, thereby inhibiting tumor growth. Skaff et al. (2015) reported an inhibitory effect of ErioT on a bacterial enzyme necessary for cell viability and suggested that eriochrome compounds may be developed into antibiotic drugs. Electropolymerized ErioT films on glassy carbon electrodes are used to create biosensors that detect specific DNA fragments (Wang et al., 2014) as well as dopamine, ascorbic acid and uric acid in biological samples (Yao et al., 2007) or L-cysteine and L-tyrosine (Liu et al., 2012).

4.3.1 Optimization of the PD LAMP assay with Eriochromeblack-T

At the time the experiments presented herein were conducted, only one publication was available reporting the application of ErioT in LAMP (Shigemoto et al., 2010). Whilst these authors used a comparatively low concentration of the dye, the concentration applied in the PD LAMP corresponded to that of the previously used HNB, yielding brighter colours than with the concentration reported by Shigemoto et al. (2010) and a high-contrast colour change. An experiment comparing the effect of ErioT and HNB on PD LAMP assay sensitivity was conducted, which proved that ErioT had no inhibitory effect on the LAMP reaction in the applied concentration since both assays using either ErioT or HNB showed equal detection limits (Figure 39). The optimization of the PD LAMP assay with ErioT resulted in a lowering of magnesium chloride concentration and the substitution of the additive betaine with polyethyleneglycol 8k (PEG 8k) in the LAMP reaction mix. Since high levels of magnesium ions can cause unspecific amplifications as reported for PCR (Innis and Gelfand, 1999; Markoulatos et al., 2002), the reduced magnesium chloride concentration possibly contributed to the robustness of the PD LAMP assay towards the formation of false positives, compared to earlier preparations using HNB with correspondingly higher magnesium concentrations. As the *Bst* DNA polymerase requires free magnesium as cofactor, the optimization of magnesium ion concentration is critical for the development of a robust and efficient LAMP assay. Template DNA, primers and dNTPs are known to bind magnesium ions (Markoulatos et al., 2002). In consequence, the magnesium chloride concentration must saturate all these magnesium complexing substances in the reaction solution, leaving an additional amount of free magnesium ions as cofactor for the polymerase (Innis and Gelfand, 1990). With ongoing DNA amplification, pyrophosphate anions are generated, which form complexes with magnesium ions as well. Using a metal indicator dye like HNB or ErioT for colorimetric product detection, an additional magnesium-complexing agent is introduced to this competition situation for magnesium (Figure 65). The binding strength of the metal indicator-magnesium-complex is most important for the choice of dye because it is necessary that the generated pyrophosphates are able to detract magnesium ions from the metal indicator complex. In consequence, the complex stability of magnesium pyrophosphate has to be higher than that of the metal indicator-magnesium-complex. During preparation of the reaction mixes with HNB, the colour of the solutions turned bluish when dNTPs were added, which was also reported by Goto et al. (2009), whereas preparations with ErioT scarcely changed their colour upon dNTP addition. Since dNTPs form complexes with magnesium, the behavior of the dyes might reflect different affinities to magnesium ions. Thus, there is a direct competition of metal indicator, dNTPs and pyrophosphate for magnesium ions, which determines, by the respective affinities to magnesium, the transition point of the dye in dependence on the pyrophosphate concentration and thereby on the DNA yield.

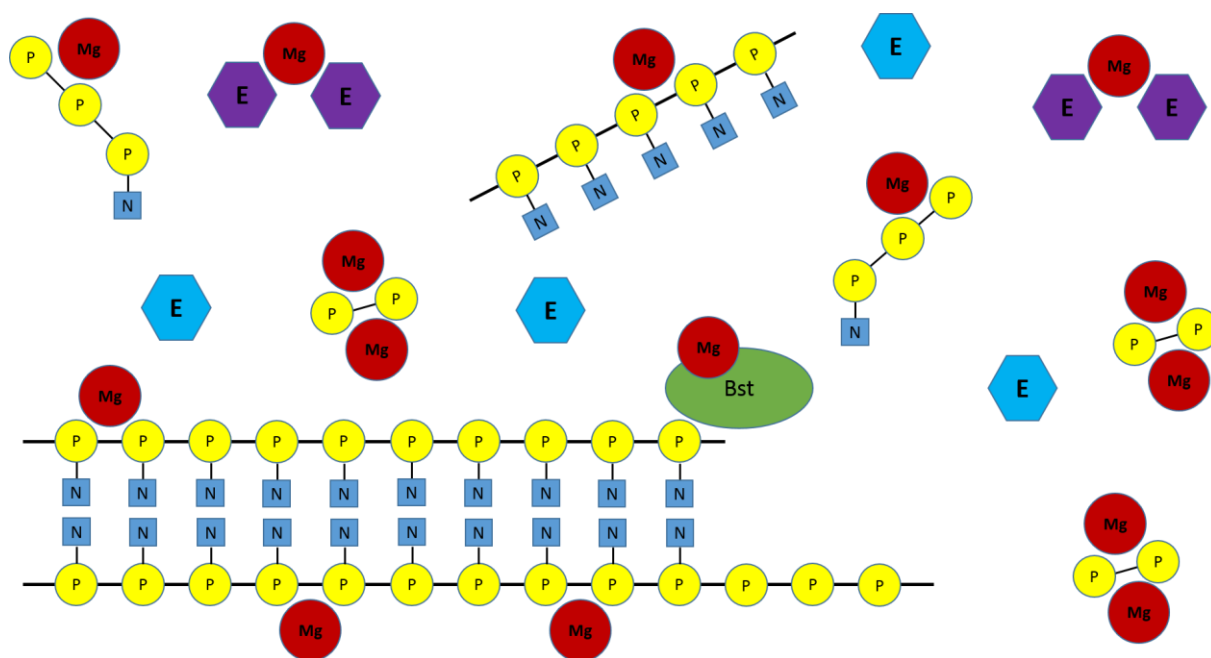


Figure 65: Schematic illustration of the competition of LAMP reagents for magnesium ions. Mg = magnesium ion; P = phosphate; N = nucleotide; N-P-P-P = dNTP; P-P = pyrophosphate anion; E = Eriochromeblack-T (purple = magnesium complex; blue = uncomplexed form); poly(P-N) single-stranded = primer; poly(P-N N-P) double-stranded = template DNA; Bst = *Bst* DNA polymerase.

In 2016, Oh et al. presented a centrifugal microdevice using ErioT for indirect LAMP product detection. In contrast to Shigemoto et al. (2010), these authors applied ErioT at a concentration of 120 μM per reaction, which is in agreement with the ErioT concentration used in this study. However, discrepancies exist in the concentrations of other LAMP reaction mix components influencing the colour and the colour change of ErioT. In this study, magnesium chloride at a concentration of 4.8 mM was used together with 0.8 mM dNTPs, in contrast to Oh et al. (2016) who applied 3.6 mM magnesium sulfate and 2.8 mM dNTPs. This might in parts explain the weak colour change, which is visible on photographs of positive and negative LAMP reaction solutions with ErioT in the publication by Oh et al. (2016).

The hitherto used additive betaine, which was applied in LAMP reactions with HNB, was replaced with the molecular crowding agent polyethylene glycol 8k (PEG 8k). A concentration series of PEG 8k confirmed the concentration of 4.8 % per reaction as reported by Denschlag et al. (2013) to be optimal in LAMP, enhancing sensitivity of the PD LAMP assay by at least one order of magnitude. However, a concentration of 6 % PEG 8k in the LAMP reaction mix considerably impaired the detection limit of the PD LAMP. Furthermore, a weakening of colour intensity of the blue-stained positive reactions was observed with high PEG 8k concentrations (Figure 41). This may be due to volume exclusion effects by enhanced PEG 8k concentrations, which results in a higher dye concentration in the aqueous phase, thereby inducing self-aggregation of ErioT. A weak staining of LAMP reaction solutions containing ErioT can also be seen in photographs presented in the publication of Oh et al. (2016). While these authors did not employ PEG 8k, they used a comparatively high concentration of betaine of 1.6 M per

reaction (as opposed to 1 M betaine used in LAMP reactions with HNB in this study), which might have a similar effect on ErioT as high concentrations of PEG 8k. The influence of PEG 8k on detection limit and specificity of the PD LAMP is discussed in detail in chapter 4.4 “Detection limit and detection range of the PD LAMP”.

Stock solutions of ErioT with either Tris-HCl (pH 8.8, corresponding to the pH of the LAMP buffer) or distilled water remained stable over a period of approximately four weeks when stored in a freezer. Older solutions exhibited a brownish discolouration, which may be due to polymerization of the dye. Similarly, at a pH below 6, ErioT shows a tendency to polymerize, which results in a yellow-brownish staining of the solution (Jander and Jahr, 2002). In consequence, ErioT solutions, which had turned brown, were discarded and fresh solutions of the dye were prepared. Except this brown staining after four weeks, the dye solutions showed no signs of degeneration before this approximate expiry date.

4.3.2 Investigation of spectrophotometric properties of Eriochromeblack-T

Similar to the work of Goto et al. (2009) with HNB, the spectrophotometric properties of ErioT were investigated with a UV/Vis spectrophotometer. Eriochromeblack-T possesses an azo bond (-N=N-) as chromophore substituted with two naphthalene moieties (de Luna et al., 2013) (Figure 66). The sulfonate group in *para*-position to the chromophore completely dissociates in water, providing for the good water solubility of ErioT (Rauf et al., 2015; Skoog et al., 2014).

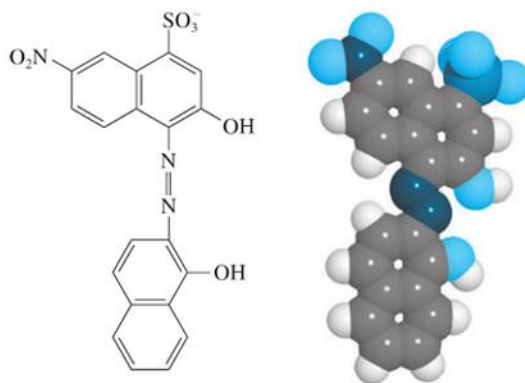


Figure 66: Structural formula and molecular model of the metal indicator Eriochromeblack-T (Skoog et al., 2014)

In this study, absorbance of aqueous ErioT solutions without adjusted pH was generally low and there was no change in absorption spectra following addition of magnesium (Figure 44). In contrast, measurements of ErioT spectra in Tris-HCl (pH 8.8) or LAMP buffer yielded distinct absorbance maxima for the metal-indicator complex and the free dye, respectively (Figure 44 - 45). This is in accordance with Young & Sweet (1955), Balsaraf et al. (2010) and Skoog et al. (2014) who reported the absorption behavior of ErioT to be dependent on the pH of the solvent. At a pH below 6, the sulfonate group is deprotonated and both hydroxyl groups are protonated.

This species is described as red. Above pH 6, one of the hydroxyl groups is deprotonated, resulting in a blue coloured anion. The second hydroxyl group dissociates at pH 12, which changes the colour to orange. Since metal complexes with ErioT are red, the recommended pH range suitable for metal indication is between 7 and 11, where the dye is in its blue form in the absence of metal ions (Young & Sweet, 1955; Lee et al., 1996; Skoog et al., 2014). The ability of an azo dye to form a complex with a metal atom requires two substituents in *ortho*-position to the azo group, one of which must be a hydroxyl group and the other a hydroxyl or carboxyl group (Ellingboe 1956). ErioT possesses two hydroxyl groups *ortho* to the azo group, which are involved in complex formation (Cakir et al., 2001; Masoud et al., 2002). In contrast to HNB, for which only 1:1 complexes with alkaline earth metals (Brittain, 1978) as well as copper (II) (Sugawara, 1977) are reported, Young and Sweet (1955) showed that ErioT forms 1:1, 2:1 and 3:1 complexes with magnesium, depending on the pH of the solvent. However, Levine and Cummings (1956) noted that at pH 10.1, a mixture of different complexes was present, and that at pH 11.5, at which presumably the 3:1 complex was formed only, absorbance values again indicated the presence of diverse complexes. Besides, 1:1 and 2:1 complexes were reported for various metals with ErioT (Kodama, 1967; Kodama & Ebine, 1967; Cakir et al., 2001; Masoud et al., 2002). At pH 8.8, which was applied in this study, the formation of 1:1 and 2:1 complexes may be likely.

The influence of individual components of the LAMP reaction mix on UV/Vis absorption spectra of ErioT was investigated (Figure 46). Absorption spectra of ErioT/Tris-HCl solutions containing either potassium chloride or ammonium sulfate showed lower peaks than the reference solution with Tris-HCl (pH 8.8) only. Inscoe et al. (1958) reported a similar effect of increasing concentrations of potassium bromide on absorption spectra of Diamine Sky Blue FF, a disazo dye. The authors attributed this to an increased aggregation tendency of the dye with increasing concentrations of inorganic salts. The aggregation of azo dyes is a frequently observed and intensely studied phenomenon. Ünal et al. (2013) investigated absorbance properties of Eriochrome Blue Black B and observed distorted isosbestic points with increasing pH values. The authors concluded that besides the pH-induced changes in acid-base-equilibria, the dye tended to form aggregates, resulting in the shift of isosbestic points. Buwalda et al. (1999) reported the absence of isosbestic points in spectra of azo dyes when cationic surfactants were added to aqueous dye solutions and ascribed this to the formation of dye aggregates. Similarly, ErioT-solutions analyzed in this study displayed distorted isosbestic points in the spectra of the metal-dye-complex and the free dye, when the solutions contained potassium chloride or ammonium sulfate. The addition of PEG 8k resulted in a stabilization of absorbance values, leading to only minor variations at the isosbestic point in the range of 0.1 units. Inscoe et al. (1958) showed that the non-ionic detergent Triton X-100 inhibits the aggregation of Methyl Violet and Chrysophenine G in a mixture, as well as the aggregation of the individual dyes. This effect is also reported for polyethylene oxide condensates (and polyethylene glycols (Martin and Standing, 1949) and may be responsible for the observed alterations of absorption

spectra when PEG 8k was added to solutions containing potassium chloride or ammonium sulfate, supporting the assumption that dye aggregates were generated in PEG 8k-deficient ErioT solutions induced by these inorganic salts. The effects of potassium chloride and ammonium sulfate on ErioT absorption spectra were more pronounced when the presence of magnesium ions caused the dye to form complexes with the metal. This may indicate that the tendency of the dye to aggregate is higher in the metal-complex-form than in the free form. However, a hypsochromic or bathochromic shift of absorption spectra, indicating the formation of H- or J-aggregates as reported by Langhals (1991) for solutions containing electrolytes, was not observed with ErioT solutions in the presence of potassium chloride or ammonium sulfate. Therefore, the type of dye aggregate generated in the analyzed ErioT solutions may be different, resulting in a lowering of overall absorption values instead of altering the absorption maximum wavelength.

The addition of PEG 8k to ErioT solutions resulted in a bathochromic shift and increased intensity of absorption peaks. Additionally, a shoulder at longer wavelengths appeared. Several explanations for these alterations of absorption spectra are conceivable. Ouyang et al. (2007) observed a bathochromic shift in the absorption spectrum of the azo dye Orange I when the solution contained PEG at various molecular weights and attributed this to the formation of J-aggregates triggered by PEG. Saad et al. (2014) reported a bathochromic shift of the absorption maximum together with the appearance of a new absorption band at a longer wavelength upon the addition of cetyltrimethylammonium bromide (CTAB) to aqueous solutions of the azo dye Acid Red 266. The authors ascribed the red-shifted absorption maximum to the formation of surfactant-dye-aggregates and the new absorption band to surfactant induced generation of J-aggregates. Nazar et al. (2010) studied the interaction of the azo dye Alizarin Yellow R with CTAB and reported red-shifted absorption maxima with increasing intensities compared to aqueous solutions upon addition of increasing CTAB concentrations. Since dye molecules can aggregate in different orientations – head-to-tail aggregation resulting in a red-shift, parallel aggregation in a blue-shift of absorbance maxima – the authors concluded that the surfactant-dye-aggregates comprised head-to-tail aggregated dye molecules. The initial decrease of absorbance values in the presence of very low CTAB concentrations was explained by the authors with surfactant-assisted self-aggregation of dye molecules, similar to the decrease of absorbance values of ErioT in the presence of potassium chloride or ammonium sulfate observed in this study. Martin and Standing (1949) found that polyethylene glycols of various molecular weights formed complexes with the azo dyes Benzopurpurine 4B, meta-Benzopurpurine 4B and Direct Fast Orange SE. In this work, the absorption spectra of magnesium-free ErioT solutions showed a bathochromic shift of the absorption maximum as well as a shoulder-like twist at longer wavelengths in the presence of PEG 8k. This may indicate the formation of PEG-ErioT-complexes, resulting in the red-shifted absorption maximum, and the generation of PEG-induced J-aggregates, causing enhanced absorption values at longer wavelengths. The less pronounced differences in absorption spectra of magnesium-containing

ErioT solutions supports this interpretation of the effect of PEG 8k on ErioT since the ErioT-magnesium-complex may be less prone to form either J-aggregates or aggregates with PEG 8k.

However, another explanation for the observed bathochromic shift of PEG 8k-containing ErioT solutions may be the azo-hydrazone-tautomerism of ErioT, which is due to conjugated hydroxyl groups in *ortho*-position to the azo group (Hamed et al., 1994; Manjunatha et al., 2014; Rauf et al., 2015). Azo-hydrazone-tautomerism requires an intramolecular proton transfer and is therefore linked with the acid-base-equilibrium of the dye (Rauf et al., 2015). The corresponding changes in electronic structure of the whole molecule result in alterations of absorption spectra (Rauf et al., 2015). Ünal et al. (2013) studied the azo-hydrazone-tautomerism of Eriochrome Blue Black B and found that besides the azo form, only one out of two possible hydrazone tautomers was present in aqueous solutions. This may presumably be transferable to the similarly built Eriochromeblack-T. Consequently, the tautomer hereinafter referred to as hydrazone tautomer of ErioT is the corresponding hydrazone-1 form as described by Ünal et al. (2013). This is in agreement with Ghosh (2010), who reported ErioT tautomerism to be triggered by sodium dodecyl benzene sulphonate (SDBS), and termed the SDBS-stabilized ErioT species a quinone-hydrazone-tautomer, which describes the same tautomeric form. Chen et al. (2012) showed that deprotonation caused by basic pH triggers the conversion of hydrazone isomers of two Disperse Yellow Dyes into their respective azo species, resulting in a shift of the azo-hydrazone equilibria in solution towards the deprotonated azo form. The spectral behavior of these dyes around pH 9 displays similarities to the spectra of free ErioT in the presence of PEG 8k recorded in this study. Here, the appearance of a new absorption band at a higher wavelengths possibly indicates a shift in the azo-hydrazone-equilibrium towards the hydrazone tautomer of ErioT. This interpretation is supported by the work of Rageh (2005) who investigated absorption spectra of the azo compound 2-[(4-sulfanylphenyl)azo]-4,5-diphenylimidazole in the presence of various organic solvents. The author stated that the absorption peak at shorter wavelengths represented the azo form of the dye and the shoulder at longer wavelengths the hydrazone form, since the latter is considered as less stable and of higher energy, requiring a lower amount of energy for excitation. Ghosh (2010) reported the stabilization of the ErioT hydrazone tautomer by SDBS as a consequence of charge transfer interaction. In this study, the bathochromic shift upon addition of PEG 8k was very weak when ErioT solutions contained magnesium ions. Since azo-hydrazone-tautomerism only occurs with the free azo dye, this observation is in line with the interpretation presented above.

A comparison of the spectra measured in this study with those presented in Oh et al. (2016) for complete LAMP reactions with ErioT again demonstrated that absorption spectra of ErioT are strongly influenced by the composition of the solvent. Absorption peaks measured in the sodium pyrophosphate titration experiment performed in this study were at 547 nm for the magnesium complex and at 648 nm for the free dye (Figure 47). In contrast, Oh et al. (2016) reported the absorption maximum of the magnesium complex to occur at 570 nm and of the free dye at 640 nm. These discrepancies may be due to the presence of the various LAMP

reaction components as dNTPs, primers and *Bst* DNA polymerase in the reaction solutions measured by Oh et al. (2016), which were excluded from spectrophotometer analysis in this study. However, the high betaine concentration used by Oh et al. (2016) might also contribute to the shifted absorption maxima as well as to the appearance of a pronounced shoulder at shorter wavelengths in spectra of the magnesium-dye-complex.

Finally, it was not possible to elucidate in detail the causes for altered absorption spectra of ErioT solutions within the scope of this work. While the formation of dye aggregates in the presence of inorganic salts is unequivocal, and undoubtedly supported by literature, the mechanism behind the shifted absorption peaks of PEG 8k-containing ErioT solutions remains unclear, not least because bathochromic shifts can have a range of different causes. Nevertheless, these shifts did not impair the contrast of the colour change. Moreover, ErioT solutions containing PEG 8k displayed colours, which appeared brighter, as reflected by enhanced absorbance values, compared to dye solutions without PEG 8.

4.3.3 Titration experiments with sodium pyrophosphate

Mori et al. (2001) proved that turbidity in LAMP derives from the amplification by-product pyrophosphate, which forms a precipitating complex with magnesium ions. The authors traced the generation of magnesium pyrophosphate in a LAMP reaction in an experiment with a constant magnesium concentration in LAMP buffer and rising potassium pyrophosphate concentrations. Based on this approach, the formation of the ErioT colour change in LAMP was traced in a titration experiment with sodium pyrophosphate (NaPP) in order to determine the colour transition point of ErioT under the given conditions. NaPP readily dissociates in an aqueous solution, thereby providing the pyrophosphate anion for the more stable magnesium pyrophosphate complex. The formation of water insoluble magnesium pyrophosphate with rising NaPP amounts reduces the concentration of free magnesium ions in the solution, resulting in the colour change of ErioT. Preliminary investigations showed that the colour change does not occur immediately after addition of NaPP to the test solutions, but takes 20 to 30 min to develop, together with the corresponding turbidity caused by precipitating magnesium pyrophosphate (data not shown). In order to simulate the mechanism behind the colour change in LAMP as precise as possible, the test solutions were incubated for 60 min at 65 °C, which corresponds the reaction conditions of the PD LAMP assay. This is in accordance with Mori et al. (2001) who chose the same reaction conditions for their titration experiment with potassium pyrophosphate. The authors reported increasing turbidity with pyrophosphate concentrations of 0.5 mM and above and concluded that below this value, the magnesium pyrophosphate complexes did not precipitate. In this study, turbidity was not measured but reaction tubes were centrifuged after incubation and whitish pellets were observed at 0.3 mM NaPP and above. It seems unlikely that the difference to the value given in Mori et al. (2001) arises from sodium instead of potassium as initial complexing salt since both are monovalent cations that immediately dissociate in aqueous solutions. Unfortunately, it is not specified in the publication

of Mori et al. (2001), which potassium pyrophosphate concentrations below 0.5 mM were tested in the simulation of turbidity generation.

The colour transition point of ErioT in the absence of dNTPs was determined at 2.5 mM NaPP by spectrophotometer measurements as well as by visual judgement of the reaction solution colours (Figures 47 and 49). The integration of dNTPs at a constant concentration into the titration experiments led to a shift of the colour transition point to 1 mM NaPP (Figure 49). The stepwise lowering of the dNTP concentration relative to the increasing NaPP concentration did not change this value (Figure 50). This indicates that magnesium consumption of pyrophosphates is mainly satisfied by the ErioT-Mg-complexes. HNB solutions containing dNTPs showed the same colour transition point as ErioT solutions. However, HNB solutions with dNTPs appeared more bluish than solutions without dNTPs and consequently, the colour change at the transition point and beyond was very weak (Figure 49). The less distinct colour change of HNB in comparison to Goto et al. (2009) is probably due to the lower magnesium concentration used in the PD LAMP (4.8 mM compared to 8 mM in Goto et al., 2009).

Based on this result, the amount of DNA produced by LAMP, which is needed to cause a colour change of ErioT, can be calculated. The result of 0.30895 $\mu\text{g}/\mu\text{l}$ is even below the DNA yield of approximately 0.5 $\mu\text{g}/\mu\text{l}$, which was stated by Nagamine et al. (2002) for LAMP reactions using loop primers within 60 min of incubation. Mori et al. (2001) reported the generation of more than 0.4 μg DNA per μl . Therefore, the suitability of the metal indicator ErioT for the colorimetric detection of LAMP products is confirmed. Moreover, the measurement of ErioT absorbance values at a given wavelength representing the free dye or the metal chelate might be a suitable method to monitor the LAMP reaction in realtime. Spectrophotometer measurements performed in the NaPP titration experiment of this study showed that tracing the absorbance values at a wavelength of 648 nm, representing the absorption maximum of the free ErioT, over the applied range of NaPP concentrations yielded a curve with a distinct rise when the colour transition point was reached (Figure 48). Similar approaches have been proposed, as for example realtime monitoring of turbidity, which relies on the generation of magnesium pyrophosphate as well (Mori et al., 2004). The use of HNB, however, has been limited to end point detection in LAMP assays up to now, which might be due to the unavailability of portable instruments to measure UV/Vis spectra. Oh et al. (2016) used a microvolume UV/Vis spectrophotometer to determine absorption spectra of LAMP reaction solutions with ErioT and reported the ratio of the absorbance values at 640 nm to 570 nm to be proportional to the amount of LAMP product. Most recently, Rodriguez-Manzano et al. (2016) presented a visual readout system with unmodified cell phones for colorimetric LAMP reactions using ErioT. However, the authors reported that a dye concentration of at least 0.175 mM was required (in contrast to 0.12 mM used in this study) to provide a colour change distinguishable by an unmodified cell phone camera. The transfer of this result visualization technique to existing LAMP assays might probably require adjustments of magnesium ion concentrations to saturate the enhanced

demand of the metal indicator dye, which may in turn result in reduced stringency of the LAMP assay due to the adverse effects of high magnesium ion concentrations.

4.4 Detection limit and detection range of the PD LAMP assay

Sensitivity of LAMP is commonly expected to be almost equal to (Kuboki et al., 2003; Poon et al., 2005) or higher (Duan et al., 2014; Kursu et al., 2015) than that of PCR. However, LAMP assays with different primer sets for the same target may show different sensitivities. Sugawara et al. (2012) reported that sensitivity differed among LAMP reactions with primer sets targeting the 16S rDNA sequence of *Candidatus* *Phytoplasma asteris* from 10-fold lower to 100-fold higher than that of PCR. This was also observed in this study with primer sets targeting the 16S rDNA sequence of *Ca. P. pyri*. In sensitivity tests, LAMP with primer set PD4 proved to be 10-fold more sensitive than with primer set PD3 (Figure 18). In comparison to conventional PCR, LAMP reactions with primer set PD4 showed a 10-fold higher sensitivity. Using primer set PD3, LAMP was equally sensitive as PCR. However, the performance of a DNA amplification assay also depends on the sample type, which determines the level of inhibitory substances as well as the amount of background DNA. While PCR and LAMP with primer set PD3 performed equally well in sensitivity tests with dilution series of DNA extracts derived from *in vitro* plants, the PD LAMP was superior, when field samples from adult pear trees were tested for the presence of phytoplasmas. This may be due to higher amounts of inhibitors present in the field samples compared to samples from *in vitro* cultured plants. A similar observation was made by Harper et al. (2010) who reported the development of a LAMP assay as well as a realtime PCR assay for the detection of the plant pathogenic bacterium *Xylella fastidiosa*. During assay development, the authors noted differences in assay performances of LAMP, conventional PCR and realtime PCR, when pathogen DNA was diluted in either water or healthy plant DNA, concluding that LAMP was less prone to inhibition than conventional PCR and realtime PCR.

In this study, the choice of additive had a strong impact on sensitivity as well as specificity of the PD LAMP assay. Two additives were examined for their influence on LAMP assay performance, betaine and polyethylene glycol 8k (PEG 8k). Betaine is an isostabilizing agent that promotes DNA strand separation by altering its melting characteristics (Jensen et al., 2010). PEG 8k is a macromolecule used to mimic the natural cellular environment, which is rather crowded by large molecules than a dilute solution. This macromolecular crowding leads to shifts in equilibria and rates of biological reactions, favoring the association of reactants (Minton, 2006). The evaluation of the detection limit of the PD LAMP assay in comparison to conventional and realtime PCR was conducted with a plasmid containing the target sequence as template (Figure 51). LAMP was able to detect 100 copies of the target per reaction, being as sensitive as PCR in two out of three repetitions when PEG 8k was used as additive in the reaction mix. As expected, realtime PCR was about 100-fold more sensitive than LAMP, yielding fluorescence signals even for the one copy of the target per reaction in all replicates.

The lower sensitivity of LAMP in comparison to realtime PCR is frequently reported for LAMP assays targeting plant pathogens (Harper et al., 2010, and references herein). Recently, De Jonghe et al. (2017) presented a LAMP assay for the detection of the fruit tree phytoplasmas of the 16SrX group. The authors reported that the developed LAMP assay was 10-fold less sensitive than a realtime PCR assay for universal phytoplasma detection according to Christensen et al. (2004). Although a direct comparison of sensitivity of the LAMP assay published by De Jonghe et al. (2017) with that of the PD LAMP assay presented herein is difficult due to the different realtime PCR assays performed for validation as well as the use of a dilution series of a DNA extract derived from an AP-infected apple tree in the sensitivity tests performed by De Jonghe et al. (2017), the apparent differences in LAMP assay sensitivities once more underline the observation that primers designed on the same target gene may lead to considerably different performances in LAMP. However, the LAMP assay developed by Pérez-López et al. (2017) for the detection of 16SrXIII phytoplasmas, which targets the *cpn60* gene, was reported to detect 100 copies of the target per reaction, which is in agreement with the detection limit determined for the PD LAMP assay developed in this study.

Since the targeted 16S rRNA gene is present in two copies in the phytoplasma genome (Schneider and Seemüller, 1994), the number of phytoplasmas per gram of sampled plant tissue necessary for a successful detection by the PD LAMP (Detectable phytoplasma number, DPN) can be estimated from the determined detection limit. The equation is given below:

$$DPN = \frac{DL}{CN} \times \frac{VE}{VL} \times \frac{1}{SM}$$

DL is the detection limit of the assay in question [copies of the target], CN the copy number of the target in the genome, VE the total volume of the DNA extract, VL the volume of the DNA extract subjected to LAMP and SM the amount of sample material [g], from which DNA was extracted. Besides the detection limit of the assay, the required phytoplasma titer depends also on the DNA extraction method because the amount of plant material, from which DNA is extracted, as well as the volume, in which the DNA is finally suspended, differ between the methods. The DNeasy Plant Mini kit (Qiagen), which was used in this study, supports a maximum amount of starting material of 100 mg wet weight. DNA is eluted with 200 µl elution buffer. Based on a detection limit of 100 copies per reaction, the calculated DPN according to the equation above is 5×10^4 cells per gram of plant tissue. A calculation for the widely used phytoplasma enrichment procedure according to Ahrens and Seemüller (1992) with 0.5 g of starting material and a final volume of 100 µl yields 5×10^3 phytoplasmas per gram of plant tissue to be detectable by the PD LAMP, when samples are processed with this DNA extraction method. These values are fairly within the range of concentrations reported from fruit tree phytoplasmas. Torres et al. (2005) measured concentrations of 9.7×10^3 to 3×10^5 phytoplasmas

per gram of plant tissue with a realtime PCR assay specific for fruit tree phytoplasmas. Besides apricots and plums, the authors tested one pear tree and reported a number of 7.7×10^4 phytoplasmas per gram of tissue. Berges et al. (2000) estimated phytoplasma concentrations using a competitive PCR assay and found considerable variation of phytoplasma concentrations in apple trees in the range of 6.5×10^2 to 1×10^8 cells per gram of tissue. Torres et al. (2010) reported an average phytoplasma concentration of 2.372×10^6 cells per gram of plant tissue in 24 pear trees, as quantified by realtime PCR.

The detection range of the PD LAMP was evaluated with phytoplasma strains representing a range of different phylogenetic groups (Figure 52). Based on the sequence information in GenBank, displaying high sequence similarity of the target sequence, the detection of other members of the 16SrX group with the PD LAMP was expected and confirmed in various experiments with the PD LAMP assay containing either PEG 8k or betaine. Extensive tests with AP and ESFY field samples proved that the PD LAMP is highly suitable for the detection of the AP and ESFY phytoplasmas, respectively. Diagnostic sensitivity and specificity calculated according to Altman and Bland (1994) both amounted to 100 % for the detection of the AP phytoplasma in DNA extracts. Using PEG 8k as additive in LAMP, all phytoplasma strains tested in this study were successfully amplified, as indicated by the colour change of the metal indicator and confirmed by subsequent agarose gel electrophoresis. However, subtle differences in the banding patterns of these samples compared to the PD positive control were observed on agarose gels. A multiple sequence alignment of the target region of the tested phytoplasma species showed several mismatches at the primer binding sites, but only very few deletions and insertions in the amplified target region (Figure 53). When betaine was used instead of PEG 8k, the assay did not yield a colour change for any phytoplasma species not belonging to the 16SrX group. On agarose gels, faint banding patterns were visible in a few cases but they were very weak, indicating amplification of the 16S rDNA target with a low efficiency due to suboptimal primer binding. Similarly, Lajin et al. (2013) reported high specificity of a tetra-primer amplification-refractory mutation system-PCR (TP-ARMS-PCR) assay in the presence of high template DNA concentrations when betaine was used as additive. Denschlag et al. (2013) observed an increase of LAMP performance in terms of a reduction of the reaction time of a LAMP assay targeting the Hyd5 gene of *Fusarium* spp. when using PEG 8k compared to the same assay without any additive. In this work, performances of a LAMP assay with either PEG 8k or betaine were compared. There was no obvious difference in the speed of the reaction between the assays, but a strong influence of the additives on sensitivity and specificity of the reaction. While PEG 8k led to an impaired specificity in favor of enhanced sensitivity, the use of betaine resulted in a 10-fold to 100-fold reduced sensitivity compared to the reaction mix with PEG 8k, in favor of a high specificity of the assay. Tong et al. (2011) presented a study on macromolecular crowding agents and their application for increasing assay performance of helicase-dependent amplification (HDA). The authors remarked that PEG had the strongest enhancing effects but also led to increased incidence of primer dimer formation in a HDA assay

for the detection of *Neisseria gonorrhoeae*. While there was no occurrence of primer dimer formation in the PD LAMP assay, the macromolecular crowding effect of PEG 8k made it possible to detect a wide range of phytoplasma strains from different phylogenetic groups. Phytoplasmas having a wide host range such as the members of the AY group, which are transmitted by polyphagous vectors, may be found occasionally in pears. Firrao et al. (2005) listed *Pyrus communis* as a host for *Candidatus Phytoplasma asteris* (group 16SrI). Lee et al. (1995) reported the detection of mixed phytoplasma infections in symptomatic pear trees. The authors suggested, that the combination of phytoplasmas was responsible for the decline of the trees. Hence, these mixed infections have to be considered pathogenic and the detection of phytoplasmas in pears in the field, regardless which taxonomic group they belong to, must lead to the classification of the trees as “diseased”. Therefore, the use of PEG 8k as additive in the PD LAMP is recommended, accepting the potential detection of phytoplasmas other than members of the 16SrX group, in favor of an enhanced assay sensitivity.

4.5 Simplified sample preparation

DNA extraction is a time-consuming and expensive prerequisite for reliable pathogen detection with PCR. The need of purified DNA for PCR analysis makes this method unsuitable for on-site applications, even if mobile devices were available. LAMP, as an isothermal DNA amplification method using a highly inhibitor-tolerant DNA polymerase, is predestined for applications in the field. To obtain an entirely laboratory-independent detection procedure, the development of a simple and rapid sample preparation method, obviating the need of DNA extraction in a laboratory, was one of the main tasks of this project. In the past, several attempts have been made to simplify DNA extraction methods because these were always a bottleneck regarding expenditure of time and cost. In general, there are two factors potentially hindering amplification that have to be overcome:

(1) DNA degradation by enzymes due to disruption/lysis of cells. In intact cells, DNA is protected against enzyme degradation by the nucleus membrane. When the cell and hence the nucleus is disrupted, DNA comes in contact with enzymes of the cytoplasm. DNA degrading enzymes (DNases) in the cytoplasm are part of the cell's defense against intruders. Therefore, the inactivation of DNases is critical during the first steps of DNA extraction.

(2) Plant metabolites inhibiting DNA amplification. Plant cells contain diverging amounts of secondary compounds as for example polyphenols or polysaccharides, which are known to inhibit many DNA polymerases. Amount and composition of these plant metabolites strongly vary between species as well as between cultivars within a species, and may even fluctuate in a single plant throughout the year (Green et al., 1999; Garcia-Chapa et al. 2003).

The inhibition of DNases is crucial during tissue homogenization and cell lysis. Low temperatures during tissue disruption, i.e. grinding of plant tissues in liquid nitrogen, as well as chemical inhibitors in the lysis buffer, as for example 2-mercaptoethanol, are widely applied

measures in plant DNA extraction protocols. While the enzymatic degradation of DNA during cell lysis is a general problem, which occurs with cells of any origin, the diversity of plant metabolites showing PCR-inhibiting effects has led to an exceeding number of DNA extraction protocols, with several protocols being especially developed for a certain plant species or even for a particular plant organ (Dellaporta et al., 1983; Katterman & Shattuck 1983; Doyle & Doyle 1990; John 1992; Lodhi et al., 1994; Kim et al., 1997; Green et al., 1999; Cheng et al., 2003; Verbylaite et al., 2010). Especially woody plants pose a challenge for the experimenter because contents of phenolic compounds and polysaccharides are very high, raising problems in downstream processes based on DNA amplification (Kim et al., 1997; Verbylaite et al., 2010).

In this work, a sample preparation procedure developed and published by Hadersdorfer et al. (2011) for the detection of the *Plum pox virus* with LAMP was examined first because it was intended for samples derived from fruit trees and worked very well at our institute. This method uses water as liquid for homogenization of plant tissues, followed by centrifugation and dilution of the homogenate. Samples derived from diseased pears were thusly prepared and subjected to LAMP. In a series of experiments, it was observed that the diluted pear homogenates inhibited the DNA amplification in LAMP despite the high tolerance of the *Bst* DNA Polymerase towards common polymerase inhibitors (Figure 26). In contrast, detection of PD phytoplasma DNA in diluted homogenates from apple and plum, to which DNA extracts containing PD phytoplasma DNA had been added, was not impaired. This indicates the presence of substances in the crude pear tissue extracts, that do not occur in apple or plum homogenates, and for which simple dilution is not sufficient to abolish their inhibitory effect.

The procedure developed in this study, which uses sodium hydroxide (NaOH) solution as liquid for homogenization of plant tissues from pear, followed by centrifugation and dilution of the homogenate, was inspired by Wang et al. (1993) who used NaOH for a quick extraction of *Arabidopsis thaliana* DNA. In a series of experiments, the authors identified alkaline pH as the most important factor for a simplified sample preparation. NaOH is a strong base, which is commonly used for extraction of plasmids from bacterial cultures. This procedure called alkaline lysis was first published in 1979 by Bimboim and Doly. In this method, NaOH is involved in breaking down the cell walls, and disrupts the hydrogen bonds of double stranded DNA. High molecular weight genomic DNA is thereby selectively denatured and, after neutralization with acidic sodium acetate, forms insoluble precipitates that are easily removed by centrifugation. However, alkaline treatment of samples can be found in several other DNA extraction protocols, and the method described by Wang et al. (1993) is, with various modifications, widely used to process different types of tissue. Groppe and Boller (1997) used the procedure according to Wang et al. (1993), extended by a NaOH incubation step, to prepare powdered grass samples for PCR analysis of endophytes. Porcar et al. (2007) modified the method of Wang et al. (1993) with a neutralization step using sodium acetate instead of diluting the homogenates for the detection of genetically modified maize with PCR. Chen et al. (2006) demonstrated the applicability of the protocol by Wang et al. (1993) with minor modifications

to samples of rice seedlings subjected to PCR and subsequent capillary electrophoresis. Collar et al. (2007) advanced the method of Wang et al. (1993) into a high-throughput method performing the whole process in a 96-well-plate. The authors reported the successful application of this method in PCR-based marker assisted selection in rice. Osmundson et al. (2013) tested the NaOH protocol of Wang et al. (1993) along with three other quick extraction protocols for their suitability for PCR diagnostics and barcoding of fungi and oomycetes and demonstrated the NaOH extraction to be superior in terms of PCR amplification success, time expenditure and cost. NaOH extracts of *Phytophthora ramorum* cultures were successfully subjected to quantitative PCR using TaqMan chemistry. Moreover, the authors reported the storage of frozen dilutions of NaOH extracts for up to 32 months without impairing PCR utility. Klimyuk et al. (1993) used a NaOH solution in combination with boiling to prepare whole plant tissue pieces for subsequent PCR analysis. The authors hypothesized that alkaline treatment makes the DNA more accessible to the polymerase. Chomczynski and Rymaszewski (2006) presented an alkaline lysis reagent with polyethylene glycol for application to a variety of samples including bacteria, blood and diverse tissues from humans, animals and plants. In this procedure, alkaline solution was used to lyse cells and release DNA from these cells. The undiluted lysates were used directly for PCR analysis. Hwang et al. (2013) used a modified version of this alkaline PEG lysis buffer for genotyping of seven different plant species with Direct PCR. Bourke et al. (1999) presented a NaOH based method for the neutralization of *Taq* inhibitors in forensic samples that failed to amplify due to contaminating substances. The authors hypothesized that many PCR inhibitors are co-eluted with DNA in standard extraction protocols because these substances intercalate into double stranded DNA, subsequently impairing PCR reactions. This intercalation might be responsible for the observation that in many cases, dilution of problematic DNA extracts does not lead to successful amplification (Bourke et al., 1999). Polyphenols such as phenolic terpenoids are known to bind to DNA and RNA after cell lysis, which makes plant species containing high contents of polyphenolic compounds, as fruit trees and conifers, very difficult to analyze with PCR (John, 1992; Kim et al., 1997). Bourke et al. (1999) argued that denaturation of DNA should result in the release of intercalating substances by reduction of their affinity to DNA, thereby enabling their removal or dilution. The authors reported that incubation and several washes with NaOH of samples containing inhibitors, which had failed to amplify under standard conditions, yielded DNA, which was successfully amplified in subsequent PCR. Satya et al. (2013) showed the NaOH extraction method to be suitable for DNA extraction from ramie (*Boehmeria nivea*), a crop containing high amounts of complex polysaccharides. Samples were subjected to PCR amplifying targets on nuclear and chloroplast DNA. Werner et al. (2002) successfully analyzed NaOH extracts from bryophytes with direct PCR and subsequent cycle sequencing.

Together with its property to break down cell walls, thus releasing the DNA to the solution, and its denaturing nature, thereby freeing the single stranded DNA from putative intercalating inhibitors, the use of NaOH provides an additional benefit: the inactivation of nucleases which

might otherwise degrade DNA during sample preparation (Wang et al., 1993). Moreover, grinding of tissues in an appropriate buffer prevents oxidative and enzymatic damage of DNA (Bellstedt et al. 2010). During the development of the NaOH-based sample preparation method in this work, experiments with different NaOH concentrations and tissue types were performed and diverging NaOH concentrations were identified as optimal for the treatment of either leaves or bark of twigs and roots, respectively (Figures 29 – 31). Unlike Wang et al. (1993) who diluted the resulting homogenate one in hundred in Tris-HCl (pH 8), distilled water was used for the dilution of the NaOH homogenates in this study, because LAMP performed better with aqueous dilutions than with dilutions using Tris-HCl in several experiments. The developed NaOH sample preparation procedure was successfully applied in a comprehensive test of pear plants belonging to a PD inoculation trial. All samples were initially tested with a LAMP assay targeting the plant cytochrome oxidase gene (COX) to verify that DNA was present in the samples (Tomlinson et al., 2010a, modified) (Figure 33). The results showed that 3.54 % of the diluted homogenates failed to amplify in the COX LAMP. This may be due to the partially poor condition of the plant material, which had been stored in a cooling chamber for four months after sampling. However, the low detection rate of the PD LAMP in these samples was most likely due to unsuccessful transmission of the pathogen, not to a failure of the DNA extraction method.

The control tests of NaOH preparations with COX LAMP were kept up in following experiments and yielded positive amplifications for preparations from fresh plant material in all cases (data not shown). DNA of *Ca. P. pyri* was successfully amplified by the PD LAMP from NaOH extracts of field samples collected in a German orchard (Figure 32). In routinely sampled *in vitro* cultures of pears used to maintain the PD phytoplasma, the pathogen was frequently detected using the NaOH sample preparation method in combination with the PD LAMP. In the cross-laboratory test for the application of the PD LAMP together with the NaOH extraction method on putative apple proliferation samples, the results of NaOH extracts in LAMP and DNA extracts in nested PCR agreed to 90.6 %, with 3 out of 32 samples yielding inconsistent results (Table 6). Diagnostic sensitivity and specificity calculated according to Altman and Bland (1994) for the PD LAMP in combination with the NaOH sample preparation method were 94.4 % and 85.7 %, respectively, whereas the calculated values for the PD LAMP in combination with conventional DNA extraction both amounted to 100 % (Tables 7 and 8). The interpretation of these results regarding the suitability of the NaOH extraction method was difficult because although the plant material used for both extraction methods derived from the same sample, the uneven distribution of phytoplasmas in the host might lead, especially at low titers, to inconsistent results for the halved sample portions (Seemüller et al., 1984; Errea et al., 2002). In order to overcome this last gap in the line of evidence, a direct PCR protocol with a commercially available kit (Phire Plant Direct PCR Kit, Thermo Scientific) and a primer pair specific for fruit tree phytoplasmas (Lorenz et al., 1995) was established. This Direct PCR protocol worked very well with the NaOH extracts, and in an experiment with samples derived

from healthy and diseased *in vitro* plants, PD LAMP and Direct PCR both yielded the same results for all 40 *in vitro* plants tested (Figure 36).

The applicability of the PD LAMP together with the NaOH sample preparation method for the detection of the ESFY phytoplasma was evaluated with field samples derived from an orchard in Tyrol, Austria. Using Direct PCR with the primer pair fO1/rO1 as reference, the diagnostic sensitivity calculated according to Altman and Bland (1994) was 100 %, whereas diagnostic specificity was 75.7 % (Table 9). This was due to nine samples being positive in LAMP and negative in Direct PCR. However, seven out of these nine samples derived from trees, for which at least one other sample was positive in both tests. This may indicate false negative results of Direct PCR rather than false positive results in LAMP due to low pathogen titers in the sampled plant parts close to PCR detection limit, or inhibition of the PCR reactions by the diluted crude plant sap.

The successful LAMP detection of the target in NaOH-based homogenates but not in water-based homogenates from leaf tissues of pears indicates the presence of substances, which are successfully removed or inactivated by NaOH. This might be due to the NaOH-mediated denaturation of DNA enabling the removal of intercalated inhibitors by centrifugation or the dilution of these inhibitors (Bourke et al., 1999). The NaOH extraction method developed in this study was successfully applied to apple and apricot samples for the detection of the apple proliferation phytoplasma and the European stone fruit yellows phytoplasma. This demonstrates the suitability of the NaOH extraction method for samples containing high amounts of secondary plant metabolites like polyphenols as they are found in fruit trees (Kim et al., 1997). However, Osmundson et al. (2013) remarked that the DNA yield of this method is low compared to standard extraction protocols as for example CTAB-based DNA extraction methods, which may be an issue for targets with low abundance. Additionally, DNA might be degraded by NaOH through hydrostatic shearing of single stranded DNA (Bourke et al., 1999), which makes crude NaOH extracts unsuitable for downstream processes, which rely on long, intact stretches of DNA, as for example Amplified fragment length polymorphism (AFLP) (Collard et al., 2007; Osmundson et al., 2013). Application to restriction enzyme digestion may also be confounded by denatured DNA in NaOH extracts (Werner et al., 2002). In spite of these limitations, NaOH-based “rapid” and “simplified” DNA extraction procedures are a reliable and inexpensive alternative to conventional DNA extraction procedures for PCR-based applications.

Although fruit tree phytoplasmas are commonly reported to occur in low titers in the host (Aldaghi et al., 2009), the experiments presented in this work demonstrate that the NaOH extraction method provides enough phytoplasma DNA for an efficient target amplification in the PD LAMP. The application of simplified sample preparation procedures using NaOH in phytoplasma detection procedures is occasionally reported in literature. A simplified extraction method based on alkaline solution for the detection of phytoplasmas with LAMP was published by Sugawara et al. (2012). The authors incubated the samples in NaOH at 95 °C, followed by

neutralization with sodium acetate and a precipitation step with isopropanol. A LAMP assay targeting the *groEL* gene of *Candidatus Phytoplasma asteris* successfully amplified phytoplasma DNA in thusly prepared samples. Guo et al. (2003) evaluated five rapid DNA extraction procedures for PCR detection of phytoplasmas and found NaOH-based methods to work best for a range a phytoplasmas in various plant tissues. The use of a homex and filter extraction bags, as in this study, was also reported by Aldaghi et al. (2009) who presented a simplified extraction protocol for subsequent detection of apple proliferation phytoplasma. Samples were ground in a commercial extraction buffer and subjected to realtime PCR using either SybrGreen I or TaqMan chemistry. Despite these examples of successful application of simplified DNA extraction protocols in phytoplasma detection procedures, CTAB-based DNA extraction methods, mostly including a “phytoplasma-enrichment-procedure” (Ahrens & Seemüller, 1992; Dellaporta et al., 1983), are until now the predominant DNA extraction methods, which are named in scientific publications dealing with DNA analysis of phytoplasmas. This may be due to frequently occurring problems caused by the uneven distribution of phytoplasmas in their host and low phytoplasma titers, especially in woody hosts, as reported by various authors (Daire et al., 1992; Berges et al., 2000; Firrao et al., 2007; Aldaghi et al., 2009; Galetto & Marzachi, 2010), but also to the presence of inhibitors, whose amount and composition unpredictably fluctuate throughout the year (Green et al., 1999). For these reasons, taking more than one sample per plant is recommended (Tomlinson et al., 2010b), which considerably raises cost and time required for DNA extraction. The DNA extraction kit, which was used in this work, is restricted to 100 mg of fresh plant material per sample, thereby limiting pooling of the samples. With the NaOH extraction method, samples can be pooled up to a total fresh weight of 1 g, which is, together with the needed amount of NaOH solution, the volumetric capacity of the filter extraction bags used in this study. The NaOH extraction method proved to be reliable, yielding enough DNA in sufficient quality to support phytoplasma detection with LAMP and Direct PCR. Since it is a cheap and rapid method to prepare samples, it is highly suitable for large-scale screenings, even if multiple samples per plant are to be tested in order to compensate for potentially low phytoplasma titers or erratic distribution.

4.6 Occurrence of false positives in LAMP

In this work, the occurrence of false positives was the most challenging problem in the development and application of the LAMP assay. Primer sets, which were newly designed, worked for some weeks and then immediately started to produce false positives systemically in entire LAMP experiments. Applying a new primer set only led to a temporary solution of the problem. Here again, false positives made it impossible to work with the assay after some weeks. Agarose gel electrophoresis revealed banding patterns, which corresponded to the patterns of positive controls, not only in negative controls but also in no template controls and all samples tested, even from demonstrably phytoplasma-free trees and *in vitro* cultures (Figure 54). In the first instance, contaminations were assumed to be responsible for these undesired amplifications and various attempts were undertaken to unravel the mysterious

source of these contaminations. First, the used reagents were replaced by fresh ones, but this measure did not lead to clean runs. Nevertheless, this was always the first step when false positives started to occur. Preparing a new primer mix and using freshly tapped water from the water purification system or ultrapure water did not solve the problem either. A PCR on LAMP reagents as samples proved that they were not contaminated with target DNA (Figure 55). Further attempts comprised preparing the LAMP reaction mix in different rooms with different equipment and using reaction tubes from new and unopened packs. The acquisition of a PCR workstation used solely for LAMP and PCR mastermix preparation was just as ineffective as systematic decontamination of surfaces and equipment in the entire laboratory.

The striking fact that false positives occurred not only in LAMP reactions targeting PD but also in LAMP assays for the detection of the *Plum pox virus* and the *Potato leafroll virus*, respectively, led to the assumption that these assays had something in common, which caused false positives in different assays, in some cases at the same time, despite the very diverging nature of the targets. Since extensive attempts to find the putative contaminants came to no result, it became obvious that “Where does the contaminant come from?” was the wrong question. Negating the existence of contaminating target DNA, the proper question to solve the problem rather was “What can cause amplification in LAMP appearing like a true positive amplification, with the respective banding pattern on an agarose gel, in the absence of the correct target sequence?” It is important to note that agarose gel electrophoresis of LAMP products does not yield information about the identity of the amplicon because unlike PCR products, which possess a defined size, LAMP amplicons consist of multiple repeats of the target sequence represented by bands of different sizes (Wastling et al., 2010). Although LAMP reactions produce characteristic ladder-like banding patterns depending on the chosen primer set, these bands on an agarose gel represent not more than the length of a range of fragments produced in the LAMP reaction. While the primers themselves are specific for the sequences they were designed on, their tolerance towards mismatches can be varied for example by incubation temperature or various additives, both influencing primer binding strength.

However, there are other factors that can have an influence on the specificity of a DNA amplification reaction. Based on the assumption that the correct target was not present in the reaction, the reason for these unspecific reactions with true positive appearance had to be sought for in the reaction mix itself, presumably displaying an imbalance of one or more components. Since this phenomenon occurred in three different assays, targeting different organisms, primers or primer mixes were unlikely to cause the problem. It had to be an ingredient, which was used in all three assays whose compositions differed mainly in the concentrations of some components. Since the ThermoPol buffer was the only LAMP ingredient consisting of multiple components, which might influence each other during storage or freeze-thaw-processes, this reagent was suspected first and foremost to provide a wavering basis for the LAMP reaction. The buffer used for all LAMP assays in our institute was the ThermoPol buffer purchased from New England Biolabs along with the *Bst* DNA polymerase. Even though for the different

assays, not one and always the same tube containing the buffer was used, it was always an aliquot of the same charge that was used equally for the different assays. Hence, the hypothesis was that some charges of the ThermoPol buffer contained fluctuating concentrations of ingredients, maybe because of variations during production or caused by precipitations during storage or freeze-thaw-processes. In a first approach, a LAMP buffer was prepared with equal composition as the hitherto used ThermoPol buffer. LAMP was performed with the freshly prepared buffer and the previously used ThermoPol buffer aliquot as control, respectively, and this experiment surprisingly confirmed the hypothesis that the ThermoPol buffer was responsible for the occurrence of false positives in the PD LAMP. While the control run with the purchased ThermoPol buffer yielded false positives in the complete run, the reaction mix with the freshly prepared buffer produced positive amplifications in positive controls only (Figure 61). This finding was the breakthrough in the development of the PD LAMP assay, finally enabling continuous work with the LAMP method.

Fluctuations of concentrations of one or more buffer component were suspected to induce the observed malfunction in LAMP, and it was hypothesized that these fluctuations were due to precipitation events during repeated freeze thaw processes or during storage of the buffer in frozen state at $-20\text{ }^{\circ}\text{C}$. A similar observation was made by Hu et al. (1992) who reported a significant impact of a PCR buffer, which had been stored as 10-fold concentrate at $-20\text{ }^{\circ}\text{C}$ for six months, on specificity of DNA amplification reactions. The authors showed that the preferential amplification of certain alleles, leading to mistyping of heterozygotes as homozygotes, was due to a considerably decreased magnesium ion concentration in the used PCR buffer, and suspected that this was due to the precipitation of magnesium in insoluble form. Slow freezing of dilute aqueous solutions at first results in crystallization of water, leaving a liquid phase, in which the solutes are concentrated in the presence of residual unfrozen water (Murase & Franks, 1989; Sundaramurthi & Suryanarayanan, 2011). The selective precipitation of buffer components depending on their respective solubilities upon cooling was reported to cause significant shifts of the pH values in the residual liquid phase of frozen buffer solutions (Williams-Smith et al., 1977; Pikal-Cleland et al., 2002; Sundaramurthi & Suryanarayanan, 2011). Kolhe et al. (2010) showed that Tris-HCl buffers undergo a shift $+1.2$ pH units when cooled from $+25\text{ }^{\circ}\text{C}$ to $-30\text{ }^{\circ}\text{C}$. Murase and Franks (1989) reported the sequential crystallization of phosphate salts in phosphate buffer mixtures during cooling to subzero temperatures. Melting of crystallized salts is endotherm, i. e. requires energy, as does ice melting. However, the amount of energy required to redissolve a precipitated salt depends on the composition of the crystallized salt. This is in agreement with Hu et al. (1992) who reported that the proper functionality of the erroneous PCR buffer was restored after heating to $90\text{ }^{\circ}\text{C}$ for 10 min, followed by vortexing. This indicates that the precipitated salt had a low solubility in the buffer solution at ambient temperature.

The influence of buffer composition on the performance of DNA amplification procedures is a well studied issue (Blanchard et al., 1993; Caetano-Anollès et al., 1994). However, no

publications were available dealing with the influence of buffer composition on LAMP reactions at the time of writing. The composition of the ThermoPol buffer, which is provided together with *Bst* DNA polymerase by New England Biolabs, corresponds to the specifications in Notomi et al. (2000) who introduced the LAMP method using the strand-displacing *Bst* DNA polymerase. Reaction buffers of identical composition are provided by several suppliers together with *Bst* DNA polymerase. Since the ThermoPol buffer had been identified as causal agent of the false positives-issue in this study, and because no information regarding the relationship of LAMP and buffer composition was available, a series of experiments was performed to evaluate the influence of varying concentrations of ThermoPol buffer ingredients on LAMP performance (Figures 62 and 63). These experiments showed that the ThermoPol buffer was well balanced, supporting highly efficient isothermal amplification by *Bst* DNA polymerase in an optimal manner. Furthermore, the altered concentrations of individual buffer ingredients did not provoke the generation of false positives.

Tris-HCl shows considerable fluctuations of pH values in dependence on the temperature (Innis & Gelfand, 1990). This was also reported for subzero temperatures (Kolhe et al., 2010). Two buffering alternatives to Tris-HCl, glycine and MOPS, were evaluated for their suitability in the PD LAMP. MOPS strongly interfered with the metal indicator dye HNB during reaction mix preparation, indicating a chelation of a considerable amount of magnesium ions. Denschlag et al. (2013) used 20 mM MOPS instead of Tris-HCl in LAMP reactions targeting the *Hyd5* gene of *Fusarium* spp. However, the authors used 8 mM magnesium chloride per reaction, exceeding the applied concentration in the PD LAMP by 2 mM per reaction. An adjustment of the magnesium ion concentration to saturate the demand of MOPS was not considered in this work since high magnesium ion concentrations are known to favor unspecific amplifications (Innis & Gelfand, 1999). Glycine is a zwitterionic buffer. Hill and Buckley (1991) suspected that zwitterionic buffers may not display pH shifts upon freezing since selective precipitation of a buffer component should not be possible in case of zwitterions. Glycine at a concentration of 20 mM per reaction enabled amplification of positive controls in LAMP reactions (Figure 64). However, these amplifications did not induce a colour change of the metal indicator. If this was due to a reduced amplification yield or an interaction of glycine with HNB was not examined in this study.

The occurrence of false positives is a common issue with all highly sensitive nucleic acid amplification methods. In most cases, contamination with genomic DNA or amplification products is assumed to be the cause and various techniques have been proposed to avoid contaminations (Martel et al., 2001; Silkie et al., 2008). However, mishybridization of primers or the formation of primer dimers may also lead to undesired PCR products, which, in the worst case, have a size similar to the expected product (Degrave et al., 1994). Where careful assay design and accurate reaction mix preparation are not sufficient, hot-start PCR techniques may be employed to overcome amplification of misprimed sequences prior to thermal cycling or in the first PCR cycle (Chou et al., 1992; Degrave et al., 1994; Kellogg et al., 1994; Lebedev et

al., 2008; Paul et al., 2010). While a “hot-start” is not possible with *Bst* DNA polymerase, an artificially modified Warmstart version of *Bst* DNA polymerase (*Bst* 2.0 Warmstart polymerase, New England Biolabs) is available, which does not show amplification activities below 50 °C. Tanner et al. (2012) reported that *Bst* 2.0 Warmstart polymerase performed equally well with or without 2 hours of preincubation at room temperature whereas wild type *Bst* DNA polymerase was negatively impacted by the preincubation at room temperature.

The generation of longer DNA stretches in the absence of background DNA can also be a result of primer dimers. Chou et al. (1992) demonstrated the occurrence of primer oligomerization in the absence of background DNA, resulting in PCR products with sizes of 75 bp and 105 bp derived from primers with lengths of 25 and 27 bp, respectively. Furthermore, the authors showed that these side reactions were initiated prior to thermal cycling, indicating polymerase activity already at low temperatures. Brownie et al. (1997) remarked that amplification of primer dimers also occurs in the absence of any complementarity. Tan et al. (2008) reported unspecific amplification in EXPAR (exponential amplification reaction), an isothermal amplification method, which uses the large fragment of *Bst* DNA polymerase, as does LAMP. The authors observed early phase and late phase background amplification, which they ascribed to template-dependent but unprimed DNA synthesis and *ab initio* DNA synthesis, respectively. Similar to LAMP, EXPAR has a feedback design, which enables high amplification speed and efficiency, advantages that contribute to its susceptibility to considerable nonspecific side reactions. *Ab initio* DNA synthesis, the enzymatic creation of oligonucleotides from dNTPs without primers or template, is reported for various DNA polymerases. Ogata and Miura (1998a) demonstrated that the DNA polymerase of the archaeon *Thermococcus litoralis* is able to synthesize double-stranded DNA stretches of 0.5 to 100 kb in the absence of primers or template DNA. Furthermore, the authors showed that the polymerase created sequences consisting of tandem repeats with unit lengths of 4-18 bp whose motifs changed when reaction conditions as temperature or ionic strength were varied. The generation of oligonucleotides with random sequences as “seed oligomers” was supposed as initial step, followed by preferential amplification of palindromic sequences, which enable the formation of self-priming hairpin structures. The authors showed that increasing reaction temperatures led to enhanced GC contents of synthesized DNA, indicating a selected amplification based on melting temperature of seed oligomers. In a second publication, these authors reported a similar behavior of the DNA polymerase of *Thermus thermophilus*, a relative of *Thermus aquaticus*, the origin of *Taq* DNA polymerase (Ogata and Miura, 1998b). The reactions were performed at a constant temperature of 74 °C. Furthermore, Ogata and Miura (2000) showed that the DNA polymerase of *Thermococcus litoralis* efficiently amplified an oligonucleotide with palindromic tandem repeats and a GC content of 25-50 % in the absence of primers and template DNA. However, elongation efficiency was reduced when the palindromic motifs were destructed or the GC content was beyond 25-50 %. Ramadan et al. (2004) reported the synthesis of short DNA

fragments by human DNA polymerase λ and DNA polymerase μ in the absence of primers and template DNA.

Zyrina et al. (2007) showed that *Bst* DNA polymerase efficiently synthesizes DNA stretches of repetitive motifs in the presence of a nicking enzyme, with the tandem repeats containing the nickase recognition site. The authors also observed insertion of random nucleotides between motif blocks and concluded that this was due to the addition of random 3' NN overhangs after elongation and end-joining of complementary overhangs in proximate amplification rounds by *Bst* DNA polymerase. However, no DNA synthesis was observed in the absence of the nicking enzyme after 4 hours of incubation. García et al. (2004) reported the generation of non-template directed 3' overhangs by the large fragment of *Escherichia coli* DNA polymerase I and DNA synthesis across discontinuous DNA strands using the overhangs as regions of microhomology (template switching). Antipova et al. (2014) studied DNA sequences produced by *Bst* DNA polymerase in the presence of three nicking endonucleases (NEases), respectively, and found random spacer sequences flanking palindromic units with NEase recognition sites. The authors remarked that *ab initio* DNA synthesis was more efficient at 37 °C than at 65 °C, the temperature optimum of *Bst* DNA polymerase, and explained this observation with stronger dNTP binding to *Bst* DNA polymerase at lower temperatures, enabling the synthesis of short oligonucleotides with random sequences (“seed oligos”). Similarly, Liang et al. (2007) reported efficient *ab initio* DNA synthesis at 50 °C by Vent DNA polymerase, whose temperature optimum for primer-dependent DNA amplification is between 70-80 °C. Kato et al. (2012) demonstrated the efficient amplification of short nonrepetitive oligonucleotides containing hairpins at each end by Vent (exo-) DNA polymerase under isothermal conditions. The obtained products consisted of tandem repeats of the seed sequences and showed sizes of more than 10 kb after 10 min of incubation. Sequences similar to those obtained in experimental *ab initio* DNA synthesis can be found in the genomes of a range of organisms. Therefore, *ab initio* DNA synthesis is considered as developing engine in early stages of evolution. However, Zyrina et al. (2007) reported that *ab initio* synthesis by *Bst* DNA polymerase alone only occurs after a lag time of several hours. The presence of nicking enzymes or restriction enzymes strongly stimulates *ab initio* DNA synthesis by *Bst* DNA polymerase, which may pose a considerable issue in isothermal amplification assays containing such enzymes, as strand displacement amplification (SDA) or rolling circle amplification (RCA) (Zyrina et al., 2014). Zyrina et al. (2012) showed that single-stranded DNA-binding proteins (SSB proteins) are able to inhibit *ab initio* DNA synthesis by *Bst* DNA polymerase in the presence of nicking enzymes.

Zyrina et al. (2014) proposed a model for *ab initio* DNA synthesis of non-palindromic sequences by *Bst* DNA polymerase. The authors suspected that due to a terminal nucleotidyl transferase activity of *Bst* DNA polymerase, random nucleotide overhangs are added to amplified seed oligos. Complementary overhangs of amplified strands derived from a seed oligo are joint by *Bst* DNA polymerase, generating sequences with oppositely directed motifs, which allows the formation of hairpins at the 3' termini. This self-priming structure exhibits

remarkable similarities with the autocycling structure of LAMP reactions. The dumbbell-like starting structure for autocycling in LAMP contains the oppositely oriented motifs F1 and F1c as well as B1 and B1c, with F1c and B1c derived from FIP and BIP, respectively. Since *ab initio* DNA synthesis by *Bst* DNA polymerase in the absence of nicking enzymes or restriction enzymes only occurs after a lag time of several hours (Zyrina et al., 2007), this may not be an issue in LAMP, which does not use endonuclease enzymes that could stimulate *ab initio* DNA synthesis. However, the presence of LAMP primers up to 45 bases in length may provoke amplification of hairpins, which can be formed in the early heating phase after onset of the LAMP reaction. The time required to heat the reaction solutions to 65 °C in a heating block after transfer from crushed ice was not recorded in this study. However, a few minutes appear sufficient for the highly efficient *Bst* DNA polymerase to synthesize a few oligonucleotides from hairpins of FIP and BIP or dimers thereof, providing starting material for subsequent autocycling. This only requires the presence of F1c and B1c complementary sequences in one DNA strand.

Hafner et al. (2001) reported the amplification and multimerization of linear DNA sequences in the presence of two primers by *Bst* DNA polymerase (linear target isothermal multimerization and amplification (LIMA)) as source of background DNA synthesis in CRCA (cascade rolling circle amplification). Similar to the hypothesis of Ogata & Miura (1998a) for the preferential amplification of seed oligomers containing certain motifs during *ab initio* DNA synthesis, Hafner et al. (2001) suspected that various inefficient replications are initiated in the early phase of the reaction, followed by preferential replication of oligomers, which are easily amplified due to their multimeric motifs (“the winner takes it all”-reactions). The result of LIMA reactions are ladder-like banding patterns on agarose gels, resembling those of LAMP and CRCA reactions. Experiments performed in this study with combinations of two LAMP primers and using a ThermoPol buffer aliquot provoking false positives under LAMP reaction conditions also yielded ladder patterns indicating the generation of multimers with various lengths (Figure 60). However, intensity of the bands as well as patterns strongly varied between the primer combinations, indicating differences in amplification efficiency. The combination of PD3 FIP and PD3 LB yielded a distinct banding pattern with band intensities equal to those of a LAMP reaction. Voisey et al. (2001) reported that *Bst* DNA polymerase amplified from primers with mismatched 3' ends to a considerable extent when they attempted to develop an isothermal method similar to allele-specific PCR (AS-PCR) to detect single nucleotide polymorphisms (SNPs). The authors judged the ability of *Bst* DNA polymerase for primer extension of mismatched 3' ends to be high. Jiang et al. (2013) observed the accumulation of false amplicons in rolling circle amplification (RCA) reactions using *Bst* DNA polymerase, in the absence of a DNA template. Similarly, Li et al. (2012) reported the occurrence of false amplification products in LAMP reactions. The authors remarked that the generation of false amplification products in the absence of template DNA was frequently observed in LAMP reactions without betaine, whereas in LAMP reactions with betaine, false positives “still

sometimes” occurred. This is in contrast to observations in this study, where false positives frequently occurred in the presence of betaine.

Kuboki et al. (2003) reported the occasional occurrence of banding patterns different from the typical pattern of the designed LAMP assay. Sequencing of these products revealed joint LAMP primers and primer fragments as well as complements thereof, together with a short fragment of the target sequence. The authors suggested that this product derived from random multimerization of primers and target DNA due to LIMA as proposed by Hafner et al. (2001). Primer fragments may derive from damage due to repeated freeze-thaw processes (Lee et al., 2009). However, Kuboki et al. (2003) judged these amplifications as target specific, although derived from an alternative amplification path. The sporadic occurrence of different banding patterns in positive samples was also reported and attributed to LIMA by Soliman and El-Matbouli (2005). In contrast, Curtis et al. (2009) who observed atypical banding patterns in reverse transcription LAMP reactions targeting HIV-1 demonstrated these products to derive from non-specific amplification by restriction digest with a restriction enzyme whose recognition site was located within the target sequence. Kuboki et al. (2003) also remarked the occasional occurrence of false positives in negative controls and attributed this to contaminations. Similarly, Inácio et al. (2008) reported atypical banding patterns as well as occasional false positives in negative controls in a LAMP assay targeting *Candida* yeast species. The authors used a lowered magnesium chloride concentration in the LAMP reaction mixes to suppress false positive amplifications in negative controls. Tanner et al. (2012) observed high rates of amplification in no template controls of a LAMP assay employing fluorescently labelled primers. However, the incidence was dependent on the primer set. The authors concluded that the occurrence of non-templated amplification in LAMP was caused by the inherent nature of the LAMP primers as well as high concentrations of primers and magnesium in LAMP reaction mixes. The dependence of the incidence of false positives on the primer set was also observed in this study. Gray et al. (2016) showed that false positives in a LAMP assay for the detection of tuberculosis were linked with low reaction volumes when too little DNA eluent was added to the dried LAMP reagents, resulting in higher concentrations of reagents, which may induce self-priming.

The generation of false positives in LAMP reactions is a rarely reported phenomenon in scientific literature. Storari et al. (2013) reported occasional occurrence of false positives in LAMP assays for the detection of *Aspergillus* species, but attributed this to cross-contaminations. Several authors have proposed solutions to avoid non-specific amplifications in LAMP without citing or reporting cases of LAMP assays, which were prone to this issue. Li et al. (2012) coupled LAMP with a catalyzed hairpin assembly (CHA) reaction specific for loop sequences of LAMP products to generate a fluorescence signal, which is strictly dependent on target-specific amplification. Jiang et al. (2015) proposed the application of a template-specific one-step strand displacement (OSD) reporter carrying a fluorophore and a quencher to distinguish template-related from background amplification, which the authors assumed to

derive from primer dimers and their multimerization due to the *Bst* DNA polymerases' intrinsic nucleotidyl transferase activity. Poole et al. (2012) reported amplification signals in no template controls with wild-type *Bst* DNA polymerase as well as *Bst* 2.0 DNA polymerase but not with *Bst* 2.0 Warmstart DNA polymerase when LAMP reactions were pre-incubated at 35 °C for 2 hours. However, the authors observed slightly slower amplification when *Bst* 2.0 WarmStart DNA polymerase was used and attributed this effect to the presence of the aptamer, which inhibits polymerase activity at temperatures below 50 °C.

The formation of hairpins is possible with several LAMP primers investigated in this study. While these secondary structures are not important at the applied reaction temperature of 65 °C, they might form in the heating phase when the reactions are transferred from ice to the heating block. Hairpins of FIP or BIP are most problematic because these oligonucleotides are constructed for autocycling. LAMP is a feedback assay that depends on the original target sequence only in the initial phase of amplification. Once the dumbbell-like starting structure for the autocycling process is generated, LAMP autocycling proceeds with the inner primers only, which is due to excess FIP and BIP concentrations relative to F3 and B3 concentrations, amplifying only these dumbbell-like structures. Furthermore, self-primed elongation of intermediate LAMP products does not require participation of primers due to the systematic incorporation of repeating motifs in the dumbbell-like starting structures, which is an essential feature of the LAMP method (Tomita et al., 2008). In consequence, a similar structure with FIP or BIP hairpins at one end and a comparable length will be amplified with the same efficiency and reaction kinetics as the original target due to the inherent primer design as demonstrated in an experiment with two LAMP primers only in the absence of template DNA presented in this study (Figure 60).

Qian et al. (2012) showed that the tendency of EXPAR templates to generate non-specific amplification of the trigger sequence is linked to the template sequence. Furthermore, unprimed amplification of EXPAR templates in the absence of a trigger indicated that the DNA polymerase was able to synthesize a complementary sequence from a single stranded oligonucleotide without the presence of a priming sequence. The authors hypothesized that a single nucleotide bound in the post-insertion site of the polymerase might function as a primer analogue. However, exponential amplification in LAMP requires not only the synthesis of complementary primer sequences but also the connection of the complementary turn-back site of the inner primers to their respective initial priming site at the 3' end. To generate the specific banding pattern on an agarose gel, the symmetric amplification of the inner primers must be obeyed. While it was demonstrated in this study, that efficient amplification producing distinct ladder-like banding patterns is possible with one inner primer and one loop primer only, the generation of false positive amplification yielding identical banding patterns as true positive reactions becomes possible if (1) complements of FIP and BIP are generated, (2) these complements are joint to FIP and BIP, (3) FIP-FIPc is connected with the complement of BIP-BIPc and vice versa. The integration of the loop primers into these sequences will further

enhance amplification efficiency. If these prerequisites are fulfilled, very few oligonucleotides are necessary to start the LAMP reaction because the feedback design of this assay creates a “the-winner-takes-it-all” situation. In other words, oligonucleotide sequences, which facilitate amplification by the formation of hairpins, thereby enabling autocycling, will be preferentially amplified. The ability of *Bst* DNA polymerase to amplify from unprimed substrates as well as end-joining of oligonucleotides due to the intrinsic nucleotidyl transferase activity was demonstrated by various authors (Zyringa et al., 2007; Tan et al., 2008; Qian et al., 2012; Zyringa et al., 2014). Furthermore, experiments with two LAMP primers only, which were performed in this study, showed that efficient amplification takes place even in the presence of a severely reduced amount of oligonucleotides compared to the complete LAMP reaction mix and with one inner primer only. The observed ladder-like banding patterns in these experiments indicate that the prerequisites for LAMP autocycling were created even from two different primer sequences only, under reaction conditions, which were supporting non-specific amplification in a very strong manner, i. e. the use of a degraded LAMP buffer. Moreover, it was demonstrated that the multicomponent buffer used in LAMP was responsible for the generation of false positives in the LAMP assay targeting the pear decline phytoplasma. Continuous work with selfmade buffer solutions confirmed that usage of the buffer longer than four weeks from assembly of its components again resulted in the occurrence of false positives.

However, when the primer set PD4 produced false positives, the primer set PD3 yielded clean controls. While this observation might indicate contamination with PD4 LAMP amplicons at first glance, it rather reflects different susceptibilities of the primer sets towards non-specific amplification. Furthermore, when a LAMP assay targeting the *Plum pox virus* was continuously generating false positives, an experiment with this primer set applied in the LAMP reaction mix optimized for PD3 surprisingly yielded clean controls although the same reagents were used as before. This demonstrates that it is not only the LAMP buffer alone but also the composition of the reaction mix as a whole, which can contribute to the susceptibility of a LAMP assay to generate false positives. In detail, the PPV LAMP reaction mix employed higher concentrations of magnesium in the form of magnesium sulfate as well as higher amounts of dNTPs.

The reported *de novo* synthesis of short oligonucleotides and unprimed amplification of these seed oligos by a range of DNA polymerases show that these enzymes possess amplification potentials far beyond conventional primed DNA synthesis. In the light of these findings, efficient amplification in the presence of a huge amount of oligonucleotides without template DNA is not surprising. While the periodic preparation of fresh LAMP buffer proved to be an efficient measure to avoid false positives in the PD LAMP, the detailed reaction conditions favoring this behavior of *Bst* DNA polymerase and LAMP primers remain to be elucidated.

4.7 Potential of the PD LAMP assay for on-site applications

Performing DNA amplification procedures directly in the field is challenging for several reasons. Outside the well-equipped environment of the laboratory, where common benchtop

facilities as a centrifuge, a clean bench and a thermal cycler or a heat block are missing, basic prerequisites as for example the maintenance of suitable reaction conditions is critical and may even fail due to the unavailability of a power source. Although isothermal DNA amplification techniques depict a huge step forward regarding operability in the field, since thermal cycling as required by PCR-based methods is omitted, a stable reaction temperature still is an essential requirement for reliable assay results. Several solutions for heating isothermal DNA amplification reactions in environments lacking electric current have been proposed. The nature of the applied techniques largely depends on the question if financial considerations are prioritized or not. Heating devices, which are intended for resource-poor settings with anticipated financial limitations, are very simple and constructed with as few and cheap components as possible. Published ideas for electricity-free heating of isothermal DNA amplification reactions employ preheated water, exothermic chemical reactions and phase-change-materials. Successful performance of LAMP reactions has been demonstrated with disposable pocket warmers (Hatano et al, 2010; Zhang et al., 2014), preheated water in a thermos cup (Nkouawa et al., 2012; Kubota et al., 2013) and modified thermos cups or food storage containers using the exothermic reaction of calcium oxide or magnesium iron alloy and water as heat source in combination with a phase change material as temperature buffer (LaBarre et al., 2011; Curtis et al., 2012; Singleton et al., 2014; Song et al., 2016; Poole et al., 2017). The incubation of recombinase polymerase amplification (RCA) reactions, which require a reaction temperature around 37 °C, was demonstrated to be possible with human body heat (Crannell et al., 2014). In contrast to these very simple constructions, portable isothermal incubation and detection devices are available, as for example Genie III (OptiGene, Horsham, UK) or the ESEQuant Tube scanner (Qiagen, Hilden, Germany), which employ fluorescence detection of isothermal amplification products. Most recently, Chen et al. (2018) reported the development of a portable turbidimeter for incubation and realtime detection of turbidity in LAMP reactions. However, purchase costs and the need for skilled personnel impede a wide distribution of this complex hardware beyond specialized laboratories (Craw & Balachandran, 2012).

The visualization of the results of isothermal DNA amplification reactions is a second problem, which needs to be overcome if a field-suitable assay has to be developed. Conventional visualization techniques, which are commonly applied in PCR and realtime PCR protocols, as agarose gel electrophoresis of amplification products and fluorescence detection of DNA-intercalated dyes or labelled probes, are largely inconvenient for on-site protocols as they require complex laboratory equipment and skilled personnel. Especially for LAMP assays, a range of visualization techniques have been proposed, which are suitable for laboratory-independent detection procedures. The generation of high amounts of the amplification by-product pyrophosphate in LAMP reactions enables indirect product detection by naked-eye observation of turbidity due to precipitation of magnesium pyrophosphate, or colorimetric detection with metal indicator dyes as HNB or calcein, which indicate reduced amounts of metal

ions in the reaction solution by a colour change (Mori et al., 2001; Tomita et al., 2008; Goto et al., 2009). Soli et al. (2013) compared colorimetric and turbidimetric end-point detection methods in three different LAMP assays and found colorimetric detection with HNB and SybrGreen I to be superior to visual inspection of turbidity as well as turbidity reading with a turbidimeter in terms of detection sensitivity. Furthermore, the authors reported that no discrepancies of the results were obtained from two independent readers of the colorimetric LAMP assays. Especially the metal indicator dye HNB is widely used for equipment-free LAMP end-point detection. A search for publications with the keywords “loop mediated isothermal amplification” and “hydroxy naphthol blue” with Google scholar (<https://scholar.google.de/>) yielded around 900 hits at the time of writing. However, commercially available LAMP test kits usually rely on turbidity measurements or fluorescence detection of DNA-intercalating dyes, which might indicate problems in the routine application of HNB as it was observed in this study. ErioT, which was shown herein to be a suitable alternative to HNB without fluctuations in colour intensity, is until now only rarely used in LAMP assays (e.g. Shigemoto et al, 2010; Wang, 2014; Oh et al., 2016; Rodriguez-Manzano et al. 2016). Although colorimetric LAMP assays still face problems in routine procedures at the moment, this mode of result visualization appears to be most suitable for the unexperienced user, given that the colour change is of high contrast and that the colours do not perceptibly vary within assays.

The integration of smartphones into detection procedures opens up new possibilities, which will facilitate result readout for users without laboratory education, and which might avoid potential readout errors due to subjective interpretation of reaction solution colours. Rodriguez-Manzano et al. (2016) used an unmodified cell phone to monitor LAMP reactions with ErioT at nanolitre scale in realtime. Liao et al. (2016) constructed a smartphone adaptor with optical excitation and emission filters for realtime fluorescence detection in a LAMP assay using the DNA-intercalating dye EvaGreen. However, the need for comparatively expensive filters to monitor fluorescence with a smartphone, as well as the large number of different phone models and softwares, is until now hindering the broad establishment of smartphones as detection devices in point-of-care diagnostics (Mauk et al., 2017).

Finally, field-suitable detection assays are worthless if they still require highly pure DNA extracts as templates and therefore laborious DNA extraction procedures. *Bst* DNA polymerase, which is commonly applied in LAMP assays, is highly tolerant towards common PCR inhibitors as they are usually present in plant-derived samples. The applicability of crude sample preparations in LAMP assays was demonstrated in this work, as well as in several publications for samples of various origins. The sample preparation method presented in this work is very simple to perform, requiring only one pipetting step for homogenate dilution. Centrifugation of the crude homogenates is necessary but does not inevitably require a benchtop centrifuge. Brown et al. (2011) used a modified salad spinner to determine hematocrit values in resource-poor settings. Priye et al. (2016) replaced the propeller blades of a drone with 3D-printed

centrifuge rotors to conduct spin column-based nucleic acid extraction. Bond & Richards-Kortum (2017) presented a simple paper-and-string centrifuge to separate the plasma fraction from blood.

The PD detection procedure presented in this work was explicitly developed and intended for on-site applications. Unfortunately, it was not possible to perform extensive field trials within the project run-time due to the recurrent occurrence of false positives whose trigger was only discovered in a late phase of the project. An experiment with disposable pocket warmers as heat source based on iron oxidation for the incubation of the PD LAMP failed, probably because the temperature provided by the pocket warmers (approximately 60 °C on average during 60 min of incubation) did not meet the specific temperature requirements of the PD LAMP assay (data not shown). The maximum temperature of 65 °C, which was stated by the manufacturer, was not reached within two hours after activation of the oxidation process. Future experiments with varying amounts of oxidation reaction components would surely yield heat packs, which are suitable for the incubation of LAMP assays requiring reaction temperatures higher than 60 °C.

However, the combination of an isothermal DNA amplification method, a colorimetric visualization of assay results and a simplified sample preparation method provides all features needed for a fully field-suitable pathogen detection protocol. Although the potential of the PD LAMP assay for field applications is therefore considered to be very high, the occurrence of false positives remains a problem to be sustainably resolved because the reparation of the LAMP buffer every three weeks as it was practiced in this study will not be suitable for the end user and furthermore contradicts the intended simplicity and field applicability. Moreover, the delivery of complete LAMP reaction mixes to the customer requires the maintenance of the cold chain, unless dried reagents are provided. PD LAMP reaction mixes, which were sent to several partners for test purposes, yielded reliable results in most cases but occasional failures and false positives were observed when the reaction mixes were shipped during the summer months (data not shown). Although the warmstart version of the *Bst* DNA polymerase 2.0 might lower the risk of LAMP failure due to moderate warming of LAMP reaction mixes during transport, dried reaction mixes would circumvent the necessity of a cold chain as well as storage in frozen state. Dried LAMP reaction mixes are already available for the detection of *Mycobacterium tuberculosis* (Mori et al., 2013). This would also be desirable for the PD LAMP assay.

5 Conclusions

5.1 Development of a field-suitable, easy-to-use detection procedure for *Candidatus Phytoplasma pyri*, the causal agent of pear decline

The objective of this work was the development of a nucleic acid-based detection procedure for the causal agent of pear decline, *Candidatus Phytoplasma pyri*. This was achieved fulfilling the specified requirements as stated in chapter 1.5 (Objective of this work):

1. An isothermal DNA amplification assay based on the LAMP method was developed for the detection of the pear decline phytoplasma. The PD LAMP assay requires no thermal cycling and is therefore highly suitable for on-site application.
2. The developed detection procedure can be performed entirely in the field, from sampling to the assessment of the results. This is achieved with a simplified sample preparation procedure, isothermal amplification of target DNA at a moderate temperature of 65 °C, and colorimetric detection of assay results. The NaOH-based sample preparation procedure is based on manual grinding of fresh sample material in alkaline solution, followed by dilution of the homogenate. Centrifugation of the crude plant sap can be achieved with a simple salad spinner.
3. The developed detection procedure is easy to perform, requiring only one pipetting step, when complete PD LAMP mastermixes are provided to the user, as well as incubation at a constant reaction temperature. The NaOH-based sample preparation procedure is easy to perform as well, involving one pipetting step only. LAMP results are easily judged by the naked eye based on the colour change of the applied metal indicator from purple to blue, when the target was successfully amplified.

5.2 Brief description of the PD LAMP detection procedure

Sampling

Samples may be leaves, shoots or roots of potentially diseased pears. Take samples from different parts of the tree. If one sample per tree is to be taken, make a pooled sample with material derived from different parts of the tree.

NaOH-based sample preparation method

Leaves, shoots and roots are processed separately. From leaves, midribs and petioles are excised and placed into filter extraction bags (Bioreba, Reinach, Switzerland). Shoots and roots are decorticated with a scalpel or razor blade. Bark and phloem tissue of shoots or roots as well as fine roots are placed into filter extraction bags. Per 100 mg of fresh plant material, 1 ml NaOH solution is added: 0.1 M NaOH for samples from shoots and roots, 0.5 M NaOH for leaf samples. Homogenize the samples with a Homex-6 machine or a manual homogenizer (Bioreba, Reinach, Switzerland). A customary hammer works as well. For manual grinding,

Conclusions

choose a hard surface. Homogenize the samples until no more intact tissues are visible, then press the crude plant sap through the filter layer in the filter extraction bag. Transfer approximately 1.8 ml of the filtered homogenate into a 2 ml reaction tube (no pipetting necessary). Centrifuge at 13,000 rpm for 2 min. Instead of a benchtop centrifuge, a modified salad spinner is also suitable. Transfer 10 μ l of the supernatant into a 1.5 ml reaction tube containing 990 μ l distilled water for a dilution of 1:100. Two μ l of the diluted homogenate is subjected to PD LAMP.

PD LAMP assay

PD LAMP reactions are optimized for a total reaction volume of 25 μ l including 2 μ l sample. Primers (Table 11) are premixed in a 10-fold primermix (Table 12). The LAMP buffer is premixed as 10-fold concentrate (Table 12). LAMP reaction mixes have to be prepared on ice, unless *Bst* 2.0 Warmstart DNA Polymerase is used (Table 13).

Table 11: PD3 Primer sequences

Primer	Sequence (5' - 3')
PD3 F3	GTCTTAACTGACGCTGAGG
PD3 B3	CATGCACCACCTGTATCC
PD3 FIP	ACGTACTACTCAGGCGGAGTACAACGATGAGTACTAAGTGTTGG
PD3 BIP	AATTGACGGGACTCCGCACTGTCAAGACCTGGTAAGGT
PD3 LF	AATGCGTAACTTCAGCACTG
PD3 LB	AAGCGGTGGATCATGTTGT

Table 12: PD3 Primer mix (10x) and LAMP buffer (10x)

Primermix (10x)				LAMP buffer (10x)	
Primer [100 μ M]	μ M (LAMP)	μ M (Premix)	μ l	Reagent	Conc.
PD3 F3	0.2	2	4	Tris-HCl (pH 8.8)	200 mM
PD3 B3	0.2	2	4	KCl	100 mM
PD3 FIP	1.6	16	32	(NH ₄) ₂ SO ₄	100 mM
PD3 BIP	1.6	16	32	Tween-20	1 %
PD3 LF	0.8	8	16		
PD3 LB	0.8	8	16		
H ₂ O			96		
Total volume			200		

Table 13: PD LAMP reaction mix

Reagents	µl per reaction	Conc. (LAMP)
ErioT [10 mM]	0.3	0.12 mM
LAMP buffer (10x)	2.5	1x
MgCl ₂ [100 mM]	1.2	4.8 mM
PEG 8k [30 % (w/v)]	4	4.8 %
dNTPs [10 mM]	2	0.8 mM
PD3 Primermix (10x)	2.5	1x
<i>Bst</i> DNA Polymerase [8 U/µl]	1	8 U
H ₂ O	9.9	
Sample	2	
Total volume	25	

Reaction conditions

Static incubation at 65 °C for 60 min in a thermal cycler, heating block or water bath.

Positive reactions will be identified by the colour change of the metal indicator dye from purple to blue.

5.3 Recommendations for further development and transfer of the PD detection procedure into practice

The problems with false positive LAMP reactions encountered during this study require further investigations on the cause and mechanism of this incidence in order to provide appropriate information for LAMP troubleshooting in future research and development. As a result, robust buffer formulations and reaction mix compositions should be selected, which are less prone to induce the generation of false positives in LAMP.

The applicability of the PD LAMP assay on-site in pear orchards may be confounded by LAMP reaction mix malfunction due to non-maintenance of the cold chain during delivery. In order to exclude this source of error, reliable procedures to provide dried LAMP reaction mixes have to be developed. Furthermore, portable devices for the performance of LAMP reactions should be introduced to the market, which are low in cost and independent of electric current.

Since pear decline is a quarantine disease, frequent screenings of pear stocks are recommended. The developed PD LAMP assay is highly suitable for on-site detection of PD infections within routine screenings in pear orchards producing fruits for the market, as well as in breeding facilities, which put pear plants and scions intended for grafting into circulation. A commercialization of the PD LAMP to make the DNA test accessible to pear growers and breeders would be desirable.

6 References

Abbasi, I., Kirstein, O. D., Hailu, A., & Warburg, A. (2016). Optimization of loop-mediated isothermal amplification (LAMP) assays for the detection of *Leishmania* DNA in human blood samples. *Acta tropica*, 162, 20-26.

Ahmadi, S., Almasi, M. A., Fatehi, F., Struik, P. C., & Moradi, A. (2013). Visual detection of Potato leafroll virus by one-step reverse transcription loop-mediated isothermal amplification of DNA with hydroxynaphthol blue dye. *Journal of Phytopathology*, 161(2), 120-124.

Ahrens, U., & Seemüller, E. (1992). Detection of DNA of plant pathogenic mycoplasma-like organisms by a polymerase chain reaction that amplifies a sequence of the 16 S rRNA gene. *Phytopathology*, 82(8), 828-832.

Aldaghi, M., Massart, S., Dutrecq, O., Bertaccini, A., Jijakli, M. H., & Lepoivre, P. (2009). A simple and rapid protocol of crude DNA extraction from apple trees for PCR and real-time PCR detection of '*Candidatus Phytoplasma mali*'. *Journal of virological methods*, 156(1), 96-101.

Altman, D. G., & Bland, J. M. (1994). Diagnostic tests. 1: Sensitivity and specificity. *BMJ: British Medical Journal*, 308(6943), 1552.

Antipova, V. N., Zheleznaya, L. A., & Zyrina, N. V. (2014). *Ab initio* DNA synthesis by *Bst* polymerase in the presence of nicking endonucleases Nt. AlwI, Nb. BbvCI, and Nb. BsmI. *FEMS microbiology letters*, 357(2), 144-150.

Arnaud, G., Malembic-Maher, S., Salar, P., Bonnet, P., Maixner, M., Marcone, C., Boudon-Padieu, E. & Foissac, X. (2007). Multilocus sequence typing confirms the close genetic interrelatedness of three distinct flavescence dorée phytoplasma strain clusters and group 16SrV phytoplasmas infecting grapevine and alder in Europe. *Applied and environmental microbiology*, 73(12), 4001-4010.

Aryan, E., Makvandi, M., Farajzadeh, A., Huygen, K., Bifani, P., Mousavi, S. L., Fateh, A., Jelodar, A., Gouya, M. M., & Romano, M. (2010). A novel and more sensitive loop-mediated isothermal amplification assay targeting IS6110 for detection of *Mycobacterium tuberculosis* complex. *Microbiological research*, 165(3), 211-220.

Asanidze, Z., Akhalkatsi, M., & Gvritshvili, M. (2011). Comparative morphometric study and relationships between the Caucasian species of wild pear (*Pyrus* spp.) and local cultivars in Georgia. *Flora-Morphology, Distribution, Functional Ecology of Plants*, 206(11), 974-986.

Bai, X., Zhang, J., Ewing, A., Miller, S. A., Radek, A. J., Shevchenko, D. V., Tsukerman, K., Walunas, T., Lapidus, A., Campbell, J.W. & Hogenhout, S. A. (2006). Living with genome instability: the adaptation of phytoplasmas to diverse environments of their insect and plant hosts. *Journal of bacteriology*, 188(10), 3682-3696.

- Balsaraf, V. M., Pawar, A. V., & Mane, P. A. (2010). Applied chemistry (Vol. 1). IK International Pvt Ltd.
- Beanland, L., Hoy, C. W., Miller, S. A., & Nault, L. R. (2000). Influence of aster yellows phytoplasma on the fitness of aster leafhopper (*Homoptera: Cicadellidae*). *Annals of the Entomological Society of America*, 93(2), 271-276.
- Bellstedt, D. U., Pirie, M. D., Visser, J. C., de Villiers, M. J., & Gehrke, B. (2010). A rapid and inexpensive method for the direct PCR amplification of DNA from plants. *American Journal of Botany*, 97(7), e65-e68.
- Bekele, B., Hodgetts, J., Tomlinson, J., Boonham, N., Nikolić, P., Swarbrick, P. & Dickinson, M. (2011). Use of a real-time LAMP isothermal assay for detecting 16SrII and XII phytoplasmas in fruit and weeds of the Ethiopian Rift Valley. *Plant Pathology* 60, 345-355.
- Bell, R. L., Quamme, H. A., Layne, R. E. C. & Skirvin, R. M. (1996). Pears. In: J. Janick and J.N. Moore (eds.). *Fruit breeding. vol I. Tree and tropical fruits*. Wiley, New York, 441–514.
- Berges, R., Rott, M., & Seemüller, E. (2000). Range of phytoplasma concentrations in various plant hosts as determined by competitive polymerase chain reaction. *Phytopathology*, 90(10), 1145-1152.
- Bertaccini, A., & Duduk, B. (2009). Phytoplasma and phytoplasma diseases: a review of recent research. *Phytopathologia Mediterranea*, 48(3), 355-378.
- Bertaccini, A., Duduk, B., Paltrinieri, S., & Contaldo, N. (2014). Phytoplasmas and phytoplasma diseases: a severe threat to agriculture. *American Journal of Plant Sciences*, 5(12), 1763.
- Betz, J. D., & Noll, C. A. (1950). Total-hardness determination by direct colorimetric titration. *Journal (American Water Works Association)*, 42(1), 49-56.
- Biedermann, W., & Schwarzenbach, G. (1948). The “complexometric” titration of alkaline earths and some other metals with Eriochromeblack T. *Chimia*, 2, 56.
- Bimboim, H. C., & Doly, J. (1979). A rapid alkaline extraction procedure for screening recombinant plasmid DNA. *Nucleic acids research*, 7(6), 1513-1523.
- Blanchard, M. M., Taillon-Miller, P., Nowotny, P., & Nowotny, V. (1993). PCR buffer optimization with uniform temperature regimen to facilitate automation. *Genome Research*, 2(3), 234-240.
- Blomquist, C. L., & Kirkpatrick, B. C. (2002). Frequency and seasonal distribution of pear psylla infected with the pear decline phytoplasma in California pear orchards. *Phytopathology*, 92(11), 1218-1226.

- Bond, M., & Richards-Kortum, R. (2017). Diagnostics for global health: Hand-spun centrifuge. *Nature Biomedical Engineering*, 1(1), 0017.
- Bourke, M. T., Scherczinger, C. A., Ladd, C., & Lee, H. C. (1999). NaOH treatment to neutralize inhibitors of *Taq* polymerase. *Journal of Forensic Science*, 44(5), 1046-1050.
- Brittain, H. G. (1978). The use of hydroxynaphthol blue in the ultramicro-determination of alkaline earth and lanthanide elements: an improved method. *Analytica Chimica Acta*, 96(1), 165-170.
- Brown, J., Theis, L., Kerr, L., Zakhidova, N., O'Connor, K., Uthman, M., Oden, Z. M., & Richards-Kortum, R. (2011). A hand-powered, portable, low-cost centrifuge for diagnosing anemia in low-resource settings. *The American journal of tropical medicine and hygiene*, 85(2), 327-332.
- Brownie, J., Shawcross, S., Theaker, J., Whitcombe, D., Ferrie, R., Newton, C., & Little, S. (1997). The elimination of primer-dimer accumulation in PCR. *Nucleic acids research*, 25(16), 3235-3241.
- Buwalda, R. T., Jonker, J. M., & Engberts, J. B. (1999). Aggregation of azo dyes with cationic amphiphiles at low concentrations in aqueous solution. *Langmuir*, 15(4), 1083-1089.
- Caetano-Anolles, G., Bassam, B. J., & Gresshoff, P. M. (1994). Buffer components tailor DNA amplification with arbitrary primers. *PCR methods and applications*, 4, 59-59.
- Çakir, O., Coskun, E. E., Bicer, E., & Çakir, S. (2001). Voltammetric and polarographic studies of eriochrome black T-nickel (II) complex. *Turkish Journal of Chemistry*, 25(1), 33-38.
- Carraro, L., Loi, N., & Ermacora, P. (2001). The 'life cycle' of pear decline phytoplasma in the vector *Cacopsylla pyri*. *Journal of Plant Pathology*, 87-90.
- Chen, W. Y., Cui, H. R., Bao, J. S., Zhou, X. S., & Shu, Q. Y. (2006). A simplified rice DNA extraction protocol for PCR analysis. *Rice Science*, 13(1), 67-70.
- Chen, X. C., Tao, T., Wang, Y. G., Peng, Y. X., Huang, W., & Qian, H. F. (2012). Azo-hydrazone tautomerism observed from UV-vis spectra by pH control and metal-ion complexation for two heterocyclic disperse yellow dyes. *Dalton transactions*, 41(36), 11107-11115.
- Chen, Z., Yang, T., Yang, H., Li, T., Nie, L., Mou, X., Deng, Y., He, N., Li, Z., Wang, L., & Li, S. (2018). A Portable Multi-Channel Turbidity System for Rapid Detection of Pathogens by Loop-Mediated Isothermal Amplification. *Journal of biomedical nanotechnology*, 14(1), 198-205.

- Cheng, Y. J., Guo, W. W., Yi, H. L., Pang, X. M., & Deng, X. (2003). An efficient protocol for genomic DNA extraction from *Citrus* species. *Plant Molecular Biology Reporter*, 21(2), 177-178.
- Chomczynski, P., & Rymaszewski, M. (2006). Alkaline polyethylene glycol-based method for direct PCR from bacteria, eukaryotic tissue samples, and whole blood. *Biotechniques*, 40(4), 454.
- Chou, Q., Russell, M., Birch, D. E., Raymond, J., & Bloch, W. (1992). Prevention of pre-PCR mis-priming and primer dimerization improves low-copy-number amplifications. *Nucleic Acids Research*, 20(7), 1717-1723.
- Christensen, N. M., Nicolaisen, M., Hansen, M., & Schulz, A. (2004). Distribution of phytoplasmas in infected plants as revealed by real-time PCR and bioimaging. *Molecular Plant-Microbe Interactions*, 17(11), 1175-1184.
- Collard, B. C. Y., Das, A., Virk, P. S., & Mackill, D. J. (2007). Evaluation of 'quick and dirty' DNA extraction methods for marker-assisted selection in rice (*Oryza sativa* L.). *Plant Breeding*, 126(1), 47-50.
- Contaldo, N., Bertaccini, A., Paltonieri, S., Windsor, H. M., & Windsor, G. D. (2012). Axenic culture of plant pathogenic phytoplasmas. *Phytopathologia Mediterranea*, 607-617.
- Crannell, Z. A., Rohrman, B., & Richards-Kortum, R. (2014). Equipment-free incubation of recombinase polymerase amplification reactions using body heat. *PloS one*, 9(11), e112146.
- Craw, P., & Balachandran, W. (2012). Isothermal nucleic acid amplification technologies for point-of-care diagnostics: a critical review. *Lab on a Chip*, 12(14), 2469-2486.
- Curtis, K. A., Rudolph, D. L., & Owen, S. M. (2009). Sequence-specific detection method for reverse transcription, loop-mediated isothermal amplification of HIV-1. *Journal of medical virology*, 81(6), 966-972.
- Curtis, K. A., Rudolph, D. L., Nejad, I., Singleton, J., Beddoe, A., Weigl, B., LaBarre, P., & Owen, S. M. (2012). Isothermal amplification using a chemical heating device for point-of-care detection of HIV-1. *PloS one*, 7(2), e31432.
- Daire, X., Boudon-Padieu, E., Berville, A., Schneider, B., & Caudwell, A. (1992). Cloned DNA probes for detection of grapevine flavescence doree mycoplasma-like organism (MLO). *Annals of Applied Biology* 121, 95-103.
- Degrave, W., Fernandes, O., Campbell, D., Bozza, M., & Lopes, U. (1994). Use of molecular probes and PCR for detection and typing of *Leishmania*-a mini-review. *Memórias do Instituto Oswaldo Cruz*, 89(3), 463-469.

References

- De Jonghe, K., De Roo, I., & Maes, M. (2017). Fast and sensitive on-site isothermal assay (LAMP) for diagnosis and detection of three fruit tree phytoplasmas. *European Journal of Plant Pathology*, 147(4), 749-759.
- Dellaporta, S. L., Wood, J., & Hicks, J. B. (1983). A plant DNA miniprep: version II. *Plant molecular biology reporter*, 1(4), 19-21.
- De Luna, M. D. G., Flores, E. D., Genuino, D. A. D., Futralan, C. M., & Wan, M. W. (2013). Adsorption of Eriochrome Black T (ErioT) dye using activated carbon prepared from waste rice hulls—Optimization, isotherm and kinetic studies. *Journal of the Taiwan Institute of Chemical Engineers*, 44(4), 646-653.
- Deng, S., & Hiruki, C. (1991). Amplification of 16S rRNA genes from culturable and nonculturable mollicutes. *Journal of microbiological methods*, 14(1), 53-61.
- Denschlag, C., Vogel, R. F., & Niessen, L. (2013). *Hyd5* gene based analysis of cereals and malt for gushing-inducing *Fusarium* spp. by real-time LAMP using fluorescence and turbidity measurements. *International journal of food microbiology*, 162(3), 245-251.
- Doi, Y., Teranaka, M., Yora, K., & Asuyama, H. (1967). Mycoplasma-or PLT group-like microorganisms found in the phloem elements of plants infected with mulberry dwarf, potato witches' broom, aster yellows, or paulownia witches' broom. *Japanese Journal of Phytopathology*, 33(4), 259-266.
- Dolatowski, J., Nowosielski, J., Podyma, W., Szymanska, M., & Zych, M. (2004). Molecular studies on the variability of Polish semi-wild pears (*Pyrus*) using AFLP. *Journal of Fruit and Ornamental Plant Research*, 12(Spec. ed. 2), 331-337.
- Doyle, J. J., & Doyle J.H. (1990). Isolation of plant DNA from fresh tissue. *Focus*, 12, 13-15.
- Duduk, B., Paltrinieri, S., Lee, I. M., & Bertaccini, A. (2013). Nested PCR and RFLP analysis based on the 16S rRNA gene. In: *Phytoplasma: Methods and Protocols*. *Methods in molecular biology*, Clifton, NJ, 938, 159-171.
- Ellingboe, J. L. (1956). Chelate ring derivatives of azo dyes. Dissertation submitted to Iowa State College. <http://lib.dr.iastate.edu/cgi/viewcontent.cgi?article=14431&context=rtd>
- Errea, P., Aguelo, V., & Hormaza, J. I. (2002). Seasonal variations in detection and transmission of pear decline phytoplasma. *Journal of Phytopathology*, 150(8-9), 439-443.
- Eurostat, Statistical Office of the European Union (2015). Permanent crops for human consumption by area, <http://ec.europa.eu/eurostat/tgm/refreshTableAction.do?tab=table&plugin=1&pcode=tag00120&language=en>, last accessed on 12.05.2017.

- Federal Statistical Office Germany (2012). Landwirtschaftliche Bodennutzung – Baumobstflächen – Fachserie 3 Reihe 3.1.4 – 2012.
- Federal Statistical Office Germany (2016). Wachstum und Ernte – Baumobst – Fachserie 3 Reihe 3.2.1 – 14/2016
- Fire, A., & Xu, S. (1995). Rolling replication of short DNA circles. *Proceedings of the National Academy of Sciences USA* 92(10), 4641-4645.
- Firrao, G., Garcia-Chapa, M., & Marzachì, C. (2007). Phytoplasmas: genetics, diagnosis and relationships with the plant and insect host. *Frontiers in Bioscience*, 12, 1353-1375.
- Fischer, T. C., Malnoy, M., Hofmann, T., Schwab, W., Palmieri, L., Wehrens, R., Schuch, L. A., Müller, M., Schimmelpfeng, H., Velasco, R., & Martens, S. (2014). F1 hybrid of cultivated apple (*Malus × domestica*) and European pear (*Pyrus communis*) with fertile F2 offspring. *Molecular breeding*, 34(3), 817-828.
- Food and Agricultural organization of the United Nation FAO (2014). Faostat_Data_pear_areaharvested, <http://www.fao.org/faostat/en/#data/QC>, last accessed on 16.05.2017.
- Galetto, L., & Marzachì, C. (2010). Real-time PCR diagnosis and quantification of phytoplasmas. In: Weintraub P.G., Jones P. (eds.): *Phytoplasmas: Genomes, Plant Hosts and Vectors*. CAB International, Wallingford, UK, 1–18.
- García, P. B., Robledo, N. L., & Islas, Á. L. (2004). Analysis of non-template-directed nucleotide addition and template switching by DNA polymerase. *Biochemistry*, 43(51), 16515-16524.
- Garcia-Chapa, M., Medina, V., Viruel, M. A., Laviña, A., & Batlle, A. (2003). Seasonal detection of pear decline phytoplasma by nested-PCR in different pear cultivars. *Plant Pathology* 52, 513-520.
- Gentili, A., Ferretti, L., Vizzaccaro, L., Durante, G., Gianinazzi, C., Lopriore, S., Chatillon, C. & Pasquiní, G. (2016). Detection of Bois noir phytoplasma by a quick-to-use isothermal amplification assay: preliminary results. *Mitteilungen Klosterneuburg, Rebe und Wein, Obstbau und Früchteverwertung*, 66(Suppl.), 70-73.
- Gétaz, M., Bühlmann, A., Schneeberger, P. H. H., Van Malderghem, C., Duffy, B., Maes, M., Pothier, J. F., & Cottyn, B. (2017). A diagnostic tool for improved detection of *Xanthomonas fragariae* using a rapid and highly specific LAMP assay designed with comparative genomics. *Plant Pathology*, 66(7), 1094-1102.
- Ghosh, S. (2010). Sodium dodecyl benzene sulphonate mediated tautomerism of Eriochrome Black-T: Effect of charge transfer interaction. *Chemical Physics Letters*, 500(4), 295-301.

- Giunchedi, L., Credi, R., Babini, A. R., & Bertaccini, A. (1982). Mycoplasma-like organisms associated with Pear moria in Italy/Corpi riferibili a micoplasmi in piante di pero affette da moria in Italia. *Phytopathologia Mediterranea*, 20-22.
- Gosch, C., Gottsberger, R. A., Stich, K., & Fischer, T. C. (2012). Blue EaLAMP—a specific and sensitive method for visual detection of genomic *Erwinia amylovora* DNA. *European journal of plant pathology*, 134(4), 835-845.
- Goto, M., Honda, E., Ogura, A., Nomoto, A., & Hanaki, K. I. (2009). Colorimetric detection of loop-mediated isothermal amplification reaction by using Hydroxy naphthol blue. *Biotechniques* 46, 167-172.
- Green, M. J., Thompson, D. A., & MacKenzie, D. J. (1999). Easy and efficient DNA extraction from woody plants for the detection of phytoplasmas by polymerase chain reaction. *Plant Disease* 83, 482-485.
- Groppe, K., & Boller, T. (1997). PCR assay based on a microsatellite-containing locus for detection and quantification of *Epichloë* endophytes in grass tissue. *Applied and environmental microbiology*, 63(4), 1543-1550.
- Gundersen, D. E., Lee, I. M., Rehner, S. A., Davis, R. E., & Kingsbury, D. T. (1994). Phylogeny of mycoplasma-like organisms (phytoplasmas): a basis for their classification. *Journal of bacteriology*, 176(17), 5244-5254.
- Guo, Y., Cheng, Z. M., & Walla, J. A. (2003). Rapid PCR-based detection of phytoplasmas from infected plants. *HortScience*, 38(6), 1134-1136.
- Hadersdorfer, J. (2013). Development of an isothermal nucleic acid amplification protocol for high-throughput monitoring of Plum pox virus infection in stone fruit production. Doctoral dissertation, München, Technische Universität München, Diss., 2013.
- Hadersdorfer, J., Neumüller, M., Treutter, D., & Fischer, T. (2011). Fast and reliable detection of Plum pox virus in woody host plants using the Blue LAMP protocol. *Annals of Applied Biology* 159(3), 456-466.
- Hafner, G. J., Yang, I. C., Wolter, L. C., Stafford, M. R., & Giffard, P. M. (2001). Isothermal amplification and multimerization of DNA by *Bst* DNA polymerase. *Biotechniques*, 30(4), 852-867.
- Hall, T.A. (1999). BioEdit: a user-friendly biological sequence alignment editor and analysis program for Windows 95/98/NT. *Nucleic Acids Symposium Series*, 41, 95-98.
- Hamed, M. M. A., Ismail, N. M., & Ibrahim, S. A. (1994). Solvent characteristics in the spectral behaviour of eriochrome black T. *Dyes and pigments*, 26(4), 297-305.

- Harper, S. J., Ward, L. I., & Clover, G. R. G. (2010). Development of LAMP and real-time PCR methods for the rapid detection of *Xylella fastidiosa* for quarantine and field applications. *Phytopathology*, 100(12), 1282-1288.
- Hatano, B., Maki, T., Obara, T., Fukumoto, H., Hagsisawa, K., Matsushita, Y., Okutani, A., Bazartseren, B., Inoue, S., Sata, T., & Katano, H. (2010). LAMP using a disposable pocket warmer for anthrax detection, a highly mobile and reliable method for anti-bioterrorism. *Japanese Journal of Infectious Diseases*, 63(1), 36-40.
- Hedrick, U.P. (1921). The pears of New York. Report of the New York Agricultural Experiment Station 1921. JB Lyon Co. Printers, Albany, N.Y.
- Hodgetts, J., & Dickinson, M. (2010). Phytoplasma phylogeny and detection based on genes other than 16S rRNA. In: Weintraub P.G., Jones P. (eds.): *Phytoplasmas: Genomes, Plant Hosts and Vectors*. CAB International, Wallingford, UK, 93–113.
- Hodgetts, J., Tomlinson, J., Boonham, N., Gonzalez-Martin, I., Nikolić, P., Swarbrick, P., Yankey, E., & Dickinson, M. (2011). Development of rapid in-field loop-mediated isothermal amplification (LAMP) assays for phytoplasmas. In *Bulletin of Insectology* (Vol. 64, No. Supplement, pp. S41-S42). Department of Agroenvironmental Sciences and Technologies.
- Hogenhout, S. A., Oshima, K., Ammar, E. D., Kakizawa, S., Kingdom, H. N., & Namba, S. (2008). Phytoplasmas: bacteria that manipulate plants and insects. *Molecular Plant Pathology*, 9(4), 403-423.
- Hummer, K. E., & Janick, J. (2009). *Rosaceae*: taxonomy, economic importance, genomics. In: *Genetics and genomics of Rosaceae*. Springer, New York, 1-17.
- Hwang, H., Bae, S. C., Lee, S., Lee, Y. H., & Chang, A. (2013). A rapid and simple genotyping method for various plants by Direct-PCR. *Plant Breeding and Biotechnology*, 1(3), 290-297.
- Inácio, J., Flores, O., & Spencer-Martins, I. (2008). Efficient identification of clinically relevant *Candida* yeast species by use of an assay combining panfungal loop-mediated isothermal DNA amplification with hybridization to species-specific oligonucleotide probes. *Journal of clinical microbiology*, 46(2), 713-720.
- Innis, M. A., & Gelfand, D. H. (1990). Optimization of PCRs. In: Innis, M. A., Gelfand, D. H., Sninsky, J. J., & White, T. J. (Eds.): *PCR protocols: A guide to methods and applications*. Academic Press, San Diego, CA, 3-12.
- Innis, M. A., & Gelfand, D. H. (1999). Optimization of PCR: conversations between Michael and David. In: Innis, M. A., Gelfand, D. H., & Sninsky, J. J. (Eds.): *PCR applications: protocols for functional genomics*. Academic Press, San Diego, CA, 3-22.

- Inscoe, M. N., Gould, J. H., Corning, M. E., & Erode, W. R. (1958). Relation between the absorption spectra and the chemical constitution of dyes: XXIX. Interaction of direct azo dyes in aqueous solution'. *Journal of Research of the National Bureau of Standards*, 60(1), 65.
- IRPCM (2004). "*Candidatus* Phytoplasma", a taxon for the wall-less, non-helical prokaryotes that colonize plant phloem and insects. *International Journal of Systematic and Evolutionary Microbiology* 54, 1243-1255.
- Jander, G., & Jahr, K.F. (2002). *Maßanalyse*. 16th Ed., Walter de Gruyter, Berlin, Germany, 213.
- Janick, J. (2000). The pear in history, literature, popular culture, and art. In VIII International Symposium on Pear 596, 41-52.
- Jansson, V., & Jansson, K. (2002). Enzymatic chemiluminescence assay for inorganic pyrophosphate. *Analytical biochemistry*, 304(1), 135-137.
- Jarausch, B., & Jarausch, W. (2010). Psyllid vectors and their control. In: Weintraub, P.G., Jones, P. (eds.): *Phytoplasmas: Genomes, Plant Hosts and Vectors*. CAB International, Wallingford, UK, 250–271.
- Jiang, Y. S., Bhadra, S., Li, B., Wu, Y. R., Milligan, J. N., & Ellington, A. D. (2015). Robust strand exchange reactions for the sequence-specific, real-time detection of nucleic acid amplicons. *Analytical chemistry*, 87(6), 3314-3320.
- John, M. E. (1992). An efficient method for isolation of RNA and DNA from plants containing polyphenolics. *Nucleic Acids Research*, 20(9), 2381.
- Karthik, K., Rathore, R., Thomas, P., Arun, T. R., Viswas, K. N., Dhama, K., & Agarwal, R. K. (2014). New closed tube loop mediated isothermal amplification assay for prevention of product cross-contamination. *MethodsX*, 1, 137-143.
- Katayama, H., Tachibana, M., Iketani, H., Zhang, S. L., & Uematsu, C. (2012). Phylogenetic utility of structural alterations found in the chloroplast genome of pear: hypervariable regions in a highly conserved genome. *Tree genetics & genomes*, 8(2), 313-326.
- Kato, T., Liang, X., & Asanuma, H. (2012). Model of elongation of short DNA sequence by thermophilic DNA polymerase under isothermal conditions. *Biochemistry*, 51(40), 7846-7853.
- Katterman, F. R. H., & Shattuck, V. I. (1983). An effective method of DNA isolation from the mature leaves of *Gossypium* species that contain large amounts of phenolic terpenoids and tannins. *Preparative Biochemistry*, 13(4), 347-359.
- Kellogg, D. E., Rybalkin, I., Chen, S., Mukhamedova, N., Vlasik, T., Siebert, P. D., & Chenchik, A. (1994). TaqStart Antibody:" hot start" PCR facilitated by a neutralizing

- monoclonal antibody directed against *Taq* DNA polymerase. *BioTechniques*, 16(6), 1134-1137.
- Kim, C. S., Lee, C. H., Shin, J. S., Chung, Y. S., & Hyung, N. I. (1997). A simple and rapid method for isolation of high quality genomic DNA from fruit trees and conifers using PVP. *Nucleic acids research*, 25(5), 1085-1086.
- Kimura, Y., de Hoon, M. J., Aoki, S., Ishizu, Y., Kawai, Y., Kogo, Y., Daub, C.O., Lezhava, A., Arner, E., & Hayashizaki, Y. (2011). Optimization of turn-back primers in isothermal amplification. *Nucleic acids research*, 39(9), e59-e59.
- Klimyuk, V. I., Carroll, B. J., Thomas, C. M., & Jones, J. D. (1993). Alkali treatment for rapid preparation of plant material for reliable PCR analysis. *The Plant Journal*, 3(3), 493-494.
- Kodama, M. (1967). Spectrophotometric studies of the solution equilibria and the kinetics of the substitution reaction between Eriochrome Black T and Cobalt (II)-Ethylenediaminetetraacetate chelate. *Bulletin of the Chemical Society of Japan*, 40(11), 2575-2579.
- Kodama, M., & Ebine, H. (1967). Spectrophotometric study of the solution equilibria between Eriochrome Black T and Zinc (II)-Nitrilotriacetate or Copper (II)-Cyclohexanediaminetetraacetate. *Bulletin of the Chemical Society of Japan*, 40(8), 1857-1861.
- Kogovšek, P., Hodgetts, J., Hall, J., Prezelj, N., Nikolić, P., Mehle, N., Lenarcic, R., Rotter, A., Dickinson, M., Boonham, N., Dermastia, M., & Ravnikar, M. (2015). LAMP assay and rapid sample preparation method for on-site detection of flavescence dorée phytoplasma in grapevine. *Plant pathology*, 64(2), 286-296.
- Kolhe, P., Amend, E., & Singh, S. K. (2010). Impact of freezing on pH of buffered solutions and consequences for monoclonal antibody aggregation. *Biotechnology progress*, 26(3), 727-733.
- Khorosheva, E. M., Karymov, M. A., Selck, D. A., & Ismagilov, R. F. (2015). Lack of correlation between reaction speed and analytical sensitivity in isothermal amplification reveals the value of digital methods for optimization: validation using digital real-time RT-LAMP. *Nucleic acids research*, 44(2), e10-e10.
- Kube, M., Schneider, B., Kuhl, H., Dandekar, T., Heitmann, K., Migdoll, A. M., Reinhardt, R., & Seemüller, E. (2008). The linear chromosome of the plant-pathogenic mycoplasma '*Candidatus* Phytoplasma mali'. *BMC Genomics*, 9(1), 306.
- Kube, M., Mitrovic, J., Duduk, B., Rabus, R., & Seemüller, E. (2012). Current view on phytoplasma genomes and encoded metabolism. *The Scientific World Journal*, 2012, 185942-185942.

- Kuboki, N., Inoue, N., Sakurai, T., Di Cello, F., Grab, D. J., Suzuki, H., Sugimoto, C., & Igarashi, I. (2003). Loop-mediated isothermal amplification for detection of African trypanosomes. *Journal of clinical microbiology*, 41(12), 5517-5524.
- Kubota, R., Labarre, P., Weigl, B. H., Li, Y., Haydock, P., & Jenkins, D. M. (2013). Molecular diagnostics in a teacup: Non-Instrumented Nucleic Acid Amplification (NINA) for rapid, low cost detection of *Salmonella enterica*. *Chinese Science Bulletin*, 58(10), 1162-1168.
- Kutzelnigg, H., & Silbereisen, R. (1995). *Pyrus*. In: *Illustrierte Flora von Mitteleuropa*. 4 (2B), Weissdorn, Jena.
- LaBarre, P., Hawkins, K. R., Gerlach, J., Wilmoth, J., Beddoe, A., Singleton, J., Boyle, D., & Weigl, B. (2011). A simple, inexpensive device for nucleic acid amplification without electricity—toward instrument-free molecular diagnostics in low-resource settings. *PloS one*, 6(5), e19738.
- Lajin, B., Alachkar, A., & Sakur, A. A. (2013). Betaine significantly improves multiplex tetra-primer ARMS-PCR methods. *Molecular biotechnology*, 54(3), 977-982.
- Langhals, H. (1991). Description of properties of binary solvent mixtures. *Studies in organic chemistry*, 42, 283-342.
- La Quintinie, J.-B. de (1690). *Instruction pour les jardins fruitiers et potagers*. [Volume 1] /, avec un *Traité des orangers*, suivy de *Quelques réflexions sur l'agriculture*, par feu M. de La Quintinye, Tome I. [-II.], p. 278. Éditeur: A Paris, chez Claude Barbin, sur le second perron de la sainte Chapelle. M.DC.LXXXX. Avec privilege de Sa Majesté. <http://gallica.bnf.fr/ark:/12148/bpt6k619796/f389.vertical>, last accessed on 17.05.2017.
- Larkin, M. A., Blackshields, G., Brown, N. P., Chenna, R., McGettigan, P. A., McWilliam, H., Valentin, F., Wallace, I. M., Wilm, A., Lopez, R., Thompson, J. D., Gibson, T. J., & Higgins, D. G. (2007). Clustal W and Clustal X version 2.0. *Bioinformatics*, 23(21), 2947–2948.
- Latscha, H. P., Linti, G. W., & Klein, H. A. (2004). *Analytische Chemie: Chemie-Basiswissen 3*. Springer-Verlag Berlin Heidelberg, p. 201.
- Lebedev, A. V., Paul, N., Yee, J., Timoshchuk, V. A., Shum, J., Miyagi, K., Kellum, J., Hogrefe, R. I., & Zon, G. (2008). Hot start PCR with heat-activatable primers: a novel approach for improved PCR performance. *Nucleic acids research*, 36(20), e131-e131.
- Lee, A. C., Xu, X., & Colombini, M. (1996). The role of pyridine dinucleotides in regulating the permeability of the mitochondrial outer membrane. *Journal of Biological Chemistry*, 271(43), 26724-26731.
- Lee, B., Park, S. Y., Heo, Y. S., Yea, S. S., & Kim, D. E. (2009). Efficient colorimetric assay of RNA polymerase activity using inorganic pyrophosphatase and ammonium molybdate. *Bulletin of the Korean Chemical Society*, 30(10), 2485-2488.

- Lee, D., La Mura, M., Allnut, T. R., & Powell, W. (2009). Detection of genetically modified organisms (GMOs) using isothermal amplification of target DNA sequences. *BMC biotechnology*, 9(1), 7.
- Lee, I.-M., Bertaccini, A., Vibio, M., & Gundersen, D. E. (1995). Detection of multiple phytoplasmas in perennial fruit trees with decline symptoms in Italy. *Phytopathology*, 85(6), 728-735.
- Lee, I.-M., Hammond, R. W., Davis, R. E., & Gundersen, D. E. (1993). Universal amplification and analysis of pathogen 16S rDNA for classification and identification of mycoplasma-like organisms. *Phytopathology*, 83(8), 834-842.
- Lee, I.-M., Gundersen-Rindal, D. E., Davis, R. E., & Bartoszyk, I. M. (1998). Revised Classification Scheme of Phytoplasmas based on RFLP analyses of 16S rRNA and ribosomal protein gene sequences. *International Journal of Systematic and Evolutionary Microbiology*, 48, 1153-1169.
- Levine, R. M., & Cummings, J. R. (1956). A sensitive, accurate spectrophotometric method for the determination of magnesium in serum. *Journal of Biological Chemistry*, 221, 735-742.
- Li, B., Chen, X., & Ellington, A. D. (2012). Adapting enzyme-free DNA circuits to the detection of loop-mediated isothermal amplification reactions. *Analytical chemistry*, 84(19), 8371.
- Liang, X., Kato, T., & Asanuma, H. (2007). Unexpected efficient *ab initio* DNA synthesis at low temperature by using thermophilic DNA polymerase. In: *Nucleic Acids Symposium Series*, 51(1), 351-352. Oxford University Press.
- Liao, S. C., Peng, J., Mauk, M. G., Awasthi, S., Song, J., Friedman, H., Bau, H. H., & Liu, C. (2016). Smart cup: a minimally-instrumented, smartphone-based point-of-care molecular diagnostic device. *Sensors and Actuators B: Chemical*, 229, 232-238.
- List, P. H., & Hörhammer, L. (1967). *Hagers Handbuch der pharmazeutischen Praxis, Allgemeiner Teil. Wirkstoffgruppen I*. Springer-Verlag Berlin Heidelberg, Germany, p. 326.
- Liu, J., Gopurenko, D., Fletcher, M. J., Johnson, A. C., & Gurr, G. M. (2017). Phytoplasmas—The “Crouching Tiger” threat of Australian plant pathology. *Frontiers in plant science*, 8, 599.
- Liu, X., Luo, L., Ding, Y., Kang, Z., & Ye, D. (2012). Simultaneous determination of L-cysteine and L-tyrosine using Au-nanoparticles/poly-eriochrome black T film modified glassy carbon electrode. *Bioelectrochemistry*, 86, 38-45.
- Lodhi, M. A., Ye, G. N., Weeden, N. F., & Reisch, B. I. (1994). A simple and efficient method for DNA extraction from grapevine cultivars and *Vitis* species. *Plant Molecular Biology Reporter*, 12(1), 6-13.

- Lorenz, K. H., Schneider, B., Ahrens, U., & Seemüller, E. (1995). Detection of the apple proliferation and pear decline phytoplasmas by PCR amplification of ribosomal and nonribosomal DNA. *Phytopathology* 85, 771-776.
- Maas, F. (2007). Evaluation of *Pyrus* and quince rootstocks for high density pear orchards. In: X International Pear Symposium, 800, 599-610.
- Manjunatha, A. S., & Sukhdev, A. (2014). Oxidative decolorisation of Eriochrome Black T with Chloramine-T: kinetic, mechanistic, and spectrophotometric approaches. *Coloration Technology*, 130(5), 340-348.
- Marcone, C., Lee, I. M., Davis, R. E., Ragozzino, A., & Seemüller, E. (2000). Classification of aster yellows-group phytoplasmas based on combined analyses of rRNA and *tuf* gene sequences. *International Journal of Systematic and Evolutionary Microbiology*, 50(5), 1703-1713.
- Markoulatos, P., Siafakas, N., & Moncany, M. (2002). Multiplex polymerase chain reaction: a practical approach. *Journal of clinical laboratory analysis*, 16(1), 47-51.
- Martel, F., Grundemann, D., & Schomig, E. (2002). A simple method for elimination of false positive results in RT-PCR. *Journal of biochemistry and molecular biology*, 35(2), 248-250.
- Martin, J. T., & Standing, H. A. (1949). 41—The effects of a polyethylene oxide condensate and some polyethylene glycols on the absorption spectra of certain azo dyes. *Journal of the Textile Institute Transactions*, 40(10), T689-T701.
- Martini, M., Lee, I. M., Bottner, K. D., Zhao, Y., Botti, S., Bertaccini, A., Harrison, N. A., Carraro, L., Marcone, C., Khan, A. J. & Osler, R. (2007). Ribosomal protein gene-based phylogeny for finer differentiation and classification of phytoplasmas. *International Journal of Systematic and Evolutionary Microbiology*, 57(9), 2037-2051.
- Martini, M., & Lee, I.-M. (2013). PCR and RFLP analyses based on the ribosomal protein operon. In: *Phytoplasma: Methods and Protocols*. Methods in molecular biology, Clifton, NJ, 938, 173-188.
- Masoud, M. S., Hammud, H. H., & Beidas, H. (2002). Dissociation constants of eriochrome black T and eriochrome blue black RC indicators and the formation constants of their complexes with Fe (III), Co (II), Ni (II), Cu (II), Zn (II), Cd (II), Hg (II), and Pb (II), under different temperatures and in presence of different solvents. *Thermochimica acta*, 381(2), 119-131.
- Mauk, M., Song, J., Bau, H. H., Gross, R., Bushman, F. D., Collman, R. G., & Liu, C. (2017). Miniaturized devices for point of care molecular detection of HIV. *Lab on a Chip*, 17(3), 382-394.

- Monte-Corvo, L., Goulão, L., & Oliveira, C. (2001). ISSR analysis of cultivars of pear and suitability of molecular markers for clone discrimination. *Journal of the American Society for Horticultural Science*, 126(5), 517-522.
- Moradi, A., Almasi, M. A., Jafary, H., & Mercado-Blanco, J. (2014). A novel and rapid loop-mediated isothermal amplification assay for the specific detection of *Verticillium dahliae*. *Journal of applied microbiology*, 116(4), 942-954.
- Mori, Y., Nagamine, K., Tomita, N., & Notomi, T. (2001). Detection of loop-mediated isothermal amplification reaction by turbidity derived from magnesium pyrophosphate formation. *Biochemical and biophysical research communications*, 289(1), 150-154.
- Mori, Y., Kitao, M., Tomita, N., & Notomi, T. (2004). Real-time turbidimetry of LAMP reaction for quantifying template DNA. *Journal of biochemical and biophysical methods*, 59(2), 145-157.
- Mori, Y., Kanda, H., & Notomi, T. (2013). Loop-mediated isothermal amplification (LAMP): recent progress in research and development. *Journal of Infection and Chemotherapy* 19(3), 404-411.
- Morris, A. D., Léonce, S., Guilbaud, N., Tucker, G. C., Pérez, V., Jan, M., Cordi, A. A., Pierré, A., & Atassi, G. (1997). Eriochrome Black T, structurally related to suramin, inhibits angiogenesis and tumor growth in vivo. *Anti-cancer drugs*, 8(8), 746-755.
- Mudge, K., Janick, J., Scofield, S., & Goldschmidt, E. E. (2009). A history of grafting. *Horticultural reviews*, 35, 437-493.
- Mullis, K. B. (1990). The unusual origin of the polymerase chain reaction. *Scientific American*, 262(4), 56-61.
- Münch, U. (1965). Mischindicator für die chelatometrische Bestimmung von Magnesium. *Fresenius' Journal of Analytical Chemistry*, 212(3), 419-420.
- Murase, N., & Franks, F. (1989). Salt precipitation during the freeze-concentration of phosphate buffer solutions. *Biophysical chemistry*, 34(3), 293-300.
- Murray, R. G. E., & Schleifer, K. H. (1994). Taxonomic notes: a proposal for recording the properties of putative taxa of procaryotes. *International Journal of Systematic and Evolutionary Microbiology*, 44(1), 174-176.
- Murray, R. G. E., & Stackebrandt, E. (1995). Taxonomic note: implementation of the provisional status *Candidatus* for incompletely described procaryotes. *International Journal of Systematic and Evolutionary Microbiology*, 45(1), 186-187.
- Nagamine, K., Hase, T., & Notomi, T. (2002). Accelerated reaction by loop-mediated isothermal amplification using loop primers. *Molecular and cellular probes*, 16(3), 223-229.

- Nagamine, K., Watanabe, K., Ohtsuka, K., Hase, T., & Notomi, T. (2001). Loop-mediated isothermal amplification reaction using a nondenatured template. *Clinical Chemistry*, 47(9), 1742-1743.
- Nair, S., Manimekalai, R., Raj, P. G., & Hegde, V. (2016). Loop-mediated isothermal amplification (LAMP) assay for detection of coconut root wilt disease and arecanut yellow leaf disease phytoplasma. *World Journal of Microbiology and Biotechnology*, 32(7), 1-7.
- Nazar, M. F., Shah, S. S., & Khosa, M. A. (2010). Interaction of azo dye with cationic surfactant under different pH conditions. *Journal of surfactants and detergents*, 13(4), 529-537.
- Nkouawa, A., Sako, Y., Li, T., Chen, X., Nakao, M., Yanagida, T., Okamoto, M., Giraudoux, P., Raoul, F., Nakaya, K., Xiao, N., Qiu, J., Qiu, D., Craig, P., & Ito, A. (2012). A loop-mediated isothermal amplification method for a differential identification of *Taenia* tapeworms from human: application to a field survey. *Parasitology international*, 61(4), 723-725.
- Notomi, T., Okayama, H., Masubuchi, H., Yonekawa, T., Watanabe, K., Amino, N., & Hase, T. (2000). Loop-mediated isothermal amplification of DNA. *Nucleic acids research*, 28(12), e63-e63.
- Oberhänsli, T., Altenbach, D., & Bitterlin, W. (2011). Development of a duplex TaqMan real-time PCR for the general detection of phytoplasmas and 18S rRNA host genes in fruit trees and other plants. *Bulletin of Insectology*, 64 (Supplement), 37-38.
- Obuchowski, M., & Wegrzyn, G. (1991). Eriochrome black T as a dye for agarose gel electrophoresis. *Acta Biochimica Polonica*, 38(1), 177-179.
- Obura, E., Masiga, D., Wachira, F., Gurja, B., & Khan, Z. R. (2011). Detection of phytoplasma by loop-mediated isothermal amplification of DNA (LAMP). *Journal of microbiological methods*, 84(2), 312-316.
- OEPP/EPPO (2006): *Candidatus* Phytoplasma pyri. *Bulletin OEPP/EPPO Bulletin* 36, 127-128.
- Ogata, N., & Miura, T. (1998a). Creation of genetic information by DNA polymerase of the archaeon *Thermococcus litoralis*: influences of temperature and ionic strength. *Nucleic acids research*, 26(20), 4652-4656.
- Ogata, N., & Miura, T. (1998b). Creation of genetic information by DNA polymerase of the thermophilic bacterium *Thermus thermophilus*. *Nucleic acids research*, 26(20), 4657-4661.
- Ogata, N., & Miura, T. (2000). Elongation of tandem repetitive DNA by the DNA polymerase of the hyperthermophilic archaeon *Thermococcus litoralis* at a hairpin-coil transitional state: A model of amplification of a primordial simple DNA sequence. *Biochemistry*, 39(45), 13993-14001.

- Oh, S. J., Park, B. H., Jung, J. H., Choi, G., Lee, D. C., & Seo, T. S. (2016). Centrifugal loop-mediated isothermal amplification microdevice for rapid, multiplex and colorimetric foodborne pathogen detection. *Biosensors and Bioelectronics*, 75, 293-300.
- Oscorbin, I. P., Belousova, E. A., Zakabunin, A. I., Boyarskikh, U. A., & Filipenko, M. L. (2016). Comparison of fluorescent intercalating dyes for quantitative loop-mediated isothermal amplification (qLAMP). *BioTechniques*, 61(1), 20.
- Oshima, K., Kakizawa, S., Nishigawa, H., Jung, H. Y., Wei, W., Suzuki, S., Arashida, R., Nakata, D., Miyata, S., Ugaki, M., & Namba, S. (2004). Reductive evolution suggested from the complete genome sequence of a plant-pathogenic phytoplasma. *Nature genetics*, 36(1), 27-29.
- Osmundson, T. W., Eyre, C. A., Hayden, K. M., Dhillon, J., & Garbelotto, M. M. (2013). Back to basics: an evaluation of NaOH and alternative rapid DNA extraction protocols for DNA barcoding, genotyping, and disease diagnostics from fungal and oomycete samples. *Molecular ecology resources*, 13(1), 66-74.
- Ouyang, C., Chen, S., Che, B., & Xue, G. (2007). Aggregation of azo dye Orange I induced by polyethylene glycol in aqueous solution. *Colloids and Surfaces A: Physicochemical and Engineering Aspects*, 301(1), 346-351.
- Park, S. Y., Lee, B., Park, K. S., Chong, Y., Yoon, M. Y., Jeon, S. J., & Kim, D. E. (2010). Facilitation of polymerase chain reaction with thermostable inorganic pyrophosphatase from hyperthermophilic archaeon *Pyrococcus horikoshii*. *Applied microbiology and biotechnology*, 85(3), 807-812.
- Paul, N., Shum, J., & Le, T. (2010). Hot start PCR. In: *RT-PCR Protocols*. Second Edition, Humana Press, Totowa, NJ, 301-318.
- Pérez-López, E., Rodríguez-Martínez, D., Olivier, C. Y., Luna-Rodríguez, M., & Dumonceaux, T. J. (2017). Molecular diagnostic assays based on cpn60 UT sequences reveal the geographic distribution of subgroup 16SrXIII-(A/I) I phytoplasma in Mexico. *Scientific Reports*, 7(1), 950.
- Pikal-Cleland, K. A., Cleland, J. L., Anchordoquy, T. J., & Carpenter, J. F. (2002). Effect of glycine on pH changes and protein stability during freeze–thawing in phosphate buffer systems. *Journal of pharmaceutical sciences*, 91(9), 1969-1979.
- Poole, C. B., Li, Z., Alhassan, A., Guelig, D., Diesburg, S., Tanner, N. A., Zhang, Y., Evans Jr., T. C., LaBarre, P., Wanji, S., Burton, R. A., & Carlow, C. K. S. (2017). Colorimetric tests for diagnosis of filarial infection and vector surveillance using non-instrumented nucleic acid loop-mediated isothermal amplification (NINA-LAMP). *PloS one*, 12(2), e0169011.

- Poole, C. B., Tanner, N. A., Zhang, Y., Evans Jr, T. C., & Carlow, C. K. (2012). Diagnosis of brugian filariasis by loop-mediated isothermal amplification. *PLoS Neglected tropical diseases*, 6(12), e1948.
- Porcar, M., Ramos, S., & Latorre, A. (2007). A simple DNA extraction method suitable for PCR detection of genetically modified maize. *Journal of the Science of Food and Agriculture*, 87(14), 2728-2731.
- PrimerExplorer V4 Manual, Eiken Chemical Co., Ltd., Tokyo, Japan.
https://primerexplorer.jp/e/v4_manual/pdf/PrimerExplorerV4_Manual_1.pdf
- Priye, A., Wong, S., Bi, Y., Carpio, M., Chang, J., Coen, M., Cope, D., Harris, J., Johnson, J., Keller, A., Lim, R., Lu, S., Millard, A., Pangelinan, A., Patel, N., Smith, L., Chan, K., & Ugaz, V. M. (2016). Lab-on-a-drone: toward pinpoint deployment of smartphone-enabled nucleic acid-based diagnostics for mobile health care. *Analytical chemistry*, 88(9), 4651-4660.
- Quartieri, M., Marangoni, B., Schiavon, L., Tagliavini, M., Bassi, D., Previati, A., & Giannini, M. (2010). Evaluation of pear rootstock selections. In: *XI International Pear Symposium* 909, 153-159.
- Qian, J., Ferguson, T. M., Shinde, D. N., Ramírez-Borrero, A. J., Hintze, A., Adami, C., & Niemz, A. (2012). Sequence dependence of isothermal DNA amplification via EXPAR. *Nucleic acids research*, 40(11), e87.
- Rageh, N. M. (2005). Low-energy electronic spectra of 2-[(4-Sulfanylphenyl) azo]-4, 5-diphenylimidazole. *Chemical Papers*, 59(4), 244-247.
- Ramadan, K., Shevelev, I. V., Maga, G., & Hübscher, U. (2004). *De novo* DNA synthesis by human DNA polymerase λ , DNA polymerase μ and terminal deoxyribonucleotidyl transferase. *Journal of molecular biology*, 339(2), 395-404.
- Rauf, M. A., Hisaindee, S., & Saleh, N. (2015). Spectroscopic studies of keto–enol tautomeric equilibrium of azo dyes. *RSC Advances*, 5(23), 18097-18110.
- Rodriguez-Manzano, J., Karymov, M. A., Begolo, S., Selck, D. A., Zhukov, D. V., Jue, E., & Ismagilov, R. F. (2016). Reading out single-molecule digital RNA and DNA isothermal amplification in nanoliter volumes with unmodified camera phones. *ACS nano*, 10(3), 3102-3113.
- Saad, S. T., Hoque, M. A., & Khan, M. A. (2014). Spectroscopic studies of the investigation of molecular interaction between Acid Red and cetyltrimethylammonium bromide. *ChemXpress*, 3(3), 111-117.
- Satya, P., Mitra, S., Ray, D. P., Mahapatra, B. S., Karan, M., Jana, S., & Sharma, A. K. (2013). Rapid and inexpensive NaOH based direct PCR for amplification of nuclear and organelle DNA

- from ramie (*Boehmeria nivea*), a bast fibre crop containing complex polysaccharides. *Industrial Crops and Products*, 50, 532-536.
- Schaper, U., & Seemüller, E. (1982). Condition of the phloem and the persistence of mycoplasma-like organisms associated with apple proliferation and pear decline. *Phytopathology*, 72, 736-742.
- Schneider, B., & Gibb, K. S. (1997). Detection of phytoplasmas in declining pears in southern Australia. *Plant Disease*, 81(3), 254-258.
- Schneider, B., Gibb, K. S., & Seemüller, E. (1997). Sequence and RFLP analysis of the elongation factor Tu gene used in differentiation and classification of phytoplasmas. *Microbiology*, 143(10), 3381-3389.
- Schneider, B., Ahrens, U., Kirkpatrick, B. C., & Seemüller, E. (1993). Classification of plant-pathogenic mycoplasma-like organisms using restriction-site analysis of PCR-amplified 16S rDNA. *Microbiology*, 139(3), 519-527.
- Schneider, B., & Seemüller, E. (1994). Presence of two sets of ribosomal genes in phytopathogenic mollicutes. *Applied and Environmental Microbiology*, 60(9), 3409-3412.
- Schneider, B., Seemüller, E., Smart, C. D., & Kirkpatrick, B. C. (1995). Phylogenetic classification of plant pathogenic mycoplasma-like organisms or phytoplasmas. *Molecular and diagnostic procedures in mycoplasmaology*, 1(369), 79.
- Schneider, H. (1970). Graft transmission and host range of the pear decline causal agent. *Phytopathology*, 60(2), 204-07.
- Seemüller, E., Kunze, L., & Schaper, U. (1984). Colonization behavior of MLO, and symptom expression of proliferation-diseased apple trees and decline-diseased pear trees over a period of several years. *Zeitschrift für Pflanzenkrankheiten und Pflanzenschutz*, 91(5), 525-532.
- Seemüller, E., & Schneider, B. (2004). '*Candidatus* Phytoplasma mali', '*Candidatus* Phytoplasma pyri' and '*Candidatus* Phytoplasma prunorum', the causal agents of apple proliferation, pear decline and European stone fruit yellows, respectively. *International Journal of Systematic and Evolutionary Microbiology*, 54(4), 1217-1226.
- Seemüller, E., Schneider, B., Jarausch, B. (2011). Pear decline phytoplasma. *Virus and virus-like diseases of pome and stone fruits*. The American Phytopathological Society, St. Paul, Minnesota, USA, 77-84.
- Seemüller, E., Schneider, B., Mäurer, R., Ahrens, U., Daire, X., Kison, H., Lorenz, K. H., Firrao, G., Avinent, L., Sears, B. B. & Stackebrandt, E. (1994). Phylogenetic classification of phytopathogenic mollicutes by sequence analysis of 16S ribosomal DNA. *International journal of systematic bacteriology*, 44(3), 440-446.

- Shiddiky, M. J., Rahman, M., Park, J. S., & Shim, Y. B. (2006). Analysis of polymerase chain reaction amplifications through phosphate detection using an enzyme-based microbiosensor in a microfluidic device. *Electrophoresis*, 27(14), 2951-2959.
- Shigemoto, N., Fukuda, S., Takao, S., Shimazu, Y., Tanizawa, Y., Kuwayama, M., & Ohara, S. (2010). Rapid detection of novel influenza A virus and seasonal influenza A (H1N1, H3N2) viruses by reverse transcription-loop-mediated isothermal amplification (RT-LAMP). *Kansenshogaku zasshi. The Journal of the Japanese Association for Infectious Diseases*, 84(4), 431-436.
- Silkie, S. S., Tolcher, M. P., & Nelson, K. L. (2008). Reagent decontamination to eliminate false-positives in *Escherichia coli* qPCR. *Journal of microbiological methods*, 72(3), 275-282.
- Silva, G. J., Souza, T. M., Barbieri, R. L., & Costa de Oliveira, A. (2014). Origin, domestication, and dispersing of pear (*Pyrus* spp.). *Advances in Agriculture*, Vol. 2014, 1-8.
- Singleton, J., Osborn, J. L., Lillis, L., Hawkins, K., Guelig, D., Price, W., Johns, R., Ebels, K., Boyle, D., Weigl, B., & LaBarre, P. (2014). Electricity-free amplification and detection for molecular point-of-care diagnosis of HIV-1. *PloS one*, 9(11), e113693.
- Siriwardhana, P. H. A. P., Gunawardena, B. W. A., & Millington, S. (2012). Detection of phytoplasma associated with Waligama Coconut Leaf Wilt Disease in Sri Lanka by loop mediated isothermal amplification assay performing alkaline polyethylene glycol based DNA extraction. *Journal of Microbiology and Biotechnology Research*, 2(5), 712-716.
- Skaff, D. A., McWhorter, W. J., Geisbrecht, B. V., Wyckoff, G. J., & Miziorko, H. M. (2015). Inhibition of bacterial mevalonate diphosphate decarboxylase by eriochrome compounds. *Archives of biochemistry and biophysics*, 566, 1-6.
- Skoog, D., West, D., Holler, F. L., & Crouch, S. (2014). *Fundamentals of analytical chemistry*. Nelson Education, p. 431.
- Soli, K. W., Kas, M., Maure, T., Umezaki, M., Morita, A., Siba, P. M., Greenhill, A. R., & Horwood, P. F. (2013). Evaluation of colorimetric detection methods for *Shigella*, *Salmonella*, and *Vibrio cholerae* by loop-mediated isothermal amplification. *Diagnostic microbiology and infectious disease*, 77(4), 321-323.
- Soliman, H., & El-Matbouli, M. (2005). An inexpensive and rapid diagnostic method of Koi Herpesvirus (KHV) infection by loop-mediated isothermal amplification. *Virology journal*, 2(1), 83.
- Solomon, M. G., Cranham, J. E., Easterbrook, M. A., & Fitzgerald, J. D. (1989). Control of the pear psyllid, *Cacopsylla pyricola*, in South East England by predators and pesticides. *Crop Protection*, 8(3), 197-205.

- Song, J., Mauk, M. G., Hackett, B. A., Cherry, S., Bau, H. H., & Liu, C. (2016). Instrument-free point-of-care molecular detection of Zika virus. *Analytical chemistry*, 88(14), 7289-7294.
- Storari, M., Rohr, R., Pertot, I., Gessler, C., & Broggini, G. A. L. (2013). Identification of ochratoxin A producing *Aspergillus carbonarius* and *A. niger* clade isolated from grapes using the loop-mediated isothermal amplification (LAMP) reaction. *Journal of applied microbiology*, 114(4), 1193-1200.
- Strauss, E. (2009). Phytoplasma research begins to bloom. *Science*, 325(5939), 388-390.
- Sugawara, K., Himeno, M., Keima, T., Kitazawa, Y., Maejima, K., Oshima, K., & Namba, S. (2012). Rapid and reliable detection of phytoplasma by loop-mediated isothermal amplification targeting a housekeeping gene. *Journal of general plant pathology*, 78(6), 389-397.
- Sugawara, M., Rokugawa, Y. I., & Kambara, T. (1977). Catalytic decomposition of the excess reagent in the spectrophotometric determination of Copper (II) with o, o'-Dihydroxyazo compounds. *Bulletin of the Chemical Society of Japan*, 50(12), 3206-3208.
- Sundaramurthi, P., & Suryanarayanan, R. (2011). Predicting the crystallization propensity of carboxylic acid buffers in frozen systems—relevance to freeze-drying. *Journal of pharmaceutical sciences*, 100(4), 1288-1293.
- Tan, E., Erwin, B., Dames, S., Ferguson, T., Buechel, M., Irvine, B., Voelkerding, K., & Niemz, A. (2008). Specific versus nonspecific isothermal DNA amplification through thermophilic polymerase and nicking enzyme activities. *Biochemistry*, 47(38), 9987.
- Tanner, N. A., Zhang, Y., & Evans Jr, T. C. (2012). Simultaneous multiple target detection in real-time loop-mediated isothermal amplification. *Biotechniques*, 53(2), 81-9.
- Tanner, N. A., Zhang, Y., & Evans Jr, T. C. (2015). Visual detection of isothermal nucleic acid amplification using pH-sensitive dyes. *BioTechniques*, 58(2), 59-68.
- Tao, Z. Y., Zhou, H. Y., Xia, H., Xu, S., Zhu, H. W., Culleton, R. L., Han, E. T., Lu, F., Fang, Q., Gu, Y. P., Liu, Y. B., Zhu, G. D., Wang, W. M., Li, J. L., Cao, J., & Gao, Q. (2011). Adaptation of a visualized loop-mediated isothermal amplification technique for field detection of *Plasmodium vivax* infection. *Parasites & vectors*, 4(1), 115.
- Tomita, N., Mori, Y., Kanda, H., & Notomi, T. (2008). Loop-mediated isothermal amplification (LAMP) of gene sequences and simple visual detection of products. *Nature protocols*, 3(5), 877-882.
- Tomlinson, J. (2013). In-field diagnostics using loop-mediated isothermal amplification. In: *Phytoplasma: Methods and Protocols*. Methods in molecular biology, Clifton, NJ, 938, 291-300.

- Tomlinson, J. A., Dickinson, M. J., & Boonham, N. (2010a). Rapid detection of *Phytophthora ramorum* and *P. kernoviae* by two-minute DNA extraction followed by isothermal amplification and amplicon detection by generic lateral flow device. *Phytopathology*, 100(2), 143-149.
- Tomlinson, J. A., Boonham, N., & Dickinson, M. (2010b). Development and evaluation of a one-hour DNA extraction and loop-mediated isothermal amplification assay for rapid detection of phytoplasmas. *Plant Pathology* 59, 465-471.
- Torres, E., Bertolini, E., Cambra, M., Montón, C., & Martín, M. P. (2005). Real-time PCR for simultaneous and quantitative detection of quarantine phytoplasmas from apple proliferation (16SrX) group. *Molecular and Cellular Probes*, 19(5), 334-340.
- Torres, E., Laviña, A., Sabaté, J., Bech, J., & Batlle, A. (2010). Evaluation of susceptibility of pear and plum varieties and rootstocks to *Ca. P. pyri* and *Ca. P. prunorum* using Real-Time PCR. *Julius-Kühn-Archiv*, 427, 395-398.
- Ünal, A., Eren, B., & Eren, E. (2013). Investigation of the azo-hydrazone tautomeric equilibrium in an azo dye involving the naphthalene moiety by UV-vis spectroscopy and quantum chemistry. *Journal of Molecular Structure*, 1049, 303-309.
- Verbylaite, R., Beiðys, P., Rimas, V., & Kuusiene, S. (2010). Comparison of ten DNA extraction protocols from wood of European aspen (*Populus tremula* L.). *Baltic Forestry*, 16(1), 30.
- Vincent, M., Xu, Y., & Kong, H. (2004). Helicase-dependent isothermal DNA amplification. *EMBO Reports* 5(8), 795-800.
- Voisey, J., Hafner, G. J., Morris, C. P., Van Daal, A., & Giffard, P. M. (2001). Interrogation of multimeric DNA amplification products by competitive primer extension using *Bst* DNA polymerase (large fragment). *BioTechniques*, 31(5), 1122-1129.
- Volk, G. M., Richards, C. M., Henk, A. D., Reilley, A. A., Bassil, N. V., & Postman, J. D. (2006). Diversity of wild *Pyrus communis* based on microsatellite analyses. *Journal of the American Society for Horticultural Science*, 131(3), 408-417.
- Vu, N. T., Pardo, J. M., Alvarez, E., Le, H. H., Wyckhuys, K., Nguyen, K. L., & Le, D. T. (2016). Establishment of a loop-mediated isothermal amplification (LAMP) assay for the detection of phytoplasma-associated cassava witches' broom disease. *Applied Biological Chemistry*, 59(2), 151-156.
- Walker, G. T., Fraiser, M. S., Schram, J. L., Little, M. C., Nadeau, J. G., & Malinowski, D. P. (1992). Strand displacement amplification—an isothermal, in vitro DNA amplification technique. *Nucleic acids research*, 20(7), 1691-1696.

- Wang, D. G. (2014). Visual detection of *Mycobacterium tuberculosis* complex with Loop-mediated isothermal amplification and Eriochrome Black T. *Applied Mechanics and Materials*, 618, 264-267.
- Wang, H., Qi, M., & Cutler, A.J. (1993). A simple method of preparing plant samples for PCR. *Nucleic Acids research*, 21(17), 4153-4154.
- Wang, L., Liao, X., Ding, Y., Gao, F., & Wang, Q. (2014). DNA biosensor based on a glassy carbon electrode modified with electropolymerized Eriochrome Black T. *Microchimica Acta*, 181(1-2), 155-162.
- Wastling, S. L., Picozzi, K., Kakembo, A. S., & Welburn, S. C. (2010). LAMP for human African trypanosomiasis: a comparative study of detection formats. *PLoS Neglected Tropical Diseases*, 4(11), e865.
- Webster, A. D. (1997). A brief review of pear rootstock development. In: VII International Symposium on Pear Growing, 475, 135-142.
- Wei, W., Davis, R. E., Lee, M., & Zhao, Y. (2007). Computer-simulated RFLP analysis of 16S rRNA genes: identification of ten new phytoplasma groups. *International Journal of Systematic and Evolutionary Microbiology*, 57(8), 1855-1867.
- Weisburg, W. G., Barns, S. M., Pelletier, D. A., & Lane, D. J. (1991). 16S ribosomal DNA amplification for phylogenetic study. *Journal of bacteriology*, 173(2), 697-703.
- Werner, O., Ros, R. M., & Guerra, J. (2002). Direct amplification and NaOH extraction: two rapid and simple methods for preparing bryophyte DNA for polymerase chain reaction (PCR). *Journal of bryology*, 24(2), 127-131.
- Wertheim, S. J. (2000). Rootstocks for European pear: a review. In: VIII International Symposium on Pear, 596, 299-309.
- Wertheim, S. J., & Vercammen, J. (2000). A multi-site pear-interstem trial in the Netherlands and Belgium. *Journal of American Pomological Society*, 54(4), 199-207.
- Williams-Smith, D. L., Bray, R. C., Barber, M. J., Tsopanakis, A. D., & Vincent, S. P. (1977). Changes in apparent pH on freezing aqueous buffer solutions and their relevance to biochemical electron-paramagnetic-resonance spectroscopy. *Biochemical Journal*, 167(3), 593-600.
- Woese, C. R. (1987). Bacterial evolution. *Microbiological reviews*, 51(2), 221-271.
- Wolko, Ł., Antkowiak, W., Lenartowicz, E., & Bocianowski, J. (2010). Genetic diversity of European pear cultivars (*Pyrus communis* L.) and wild pear (*Pyrus pyraster* (L.) Burgsd.) inferred from microsatellite markers analysis. *Genetic resources and crop evolution*, 57(6), 801-806.

- Yamamoto, T., & Chevreau, E. (2009). Pear genomics. In: Genetics and Genomics of Rosaceae. Springer, New York, 163-186.
- Yao, H., Sun, Y., Lin, X., Tang, Y., & Huang, L. (2007). Electrochemical characterization of poly (eriochrome black T) modified glassy carbon electrode and its application to simultaneous determination of dopamine, ascorbic acid and uric acid. *Electrochimica Acta*, 52(20), 6165-6171.
- Yeh, H. Y., Shoemaker, C. A., & Klesius, P. H. (2005). Evaluation of a loop-mediated isothermal amplification method for rapid detection of channel catfish *Ictalurus punctatus* important bacterial pathogen *Edwardsiella ictaluri*. *Journal of microbiological methods*, 63(1), 36-44.
- Young, A., & Sweet, T. R. (1955). Complexes of Eriochrome Black T with calcium and magnesium. *Analytical Chemistry*, 27(3), 418-420.
- Zhang, Y., Zhang, L., Sun, J., Liu, Y., Ma, X., Cui, S., Ma, L., Xi, J. J., & Jiang, X. (2014). Point-of-care multiplexed assays of nucleic acids using microcapillary-based loop-mediated isothermal amplification. *Analytical chemistry*, 86(14), 7057-7062.
- Zhao, Y., & Davis, R. E. (2016). Criteria for phytoplasma 16Sr group/subgroup delineation and the need of a platform for proper registration of new groups and subgroups. *International journal of systematic and evolutionary microbiology*, 66(5), 2121-2123.
- Zhao, Y., Davis, R. E., Wei, W., & Lee, I.-M. (2015). Should ‘*Candidatus* Phytoplasma’ be retained within the order *Acholeplasmatales*? *International journal of systematic and evolutionary microbiology*, 65(3), 1075-1082.
- Zhao, Y., Wei, W., Davis, R. E., & Lee, I.-M. (2010). Recent advances in 16S rRNA gene-based phytoplasma differentiation, classification and taxonomy. In: Weintraub P.G., Jones P. (eds.): *Phytoplasmas: Genomes, Plant Hosts and Vectors*. CAB International, Wallingford, UK, 64-92.
- Zyrina, N. V., Antipova, V. N., & Zheleznaya, L. A. (2014). *Ab initio* synthesis by DNA polymerases. *FEMS Microbiology Letters*, 351(1), 1-6.
- Zyrina, N. V., Artyukh, R. I., Svad'bina, I. V., Zheleznaya, L. A., & Matvienko, N. I. (2012). The effect of single-stranded DNA binding proteins on template/primer-independent DNA synthesis in the presence of nicking endonuclease Nt. BspD6I. *Russian Journal of Bioorganic Chemistry*, 38(2), 171-176.
- Zyrina, N. V., Zheleznaya, L. A., Dvoretzky, E. V., Vasiliev, V. D., Chernov, A., & Matvienko, N. I. (2007). N. BspD6I DNA nickase strongly stimulates template-independent synthesis of non-palindromic repetitive DNA by *Bst* DNA polymerase. *Biological chemistry*, 388(4), 367-372.